Université de Montréal

Application de la tectonique moléculaire à des systèmes auto-assemblés non cristallins à l'aide des diarylbiguanides et des diarylaminotriazines

Par

Olivier Lebel

Département de Chimie

Faculté des Arts et des Sciences

Thèse présentée à la Faculté des études supérieures

en vue de l'obtention du grade de

Philisophiae Doctor (Ph.D.)

en chimie

Avril 2006

Université de Montréal

Faculté des études supérieures

Cette thèse intitulée :

Application de la tectonique moléculaire à des systèmes auto-assemblés non cristallins à l'aide des diarylbiguanides et des diarylaminotriazines

présentée par :

Olivier Lebel

a été évaluée par un jury composé des personnes suivantes :

Professeur Stephen Hanessian	président-rapporteur
Professeur James D. Wuest	directeur de recherche
Professeur Andreea Schmitzer	membre du jury
Professeur Yue Zhao	examinateur externe
Professeur Jeffrey W. Keillor	représentant du doyen de la FES

Sommaire

La chimie supramoléculaire vise à exploiter de façon stratégique les interactions non-covalentes afin de moduler les propriétés des composés. La tectonique moléculaire, qui est une branche de la chimie supramoléculaire développée au sein du groupe Wuest, consiste à créer de nouveaux matériaux ordonnés par auto-assemblage. Bien que jusqu'à présent cette technique ait seulement été utilisée afin de générer des matériaux cristallins poreux, il est envisageable d'utiliser les principes de la tectonique moléculaire dans la conception de matériaux auto-assemblés d'un moindre degré d'ordre, comme les cristaux liquides, les gels et les matériaux amorphes.

Les études effectuées dans le cadre de cette thèse visent à utiliser les connaissances acquises en tectonique moléculaire au cours des quinze dernières années afin de développer des composés capables d'auto-assemblage favorisant la formation de gels ou de solides amorphes plutôt que de cristaux.

Pour ce faire, nous avons utilisé les 1,5-diarylbiguanides comme précurseurs synthétiques. Étant donné que ces composés sont plutôt méconnus, nous avons d'abord cherché à établir des procédures simples d'usage pour leur synthèse et leur caractérisation. Nous avons également étudié certains de ces composés et leurs sels à l'état cristallin.

Afin d'évaluer le potentiel des biguanides et de leurs sels comme groupes de reconnaissance en tectonique moléculaire, nous avons ensuite étudié les structures cristallographiques du 1,3- et du 1,4-phénylènebis(biguanide) et de leurs sels pour vérifier la présence de motifs d'association généraux et récurrents. Ces études ont démontré que bien que ces groupes fonctionnels affichent certaines préférences quant à leurs motifs d'auto-assemblage, leur flexibilité et leur vaste nombre de sites pouvant former des ponts hydrogène limitent la prévisibilité de ces motifs.

Dans un deuxième temps, nous avons étudié les sels de sodium des 4,6-diarylamino-1,3,5-triazine-2-carboxylates comme gélateurs de bas poids moléculaire. En effet, ces composés préfèrent s'associer selon une dimension de l'espace pour former des fibres dont l'enchevêtrement provoque la gélification du DMSO à très basse concentration. Nous avons étudié l'effet du contre-ion, du solvant et des substituants présents sur les groupes aryles, et nous avons découvert que tous trois sont étroitement liés avec la capacité de ces composés à former des gels. Des études morphologiques ainsi que l'obtention d'une structure cristallographique de l'un de ces composés ont démontré que les molécules s'assemblent par coordination au sodium pour former des fibres d'environ 25 à 30 nm de diamètre.

Finalement, nous avons découvert que des dérivés 1,5-diarylbiguanide et 4,6-diarylamino-1,3,5-triazine portant des groupes méthyles aux positions 3- et 5- des groupes aryles favorisent la formation de solides amorphes malgré leur capacité à s'associer à l'aide de ponts hydrogène. À l'aide de la synthèse de nouveaux dérivés, d'une structure cristallographique et d'études spectroscopiques, nous avons confirmé la présence d'association par ponts hydrogène à l'état amorphe, et nous avons démontré l'importance de l'auto-assemblage pour la formation de solides amorphes ainsi que leur stabilité.

Mots clés : Chimie supramoléculaire, génie cristallin, matériaux, auto-assemblage, ponts hydrogène, gels, verres moléculaires, biguanides, diarylaminotriazines, microscopie.

Summary

Supramolecular chemistry seeks to exploit non-covalent interactions strategically to modulate the properties of compounds. Molecular tectonics, which is a branch of supramolecular chemistry developed in the Wuest group, involves the design of novel ordered materials through self-assembly. Although until now molecular tectonics has only been used to generate porous crystalline materials, it would be in principle possible to translate the principles of molecular tectonics to less-ordered materials such as liquid crystals, gels or amorphous materials.

The studies described in this thesis aim to use the knowledge acquired in the course of exploring molecular tectonics during the last fifteen years to develop compounds that are capable of self-association but favor the formation of gels or amorphous solids rather than crystals.

Towards this goal, we have used 1,5-diarylbiguanides as synthetic precursors. Since these compounds are poorly known, we have first sought to establish simple procedures for their synthesis and characterization. We have also studied the crystal structures of parent compound 1,5-diphenylbiguanide and its hydrochloride salt.

In order to assess the potential of biguanides and their salts as sticky sites in molecular tectonics, we have then studied the crystallographic structures of 1,3- and 1,4-phenylenebis(biguanide) and their salts in order to confirm the presence of recurring and general recognition motifs. These studies have demonstrated that even though biguanides show certain preferences in their self-assembly patterns, their flexibility and their large number of hydrogen-bonding sites limit the predictability of these patterns.

In the second part of this work, we discuss the use of sodium salts of 4,6-diarylamino-1,3,5-triazine-2-carboxylates as low-molecular-weight gelators. These compounds associate in a unidimensional fashion to form fibres. The fibres in turn form three-dimensional networks that can gel DMSO at very low concentration. We have

studied the effect of counterion, solvent and substituents on the aryl groups on gelling efficiency, and we have discovered that there is a very close relationship between the ability of a compound to form a gel and all three of these parameters. Morphological studies, along with the crystallographic structure of one of these compounds, have shown that gelator molecules self-assemble through sodium coordination to form fibres ranging approximately from 25 to 30 nm in diameter.

Finally, we have discovered that certain 1,5-diarylbiguanide and 4,6-diarylamino-1,3,5-triazine derivatives bearing methyl groups at the 3- and 5-positions of the aryl groups favor the formation of amorphous solids in spite of their capacity to self-assemble through hydrogen bonding. Through the synthesis of novel derivatives, crystallography and spectroscopic studies, we have confirmed that hydrogen-bonded self-assembly is present in the amorphous solid state, and we have established the importance of self-assembly for the formation and stability of amorphous solids.

Keywords : Supramolecular chemistry, crystal engineering, materials science, self-assembly, hydrogen bonds, gels, molecular glasses, biguanides, diarylaminotriazines, microscopy.

Table des matières

Chapitre 1 : Introduction

Chapitre 2 : Synthèse et caractérisation des arylbiguanides et des diarylbiguanides

Chapitre 3 : Étude des arylbis(biguanides) et de leurs sels dans l'état cristallin

Chapitre 4 : Propriétés gélifiantes des 4,6-diarylamino-1,3,5-triazine-2-carboxylates de sodium

Chapitre 5 : Vers la conception de matériaux moléculaires amorphes auto-assemblés

Chapitre 6 : Conclusions et perspectives

Liste des tableaux

Liste des schémas

Liste des figures

Liste des abréviations

A	: adénine
Å	: Ångström
Ac	: acétyle
ADN	: acide désoxyribonucléique
AFM	: atomic force microscopy
Anal.	: analyse
APPI	: Atmospheric Pressure Photo-Ionization
aq	: aqueux
Ar	: aryle
a.u.	: arbitrary unit
Boc	: *tert*-butoxycarbonyle
br	: broad (en RMN)
C	: cytosine
°C	: degré Celsius
calcd	: calculated
CCD	: Charge-Coupled Device
cm	: centimètre
Δ	: chaleur
δ	: déplacement chimique
°	: degré
d	: doublet (en RMN)
d	: densité
dd	: doublet de doublets (en RMN)
DMF	: N,N-diméthylformamide
DMSO	: diméthyl sulfoxyde
DSC	: differential scanning calorimetry
dt	: doublet de triplets (en RMN)
e	: électron
eq	: équivalent

ESI	: electrospray ionisation
Et	: éthyle
FAB	: fast atom bombardment
FE-SEM	: field effect scanning electron microscopy
FTIR	: Fourier transform infrared
Fw	: formula weight
g	: gramme
G	: guanine
GoF	: goodness-of-fit
h	: heure
HRMS	: high resolution mass spectrometry
$h\nu$	: sous irradiation
Hz	: hertz
IR	: infrarouge
J	: constante de couplage
K	: Kelvin
λ	: longueur d'onde
M	: molaire
m	: masse ou multiplet (en RMN)
μ	: coefficient d'absorption
MAB	: metastable atom bombardment
mDSC	: modulated differential scanning calorimetry
Me	: méthyle
m/e	: rapport masse / charge
mg	: milligramme
MHz	: mégahertz
µm	: micromètre
min	: minute
mL	: millilitre
mm	: millimètre
mM	: millimolaire

mmol	: millimole
mol	: mole
mp	: melting point
MS	: mass spectrometry
nm	: nanomètre
NMR	: nuclear magnetic resonance
OLED	: organic light-emitting diode
ORTEP	: Oak Ridge Thermal Ellipsoid Program
P	: porosity
Ph	: phényle
π	: électron π
q	: quadruplet (en RMN)
quint	: quintuplet (en RMN)
R_1	: facteur d'accord sur les réflexions observées
wR_2	: facteur d'accord pondéré
RMN	: résonance magnétique nucléaire
rt	: room temperature
s	: singulet (en RMN)
SEM	: scanning electron microscopy
t	: triplet (en RMN)
T	: thymine
% T	: transmittance
TEM	: transmission electron microscopy
T_g	: température de transition vitreuse
T_{gel}	: température de transition sol-gel
THF	: tétrahydrofurane
TMS	: triméthylsilyle
UV	: ultraviolet
V	: volume
W	: Watt
wt	: weight

Z	: nombre d'unités formulaires par maille

Remerciements

Je souhaiterais tout d'abord remercier mon directeur de recherche, le professeur James D. Wuest, pour m'avoir accepté dans son groupe de recherche comme étudiant gradué. Il m'a permis d'apprendre énormément sur la chimie et sur moi-même au cours de ce long processus d'évolution qu'est le Ph.D. De plus, il m'a toujours donné la latitude pour exprimer ma créativité et pour diriger mes projets de recherche de façon indépendante, dans la réussite comme dans l'échec.

Ensuite, je voudrais remercier le docteur Thierry Maris ainsi que Marie-Ève Perron, non seulement pour avoir contribué de façon significative dans mes projets de recherche, mais également pour leurs conseils avisés, leur professionnalisme et leur compétence quasi légendaire.

Je tiens également à remercier tous les membres du groupes, présents et passés, avec lesquels j'ai eu l'occasion de travailler. Les discussions que nous avons eues ont été soit des plus enrichissantes, soit des plus insignifiantes, mais elles ont toujours été appréciées.

Je remercie les professeurs Jeffrey Keillor, William Lubell et André Charette pour m'avoir fait découvrir la chimie organique, ainsi que Minh Tan Phan Viet, Sylvie Bilodeau et Cédric Malveau du laboratoire de RMN, Alexandra Furtos du laboratoire de spectrométrie de masse et Huguette Dinel du laboratoire d'analyse élémentaire, ainsi que tout le personnel administratif du département de chimie.

Merci à tous les membres de ma famille et tous mes amis, en particulier mes parents, pour m'avoir toujours encouragé à aller jusqu'au bout de mes rêves sans jamais m'imposer de pression.

Finalement, je tiens particulièrement à remercier ma douce Patricia pour avoir cru en moi quand j'en avais le plus besoin, pour m'avoir soutenu quand j'en avais le

plus besoin, et pour m'avoir botté le derrière quand j'en avais le plus besoin. Je ne me serais jamais rendu où j'en suis sans ton aide et ta présence.

À Patricia et Samantha

Notes

Pour simplifier l'insertion des articles et ainsi faciliter la lecture de cette thèse, l'auteur a fait les modifications suivantes :

- La numérotation des molécules, des tableaux, des schémas et des figures dans les articles a été modifiée afin de suivre une numérotation générale pour toute la thèse.
- Les références contenues dans les articles sont placées à la fin de chaque article et sont indépendantes du chapitre dans lequel l'article est inséré.
- Toutes les informations des articles sont préservées dans la même section. Par contre, les parties « Supporting Information » pour chaque article sont disponibles en annexe.
- La nomenclature utilisée à travers la thèse est la nomenclature IUPAC.

La liste suivante démontre la contribution personnelle d'Olivier Lebel dans les articles présentés dans cette thèse :

- Toutes les synthèses ainsi que les cristallisations des molécules dans tous les articles ont été effectuées par Olivier Lebel.
- Les études de RMN à température variable contenues dans les articles 1 et 3, les études de spectroscopie infrarouge contenues dans l'article 4, ainsi que les mesures de concentration minimale de gélateur et les mesures de T_{gel} par la méthode « dropping-ball » contenues dans l'article 3 ont été effectuées par Olivier Lebel.
- Toutes les structures cristallographiques ont été résolues par le Dr Thierry Maris, et l'acquisition des données pour l'article 4 a été effectuée par le Dr. Alan Lough.
- Les images de microscopie optique contenues dans l'article 3 ont été effectuées par Marie-Ève Perron.

- Les images de microscopie électronique à balayage contenues dans l'article 3 ont été enregistrées par le Dr Sylvia Francis Zalzal.
- Les images de microscopie à force atomique contenues dans l'article 3 ont été enregistrées par le Dr Daniel Yi.
- Les mesures de calorimétrie à balayage différentiel ont été effectuées par Marie-Ève Perron et Eric Demers.
- Tous les articles ont été rédigés par Olivier Lebel et corrigés par les co-auteurs respectifs.

Chapitre 1 :

Introduction

1.1 La chimie supramoléculaire

1.1.1 Historique

Malgré le fait que les interactions non-covalentes, comme les interactions de van der Waals[1] et les ponts hydrogène,[2] ont été découvertes en 1873 et en 1920, respectivement, et malgré le fait que de nombreuses informations concernant la présence de liens non-covalents dans les biomolécules ont été rassemblées (par exemple, la structure en double hélice de l'ADN, qui est la conséquence de nombreux ponts hydrogène et d'interactions π-π, a été élucidée par Watson et Crick en 1953),[3] personne n'a alors tenté d'utiliser les liens non-covalents dans le but de générer de nouvelles structures chimiques. Pour ce faire, il fallut attendre que Charles J. Pedersen découvre entre 1962 et 1967 une série de polyéthers macrocycliques, tels que le composé **1**, qu'il baptisa « éthers couronne » en raison de leur forme. Ces composés ont la capacité de lier sélectivement des cations métalliques (Schéma 1.1).[4]

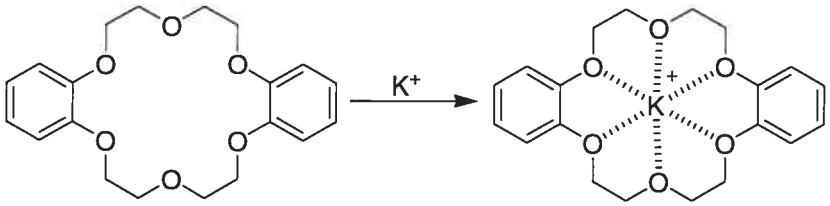

1

Schéma 1.1 Liaison d'un métal alcalin par un éther couronne.

Donald J. Cram[5] et Jean-Marie Lehn[6] poursuivirent ces travaux en synthétisant des molecules similaires comportant des cavités tridimensionnelles, nommées *cryptands*, qui ont la capacité de lier des substrats spécifiques avec une affinité encore plus grande. Les composés **2** et **3** sont des exemples de cryptands. Le travail combiné de Pedersen, Cram et Lehn leur valut un prix Nobel en 1987.[7]

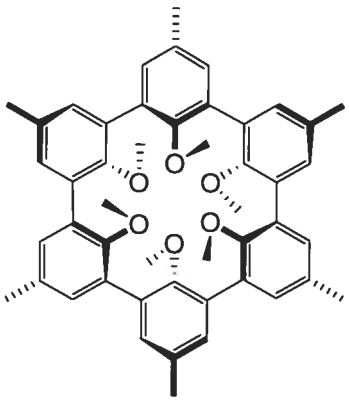

2

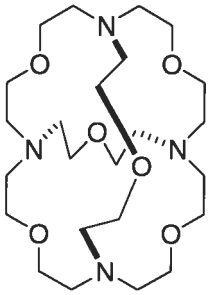

3

1.1.2 Les avantages des liaisons non-covalentes

Les interactions non-covalentes, bien que plus faibles que les liens covalents, ont l'avantage d'être réversibles, ce qui permet de générer des structures dynamiques qui prennent forme spontanément. Les différentes structures possibles sont triées par contrôle thermodynamique, ce qui permet de converger vers les espèces les plus stables. De plus, il est possible de provoquer la formation ou la rupture des assemblages à l'aide de stimuli externes (lumière, pH, métaux, chaleur, etc.). Différentes interactions non-covalentes travaillant ensemble de façon concertée peuvent résulter en la formation d'espèces chimiques posssédant des propriétés jusqu'alors inaccessibles.

1.1.3 Les sources d'inspiration de la chimie supramoléculaire

De la même manière que les moines Shaolin ont développé des styles de combat en se basant sur les mouvements des animaux,[8] les chimistes supramoléculaires se sont en grande partie inspirés de la nature qui regorge d'exemples de l'usage des interactions non-covalentes.

Les protéines sont possiblement le meilleur exemple de l'effet des interactions non-covalentes. La structure primaire (séquence d'acides aminés) d'une protéine dicte sa structure tertiaire (structure tridimensionnelle) à l'aide d'un mélange de ponts hydrogène, d'interactions électrostatiques, d'interactions de van der Waals et d'interactions π-π impliquant à la fois le squelette d'acides aminés et les chaînes latérales. La diversité de fonctions accomplies par les protéines est impressionnante. Les

enzymes sont des catalyseurs d'une extrême sélectivité et efficacité qui lient leur substrat à l'aide d'interactions non-covalentes.[9] Par ailleurs, les protéines comme le collagène, la kératine et la fibroïne de la soie sont des protéines fibreuses d'une grande résistance (qui leur est conférée par de nombreux ponts hydrogène) qui jouent un rôle important dans la structure des êtres vivants.

L'ADN forme une hélice bicaténaire à l'aide d'un mélange de ponts hydrogène et d'interactions π-π. La complémentarité des chaînes est assurée par la reconnaissance sélective entre les paires de nucléotides adénine-thymine et guanine-cytosine qui dépend à la fois du nombre de ponts hydrogène et de leur taille (Figure 1.1).

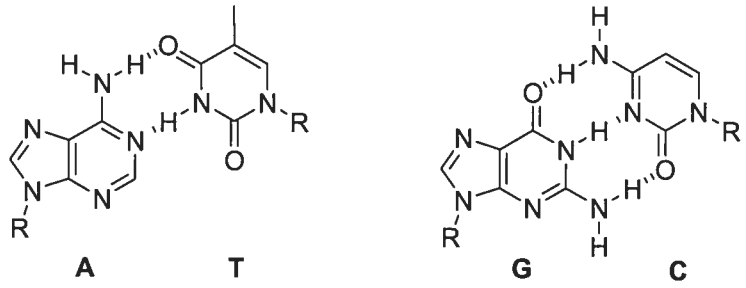

Figure 1.1 Reconnaissance sélective des unités de base dans les nucléotides par ponts hydrogène.

1.1.4 La chimie supramoléculaire en solution

La chimie supramoléculaire en solution repose en grande partie 1) sur l'auto-assemblage pour former des suprastructures de forme définie ou 2) sur la reconnaissance de substrats spécifiques. Par exemple, des molécules de forme hémisphérique peuvent s'assembler pour former des capsules qui peuvent contenir des molécules invitées.[10] Le composé **4** peut s'assembler pour former un tétramère qui ressemble à une balle de tennis[11] (Figure 1.2). Ces tétramères peuvent contenir des petites molécules telles le dichlorométhane, le benzène, le toluène, et des petites cétones cycliques.

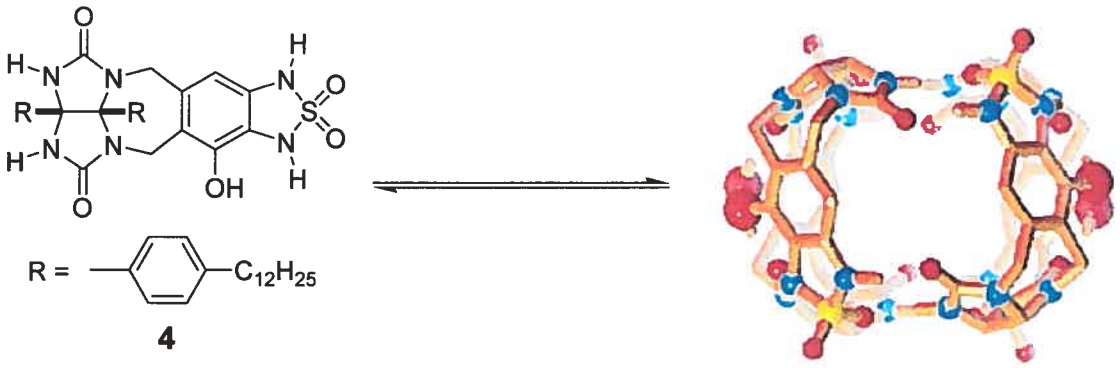

4

Figure 1.2 Auto-assemblage du composé **4** pour former un tétramère sphérique.[11]

Plusieurs applications peuvent découler de l'association moléculaire en solution. Par exemple, un composé capable de lier un substrat avec une grande sélectivité et possédant un chromophore peut s'avérer d'une grande utilité comme récepteur artificiel pouvant détecter des biomolécules (comme le glucose, par exemple)[12] ou des espèces dangereuses pour l'environnement, comme Hg^{2+}.[13] Par exemple, le composé **5** peut agir comme un senseur colorimétrique pour plusieurs anions tels le fluorure, l'acétate et le pyrophosphate.[14]

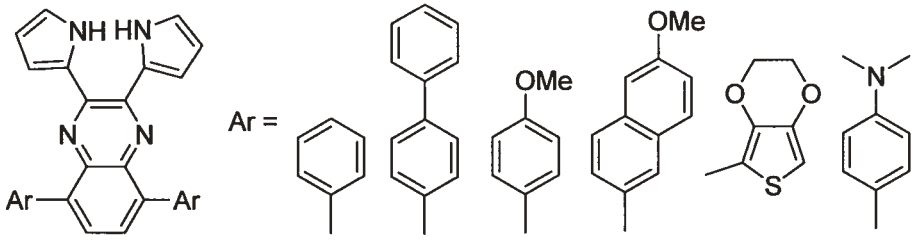

5

Il est aussi possible de générer des catalyseurs pour la synthèse stéréosélective capables de lier les différents réactifs à l'aide d'interactions non-covalentes. Le ligand **6**, synthétisé par Shibasaki,[15,16] est un tel exemple, capable de catalyser des réactions de cyanosilylation de type Strecker ou Reissert (Schéma 1.2). Les auteurs ont proposé que le substrat se lie sur l'aluminium et le cyanotriméthylsilane se lie sur un oxyde de phosphine à l'aide d'interactions acide de Lewis-base de Lewis, ce qui rapproche les deux réactifs et les maintient dans la bonne orientation (Figure 1.3).

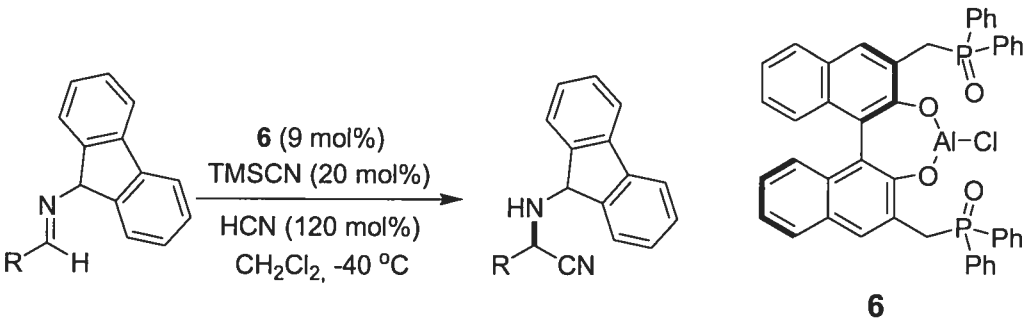

Schéma 1.2 Réaction de Strecker asymétrique catalysée par le ligand **6**.[15]

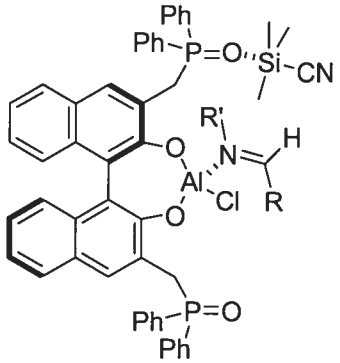

Figure 1.3 Modèle mécanistique proposé pour le rôle du ligand **6** dans la réaction de Strecker asymétrique.

1.1.5 La chimie supramoléculaire dans les couches et d'autres structures semi-ordonnées

Un aspect actif de la chimie supramoléculaire porte sur l'association de molécules pour former des systèmes partiellement ordonnés, tels les monocouches et les gels. Les surfaces inorganiques, comme les métaux ou les oxydes métalliques, peuvent être recouvertes d'une monocouche d'un composé organique en exploitant de façon stratégique l'affinité des surfaces pour certains groupes fonctionnels. Une monocouche auto-assemblée est ainsi formée.[17] Par exemple, les thiols (**7** par exemple) possèdent une forte affinité pour des métaux comme l'or (Schéma 1.3),[18] tandis que les composés comportant des groupes hydroxyles peuvent s'assembler sur des oxydes tels SiO_2, Al_2O_3 et TiO_2. Un tel composé est le dihydroxytétracène (**8**), qui peut s'assembler sur HfO_2, ZrO_2, Y_2O_3 et Al_2O_3 (Schéma 1.4).[19] En utilisant différentes interactions non-covalentes (les ponts hydrogène par exemple), il est possible de construire des architectures comportant plusieurs couches ordonnées par auto-assemblage.[20]

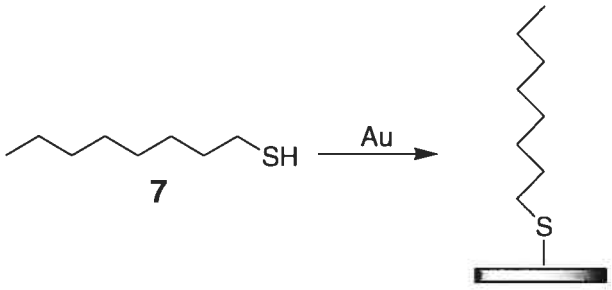

7

Schéma 1.3 Assemblage de l'octanethiol (**7**) sur une surface d'or pour former une monocouche.

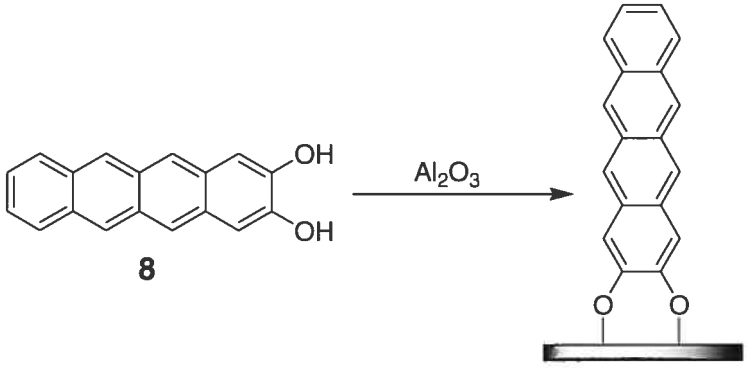

8

Schéma 1.4 Assemblage du composé **8** sur Al_2O_3.

Il est également possible de former des monocouches auto-assemblées sur des nanoparticules métalliques générées *in situ*.[21] Par exemple, la réduction d'un sel de tétrachloroaurate en présence d'un thiol résulte en la formation de nanoparticules d'or couvertes d'une monocouche du thiol dont la taille peut être contrôlée par la concentration et la stoechiométrie des réactifs.[22]

La microscopie tunnel à balayage[23] permet d'observer des monocouches physisorbées sur des surfaces avec une résolution atomique. Les monocouches peuvent être générées par déposition de vapeur ou par déposition en solution à l'interface solide-liquide. Les dicarbamates **9a-c**, par exemple, s'assemblent sur une surface de graphite pour former des motifs dont la forme est contrôlée par des ponts hydrogène ainsi que par la taille des chaînes alkyles (Figure 1.4).[24]

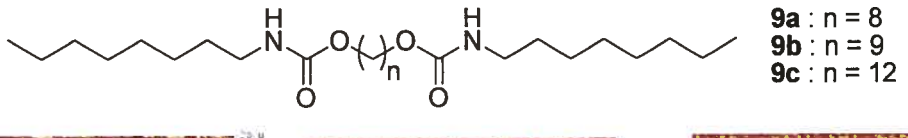

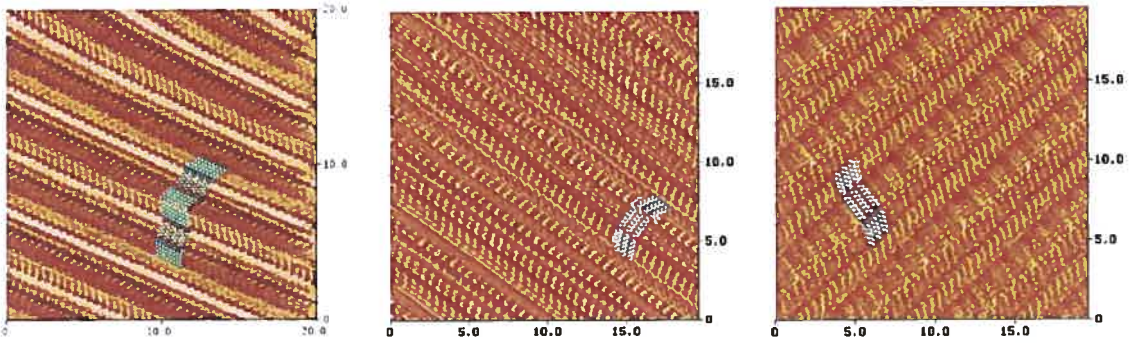

9a **9b** **9c**

Figure 1.4 Images par microscopie tunnel à balayage de monocouches physisorbées des composés **9a-c** sur du graphite pyrolytique hautement ordonné à l'interface liquide-solide. Des molécules sont représentées dans chaque cas. L'échelle est indiquée.[24]

Dans la plupart des cas, le refroidissement d'une solution sursaturée a pour effet la formation de cristaux, mais certains composés peuvent également former des fibres unidimensionnelles dont la croissance simultanée entraîne la formation d'un réseau. Les molécules de solvant sont retenues par ce réseau dont un gel est la conséquence macroscopique. Dans le cas des gélateurs polymériques, ces fibres sont liées par des liens covalents, tandis que dans le cas des gélateurs de bas poids moléculaire, ces fibres sont d'origine supramoléculaire. La présence simultanée de plusieurs types différents d'interactions non-covalentes est à la base de cet auto-assemblage. Les dérivés d'acides aminés **10**[25] et **11**[26] sont deux exemples de gélateurs de bas poids moléculaire, qui s'associent à l'aide de ponts hydrogène et d'interactions de van der Waals.

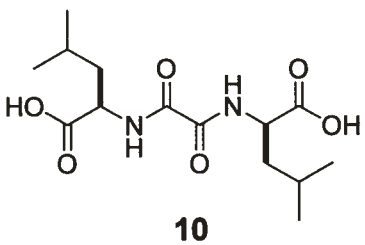

10

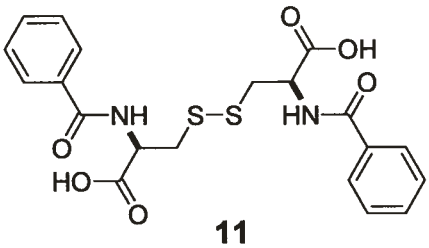

11

1.1.6 La chimie supramoléculaire à l'état cristallin

L'objectif de cette branche de la chimie supramoléculaire consiste en la conception de molécules capables de former des architectures auto-assemblées à l'état

cristallin où la présence d'interactions non-covalentes permet de contrôler et de prédire jusqu'à un certain degré la structure cristalline.

Il est connu que la mélamine forme un complexe 1 : 1 avec l'acide cyanurique.[27] L'association de mélamines substituées avec des dérivés des acides cyanurique ou barbiturique à l'état cristallin[28] a démontré que les molécules peuvent s'assembler pour former des rubans linéaires (**12**) ou plissés (**13**), ou encore des hexamères en forme de rosette (**14**) selon la taille des substituants (Figure 1.5).[29]

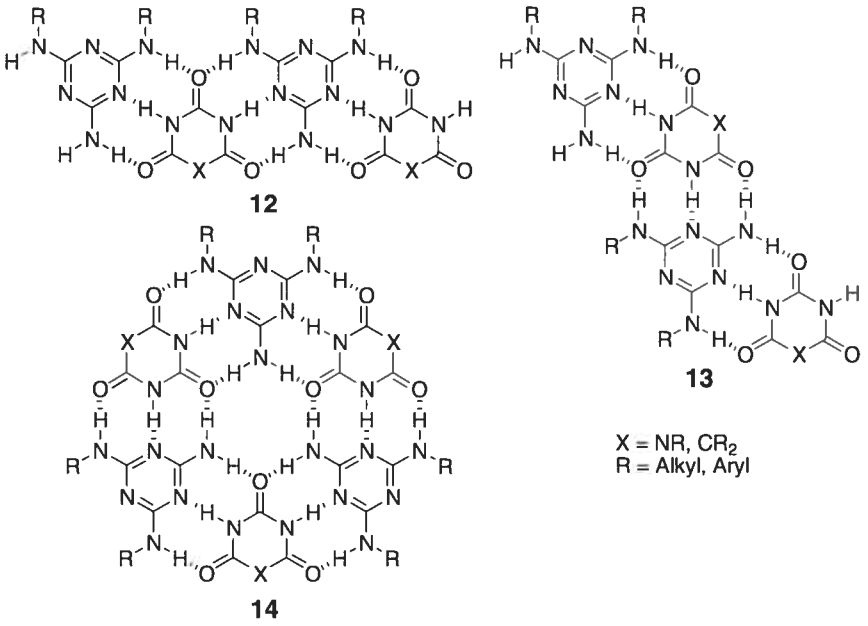

Figure 1.5 Différents motifs résultant de la co-cristallisation de mélamines disubstituées avec des dérivés des acides cyanurique ou barbiturique.

À l'aide de petites molécules organiques possédant plusieurs sites pouvant coordonner des métaux de transition, il est possible de générer des architectures cristallines où la structure est dirigée par la coordination aux métaux. Ces cristaux sont souvent d'une grande robustesse et d'une grande porosité, le volume libre pouvant être occupé par des solvants, des contre-ions ou des molécules de gaz.[30] À partir d'acides carboxyliques simples, tels que **15**, **16** ou **17** et des sels de fer, de zinc, de cuivre ou de nickel, de tels cristaux peuvent être obtenus.

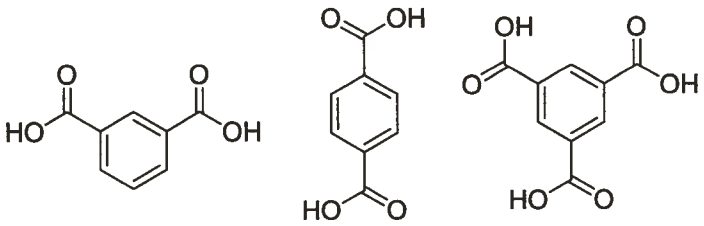

15 **16** **17**

Par exemple, la diffusion de triéthylamine dans une solution du composé **16** et de nitrate de zinc(II) dans un mélange DMF/chlorobenzène produit des cristaux où la coordination de **16** au zinc résulte en un réseau cubique où 55-61 % du volume est accessible à des molécules invitées (Figure 1.6).[31] Les molécules de solvant présentes dans les canaux peuvent être enlevées et remplacées par des molécules de gaz, par exemple.

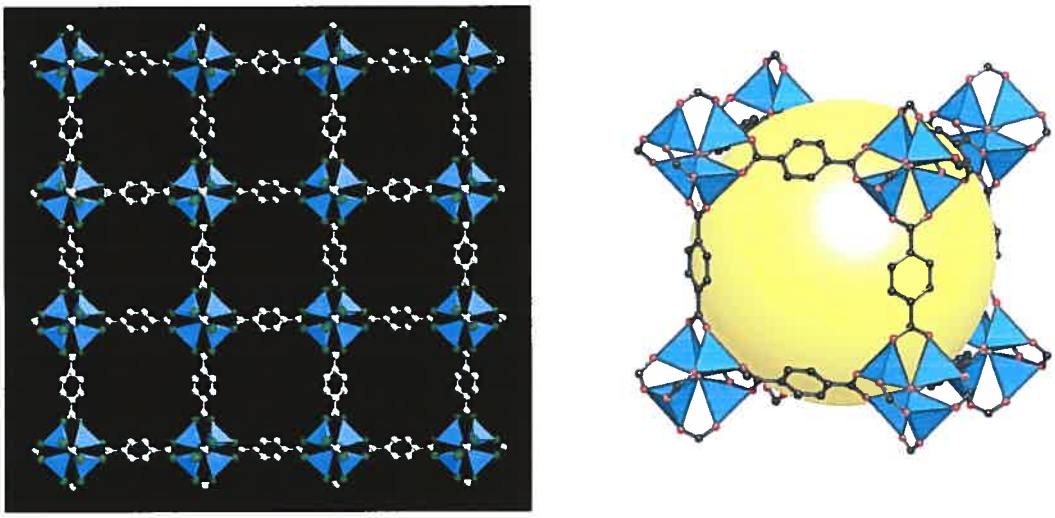

a **b**

Figure 1.6. a) Représentation schématique de la structure cristallographique du complexe de zinc du composé **16** cristallisé dans DMF/chlorobenzène. b) Représentation schématique du volume accessible aux molécules invitées, représenté par une sphère jaune. Les molécules de solvant ont été omises. Les atomes de zinc et leurs ligands sont représentés par des tétraèdres bleus.[31]

1.1.7 La tectonique moléculaire

La tectonique moléculaire est une branche du génie cristallin qui consiste en la conception de petites molécules appelées *tectons* (du mot grec pour constructeur)

portant des groupes fonctionnels capables de s'associer d'une façon forte, directionnelle et réversible à l'aide d'interactions non-covalentes.[32] La cristallisation des tectons est donc dirigée par l'auto-assemblage des groupes de reconnaissance plutôt que par l'empilement compact, comme démontré à la Figure 1.7.

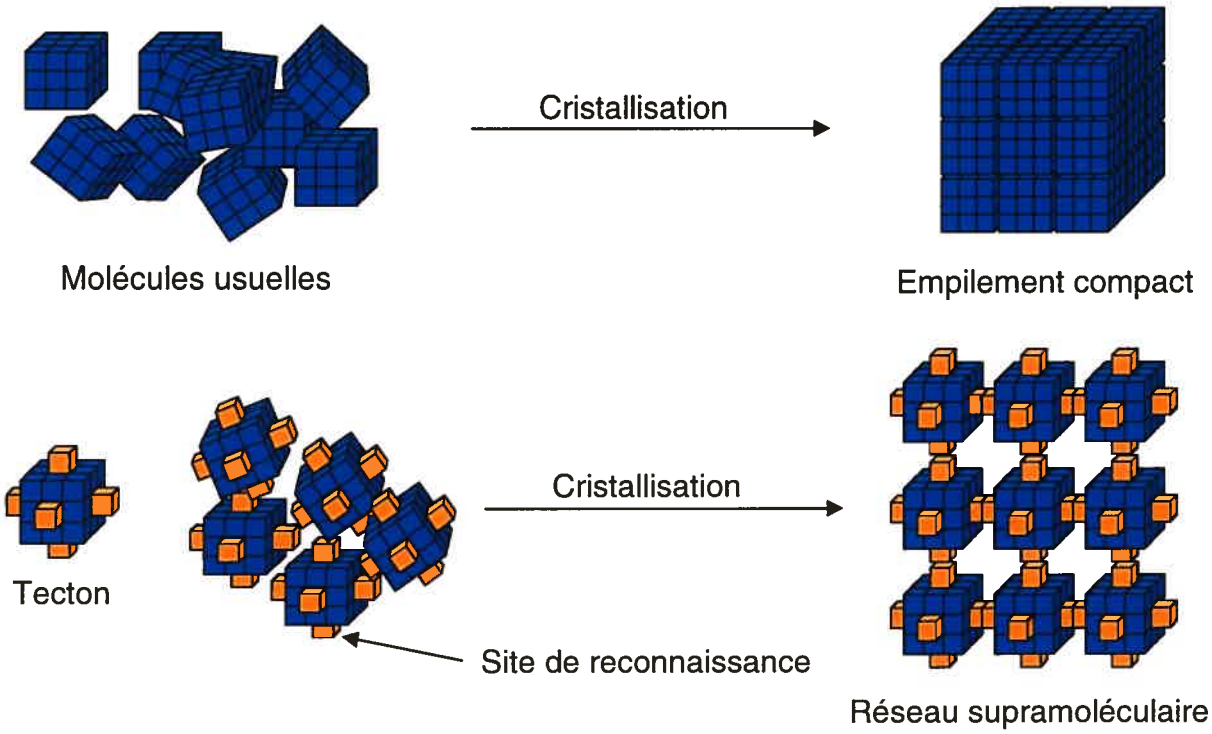

Figure 1.7 Représentation schématique de la cristallisation de molécules usuelles pour former des cristaux où les molécules sont empilées de façon compacte (ci-haut), et cristallisation d'un tecton pour former un réseau supramoléculaire où l'auto-assemblage dirige la structure cristalline (ci-dessous).

Dans les cristaux des tectons, l'assemblage dû aux groupes de reconnaissance a souvent pour conséquence la présence de canaux pouvant contenir de vastes quantités de molécules invitées (du solvant, par exemple). Le tecton **18**, par exemple, cristallise à partir d'un mélange DMSO/dioxane pour donner une structure dans laquelle 75% du volume du cristal est accessible aux molécules de solvant (Figure 1.8).[33]

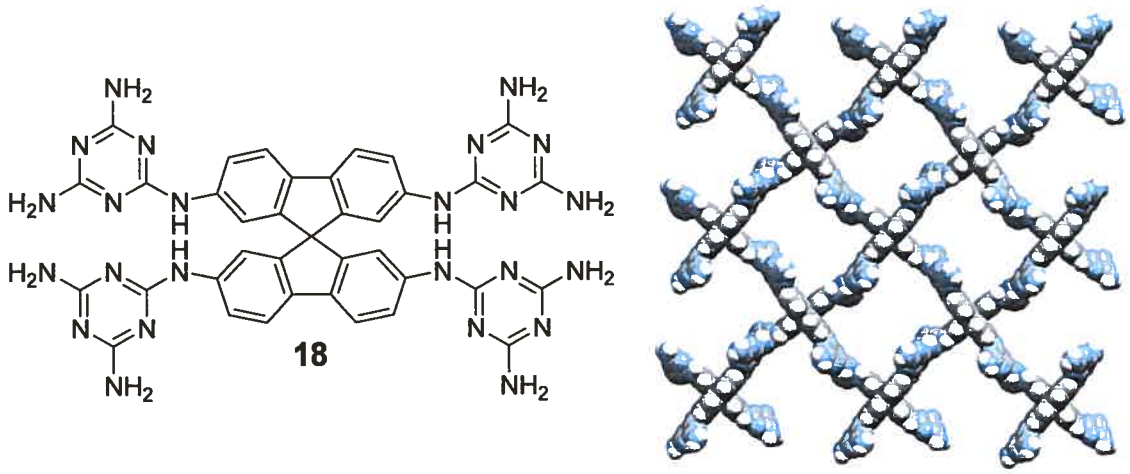

Figure 1.8 Vue selon l'axe *c* de la structure cristallographique du composé **18** cristallisé dans DMSO/dioxane, révélant la présence de canaux d'environ 13 X 13 Å. Les molécules de solvant ont été omises.[33]

1.2 Objectifs de cette thèse

Depuis les quinze dernières années, l'objectif de la tectonique moléculaire a reposé sur la formation de cristaux poreux. Par contre, les principes de la tectonique moléculaire peuvent être étendus à la compréhension et au contrôle de la formation d'autres états solides d'un plus faible degré d'ordre. Le but ultime de cette stratégie est d'arriver à comprendre et à contrôler l'association moléculaire et les propriétés mécaniques des matériaux à partir de leur structure moléculaire. Le savoir ainsi accumulé peut être utilisé pour générer de nouveaux matériaux possédant des propriétés jusqu'alors inconnues ou améliorées par rapport à celles des composés connus.

Par exemple, les gélateurs de bas poids moléculaire et les matériaux moléculaires amorphes (ou verres moléculaires) sont deux classes de composés encore largement méconnues malgré plus de vingt ans d'études approfondies. Dans les deux cas, les connaissances acquises sont d'origine empirique plutôt que d'une véritable compréhension des éléments responsables de leur formation au niveau moléculaire.

Nous avons donc tenté d'utiliser le concept de la tectonique moléculaire ainsi que les connaissances acquises au cours des 15 dernières années afin de générer des composés pouvant s'auto-assembler à l'aide d'interactions non-covalentes mais où cette association résulte en la formation de gels ou de solides amorphes plutôt que de cristaux.

Nous avons également tenté d'élucider les structures obtenues au niveau moléculaire de façon à approfondir nos connaissances sur ces systèmes.

Notre point de départ dans les deux cas consiste en l'exploration des arylbiguanides comme précurseurs synthétiques. Les biguanides sont une classe de composés connus depuis plus d'un siècle mais peu utilisés et encore méconnus de nos jours. Leur utilisation a d'abord demandé le développement de méthodes de synthèse et de caractérisation simples et efficaces. Nous avons également étudié brièvement l'association de certains biguanides et de leurs sels à l'état cristallin afin d'évaluer leur potentiel comme groupes de reconnaissance en tectonique moléculaire.

Cette thèse est divisée comme suit : le chapitre 2 traite de la synthèse et de la caractérisation des aryl- et diarylbiguanides qui sont utilisés comme précurseurs synthétiques pour la majorité de la recherche effectuée. Dans le chapitre 3 sont décrites les études cristallographiques de dérivés de bis(biguanides) simples afin d'évaluer leur utilité en tectonique moléculaire. La synthèse de 4,6-diarylamino-1,3,5-triazine-2-carboxylates de sodium et la caractérisation des gels formés par ces composés sont détaillées au chapitre 4, tandis que le chapitre 5 aborde la synthèse et la caractérisation de verres moléculaires basés sur des dérivés de la 4,6-bis[(3,5-diméthylphényl)amino]-1,3,5-triazine. Finalement, le chapitre 6 conclut la recherche effectuée et apporte des perspectives pour des travaux futurs.

Références

1. a) van der Waals, J.D. *Die Continuidt des gasförmigen und flüssigen Zustandes*, 1900. b) chemed.chem.purdue.edu/genchem/history/vanderwaals.html c) www.chemguide.co.uk/atoms/bonding/vdw.html
2. Latimer, W.M.; Rodebush, W.H. *J. Am. Chem. Soc.* **1920**, *42*, 1419.
3. a) Watson, J.D.; Crick, F.H.C. *Nature*, **1953**, *171*, 737. b) Watson, J.D. *The Double Helix*, Signet, 1969.
4. Pedersen, C.J. *J. Am. Chem. Soc.* **1967**, *89*, 2495.
5. Cram, D.J.; Kaneda, T.; Helgeson, R.C.; Lein, G.M. *J. Am. Chem. Soc.* **1979**, *101*, 6752.

6. Graf, E.; Lehn, J.-M. *J. Am. Chem. Soc.* **1975**, *97*, 5022.
7. a) Frängsmyr, T.; Malmström, B.G. *Nobel Lectures, Chemistry 1981-1990*, World Scientific Publishing Co., 1992. b) nobelprize.org/chemistry/laureates/1987
8. www.shaolin.com
9. a) Voet, D.; Voet, J.G. *Biochemistry*, 3rd edition, Wiley, 2004. b) Alberts, B.; Johnson, A.; Lewis, J.; Raff, M.; Roberts, K.; Walter, P. *Molecular Biology of the Cell*, 4th edition, Garland Publishing, 2002.
10. Conn, M.M.; Rebek, J., Jr. *Chem. Rev.* **1997**, *97*, 1647.
11. a) Martin, T.; Obst, U.; Rebek, J., Jr. *Science* **1998**, *281*, 1842. b) Nuckolls, C.; Hof, F.; Martin, T.; Rebek, J., Jr. *J. Am. Chem. Soc.* **1999**, *121*, 10281.
12. McQuade, D.T.; Pullen, A.E.; Swager, T.M. *Chem. Rev.* **2000**, *100*, 2537.
13. Kao, T.-L.; Wang, C.-C.; Pan, Y.-T.; Shiao, Y.-J.; Yen, J.-Y.; Shu, C.-M.; Lee, G.-H.; Peng, S.-M.; Chung, W.-S. *J. Org. Chem.* **2005**, *70*, 2912.
14. Aldakov, D.; Palacios, M.A.; Anzenbacher, P., Jr. *Chem. Mater.* **2005**, *17*, 5238.
15. Takamura, M.; Hamashima, Y.; Usuda, H.; Kanai, M.; Shibasaki, M. *Angew. Chem. Int. Ed.* **2000**, *39*, 1650.
16. a) Takamura, M.; Funabashi, K.; Kanai, M.; Shibasaki, M. *J. Am. Chem. Soc.* **2000**, *122*, 6327. b) Takamura, M.; Funabashi, K.; Kanai, M.; Shibasaki, M. *J. Am. Chem. Soc.* **2001**, *123*, 6801. c) Funabashi, K.; Ratni, H.; Kanai, M.; Shibasaki, M. *J. Am. Chem. Soc.* **2001**, *123*, 10784.
17. a) Badia, A.; Lennox, R.B.; Reven, L. *Acc. Chem. Res.* **2000**, *33*, 475. b) Love, J.C.; Estroff, L.A.; Kriebel, J.K.; Nuzzo, R.G.; Whitesides, G.M. *Chem. Rev.* **2005**, *105*, 1103.
18. Bain, C.D.; Troughton, E.B.; Tao, Y.-T.; Evall, J.; Whitesides, G.M.; Nuzzo, R.G. *J. Am. Chem. Soc.* **1989**, *111*, 321.
19. Tulevski, G.S.; Miao, Q.; Fukuto, M.; Abram, R.; Ocko, B.; Pindak, R.; Steigerwald, M.L.; Kagan, C.R.; Nuckolls, C. *J. Am. Chem. Soc.* **2004**, *126*, 15048.
20. Facchetti, A.; Annoni, E.; Beverina, L.; Morone, M.; Zhu, P.; Marks, T.J.; Pagani, G.A. *Nature Mater.* **2004**, *3*, 910.

21. Brust, M.; Walker, M.; Bethell, D.; Schiffrin, D.J.; Whyman, R. *J. Chem. Soc., Chem. Commun.* **1994**, 801.

22. a) Templeton, A.C.; Hostetler, M.J.; Warmoth, E.K.; Chen, S.W.; Hartshorn, C.M.; Krishnamurthy, V.M.; Forbes, M.D.E.; Murray, R.W. *J. Am. Chem. Soc.* **1998**, *120*, 4845. b) Shenhar, R.; Rotello, V.M. *Acc. Chem. Res.* **2003**, *36*, 549.

23. Binnig, G.; Rohrer, H.; Gerber, C.; Weibel, E. *Phys. Rev. Lett.* **1982**, *49*, 57.

24. Kim, K.; Plass, K.E.; Matzger, A.J. *J. Am. Chem. Soc.* **2005**, *127*, 4879.

25. Makarevic, J.; Jokic, M.; Peric, B.; Tomisic, V.; Kojic-Prodic, B.; Zinic, M. *Chem. Eur. J.* **2001**, *7*, 3328.

26. Menger, F.M.; Caran, K.L. *J. Am. Chem. Soc.* **2000**, *122*, 11679.

27. a) Kazuo, M.; Hironobu, K.; Koichiso, Y.; Junichi, N. *Jpn. Kokai Tokkyo Koho* **1979**, *79*, 588. b) Seto, C.T.; Whitesides, G.M. *J. Am. Chem. Soc.* **1990**, *112*, 6409.

28. Zerkowski, J.A.; Seto, C.T.; Wierda, D.A.; Whitesides, G.M. *J. Am. Chem. Soc.* **1990**, *112*, 9025.

29. Zerkowski, J.A.; Seto, C.T.; Whitesides, G.M. *J. Am. Chem. Soc.* **1992**, *114*, 5473.

30. a) Li, H.; Davis, C.E.; Groy, T.L.; Kelley, D.G.; Yaghi, O.M. *J. Am. Chem. Soc.* **1998**, *120*, 2186. b) Yaghi, O.M.; Li, H.; Davis, C.; Richardson, D.; Groy, T.L. *Acc. Chem. Res.* **1998**, *31*, 474. c) Chae, H.K.; Siberio-Pérez, D.Y.; Kim, J.; Go, Y.; Eddaoudi, M.; Matzger, A.J.; O'Keeffe, M.; Yaghi, O.M. *Nature* **2004**, *427*, 523.

31. Li, H.; Eddaoudi, M.; O'Keeffe, M.; Yaghi, O.M. *Nature* **1999**, *402*, 276.

32. Pour des articles de revue voir : Wuest, J.D. *Chem. Commun.* **2005**, 5830.

33. Fournier, J.-H.; Maris, T.; Wuest, J.D. *J. Org. Chem.* **2004**, *69*, 1762.

Chapitre 2 :

Synthèse et caractérisation des arylbiguanides et des diaryl-biguanides

2.1 Les biguanides

Le biguanide (**19**) a été synthétisé en 1892 par Bamberger et Dieckmann[1] en chauffant du dicyandiamide avec du chlorure d'ammonium. Depuis ce temps, quelques méthodes ont été développées afin de synthétiser des biguanides substitués.[2] Par contre, les biguanides représentent une classe de composés méconnus, et les méthodes de synthèse et de caractérisation demeurent encore archaïques.

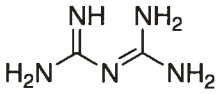

19

2.2 L'utilité des biguanides

Les biguanides n'en demeurent pas moins une classe de composés d'une grande utilité. Ils peuvent servir de précurseurs synthétiques pour divers hétérocycles tels les triazines,[3] les imidazoles,[4] ou les pyrimidines,[5] en plus d'être à la base de plusieurs agents thérapeutiques.[6] En chimie inorganique, les biguanides s'avèrent utiles comme ligands bidentates possédant une affinité pour plusieurs métaux de transition.[7] Malgré le fait que les biguanides n'ont pas fait l'objet de beaucoup d'études en chimie supramoléculaire, leur grand nombre de sites pouvant donner ou accepter des ponts hydrogène en font des candidats potentiels.

2.3 Le temple de la renommée des biguanides

Environ 50 biguanides sont disponibles commercialement, mais quatre composés se sont démarqués par l'importance de leur usage et de leur production commerciale importante.

2.3.1 Metformin

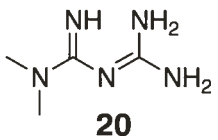

20

Le 1,1-diméthylbiguanide, ou metformin (**20**), a initialement été synthétisé par Slotta et Tschesche en 1929,[8] mais il a seulement été approuvé pour l'usage thérapeutique en 1994 sous le nom de Glucophage.[9] Le metformin est un agent hypoglycémique utilisé pour traiter le diabète de type 2. Son mécanisme d'action implique l'augmentation de l'absorption de l'insuline par le foie, les muscles et les tissus adipeux. Contrairement aux autres médicaments utilisés pour traiter le diabète de type 2, le metformin n'augmente pas la production d'insuline et ne cause pas d'hypoglycémie. Par contre, de rares cas d'acidose lactique ont été observés.

2.3.2 Chlorhexidine

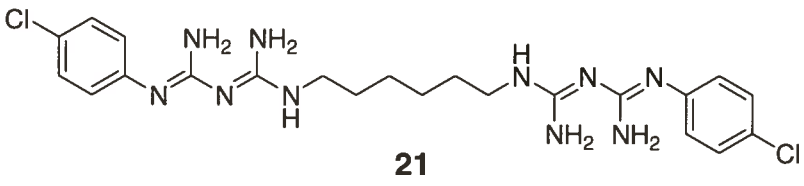

21

La chlorhexidine (**21**) est un bis(biguanide) qui possède des propriétés antibactériennes et antiseptiques.[10] La chlorhexidine est le désinfectant le plus couramment utilisé dans les hôpitaux, en plus d'être utilisé en médecine vétérinaire et dans des rince-bouche contre la gingivite.[11] La chlorhexidine est d'une grande efficacité à la fois contre les bactéries Gram-positives et Gram-négatives en causant la rupture de leur paroi cellulaire. De plus, elle est faiblement active contre les moisissures, les spores et les virus. Le plus grand avantage de la chlorhexidine est sa durée d'action qui peut atteindre une semaine, ce qui prévient la croissance des bactéries après l'application.

2.3.3 PHMB (poly(hexaméthylènebiguanide))

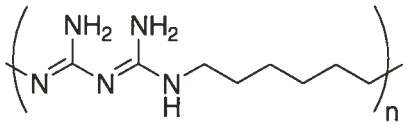

22

Le poly(hexaméthylènebiguanide) (PHMB, **22**), utilisé sous la forme de son hydrochlorure, est un biguanide polymérique qui possède aussi une importante activité antimicrobienne.[12] Le PHMB fut initialement utilisé sous le nom commercial de Vantocil comme désinfectant pour les verres de contact ou en milieu hospitalier, ainsi que comme préservatif dans les industries alimentaire et cosmétique.[13] Vers la fin des années 1970, le PHMB a également été commercialisé sous le nom de Baquacil[14] en tant que désinfectant pour piscines. Le PHMB constitue une alternative pour remplacer le chlore, car il se dégrade lentement et est moins irritant et moins corrosif.[15]

2.3.4 Paludrine

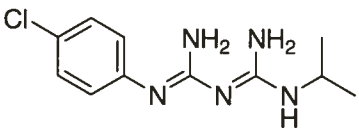

23

Le 1-(4-chlorophényl)-5-isopropylbiguanide (**23**), ou paludrine,[2a] est un agent antimalarial qui prévient la reproduction des parasites *Plasmodium* dans les globules rouges.[16] Par contre, étant donné que son activité est faible, la paludrine est souvent administrée avec la chloroquine (**24**).[17] Bien que la paludrine soit utilisée en Europe et au Canada par les voyageurs, son usage n'est pas encore permis aux États-Unis.

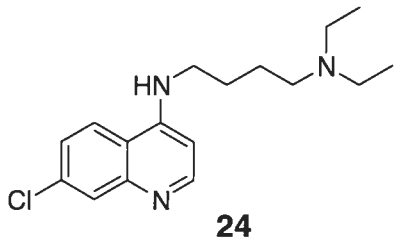

24

2.4 Objectifs

Bien que les biguanides soient d'une grande utilité, nous avons heurté quelques obstacles en tentant de les employer dans le cadre de notre recherche. Tout d'abord, les méthodes connues pour leur synthèse sont peu documentées et plusieurs voies synthétiques se sont avérées laborieuses. Deuxièmement, les seules méthodes rapportées dans la littérature pour leur caractérisation sont leur point de fusion et l'analyse élémentaire. Nous avons d'abord souhaité combler ces lacunes en établissant des méthodes de synthèse précises et simples d'usage ainsi que des procédures de caractérisation spectroscopiques de routine.

2.5 Article 1 :

A Practical Guide to Arylbiguanides – Synthesis and Structural Characterization.

Olivier Lebel, Thierry Maris, Hugues Duval, James D. Wuest. *Canadian Journal of Chemistry* **2005**, *83*, 615-625.

Submitted to *Can. J. Chem.*
Revised Version of February 21, 2005

A Practical Guide to Arylbiguanides: Synthesis and Structural Characterization[1]

Olivier LeBel, Thierry Maris, Hugues Duval, and James D. Wuest

Dedicated with respect and affection to Professor Howard Alper on the occasion of his 65th birthday, for his friendship, wise counsel, pioneering research, and tireless service to Canadian chemistry.

Olivier Lebel,[2] Thierry Maris, Hugues Duval, and James D. Wuest.[3] Département de Chimie, Université de Montréal, Montréal, Québec, H3C 3J7, Canada.

[1] This article is part of a Special Issue dedicated to Professor Howard Alper.

[2] Fellow of the Ministère de l'Éducation du Québec, 2002-2004.

[3] Corresponding author [redacted]

Abstract: Monohydrochloride salts of diverse 1-arylbiguanides and 1,5-diarylbiguanides were synthesized by the reaction of anilinium chlorides with dicyandiamide or sodium dicyanamide, and the biguanidinium chlorides were converted into the corresponding biguanides by deprotonation with methanolic $NaOCH_3$. The resulting biguanides and their salts were fully characterized by spectroscopic methods, and the structures of representative compounds were determined by X-ray crystallography.

Key words: biguanide, biguanidinium, synthesis, structure, hydrogen bonds, non-covalent interactions, supramolecular chemistry.

Introduction

The general class of compounds called biguanides has been known for more than 100 years (1-3). An early method for preparing salts of biguanide itself (**25**) was reported in 1892 by Bamberger and Dieckmann (4), who heated dicyandiamide (**26**)

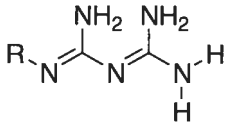

25 (R = H)
27 (R = Ph)
37 (R = CH_2CH_2Ph)

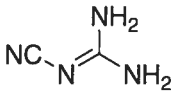

26

with ammonium chloride and then isolated the product by forming an intermediate biguanide-copper (II) complex.[4] Since then, biguanides have proven to be broadly useful. In medicine, they have important applications as antiseptics (5), antimalarials (6-7), serotoninergic antagonists (8), antitumoral agents (9), and hypoglycemic agents (10-11). In addition, the ability of biguanides to chelate metals has been widely used in coordination chemistry since the initial observations of Bamberger and Dieckmann (1, 3). Moreover, biguanides are strong bases (12-13), and they are also valuable precursors for synthesizing a wide range of heterocyclic compounds (2, 14). Of special interest among the heterocyclic derivatives of biguanides are aminotriazines, which are themselves an extremely useful family of compounds. For example, they are widely used in supramolecular chemistry because they incorporate a characteristic pattern of multiple sites that can donate or accept hydrogen bonds, thereby directing molecular recognition and association. In particular, recent applications of aminotriazines in crystal engineering have highlighted their ability to direct crystallization by self-associating according to reliable hydrogen-bonding motifs (15-16).

[4] For the sake of simplicity, biguanides, dicyandiamide, and related compounds are normally represented in this paper as single tautomers.

Our motivation for studying substituted biguanides stems from their potential as precursors of novel aminotriazines and from the possibility that the multiple sites of hydrogen bonding in the biguanides themselves may make them valuable components in supramolecular assembly. Unfortunately, despite the demonstrated utility of biguanides and the likelihood of new applications, few detailed syntheses and structural characterizations have been previously reported, and information about 1-aryl- and 1,5-diarylbiguanides remains particularly sparse (17-38). To supply missing data and give other researchers a practical guide to the field, we report here the synthesis and full characterization of a series of arylbiguanides, along with crystal structures of representative compounds.

Results and discussion

Synthesis of 1-arylbiguanides

To synthesize monosubstituted 1-arylbiguanides, we used a modification of a procedure reported in a 1946 patent by Curd and Rose (23), who heated anilinium salts with dicyandiamide in water (Scheme 2.1). The hydrochloride salts of the arylbiguanides generally crystallize from the reaction mixture in good yield and in

Scheme 2.1

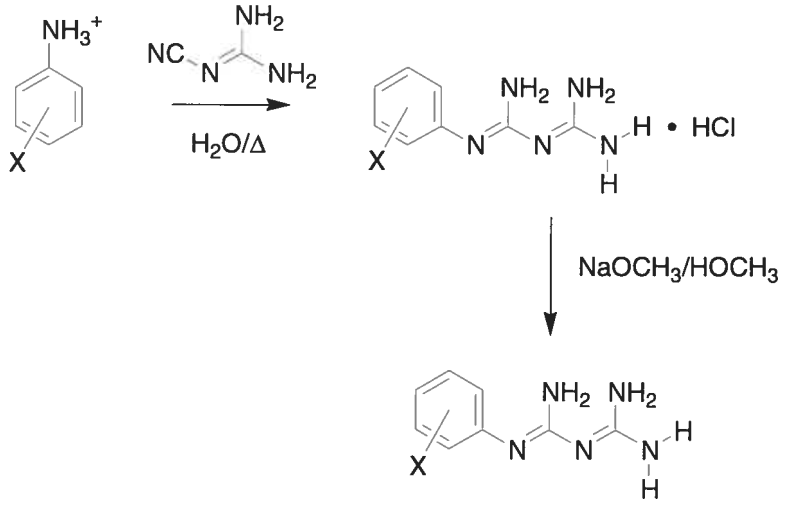

high purity, and they can be deprotonated with methanolic sodium methoxide in nearly quantitative yield. Detailed procedures for making 1-phenylbiguanide (**27**) and its hydrochloride salt by these methods are provided in the experimental section, and other aryl-substituted derivatives can be made in the same way. When 1,4- or 1,3-phenylenediamine dihydrochloride reacted under these conditions with two equivalents of dicyandiamide, the corresponding bis(biguanide) **28** or **29** was obtained after deprotonation (39), whereas 1,2-phenylenediamine dihydrochloride gave 2-guanidinobenzimidazole (40).

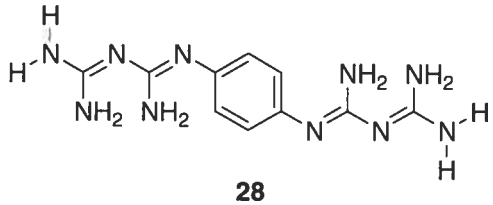

28

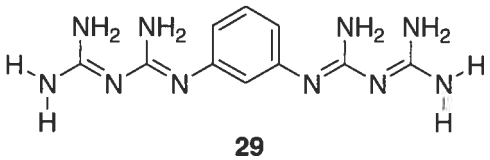

29

Synthesis of 1,5-diarylbiguanides

1,5-Diarylbiguanides **30a-j** could be synthesized in good yield by a one-pot procedure based on a method reported by Neelakantan (22), in which two equivalents of an anilinium chloride are added to sodium dicyanamide in boiling water (Scheme 2.2). In the case of anilines with low solubility in water, the reaction can be performed

Scheme 2.2

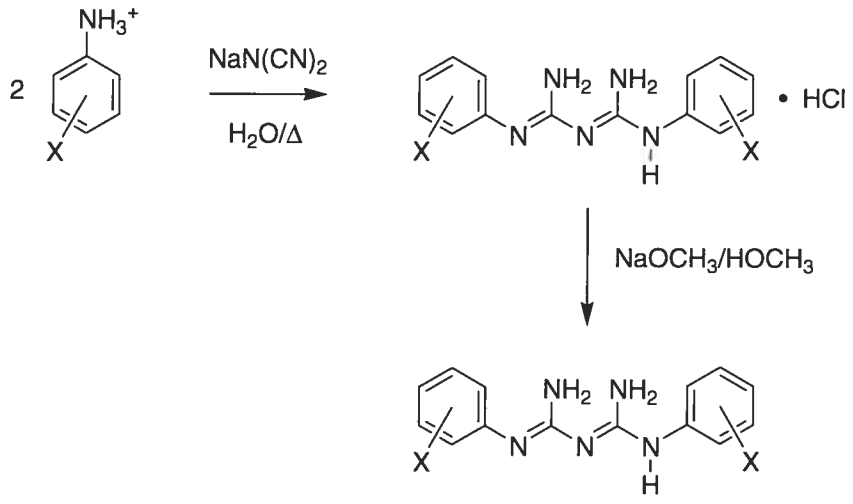

30a (X = X' = H)
30b (X = X' = 2-CH_3)
30c (X = X' = 3-CH_3)
30d (X = X' = 4-CH_3)
30e (X = X' = 4-OCH_3)
30f (X = X' = 4-CN)
30g (X = X' = 2-Br)
30h (X = X' = 4-Br)
30i (X = X' = 3,5-CH_3)
30j (X = X' = 2,4,6-CH_3)

in ethanol or in water/ethanol mixtures. Of all anilines tested, only 4-nitroaniline failed to give the desired product, presumably because its basicity and nucleophilicity are too low. A monosubstituted aryldicyandiamide **31** typically precipitated at an initial stage of

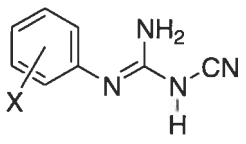

31

each reaction, but the intermediate was eventually converted into the desired diarylbiguanide as its hydrochloride salt. It is possible to isolate the intermediate

monoaryldicyandiamides and use them to synthesize unsymmetric 1,5-diarylbiguanides. For example, phenyldicyandiamide (**31**, X = H) was obtained in this way in 87% yield.

After the reaction of two equivalents of an anilinium chloride with sodium dicyanamide, the crude product typically consisted of the desired diarylbiguanide hydrochloride along with small amounts of the intermediate monoaryldicyandiamide. This impurity could be removed by dissolving the product in a small volume of DMF and then precipitating the biguanide hydrochloride by the addition of toluene. The resulting product normally required no further purification, but it could be recrystallized from hot water. Pure samples of the corresponding free base could be obtained in nearly quantitative yield by treating the salt with methanolic sodium hydroxide.

Spectroscopic characterization of arylbiguanides

Arylbiguanides typically have poor solubility in organic solvents and water, and DMSO-d_6 proved to be best suited for obtaining NMR spectra of most of the compounds synthesized. The -NH and -NH_2 protons in these compounds generally show broad, poorly resolved peaks in the range δ 5-9. However, the corresponding monohydrochloride salts produce spectra in which the -NH and -NH_2 signals are better resolved and easier to identify. In the salts, the aryl -NH protons tend to give rise to a singlet near δ 9-10, and -NH_2 groups yield signals in the range δ 7-8.

To assess the possible importance of slow interconversion of tautomers or slow rotations around C-N bonds, ^{1}H NMR spectra of 1,5-diphenylbiguanide (**30a**) and its hydrochloride salt were recorded in DMSO-d_6 at temperatures ranging from 298 to 378 K (see Supplementary Material).[5] The spectra of both compounds are indeed temperature-dependent and become better resolved at higher temperatures, possibly

[5] Supplementary data may be purchased from the Directory of Unpublished Data, Document Delivery, CISTI, National Research Council Canada, Ottawa, ON K1A 0S2, Canada (http://www/nrc.ca/cisti/irm/unpub_e.shtml for information on ordering electronically).

because rotations or tautomeric interconversions are accelerated. Partial decomposition was noted in spectra of the free base recorded at higher temperatures.

In general, the hydrochloride salts of both 1-arylbiguanides and 1,5-diarylbiguanides gave well-resolved ^{13}C NMR spectra in DMSO-d_6 at 298 K. The biguanide carbons have characteristic chemical shifts in the range δ 155-165. In contrast, the ^{13}C NMR spectra of the corresponding free bases are less easy to analyze, and broad signals are often observed for the biguanide carbons.

FT-IR spectra of arylbiguanides and their monohydrochloride salts in KBr both show multiple strong broad bands in the range 2900-3300 cm^{-1}. In addition, the free bases exhibit a pair of sharper but weaker bands near 3440 and 3350 cm^{-1}, presumably due to $-NH_2$ groups. In both the free bases and salts, strong C=N stretching bands normally appear near 1640-1610 cm^{-1}.

FAB and MAB mass spectra proved to be useful for characterizing arylbiguanides, and $[M + H]^+$ is typically the peak of highest intensity. Diagnostic fragments usually include $[M + H - NH_3]^+$, $[M + H - ArNH_2]^+$, $[M + H - ArNHCN]^+$, and $[M + H - ArN{=}C(NH_2)_2]^+$.

Crystal structures of 1,5-diphenylbiguanide (30a) and its monohydrochloride salt

Few structures of simple biguanidinium salts or biguanides have been reported (25-38), and in none of these cases have aryl groups been present at positions 1 and 5. As a result, we elected to determine the structures of 1,5-diphenylbiguanide (**30a**) and its monohydrochloride salt. The salt crystallized from hot water in the monoclinic space group $P2_1/n$ (Table 2.1).[5,6] The structure was determined by X-ray diffraction, and views

[6] CCDC 258751-258752 contain the supplementary crystallographic data for this paper. These data can be obtained free of charge via www.ccdc.cam.ac.uk/conts/retrieving.html (or from the Cambridge Crystallographic Data Centre, 12 Union Road, Cambridge CB2 1EZ, U. K. (Fax: +44 1223 336033 or e-mail: deposit@ccdc.cam.ac.uk).

of a single biguanidinium cation are shown in Fig. 2.1. The narrow range of guanidinium C-N bond lengths (1.343-1.394 Å) provides evidence of extensive delocalization, although the structure is not fully symmetric. It is noteworthy that the cation can be represented by localized structure **32** and its resonance hybrids,

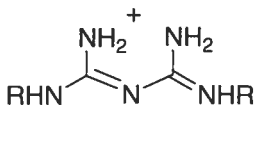

32

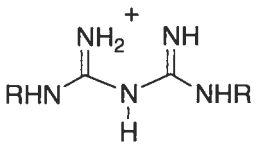

33

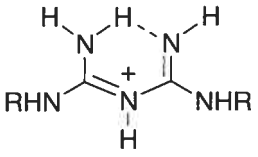

34

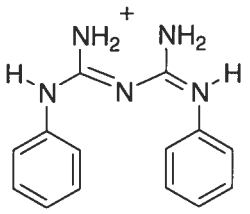

35

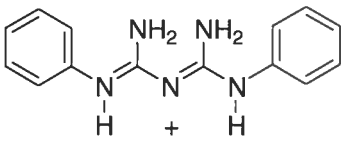

36

whereas alternatives in which the central nitrogen atom is protonated (**33**) or an intramolecular hydrogen bond is formed (**34**) are not favored in the solid state. Similar observations have been made in all previous structural studies of biguanidinium cations (25, 26, 28-34, 36-38), so protonation of biguanides to give structure **32** appears to be a fundamental preference, both in the solid state and in solution (2).

The two guanidinium subunits that can be considered to make up the biguanidinium cation lie in two distinct planes that form an angle of 22.8(4)°. The non-planarity of the biguanidinium core presumably reduces allylic strain while permitting a significant degree of conjugation. Again, similar observations have been made in all previous structural studies of biguanidinium salts, so non-planarity of the biguanidinium core appears to be a universal characteristic. The two phenyl rings are tilted from the guanidinium planes by angles of 52.4(1)° and 39.5(1)°, and together they form an angle of 88.8(1)°, thereby permitting an intramolecular C-H···π interaction in which the shortest C-C distance is 3.773 Å (Fig. 2.1). This may explain why the 1,5-

diphenylbiguanidinium cation adopts the compact conformation represented by structure **35**, rather than extended conformation **36**.

The crystal structure of diphenylbiguanidinium salt **30a** • HCl is closed-packed (Fig. 2.2) and can be considered to consist of bilayers, with hydrophilic biguanidium cations and chloride anions occupying the core and hydrophobic phenyl groups forming the exterior.[7] The bilayers then stack along the *c* axis. Within the core of each bilayer, the principal interactions are hydrogen bonds and ionic attractions between biguanidinium and chloride. The biguanidinium ions do not interact directly with each other by forming hydrogen bonds. The absence of inter-cationic hydrogen bonds has been noted in most other biguanidinium salts (28, 29, 31, 34, 36-38), but they are nevertheless present in certain cases (25, 26, 32). Each chloride ion accepts a total of six hydrogen bonds from four neighboring biguanidinium cations (Fig. 2.3), two of which chelate chloride by donating two hydrogen bonds and two of which each contribute a single hydrogen bond. In turn, each biguanidinium cation forms hydrogen bonds with a total of four neighboring chloride ions, of which two are chelated and the others each accept a single hydrogen bond. Similar interactions between biguanidinium ions and halide have been observed previously (25, 28, 31, 34, 36-38). In addition, the phenyl groups of each biguanidinium cation engage in multiple aromatic contacts or interactions with phenyl groups provided by neighboring cations (Fig. 2.4). In total, each biguanidinium cation has four face-to-face and six edge-to-face aromatic contacts with six neighbors.

The corresponding free base, 1,5-diphenylbiguanide (**30a**), crystallized from hot ethanol in the monoclinic space group Pc, and one of two symmetry-independent molecules in the unit cell is shown in Fig. 2.5. The other molecule is closely similar and is not illustrated. Unlike the twisted biguanidinium cation, the biguanide unit has a roughly planar geometry, maintained by an intramolecular N-H···N hydrogen bond

[7] A similar bilayer organization has been noted in the structure of the monohydrochloride salt of phenformin (**37**) (32).

(2.06(1) Å). Similar features appear in all previous structural studies of biguanides (27, 33, 34), so a nearly planar geometry and an intramolecular hydrogen bond appear to be fundamental preferences. The C-N bond lengths within the biguanide unit range from 1.294(8) to 1.406(8) Å, suggesting significant delocalization of C-N single and double bonds, but slightly less than in the corresponding biguanidinium salt. Unlike the salt, free base **30a** favors a conformation in which no intramolecular aromatic interactions are present.

Like the corresponding biguanidinium salt, biguanide **30a** forms a closed-packed layered structure consisting of alternating hydrophobic and hydrophilic domains (Fig. 2.6). In the free base **30a**, however, the neutral biguanide units interact directly by hydrogen bonding. Each molecule donates two hydrogen bonds to one neighbor and accepts two hydrogen bonds from another, thereby forming a corrugated ribbon (Fig. 2.7). Similar intermolecular hydrogen bonding has been previously observed in the structures of biguanide (**25**) and 1-phenylbiguanide (**27**) (27, 33, 34). Curiously, the donor sites that form the shortest intermolecular hydrogen bonds are the $-NH_2$ groups already involved as donors in intramolecular hydrogen bonding. As expected, one of the acceptor sites is the unprotonated central nitrogen atom in each biguanide unit. The other acceptor site is the nitrogen atom of the $-NH_2$ group not involved in intramolecular hydrogen bonding, which forms the longest C-N bond in the biguanide unit (1.406 Å).

Individual corrugated ribbons formed by intermolecular hydrogen bonding form face-to-face aromatic interactions and stack along the *ab* diagonal to create layers (Fig. 2.8a). Stacking of the layers along the *c* axis then permits the formation of multiple C-H$\cdots\pi$ interactions (Fig. 2.8b), with shortest C-C distances ranging from 3.600(x) to 3.764(y) Å.

Conclusions

Biguanides are an intrinsically interesting class of compounds with many known or potential applications. Despite these attractive properties, biguanides remain poorly

studied. Few detailed procedures for their synthesis have been published, and full spectroscopic characterizations and structural studies are rare. As a practical guide to assist other researchers interested in using biguanides, we have summarized our experience with 1-arylbiguanides, 1,5-diarylbiguanides, and their monohydrochloride salts. Various substituted derivatives can be synthesized in good yields and high purity by simple methods based on published procedures, and these compounds can be fully characterized by standard spectroscopic methods. Structural analyses of representative compounds by X-ray diffraction confirm that arylbiguanides and their salts can form networks held together by characteristic patterns of hydrogen bonds. As a result, arylbiguanides and their salts show promise as components in supramolecular construction.

Experimental

Anilines were purified by recrystallization or distillation prior to use. All other reagents were commercial products that were used without further purification. All NMR spectra were recorded at 298 K unless noted otherwise. Mass spectra are provided only for the neutral biguanides.

1-Phenylbiguanide (27) • HCl

In a 2-L round-bottom flask equipped with a magnetic stirrer, aniline (91.3 mL, 93.3 g, 1.00 mol) was added to aqueous HCl (1 L, 1 M), and the mixture was stirred until it became homogeneous. Dicyandiamide (84.1 g, 1.00 mol) was then added, and the mixture was heated at reflux with constant stirring for 12 h. The mixture was cooled to 25 °C, and the resulting colorless crystals were separated by filtration and washed with THF, hexane, and acetone to yield an initial crop of 1-phenylbiguanide (**27**) monohydrochloride (159 g). Concentration of the filtrate followed by crystallization and filtration provided an additional crop of product, giving a total yield of 181 g (0.839 mol, 84%), mp 244 to 245 °C. IR (KBr) 3301 (s), 3168 (s), 1643 (s), 1604 (s), 1557 (s),

1529 (s), 1490 (s), 1455 (m), 1373 (m), 1287 (m), 1252 (w), 1075 (m) cm^{-1}. ^1H NMR (300 MHz, DMSO-d_6) δ: 9.96 (s, 1H), 7.42 (s, 4H), 7.38 (d, ^3J = 8 Hz, 2H), 7.27 (t, ^3J = 8 Hz, 2H), 7.15 (s, 2H), 7.02 (t, ^3J = 8 Hz, 1H). ^{13}C NMR (75 MHz, DMSO-d_6) δ: 162.1, 156.1, 139.5, 129.5, 124.1, 121.6. Anal. calcd. for $C_8H_{12}ClN_5$: C 44.97, H 5.66, N 32.78; found: C 44.84, H 5.71, N 32.58.

1-Phenylbiguanide (27)

In a 1-L round-bottom flask equipped with a magnetic stirrer, 1-phenylbiguanide (**3**) monohydrochloride (214 g, 1.00 mol) was added to a mixture of methanol (200 mL) and methanolic $NaOCH_3$ (230 mL, 25% by weight, 1.0 mol). The resulting mixture was then stirred at 25 °C for 1 h. Suspended NaCl was separated by filtration, and solvent was removed from the filtrate by evaporation under reduced pressure. The gummy residue was triturated with hot ethanol (600 mL), and undissolved solids were removed by filtration. The filtrate was concentrated to 150 mL by partial evaporation under reduced pressure, and then hexane was added to precipitate the desired product, which was separated by filtration and dried under reduced pressure. This yielded pure 1-phenylbiguanide (**27**) as a colorless solid (168 g, 0.948 mol, 95%), mp 138 to 139 °C. IR (KBr) 3428 (w), 3375 (m), 3324 (m), 3153 (m), 2988 (m), 1665 (s), 1603 (s), 1555 (s), 1482 (m), 1445 (w), 1387 (m), 1363 (m), 1247 (m), 1071 (w), 756 (w), 695 (m) cm^{-1}. ^1H NMR (300 MHz, DMSO-d_6) δ: 7.20 (t, ^3J = 7.6 Hz, 2H), 6.85 (t, ^3J = 7.6 Hz, 1H), 6.80 (d, ^3J = 7.6 Hz, 2H), 6.70 (bs, 4H), 4.92 (bs, 2H). ^{13}C NMR (75 MHz, DMSO-d_6) δ: 160.2, 158.7, 151.7, 129.8, 123.7, 121.5. MAB-HR-MS (N_2) calcd. for $C_8H_{11}N_5$ *m/e*: 177.1014; found: 177.1022. Anal. calcd. for $C_6H_{11}N_5$ • 1/8 H_2O: C 53.54, H 6.32, N 39.02; found: C 53.58, H 6.30, N 39.03.

1,4-Phenylenebis(biguanide) (28) • 2 HCl

In a 250-mL round-bottom flask equipped with a magnetic stirrer, 1,4-phenylenediamine (5.24 g, 48.5 mmol) was added to aqueous HCl (96 mL, 1.0 M, 96 mmol). Dicyandiamide (8.15 g, 96.9 mol) was then added, and the mixture was heated at reflux for 3 h. Solvent was then removed by evaporation under reduced pressure, and the residual oil was triturated with hot ethanol. The resulting solid was separated by filtration, washed with hot ethanol, and crystallized from water/acetone. The crystals were separated by filtration, washed with acetone, and dried under reduced pressure to provide pure 1,4-phenylenebis(biguanide) (**28**) dihydrochloride (10.3 g, 29.5 mmol, 61%) as a colorless solid, mp 254 to 255 °C (lit. (39) mp 270 to 278 °C (dec.)). IR (KBr) 3428 (m), 3302 (s), 3186 (s), 3153 (s), 1632(s), 1547 (s), 1497 (s), 1415 (s), 1377 (m), 1295 (w), 1240 (m), 1017 (m), 826 (m), 717 (m) cm^{-1}. ^1H NMR (300 MHz, DMSO-d_6) δ: 9.74 (s, 2H), 7.26 (s, 12H), 7.04 (s, 4H). ^{13}C NMR (75 MHz, DMSO-d_6) δ: 161.8, 156.4, 135.1, 122.4. Anal. calcd. for $C_{10}H_{18}Cl_2N_{10} \cdot 1/4\ H_2O$: C 33.95, H 5.27, N 39.60; found: C 34.17, H 5.56, N 39.60.

1,3-Phenylenebis(biguanide) (29) • 2 HCl

Applied to 1,3-phenylenediamine (5.24 g, 48.5 mmol), the procedure described above provided pure 1,3-phenylenebis(biguanide) (**29**) dihydrochloride (8.59 g, 24.6 mmol, 51%) as a colorless solid, mp 220 to 221 °C. IR (KBr) 3313 (s), 3148 (s), 1654 (s), 1544 (s), 1454 (m), 1382 (m), 1278 (w), 1193 (w), 1083 (w), 1045 (w), 920 (w), 780 (w), 733 (w) cm^{-1}. ^1H NMR (300 MHz, DMSO-d_6) δ: 9.78 (s, 2H), 7.34 (s, 8H), 7.21-7.08 (m, 4H), 7.05 (s, 4H). ^{13}C NMR (75 MHz, DMSO-d_6) δ: 162.0, 156.0, 139.8, 129.6, 116.7, 114.0. Anal. calcd. for $C_{10}H_{18}Cl_2N_{10}$: C 34.39, H 5.20; found: C 34.27, H 5.59.

1,4-Phenylenebis(biguanide) (28)

In a 100-mL round-bottom flask equipped with a magnetic stirrer, the dihydrochloride of 1,4-phenylenebis(biguanide) (**28**; 1.05 g, 3.01 mmol) was added to a mixture of methanol (20 mL) and methanolic $NaOCH_3$ (1.6 mL, 25% by weight, 7.0 mmol). The resulting mixture was stirred at 25 °C for 1 h. The precipitate was separated by filtration, washed with cold water (10 mL) and ethanol (10 mL), and dried under reduced pressure to give pure 1,4-phenylenebis(biguanide) (**28**; 0.741 g, 2.68 mmol, 89%) as a colorless solid, mp 218 to 219 °C (lit. (39) mp 218 to 219 °C (dec.)). IR (KBr) 3467 (m), 3434 (m), 3357 (m), 3329 (m), 3159 (m), 1641 (s), 1614 (s), 1548 (s), 1520 (s), 1493 (s), 1399 (s), 1378 (s), 1242 (s), 1090 (w), 883 (m), 840 (w), 758 (w), 722 (w) cm^{-1}. ^1H NMR (300 MHz, D_2O) δ: 6.86 (s, 4H). ^{13}C NMR (75 MHz, D_2O) δ: 159.8, 159.4, 142.0, 124.8. FAB-MS (3-nitrobenzyl alcohol) *m/e*: 277. FAB-HR-MS (3-nitrobenzyl alcohol) calcd. for $C_{10}H_{17}N_{10}$ *m/e*: 277.1638; found: 277.1649. Anal. calcd. for $C_{10}H_{16}N_{10} \cdot H_2O$: C 40.81, H 6.16, N 47.59; found: C 40.68, H 6.19, N 47.17.

1,3-Phenylenebis(biguanide) (29)

Applied to the dihydrochloride of 1,3-diphenylenebis(biguanide) (**29**), the procedure described above gave pure 1,3-phenylenebis(biguanide) (**29**) as a colorless solid, mp °C. IR (KBr) 3479 (m), 3428 (m), 3335 (m), 3109 (m), 1610 (s), 1517 (s), 1470 (s), 1369 (s), 1284 (m), 1186 (m) cm^{-1}. ^1H NMR (300 MHz, D_2O) δ: 7.15 (t, ^3J = 7.8 Hz, 1H), 6.57 (dd, ^4J = 2.1 Hz, ^3J = 7.8 Hz, 2H), 6.46 (t, ^3J = 2.1 Hz, 1H). ^{13}C NMR (75 MHz, D_2O) δ: 159.7, 159.1, 148.3, 130.8, 118.6, 118.3. FAB-MS (3-nitrobenzyl alcohol) *m/e*: 277, 218. TOF-HR-MS calcd. for $C_{10}H_{17}N_{10}$ *m/e*: 277.1632; found: 277.1631. Anal. calcd. for $C_{10}H_{16}N_{10} \cdot 1.5\ H_2O$: C 39.60, H 6.31; found: C 39.79, H 5.97.

1,5-Diphenylbiguanide (30a) • HCl

In a 250-mL round-bottom flask equipped with a magnetic stirrer, aniline (9.31 g, 100 mmol) was added to aqueous HCl (100 mL, 1 M, 100 mmol). The mixture was stirred until it became homogeneous. Sodium dicyanamide (4.45 g, 50.0 mol) was then added, and the mixture was heated at reflux. Within 1 h, phenyldicyandiamide (**31**, X = H) had precipitated from the mixture, and heating was continued. After a total of 12 h, the mixture was cooled to 25 °C, and the precipitate was separated by filtration, washed with water, and dried under reduced pressure. The solid was dissolved in hot DMF (20 mL), and toluene (150 mL) was then added, causing the formation of a gel-like precipitate. The precipitate was separated by filtration and washed successively with toluene, hexane, and water. The product could be used without further treatment, but further purification could be achieved by crystallization from hot water, which provided the monohydrochloride of 1,5-diphenylbiguanide (**30a**; 10.1 g, 34.9 mmol, 70%) as a colorless solid, mp 230 to 232 °C (lit. (41) mp 232 °C, lit. (22) mp 220 °C). IR (KBr) 3401 (w), 3307 (m), 3181 (w), 3120 (w), 1629 (m), 1602 (m), 1577 (m), 1519 (s), 1489 (m), 1445 (m), 1382 (w), 1245 (w), 754 (w), 732 (w), 688 (w) cm^{-1}. ^{1}H NMR (300 MHz, DMSO-d_6) δ: 9.90 (s, 2H), 7.44 (s, 4H), 7.29 (m, 8H), 7.08 (m, 2H). ^{13}C NMR (75 MHz, DMSO-d_6) δ: 157.7, 138.8, 129.7, 125.0, 122.4. Anal. calcd. for $C_{14}H_{16}ClN_5$: C 58.03, H 5.57, N 24.17; found: C 57.94, H 5.67, N 24.20.

The monohydrochloride salts of 1,5-bis(2-methylphenyl)biguanide (**30b**), 1,5-bis(3-methylphenyl)biguanide (**30c**), 1,5-bis(4-methylphenyl)biguanide (**30d**), 1,5-bis(4-methoxyphenyl)biguanide (**30e**), 1,5-bis(4-cyanophenyl)biguanide (**30f**), 1,5-bis(2-bromophenyl)biguanide (**30g**), 1,5-bis(4-bromophenyl)biguanide (**30h**), 1,5-bis(3,5-dimethylphenyl)biguanide (**30i**), and 1,5-bis(2,4,6-trimethylphenyl)biguanide (**30j**) were prepared in the same way. Yields, melting points, spectroscopic data, and elemental analyses are provided in the Supplementary Material.[5]

1,5-Diphenylbiguanide (30a)

In a 200-mL round-bottom flask equipped with a magnetic stirrer, the monohydrochloride of 1,5-diphenylbiguanide (8.69 g, 30.0 mmol) was added to a mixture of methanol (60 mL) and methanolic $NaOCH_3$ (8.2 mL, 25% by weight, 36 mmol). The mixture was stirred at 25 °C for 1 h, and then water was added. The resulting precipitate was separated by filtration, washed with water, and dried under reduced pressure to give 1,5-diphenylbiguanide (**30a**; 7.30 g, 28.8 mmol, 96%) as a colorless solid, mp 147 to 148 °C (dec.) (lit. (41) mp 145 to 146 °C). IR (KBr) 3439 (m), 3351 (m), 3214 (m), 3071 (m), 1621 (s), 1593 (m), 1544 (s), 1522 (s), 1495 (m), 1481 (m), 1443 (m), 1380 (m), 1349 (s), 1289 (w), 1231 (s), 1155 (w), 1067 (w), 757 (m), 738 (m), 716 (m), 688 (m), 611 (m) cm^{-1}. ^1H NMR (400 MHz, DMSO-d_6) δ: 7.24 (m, 8 H), 6.93 (m, 2H), 9-5 (bs, 5H). ^{13}C NMR (75 MHz, DMSO-d_6) δ: 156.6, 146.0, 129.7, 122.3. FAB-MS (3-nitrobenzyl alcohol) *m/e*: 254, 237, 161, 136, 119. FAB-HR-MS (3-nitrobenzyl alcohol) calcd. for $C_{14}H_{16}N_5$: 254.1406; found: 254.1402. Anal. calcd. for $C_{14}H_{15}N_5$: C 66.38, H 5.97, N 27.65; found: C 66.41, H 6.05, N 27.80.

1,5-Bis(2-methylphenyl)biguanide (**30b**), 1,5-bis(3-methylphenyl)biguanide (**30c**), 1,5-bis(4-methylphenyl)biguanide (**30d**), 1,5-bis(4-methoxyphenyl)biguanide (**30e**), 1,5-bis(4-cyanophenyl)biguanide (**30f**), bis(2-bromophenyl)biguanide (**30g**), 1,5-bis(4-bromophenyl)biguanide (**30h**), 1,5-bis(3,5-dimethylphenyl)biguanide (**30i**), and 1,5-bis(2,4,6-trimethylphenyl)biguanide (**30j**) were prepared in similar yields in the same way. Yields, melting points, spectroscopic data, and elemental analyses are provided in the Supplementary Material.[5]

Phenyldicyandiamide (31, X = H)

In a 100-mL round-bottom flask equipped with a magnetic stirrer, aniline (2.45 g, 26.3 mmol) was added to aqueous HCl (25 mL, 1 M, 25 mmol), and the mixture was stirred until it became homogeneous. Sodium dicyanamide (2.23 g, 25.0 mmol) was then added, and the mixture was heated at reflux for 2 h with constant stirring. During this period the product precipitated, and it was separated by filtration and recrystallized from

CH_3CH_2OH to give pure phenyldicyandiamide (**31**, X = H; 3.49 g, 21.8 mol, 87%) as a colorless solid, mp 197 to 198 °C (lit. (41) mp 196 to 197 °C). IR (KBr) 3407 (m), 3319 (m), 3215 (m), 3154 (m), 2973 (m), 2176 (s), 2143 (m), 1660 (m), 1608 (m), 1585 (s), 1555 (s), 1495 (s), 1449 (m), 1393 (s), 1298 (m), 1208 (m), 1065 (m), 1051 (s), 895 (w), 744 (m), 714 (m), 686 (w), 637 (w) cm^{-1}. ^1H NMR (300 MHz, DMSO-d_6) δ: 9.03 (s, 1H), 7.35 (d, ^3J = 8.4 Hz, 2H), 7.30 (t, ^3J = 7.0 Hz, 2H), 7.07 (t, ^3J = 7.0 Hz, 1H), 6.98 (s, 2H). ^{13}C NMR (75 MHz, DMSO-d_6) δ: 160.4, 138.8, 129.7, 124.6, 122.2, 118.1. MAB-HR-MS (N_2) calcd. for $C_8H_8N_4$ *m/e*: 160.0749; found: 160.0750. Anal. calcd. for $C_8H_8N_4$: C 59.99, H 5.03, N 34.98; found: C 60.07, H 5.13, N 35.20.

X-Ray Crystallographic Studies

The structures were solved by direct methods using SHELXS-97 (44) and refined with SHELXL-97 (45). All non-hydrogen atoms were refined anisotropically. Hydrogen atoms were refined as riding atoms. They were located by a difference Fourier map for compound **30a** • HCl, whereas they were placed in ideal positions for compound **30a**.

Crystallization of Compounds 30a and 30a • HCl

Single crystals of compound **30a** • HCl suitable for analysis by X-ray diffraction were grown from hot water, and crystals of free base **30a** were grown from hot ethanol.

Acknowledgments

We are grateful to the Natural Sciences and Engineering Research Council of Canada, the Ministère de l'Éducation du Québec, the Canada Foundation for Innovation, the Canada Research Chairs Program, and Merck Frosst for financial support. In addition, we thank Prof. Jurgen Sygusch for providing access to a Bruker SMART 6000 CCD diffractometer equipped with a rotating anode.

References

1. P. Hubberstey and U. Suksangpanya. Struct. Bond. **111**, 33 (2004).
2. F. Kurzer and E. D. Pitchfork. Fortschr. Chem. Forsch. **10**, 375 (1968).
3. P. Ray. Chem. Rev. **61**, 313 (1961).
4. E. Bamberger and W. Dieckmann. Ber. **25**, 543 (1892).
5. H. Tsubouchi, K. Ohguro, K. Yasumura, H. Ishikawa, and M. Kikuchi. Bioorg. Med. Chem. Lett. **7**, 1721 (1997).
6. D. Sweeney, M. L. Raymer, and T. D. Lockwood. Biochem. Pharm. **66**, 663 (2003).
7. F. L. Rose. J. Chem. Soc. 1951 (2770).
8. R. A. Glennon, M. K. Daoud, M. Dukat, M. Teitler, K. Herrick-Davis, A. Purohit, and H. Syed. Bioorg. Med. Chem. **11**, 4449 (2003).
9. Z. Brzozowski, F. Sączewski, and M. Gdaniec. Eur. J. Med. Chem. **35**, 1053 (2000).
10. R. S. Hundal and S. E. Inzucchi. Drugs **63**, 1879 (2003).
11. K. H. Slotta and R. Tschesche. Ber. **62B**, 1398 (1929).
12. B. Kovačević and Z. B. Maksić. Org. Lett. **3**, 1523 (2001).
13. I. Kaljurand, T. Rodima, I. Leito, I. A. Koppel, and R. Schwesinger. J. Org. Chem. **65**, 6202 (2000).
14. C. G. Overberger, F. W. Michelotti, and P. M. Carabateas. J. Am. Chem. Soc. **79**, 941 (1957).
15. D. Laliberté, T. Maris, and J. D. Wuest. J. Org. Chem. **69**, 1776 (2004).
16. J. H. Fournier, T. Maris, and J. D. Wuest. J. Org. Chem. **69**, 1762 (2004).
17. S. Mayer, D. M. Daigle, E. D. Brown, J. Khatri, and M. G. Organ. J. Comb. Chem. **6**, 776 (2004).
18. S. N. Holter and W. C. Fernelius. Inorg. Syn. **7**, 58 (1963).
19. D. Karipides and W. C. Fernelius. Inorg. Syn. **7**, 56 (1963).
20. K. Shirai and K. Sugino. J. Org. Chem. **25**, 1045 (1960).
21. S. L. Shapiro, V. A. Parrino, E. Rogow, and L. Freedman. J. Am. Chem. Soc. **81**, 3725 (1959).

22. L. Neelakantan. J. Org. Chem. **22**, 1587 (1957).

23. F. H. S. Curd and F. L. Rose. British Patent 581,346 (1946).

24. B. Clement and U. Girreser. Magn. Reson. Chem. **37**, 662 (1999).

25. G. López-Olvera and M. Soriano-García. Anal. Sci. **20**, x151 (2004).

26. A. Martin, A. A. Pinkerton, and A. Schiemann. Acta Crystallogr. **C52**, 966 (1996).

27. A. Dalpiaz, V. Ferretti, P. Gilli, and V. Bertolasi. Acta Crystallogr. **B52**, 509 (1996).

28. M. Hariharan, S. S. Rajan, and R. Srinivasan. Acta Crystallogr. **C45**, 911 (1989).

29. J. M. Amigó, J. M. Martínez-Calatayud, A. Cantarero, and T. Debaerdemaeker. Acta Crystallogr. **C44**, 1452 (1988).

30. J. M. Amigó, J. Martínez-Calatayud, and T. Debaerdemaeker. Bull. Soc. Chim. Belg. **94**, 119 (1985).

31. C. J. Brown and L. Sengier. Acta Crystallogr. **C40**, 1294 (1984).

32. C. Herrnstadt, D. Mootz, and H. Wunderlich. J. Chem. Soc., Perkin Trans 2 735 (1979).

33. A. A. Pinkerton and D. Schwarzenbach. J. Chem. Soc., Dalton 989 (1978).

34. S. R. Ernst. Acta Crystallogr. **B33**, 237 (1977).

35. S. R. Ernst and F. W. Cagle, Jr. Acta Crystallogr. **B33**, 235 (1977).

36. R. Handa and N. N. Saha. Acta Crystallogr. **B29**, 554 (1973).

37. R. Handa and N. N. Saha. J. Cryst. Mol. Struct. **1**, 235 (1971).

38. C. J. Brown. J. Chem. Soc. A 60 (1967).

39. S. R. Safir, S. Kushner, L. M. Brancone, and Y. Subbarow. J. Org. Chem. **13**, 924 (1948).

40. F. E. King, R. M. Acheson, and P. C. Spensley. J. Chem. Soc. 1366 (1948).

41. F. H. S. Curd and F. L. Rose. J. Chem. Soc. 729 (1946).

42. A. B. Sen and P. R. Singh. J. Ind. Chem. Soc. **39**, 41 (1962).

43. Ashley, J. N.; Berg, S. S.; MacDonald, R. D. J. Chem. Soc. 4525 (1960).

44. G. M. Sheldrick. SHELXS-97, Program for the Solution of Crystal Structures; Universität Göttingen: Göttingen, Germany, 1997.

45. G. M. Sheldrick. SHELXL-97, Program for the Refinement of Crystal Structures; Universität Göttingen: Göttingen, Germany, 1997.

Table 2.1. Crystallographic data for the hydrochloride salt of 1,5-diphenylbiguanide (**30a** • HCl) and for 1,5-diphenylbiguanide (**30a**).

Fig. 2.1. Two views of the structure of individual biguanidinium cations in crystals of the hydrochloride salt of 1,5-diphenylbiguanide (**30a** • HCl) grown from water. Hydrogen atoms appear in white, carbon atoms in gray, and nitrogen atoms in black. The upper view provides C-N bond lengths, and the lower view shows the intramolecular C-H···π interaction (broken line) present in the biguanidinium ion. All bond lengths are in Å (with standard deviations provided in the Supplementary Material[5]), and the shortest C-C distance between the phenyl rings is used to define the aromatic interaction.

Fig. 2.2. View along the *b* axis of the structure of crystals of the hydrochloride salt of 1,5-diphenylbiguanide (**30a** • HCl) grown from water. The image reveals bilayers with an ionic core and a hydrophobic exterior. The view shows a 3 × 1 × 1 array of unit cells with atoms represented by spheres of van der Waals radii. Hydrogen atoms appear in white, chlorine atoms in light gray, carbon atoms in dark gray, and nitrogen atoms in black.

Fig. 2.3. View of the structure of crystals of the hydrochloride salt of 1,5-diphenylbiguanide (**30a** • HCl), showing how each chloride anion is surrounded by four biguanidinium cations and accepts six ionic N-H···Cl hydrogen bonds (broken lines). Two biguanidinium cations chelate chloride and two donate single hydrogen bonds.

Fig. 2.4. View along the *c* axis of the layered structure of crystals of the hydrochloride salt of 1,5-diphenylbiguanide (**30a** • HCl), showing multiple intermolecular aromatic interactions (broken lines) within a single layer. Hydrogen atoms appear in white, carbon atoms in gray, and nitrogen atoms in black. Each biguanidinium cation has four face-to-face and six edge-to-face aromatic contacts with six neighbors, as well as one intramolecular edge-to-face interaction (not marked by a broken line). The shortest C-C distances between phenyl rings are shown in Å.

Fig. 2.5. View of the structure of crystals of 1,5-diphenylbiguanide (**30a**) grown from ethanol. Hydrogen atoms appear in white, carbon atoms in gray, and nitrogen atoms in black. The intramolecular N-H···N hydrogen bond is represented by a broken line, and bond lengths are shown in Å, with standard deviations provided in the Supplementary Material.[5]

Fig. 2.6. View along the *a* axis of the structure of crystals of 1,5-diphenylbiguanide (**30a**) grown from ethanol. The image reveals bilayers with a hydrophilic core and a hydrophobic exterior. The view shows a 1 × 3 × 2 array of unit cells with atoms represented by spheres of van der Waals radii. Hydrogen atoms appear in white, carbon atoms in dark gray, and nitrogen atoms in black.

Fig. 2.7. View along the *ab* diagonal of the structure of 1,5-diphenylbiguanide (**30a**) showing inter- and intramolecular hydrogen bonds. The hydrogen bonds are represented

by broken lines, and lengths are shown in Å, with standard deviations provided in the Supplementary Material.[5] Hydrogen atoms appear in white, carbon atoms in gray, and nitrogen atoms in black. Each molecule donates two hydrogen bonds to one neighbor and accepts two hydrogen bonds from another, thereby forming a corrugated ribbon.

Fig. 2.8. a) View along the *ab* diagonal of the structure of 1,5-diphenylbiguanide (**30a**), showing how individual corrugated ribbons formed by intermolecular hydrogen bonding (broken lines) form face-to-face aromatic interactions and stack to create layers. Hydrogen atoms appear in white, carbon atoms in gray, and nitrogen atoms in black. b) View along the *b* axis, showing multiple edge-to-face aromatic interactions between layers. The shortest C-C distances between phenyl rings are shown in Å.

Compound	**30a** • HCl	**30a**
Formula	$C_{14}H_{16}ClN_5$	$C_{14}H_{15}N_5$
Fw	289.77	253.31
F(000)	608	536
Crystal system	Monoclinic	Monoclinic
Space group	$P2_1/n$	Pc
a (Å)	9.627(5)	9.0317(3)
b (Å)	4.9751(5)	6.3945(2)
c (Å)	35.2533(5)	22.5874(8)
α (°)	90	90
β (°)	95.79(2)°	99.588(2)°
γ (°)	90°	90°
Volume (Å^3)	1679.9(9)	1286.27(7)
R_1	0.0587	0.0728
wR2	0.1874	0.2183
GoF	1.069	1.032

Table 2.1. Crystallographic data for the hydrochloride salt of 1,5-diphenylbiguanide (**30a** • HCl) and for 1,5-diphenylbiguanide (**30a**).

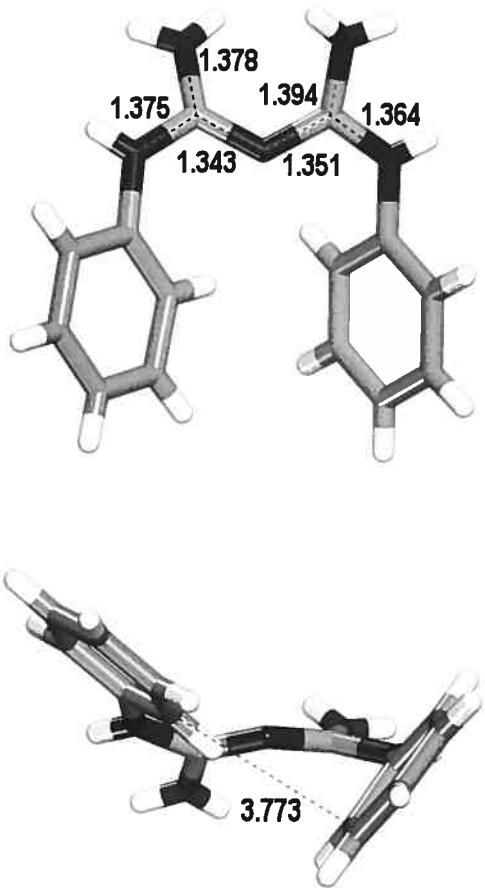

Fig. 2.1. Two views of the structure of individual biguanidinium cations in crystals of the hydrochloride salt of 1,5-diphenylbiguanide (**30a** • HCl) grown from water. Hydrogen atoms appear in white, carbon atoms in gray, and nitrogen atoms in black. The upper view provides C-N bond lengths, and the lower view shows the intramolecular C-H···π interaction (broken line) present in the biguanidinium ion. All bond lengths are in Å (with standard deviations provided in the Supplementary Material[5]), and the shortest C-C distance between the phenyl rings is used to define the aromatic interaction.

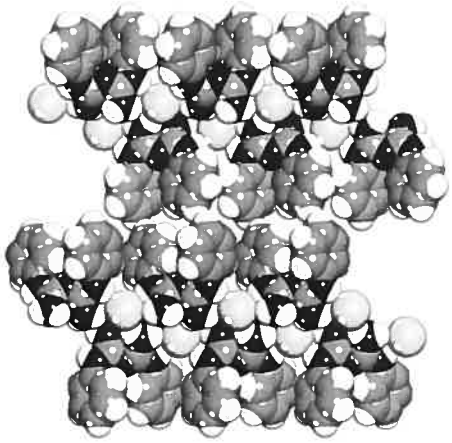

Fig. 2.2. View along the *b* axis of the structure of crystals of the hydrochloride salt of 1,5-diphenylbiguanide (**30a** • HCl) grown from water. The image reveals bilayers with an ionic core and a hydrophobic exterior. The view shows a 3 × 1 × 1 array of unit cells with atoms represented by spheres of van der Waals radii. Hydrogen atoms appear in white, chlorine atoms in light gray, carbon atoms in dark gray, and nitrogen atoms in black.

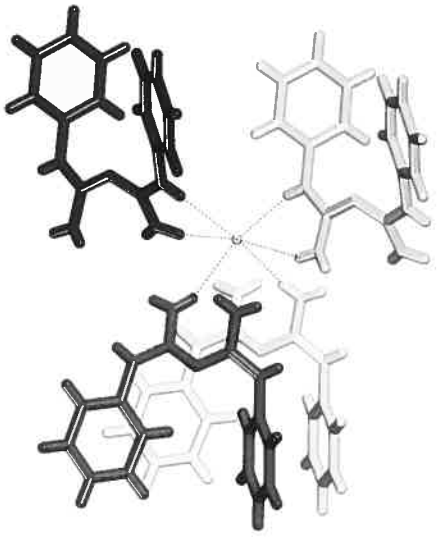

Fig. 2.3. View of the structure of crystals of the hydrochloride salt of 1,5-diphenylbiguanide (**30a** • HCl), showing how each chloride anion is surrounded by four biguanidinium cations and accepts six ionic N-H···Cl hydrogen bonds (broken lines). Two biguanidinium cations chelate chloride and two donate single hydrogen bonds.

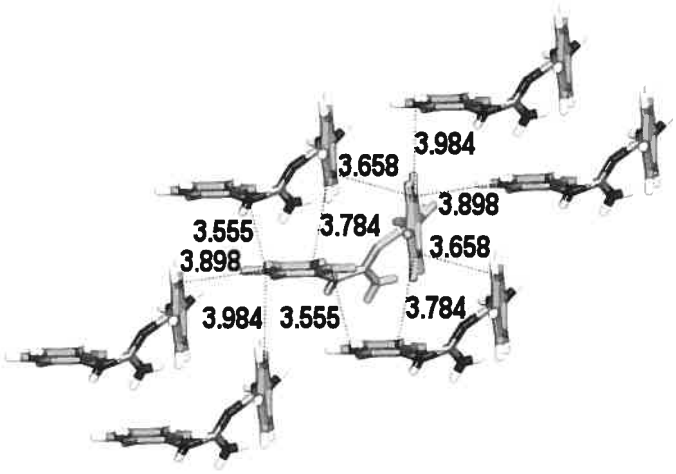

Fig. 2.4. View along the *c* axis of the layered structure of crystals of the hydrochloride salt of 1,5-diphenylbiguanide (**30a** • HCl), showing multiple intermolecular aromatic interactions (broken lines) within a single layer. Hydrogen atoms appear in white, carbon atoms in gray, and nitrogen atoms in black. Each biguanidinium cation has four face-to-face and six edge-to-face aromatic contacts with six neighbors, as well as one intramolecular edge-to-face interaction (not marked by a broken line). The shortest C-C distances between phenyl rings are shown in Å.

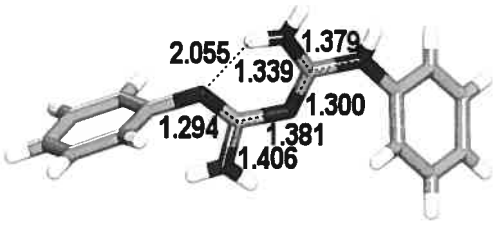

Fig. 2.5. View of the structure of crystals of 1,5-diphenylbiguanide (**30a**) grown from ethanol. Hydrogen atoms appear in white, carbon atoms in gray, and nitrogen atoms in black. The intramolecular N-H···N hydrogen bond is represented by a broken line, and bond lengths are shown in Å, with standard deviations provided in the Supplementary Material.[5]

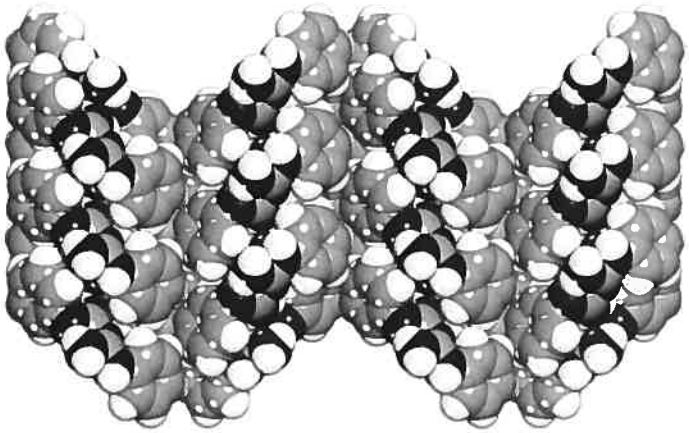

Fig. 2.6. View along the *a* axis of the structure of crystals of 1,5-diphenylbiguanide (**30a**) grown from ethanol. The image reveals bilayers with a hydrophilic core and a hydrophobic exterior. The view shows a 1 × 3 × 2 array of unit cells with atoms represented by spheres of van der Waals radii. Hydrogen atoms appear in white, carbon atoms in dark gray, and nitrogen atoms in black.

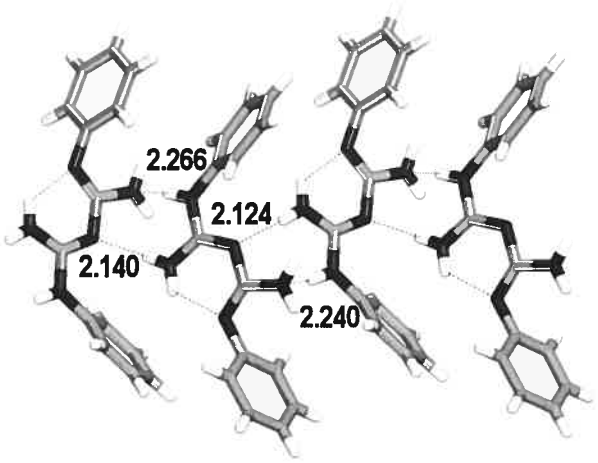

Fig. 2.7. View along the *ab* diagonal of the structure of 1,5-diphenylbiguanide (**30a**) showing inter- and intramolecular hydrogen bonds. The hydrogen bonds are represented by broken lines, and lengths are shown in Å, with standard deviations provided in the Supplementary Material.[5] Hydrogen atoms appear in white, carbon atoms in gray, and nitrogen atoms in black. Each molecule donates two hydrogen bonds to one neighbor and accepts two hydrogen bonds from another, thereby forming a corrugated ribbon.

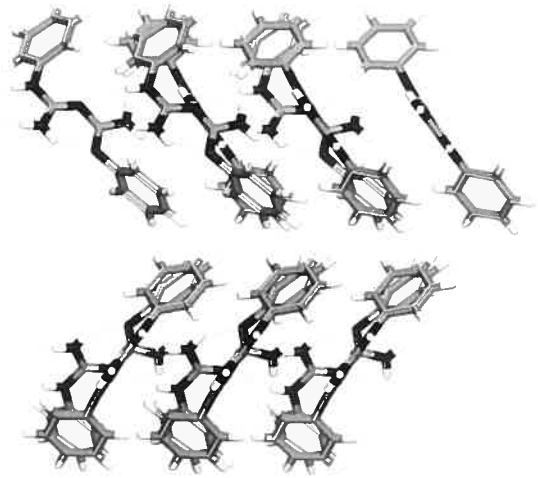

a

b

Fig. 2.8. a) View along the *ab* diagonal of the structure of 1,5-diphenylbiguanide (**30a**), showing how individual corrugated ribbons formed by intermolecular hydrogen bonding (broken lines) form face-to-face aromatic interactions and stack to create layers. Hydrogen atoms appear in white, carbon atoms in gray, and nitrogen atoms in black. b) View along the *b* axis, showing multiple edge-to-face aromatic interactions between layers. The shortest C-C distances between phenyl rings are shown in Å.

2.6 Conclusions

Pour conclure, nous avons établi à la fois des méthodes de synthèse et de purification qui sont simples, pratiques et efficaces. Nous avons également démontré que la spectroscopie infrarouge et RMN ainsi que la spectrométrie de masse permettent de caractériser les produits obtenus, ce qui devrait à l'avenir fournir les outils nécessaires à toute personne désirant faire la synthèse de dérivés arylbiguanide. Bien que nos synthèses aient été effectuées à l'aide de précurseurs simples, ces méthodes sont également applicables à la synthèse de composés d'une plus grande complexité.

Les structures cristallographiques que nous avons obtenues nous ont aidé à accroître notre compréhension à propos des formes tautomériques prédominantes ainsi que des préférences conformationnelles des diarylbiguanides à l'état solide selon leur degré de protonation. Ces données peuvent s'avérer d'une grande utilité comme point de départ pour des études plus poussées des biguanides en génie cristallin.

Références

1. Bamberger, E.; Dieckmann, W. *Ber.* **1892**, *25*, 543.
2. a) Curd, F.H.S.; Rose, F.L. *J. Chem. Soc.* **1946**, 729. b) Neelakantan, L. *J. Org. Chem.* **1957**, *22*, 1587. c) Suyama, T.; Soga, T.; Miyauchi, K. *Nippon Kagaku Kaishi* **1989**, *5*, 884. d) Sakai, J.; Uohama, M. JP 97-232411 (1997).
3. a) Overberger, C.G.; Shapiro, S.L. *J. Am. Chem. Soc.* **1954**, *76*, 93. b) Tsuji, T.; Momona, H.; Ueda, T. *Chem. Pharm. Bull.* **1968**, *16*, 799.
4. King, F.E.; Acheson, R.M.; Spensley, P.C. *J. Chem. Soc.* **1948**, 1366.
5. a) Curd, F.H.S.; Rose, F.L. *J. Chem. Soc.* **1946**, 362. b) Shuto, Y.; Taniguchi, E.; Maekawa, K. *J. Fac. Agr., Kyushu Univ.* **1974**, *18*, 221.
6. a) Dukat, M.; Abdel-Rahman, A.A.; Ismaiel, A.M.; Ingher, S.; Teitler, M.; Gyermek, L.; Glennon, R.A. *J. Med. Chem.* **1996**, *39*, 4017. b) Tsubouchi, H.; Ohguro, K.; Yasumura, K.; Ishikawa, H.; Kikuchi, M. *Bioorg. Med. Chem. Lett.* **1997**, *7*, 1721. c) Brzozowski, Z.; Saczewski, F.; Gdaniec, M. *Eur. J. Med. Chem.* **2000**, *35*, 1053.
7. Voir par exemple : Das, G.; Bharadwaj, P.K.; Ghosh, D.; Chaudhuri, B.; Banerjee, R. *Chem. Commun.* **2001**, 323.

8. Slotta, K.H.; Tschesche, R. *Ber.* **1929**, *62B*, 1398.
9. a) Lee, A.J. *Pharmacotherapy* **1996**, *16*, 327. b)www.drugs.com/metformin.html c) www.medicinenet.com/metformin/article.htm
10. a) Davies, G.E.; Francis, J.; Martin, A.R.; Rose, F.L.; Swain, G. *Brit. J. Pharmacol. Chemotherapy* **1954**, *9*, 192. b) Rose, F.L.; Swain, G. GB Pat. 705838 (1954). c) Rose, F.L.; Swain, G. US Pat. 2384924 (1954).
11. a) Russell, A.D. *Infection* **1986**, *14*, 212. b) Gjermo, P. *J. Dental Res.* **1989**, *68*, 1602. c) Oie, S. *Infection Control* **2002**, *11*, 392. d) www.nlm.nih.gov/medlineplus e) www.drugs.com/cons/chlorhexidine.html
12. Davies, A.; Field, B.S. *Biochem. J.* **1968**, *106*, 46P.
13. a) Leeming, P.A.; Thomas, G.A. S. African Pat. ZA 6702673 (1968). b) Drain, D.J.; Simmonite, D. Ger. Offen. DE 2318137 (1973).
14. a) MacLeod, N.A.; Webb, C.P.N. Ger. Offen. DE 2826019 (1979). b) www.baquacil.com
15. a) Millis, N.F.; Eager, E.; Hay, A.J.; Kasian, P.A.; Pickering, W.J.; Tan, M.A. *Med. J. Australia* **1981**, *1*, 573. b) www.poolcenter.com/biguan.htm c) www.mareva.fr/eu-fr/phmb
16. a) Greenwood, D. *J. Antimicrobial Chemotherapy* **1995**, *36*, 857. b) www.netdoctor.co.uk/medicines/100001985.html
17. Surrey, A.R.; Hammer, H.F. *J. Am. Chem. Soc.* **1946**, *68*, 113.

Chapitre 3 :

Étude des arylbis(biguanides) et de leurs sels dans l'état cristallin

3.1 Les biguanides en génie cristallin

Étant donné que les biguanides possèdent de nombreux sites donneurs et accepteurs de ponts hydrogène, il est envisageable de les utiliser en génie cristallin afin de diriger l'association des molécules.[1] De plus, les biguanides étant des bases modérément fortes, il est possible de les co-cristalliser en présence de divers acides pour former des sels où les contre-ions peuvent jouer un rôle dans le réseau cristallin.[2] Finalement, les biguanides s'avèrent être des ligands bidentates pouvant coordonner une variété de métaux de transition[3] ou des lanthanides[4] (Figure 3.1).

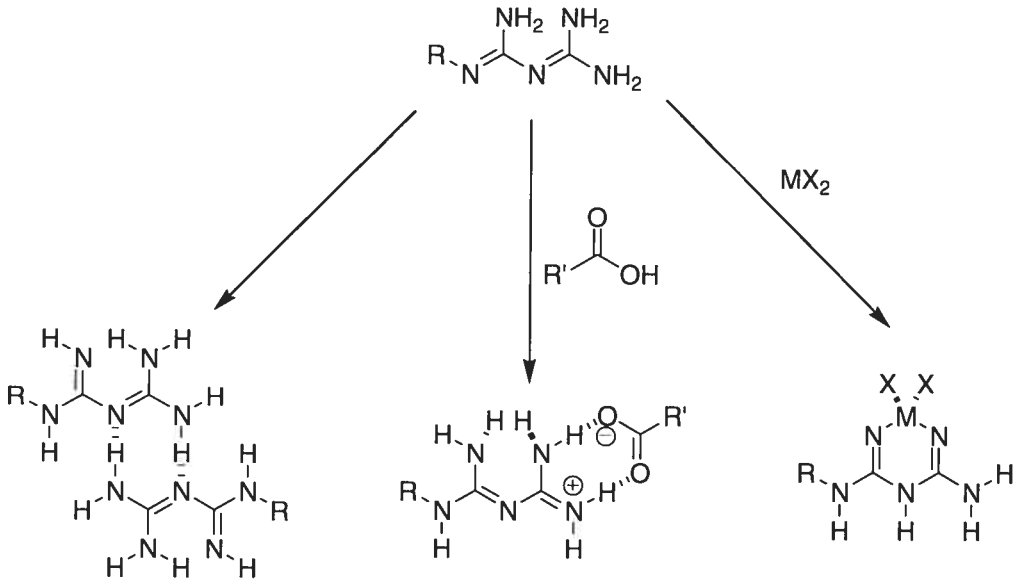

Figure 3.1 Modes d'association potentiels des biguanides en génie cristallin.

Cependant, bien que les biguanides aient fait l'objet de plusieurs études cristallographiques, les structures cristallines rapportées dans la littérature de composés portant plus d'un groupe biguanide sont très limitées, les seuls exemples étant des complexes de l'éthylènebis(biguanide) (**38**) avec des métaux tels l'argent, le nickel, le cuivre et le manganèse.[5]

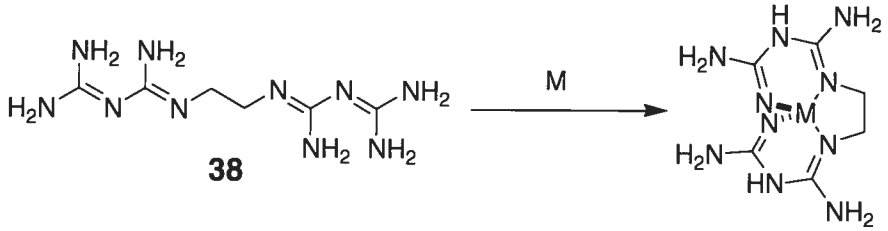

38

M = Ag(II), Ni(II), Cu(II), Mn(II)

3.2 Objectifs

Pour ces raisons, nous avons souhaité explorer l'utilité des biguanides en tant que groupes de reconnaissance en tectonique moléculaire. Pour ce faire, nous souhaitions utiliser des dérivés simples comme cibles lors d'études préliminaires. Nous avons donc cristallisé le 1,4-phénylènebis(biguanide) (**28**) et son dihydrochlorure, ainsi que le dihydrochlorure et le carbonate du 1,3-phénylènebis(biguanide) (**29**). La synthèse de ces composés a déjà été décrite au Chapitre 2, sauf dans le cas du sel de carbonate de **29**, dont des cristaux ont été obtenus à partir d'une solution de **29** en présence d'air.

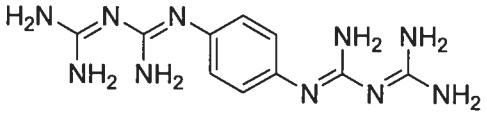

28

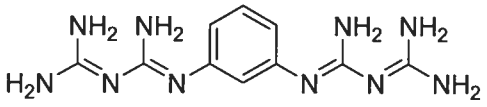

29

3.3 Article 2 :

Hydrogen-Bonded Networks in Crystals Built from Bis(biguanides) and their Salts

Olivier Lebel, Thierry Maris, James D. Wuest. *Canadian Journal of Chemistry*, sous presse.

Submitted to *Can. J. Chem.*
Version of March 18, 2006

Hydrogen-Bonded Networks in Crystals Built from Bis(biguanides) and Their Salts[1]

Olivier Lebel, Thierry Maris, and James D. Wuest

Dedicated with respect and affection to Dr. Alfred Bader, for his friendship, encouragement, generosity, entreprenurial spirit, love of art, and enduring service to chemistry.

Olivier Lebel,[2] Thierry Maris, and James D. Wuest.[3] Département de Chimie, Université de Montréal, Montréal, Québec, H3C 3J7, Canada.

[1] This article is part of a Special Issue dedicated to Dr. Alfred Bader.

[2] Fellow of the Ministère de l'Éducation du Québec, 2002-2004.

[3] Corresponding author [redacted]

Abstract: Biguanide groups and biguanidinium cations incorporate multiple sites that can donate or accept hydrogen bonds. To assess their ability to associate and to direct the formation of extended hydrogen-bonded networks, we examined the structure of crystals of four compounds in which two neutral biguanide groups or the corresponding cations are attached to the 1,4- and 1,3-positions of phenylene spacers. As expected, all four structures incorporate extensive networks of hydrogen bonds and reveal other reliable features. In particular, 1) neutral biguanide groups favor a roughly planar conformation with an intramolecular hydrogen bond, and they associate as hydrogen-bonded pairs; 2) despite coulombic repulsion, biguanidinium cations can also associate as hydrogen-bonded pairs; and 3) the 1,3-phenylenebis(biguanidinium) dication favors a pincer-like conformation that allows chelation of suitable counterions. However, the precise patterns of hydrogen bonding in the structures vary substantially, limiting the usefulness of biguanide and biguanidinium as groups for directing supramolecular assembly.

Key words: bis(biguanide), bis(biguanidinium), structure, hydrogen-bonded network, non-covalent interaction, supramolecular chemistry, crystal engineering.

Introduction

The general family of compounds that includes biguanide (**19**) has been known for over 100 years (1-3).[4] Members of the family have important applications as medicines, as ligands in coordination chemistry, as bases, and as precursors for the

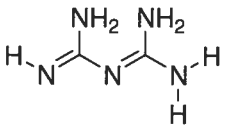

19

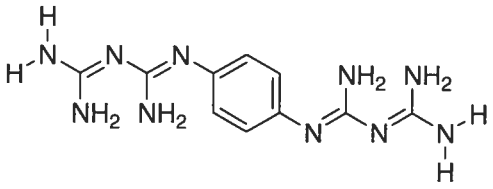

28

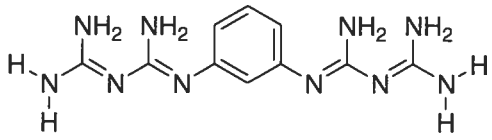

29

synthesis of various heterocyclic compounds (4). In addition, biguanide groups and biguanidinium cations incorporate characteristic patterns of sites that can donate or accept hydrogen bonds, thereby allowing them to associate and engage in supramolecular assembly (4).

A productive strategy for engineering predictably ordered supramolecular materials is to build them from compounds incorporating multiple sticky sites that participate in directional intermolecular interactions (5). These interactions tend to place adjacent molecules in specific positions, leading to the formation of extensive networks with predetermined architectures. In this paper, we assess the potential of multiple biguanide and biguanidinium groups to serve in this way as sticky sites, and we describe the hydrogen-bonded networks present in crystals of bis(biguanide) **28**, its dihydrochloride, and the dihydrochloride and carbonate of isomeric bis(biguanide) **29**. Previous use of such compounds in supramolecular chemistry has been limited to the chelation of metals by ethylenebis(biguanide) (6,7).

---

[4] For the sake of simplicity, biguanides and their salts are normally represented in this paper as single tautomers.

Results and discussion

Crystal structure of bis(biguanide) 28

Bis(biguanide) **28** was prepared by a published method (4) and was crystallized from hot water. X-ray diffraction established that the crystals belong to the triclinic space group P-1 and exist as a pair of non-merohedral twins (8). The crystals have the composition **28** • H_2O, and each unit cell contains six molecules of bis(biguanide) **28** and six molecules of H_2O. Crystallographic parameters are given in Table 3.1, views of the structure appear in Figs. 3.2-3.3, and additional information is provided as supplementary data.[5] Multiple symmetry-independent biguanide groups are present in the unit cell, but all correspond to tautomeric form **I** (Scheme 3.1) and have a roughly planar

Scheme 3.1

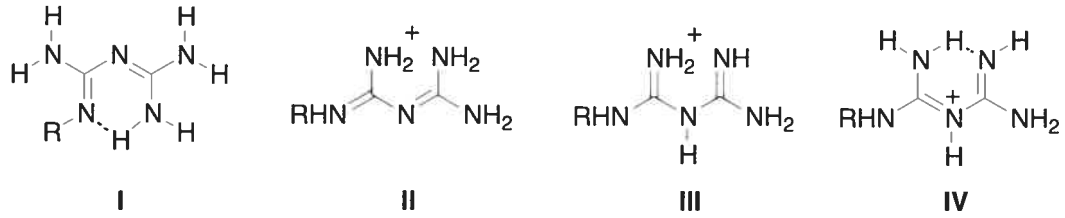

geometry, with internal torsion angles in the range 2.5(3)-29.8(3)°. This geometry is enforced by an intramolecular N-H···N hydrogen bond, with N···H distances of normal

[5] Supplementary data for this article are available on the Web site or may be purchased from the Directory of Unpublished Data, Document Delivery, CISTI, National Research Council Canada, Ottawa, ON K1A 0S2, Canada. DUD 3662. For more information on obtaining material refer to http://cisti-icist.nrc-cnrc.gc.ca/irm/unpub_e.shtml. CCDC 291494-291497 contain the crystallographic data for this manuscript. These data can be obtained, free of charge, via www.ccdc.cam.ac.uk/conts/retrieving.html (or from the Cambridge Crystallographic Data Centre, 12 Union Road, Cambridge CB2 1EZ, UK; fax +44 1223 336033; or deposit@ccdc.cam.ac.uk).

values (1.993(5)-2.263(5) Å). Similar features appear in all previous structural studies of neutral biguanides (4, 9-11), so a nearly planar geometry and an intramolecular hydrogen bond appear to be structural features of biguanides that can be used reliably by crystal engineers. The average planes defined by the biguanide groups form dihedral angles in the range 67.6(1)-88.7(1)° with respect to the plane of the central aromatic ring.

Intermolecular hydrogen bonds involving both bis(biguanide) **28** and water create a complex network (Figs. 3.2-3.3), with over 40 hydrogen bonds per unit cell. A primary motif in this network is the ribbon shown in Fig. 3.2, which links molecules of bis(biguanide) **28** end-to-end by novel bifurcated hydrogen bonds. Each molecule in the ribbon serves either as a double acceptor or double donor of these bifurcated bonds. The resulting ribbons are aligned with the *ac* diagonal and linked by additional hydrogen bonds between biguanide groups, as well as by bridging molecules of water (Fig. 3.3).

Crystal structure of the dihydrochloride salt of bis(biguanide) 28

Crystals were grown by allowing acetone to diffuse slowly into an aqueous solution of bis(biguanidinium) dichloride (**28** • 2HCl), which was prepared by a known method (4). X-ray diffraction demonstrated that the crystals belong to the triclinic space group P-1 and have the composition **28** • 2HCl • H_2O. Each unit cell contains two symmetry-equivalent molecules of bis(biguanidium) dichloride and two molecules of H_2O. There are four potential sites for H_2O, associated in pairs within van der Waals distances, but only half are occupied. Crystallographic parameters appear in Table 3.1, views of the structure are shown in Figs. 3.4-3.5, and additional information is given as supplementary data.[5] The biguanidinium groups are extensively delocalized, as demonstrated by the similarity of the C-N distances (1.310(3)-1.366(2) Å). Each biguanidinium group can be represented by structure **II** (Scheme 3.1) and its resonance hybrids, and alternatives in which the central atom of nitrogen is protonated (structure **III**) or in which an intramolecular hydrogen bond is present (structure **IV**) are not favored in the solid state. Similar conclusions have been reached in all previous structural analyses of biguanidinium cations (4, 10-21), so protonation of biguanides to give structure **II** (Scheme 3.1) appears to be a fundamental preference, both in solution

(2) and in the solid state. Although the biguanidium groups in the dihydrochloride salt of compound **28** can be represented by structure **II**, they are not planar. The two guanidinium subunits that can be considered to be present in each biguanidinium group are individually planar, but their planes define dihedral angles of 39.2(1)° and 45.5(1)° in the two arms of each dication.

The structure of the dihydrochloride salt of bis(biguanide) **28** can be described as a complex network held together in part by hydrogen-bonded pairing of biguanidinium cations (Fig. 3.4a). The N···N distance in these cationic pairs is 3.033(3) Å. Inter-cationic hydrogen bonding is disfavored by coulombic repulsion and is absent in most biguanidinium salts (4, 11, 14, 15, 17, 19-21), although it has previously been observed in a few cases (12, 13, 18). Slightly offset face-to-face aromatic interactions are also observed in the structure of salt **28** • 2HCl (Fig. 3.4b), with a center-to-center separation of 3.879(2) Å. In addition, the structure of the salt reveals multiple ionic hydrogen bonds between biguanidium cations and chloride (Fig. 3.5). There are two distinct types of chloride ion in the structure, each of which accepts hydrogen bonds from N-H groups provided by neighboring bis(biguanidium) dications. One type (Cl1) accepts five hydrogen bonds from four dications (Fig. 3.5a), and the other type (Cl2) accepts six hydrogen bonds from four dications, two of which are involved in chelation of chloride (Fig. 3.5b). Each bis(biguanidinium) dication is linked by hydrogen bonding to eight chloride ions, two molecules of water, and one other bis(biguanidinium) dication. The resulting network defines small channels along the *a* axis that are occupied by included molecules of water.

Crystal structure of the dihydrochloride salt of bis(biguanide) 29

Bis(biguanidinium) dichloride **29** • 2HCl was prepared by a known method (4) and was crystallized from acetone/water. X-ray diffraction revealed that 1) the crystals belong to the triclinic space group P-1, 2) their composition corresponds to **29** • 2HCl • $3H_2O$, and 3) each unit cell contains two equivalent molecules of bis(biguanidium) dichloride and six molecules of H_2O. Crystallographic parameters are given in Table 3.1, views of the structure appear in Figs. 3.6 and 3.7a, and additional information is provided in the supplementary data.[5] As noted in other biguanidinium salts, the cations

are extensively delocalized, and the C-N distances have similar values (1.320(5)-1.353(5) Å). Again, each biguanidinium group can be represented by structure **II** (Scheme 3.1). This further reinforces the conclusion, drawn previously from analysis of salt **28** • 2HCl and related compounds (4), that structure **II** is a fundamental preference of biguanidinium cations and can be used dependably by crystal engineers. As in the case of analogue **28** • 2HCl, the two biguanidinium groups in each bis(biguanidinium) dication are distinctly nonplanar, and the planes of the guanidinium subunits that can be considered to be present define dihedral angles of 52.6(2)° and 54.8(2)°.

Various important interactions can be identified in the structure of the dihydrochloride salt of bis(biguanide) **29**. As in the structure of analogous salt **28** • 2HCl, a network is formed by hydrogen-bonded pairing of biguanidinium cations (Fig. 3.6a), with N···N distances similar to those observed previously (2.979(4) and 3.028(4) Å). It is noteworthy that this uncommon hydrogen-bonded dimeric motif is observed in the structures of both bis(biguanidinium) salts, despite its coulombic disadvantage. Nevertheless, its absence in the structures of most other biguanidinium salts (4, 11, 14, 15, 17, 19-21) suggests that it does not define a motif that can be used reliably in supramolecular construction.

Additional cohesive forces in the structure of salt **29** • 2HCl, also observed in that of analogue **28** • 2HCl, are contributed by face-to-face aromatic interactions, with a center-to-center separation of 3.687(2) Å (Fig. 3.6b). The structure of salt **29** • 2HCl, like that of analogue **28** • 2HCl, reveals multiple ionic hydrogen bonds between biguanidium cations and chloride (Fig. 3.7a). Again, there are two distinct types of chloride ion in the structure. One accepts a total of six hydrogen bonds from N-H groups provided by three neighboring bis(biguanidium) dications (Fig. 3.7a). This type of chloride accepts an additional hydrogen bond from one of the included molecules of water. The dications adopt a pincer-like conformation that favors binding of chloride by allowing each biguanidinium group to donate two hydrogen bonds to a single chloride, resulting in a characteristic chelation (Fig. 3.7a). Binding of chloride in this way generates tapes that run along the *ab* diagonal. The second type of chloride forms additional ionic hydrogen bonds that help bridge the tapes, and further links between the tapes are created by the hydrogen-bonded pairing of biguanidinium cations (Fig. 3.6a).

Crystal structure of the carbonate salt of bis(biguanide) 29

In contact with air, solutions of bis(biguanide) **29** in dioxane/water yielded crystals of the corresponding carbonate. X-ray diffraction established that 1) the crystals belong to the triclinic space group P-1, 2) their composition corresponds to **29** • H_2CO_3 • H_2O • 0.5dioxane, and 3) each unit cell contains two equivalent molecules of bis(biguanidium) carbonate. Crystallographic parameters are provided in Table 3.1, a view of the structure appears in Fig. 3.7b, and additional information is given in the supplementary data.[5] The bis(biguanidinium) dications adopt essentially the same pincer-like conformation observed in dichloride **29** • 2HCl, and the two structures are strikingly similar. Chelation of carbonate leads to the assembly of sheets rather than tapes (Fig. 3.7b). Hydrogen-bonded pairing of biguanidinium cations, also observed in the other salts of bis(biguanides) **28** and **29**, then joins the sheets in a three-dimensional network. Each carbonate also accepts an additional hydrogen bond from an adjacent sheet, and molecules of dioxane are held between the sheets by multiple hydrogen bonds.

Conclusions

Biguanides are an intrinsically interesting class of compounds with many known or potential applications. Because biguanides and biguanidinium salts incorporate multiple sites that can donate or accept hydrogen bonds, they are inherently disposed to associate, making them attractive candidates for applications in crystal engineering and other areas of supramolecular chemistry. To evaluate their potential, we have linked two biguanide or biguanidinium groups to rigid aromatic spacers, and we have determined how the resulting bis(biguanides) and bis(biguanidinium) dications interact in the crystalline state. These studies, along with previous structural analyses, have confirmed that the biguanide and biguanidinium groups can be counted on to engage in multiple hydrogen bonds, leading to the formation of extended networks. However, the precise patterns of hydrogen bonding vary significantly, suggesting that other groups are inherently more suitable for fully controlling molecular aggregation.

Experimental

Crystallization of bis(biguanide) 28

Bis(biguanide) **28** was prepared according to a published procedure (4) and crystallized from hot water.

Crystallization of the dihydrochloride salt of bis(biguanide) 28

The dihydrochloride salt of bis(biguanide) **28** was prepared according to a published procedure (4). Single crystals suitable for X-ray diffraction were grown by allowing acetone to diffuse slowly into an aqueous solution of the salt.

Crystallization of the dihydrochloride salt of bis(biguanide) 29

The dihydrochloride salt of bis(biguanide) **29** was prepared according to a published procedure (4). Single crystals suitable for X-ray diffraction were grown by allowing acetone to diffuse slowly into an aqueous solution of the salt.

Crystallization of the carbonate salt of bis(biguanide) 29

Bis(biguanide) **29** was prepared according to a published procedure (4). Single crystals of the carbonate salt suitable for X-ray diffraction were grown by allowing dioxane to diffuse slowly into an aqueous solution of compound **29** in contact with air.

X-Ray Crystallographic Studies

The structures were solved by direct methods using SHELXS-97 (22) and refined with SHELXL-97 (23). All non-hydrogen atoms were refined anisotropically. Hydrogen atoms bonded to nitrogen atoms were located from difference Fourier maps, whereas hydrogen atoms bonded to the carbon atoms of aryl groups were placed in idealized positions. All hydrogen atoms were refined as riding atoms. The structure of bis(biguanide) **28** was refined as a two-component twin with twin element scale factors of 0.512(1) and 0.488(1) (24).

Acknowledgments

We are grateful to the Natural Sciences and Engineering Research Council of Canada, the Ministère de l'Éducation du Québec, the Canada Foundation for Innovation, and the Canada Research Chairs Program for financial support. In addition, we thank Prof. Jurgen Sygusch for providing access to a Bruker SMART 6000 CCD diffractometer equipped with a rotating anode.

References

1. P. Hubberstey and U. Suksangpanya. Struct. Bond. **111**, 33 (2004).
2. F. Kurzer and E. D. Pitchfork. Fortschr. Chem. Forsch. **10**, 375 (1968).
3. P. Ray. Chem. Rev. **61**, 313 (1961).
4. O. LeBel, T. Maris, H. Duval, and J. D. Wuest. Can. J. Chem. **83**, 615 (2005).
5. J. D. Wuest. Chem. Commun. 5830 (2005).
6. A. Das and S. Mukhopadhyay. Polyhedron **23**, 895 (2004).
7. A. De. Acta Crystallogr. **C46**, 1004 (1990).
8. C. Giacovazzo. Fundamentals of Crystallography. Oxford University Press, New York, 1992. pp. 83-87.
9. A. Dalpiaz, V. Ferretti, P. Gilli, and V. Bertolasi. Acta Crystallogr. **B52**, 509 (1996).
10. A. A. Pinkerton and D. Schwarzenbach. J. Chem. Soc., Dalton 989 (1978).

11. S. R. Ernst. Acta Crystallogr. **B33**, 237 (1977).
12. G. López-Olvera and M. Soriano-García. Anal. Sci.: X-ray Struct. Anal. [online], **20**, x151 (2004).
13. A. Martin, A. A. Pinkerton, and A. Schiemann. Acta Crystallogr. **C52**, 966 (1996).
14. M. Hariharan, S. S. Rajan, and R. Srinivasan. Acta Crystallogr. **C45**, 911 (1989).
15. J. M. Amigó, J. M. Martínez-Calatayud, A. Cantarero, and T. Debaerdemaeker. Acta Crystallogr. **C44**, 1452 (1988).
16. J. M. Amigó, J. Martínez-Calatayud, and T. Debaerdemaeker. Bull. Soc. Chim. Belg. **94**, 119 (1985).
17. C. J. Brown and L. Sengier. Acta Crystallogr. **C40**, 1294 (1984).
18. C. Herrnstadt, D. Mootz, and H. Wunderlich. J. Chem. Soc., Perkin Trans 2 735 (1979).
19. R. Handa and N. N. Saha. Acta Crystallogr. **B29**, 554 (1973).
20. R. Handa and N. N. Saha. J. Cryst. Mol. Struct. **1**, 235 (1971).
21. C. J. Brown. J. Chem. Soc. A 60 (1967).
22. G. M. Sheldrick. SHELXS-97, Program for the Solution of Crystal Structures; Universität Göttingen: Göttingen, Germany, 1997.
23. G. M. Sheldrick. SHELXL-97, Program for the Refinement of Crystal Structures; Universität Göttingen: Göttingen, Germany, 1997.
24. R. Herbst-Irmer and G. M. Sheldrick. Acta Crystallogr. **B54**, 443 (1998).

Table 3.1. Crystallographic data for bis(biguanide) **28**, its dihydrochloride, and the dihydrochloride and carbonate of isomeric bis(biguanide) **29**.

Fig. 3.2. View of the structure of crystals of neutral bis(biguanide) **28** grown from water. The view reveals that each biguanide group incorporates an internal N-H···N hydrogen bond and favors tautomeric form **I** (Scheme 1). In addition, the view shows bifurcated intermolecular hydrogen bonds that link compound **28** into continuous ribbons, as well as additional hydrogen bonds involving water. Hydrogen bonds are represented by broken lines. Hydrogen atoms appear in white, carbon in gray, nitrogen in blue, and oxygen in red.

Fig. 3.3. a) View along the *b* axis of the structure of crystals of neutral bis(biguanide) **28**, with two hydrogen-bonded ribbons highlighted in red and green. The two highlighted ribbons run in opposite directions along the *ac* diagonal. b) View along the *a* axis showing secondary hydrogen bonds (represented by broken lines) between the characteristic ribbons. In both views, water molecules are omitted for clarity.

Fig. 3.4. Views of the structure of crystals of the dihydrochloride salt of bis(biguanide) **28** grown from acetone/water. a) The biguanidinium cations favor structure **II** (Scheme 1) and form hydrogen-bonded pairs. b) Addition cohesion is contributed by slightly offset face-to-face aromatic interactions. Hydrogen bonds and the aromatic interaction are represented by broken lines, and included water molecules are omitted for simplicity. Hydrogen atoms appear in white, carbon in gray, and nitrogen in blue.

Fig. 3.5. Views of the structure of crystals of the dihydrochloride salt of bis(biguanide) **28**, showing ionic hydrogen bonds involving chloride. a) One set of chloride ions (Cl1) accepts hydrogen bonds donated by five N-H groups in four different bis(biguanidinium) dications. b) The other type of chloride (Cl2) accepts six hydrogen bonds (four involving chelation), contributed again by N-H groups in four different bis(biguanidinium) dications. In both views, hydrogen bonds are represented by broken lines. Hydrogen atoms appear in white, carbon in gray, nitrogen in blue, and chlorine in green.

Fig. 3.6. Views of the structure of crystals of the dihydrochloride salt of bis(biguanide) **29** grown from acetone/water. a) The biguanidinium cations favor structure **II** (Scheme 1) and form hydrogen-bonded pairs. b) Addition cohesion is contributed by face-to-face aromatic interactions. Hydrogen bonds and the aromatic interaction are represented by broken lines, and included water molecules are omitted for simplicity. Hydrogen atoms appear in white, carbon in gray, and nitrogen in blue.

Fig. 3.7. a) View along the *c* axis of the structure of crystals of the dihydrochloride salt of bis(biguanide) **29** grown from acetone/water. The view shows a tape constructed by ionic hydrogen bonding involving one of the two types of chloride ions in the structure. Each bis(biguanidinium) dication adopts a pincer-like conformation that permits chelation of chloride by the simultaneous donation of four hydrogen bonds. b) View along the *c* axis of the closely related structure of crystals of the carbonate salt of

bis(biguanide) **29** grown from dioxane/water. In both views, hydrogen bonds are represented by broken lines. Hydrogen atoms appear in white, carbon in gray, nitrogen in blue, oxygen in red, and chlorine in green.

Table 3.1. Crystallographic data for bis(biguanide) **28**, its dihydrochloride, and the dihydrochloride and carbonate of isomeric bis(biguanide) **29**.

Compound	**28** • H_2O	**28** • 2HCl • H_2O	**29** • 2HCl • $3H_2O$	**29** • H_2CO_3 • H_2O • 0.5dioxane
Temperature (K)	100	293	100	100
λ (Å)	1.54178	1.54178	1.54178	1.54178
Formula	$C_{10}H_{18}N_{10}O$	$C_{10}H_{20}Cl_2N_{10}O$	$C_{10}H_{24}Cl_2N_{10}O_3$	$C_{13}H_{24}N_{10}O_5$
Fw	294.34	367.26	403.29	400.42
F(000)	936	384	424	424
Crystal system	Triclinic	Triclinic	Triclinic	Triclinic
Z	6	2	2	2
d (g cm^{-3})	1.432	1.420	1.435	1.420
μ (mm^{-1})	0.863	3.591	3.437	0.947
Space group	P-1	P-1	P-1	P-1
a (Å)	10.0311(16)	5.8749(8)	9.3537(3)	9.9072(3)
b (Å)	10.8820(18)	12.036(5)	9.6015(3)	10.1769(3)
c (Å)	21.127(3)	13.084(5)	11.4402(4)	11.0195(5)
α (°)	88.090(7)	105.66(3)	82.983(2)	77.297(2)
β (°)	87.280(7)	95.65(3)	71.193(2)	67.906(2)
γ (°)	62.735(6)	102.12(2)	73.759(2)	65.826(2)
Volume ($Å^3$)	2047.5(6)	859.1(5)	933.19(5)	936.32(6)
θ max (°)	58.01	70.01	70.01	72.03
h, *k*, *l* max	10/11/23	7/14/15	11/11/14	12/12/13
Unique	6951	3241	3545	3557
Observed ($I > 2\sigma(I)$)	3715	2766	2583	2403
R_1	0.0600	0.0456	0.0745	0.0487
wR2	0.0903	0.1109	0.2142	0.1277
R1 (all data)	0.1294	0.0463	0.0818	0.0699
wR2 (all data)	0.1012	0.1110	0.2351	0.1357
Diff. peak and hole ($e/Å^3$)	0.318/-0.360	0.323/-0.396	0.913/-0.626	0.397/-0.479

GoF	1.012	1.105	1.058	0.942

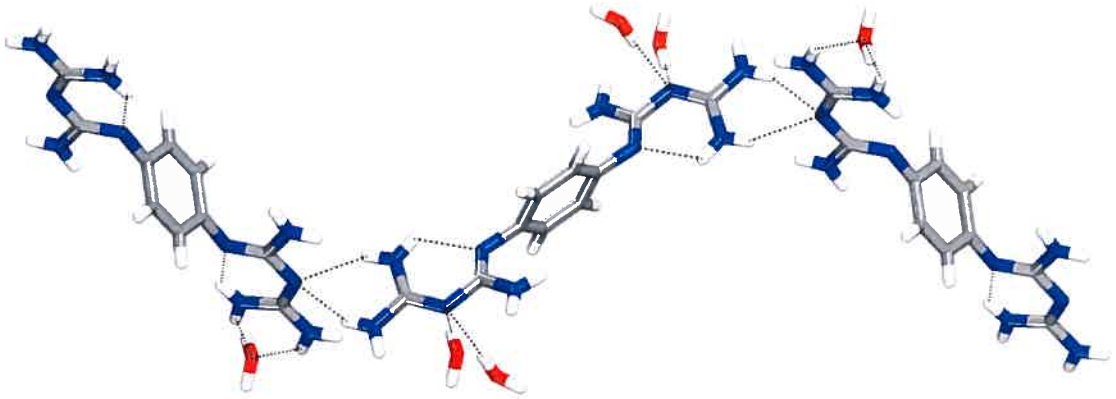

Fig. 3.2. View of the structure of crystals of neutral bis(biguanide) **28** grown from water. The view reveals that each biguanide group incorporates an internal N-H···N hydrogen bond and favors tautomeric form **I** (Scheme 1). In addition, the view shows bifurcated intermolecular hydrogen bonds that link compound **28** into continuous ribbons, as well as additional hydrogen bonds involving water. Hydrogen bonds are represented by dotted lines. Hydrogen atoms appear in white, carbon in gray, nitrogen in blue, and oxygen in red.

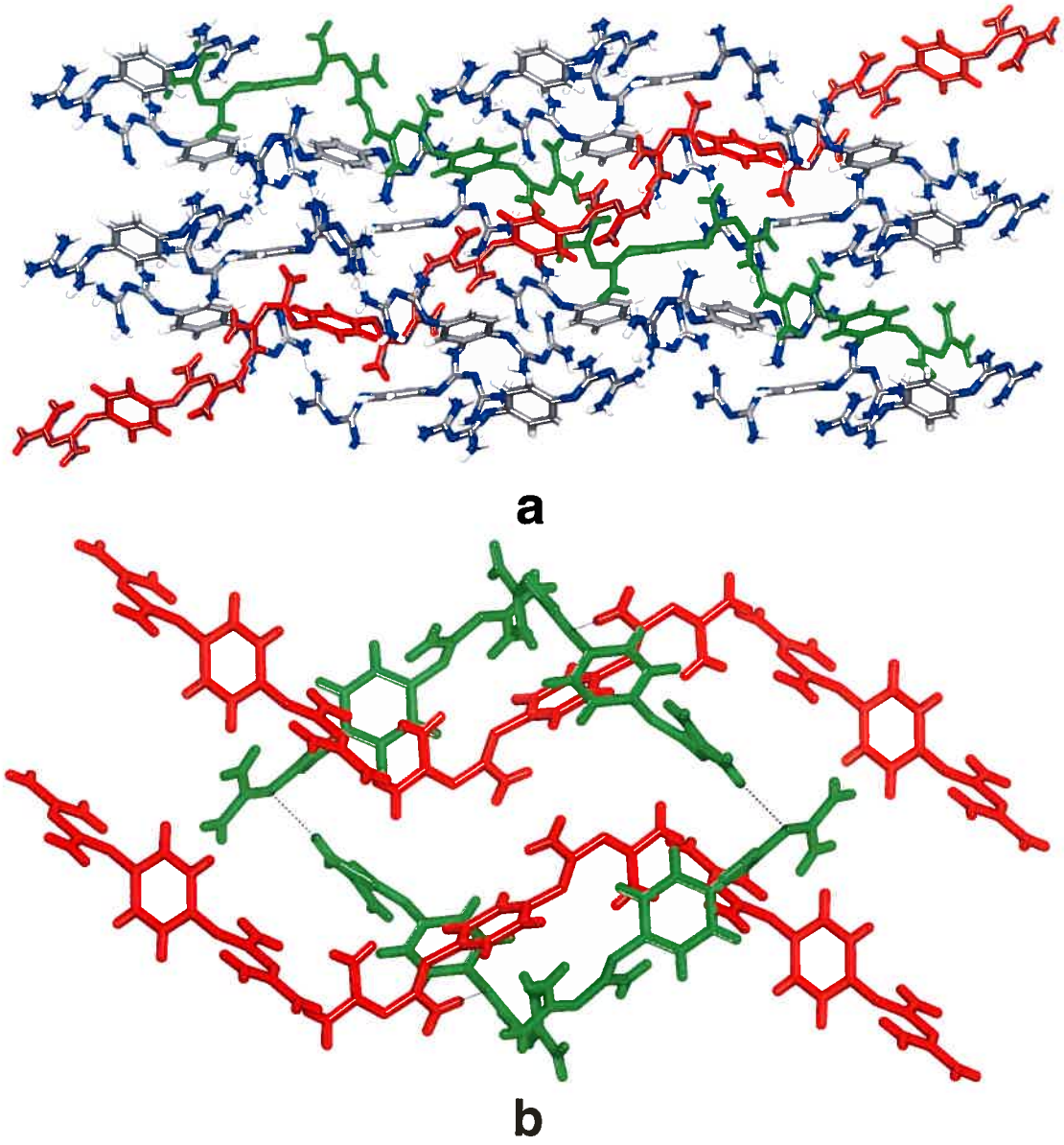

Fig. 3.3. a) View along the *b* axis of the structure of crystals of neutral bis(biguanide) **28**, with two hydrogen-bonded ribbons highlighted in red and green. The two highlighted ribbons run in opposite directions along the *ac* diagonal. b) View along the *a* axis showing secondary hydrogen bonds (represented by dotted lines) between the characteristic ribbons. In both views, water molecules are omitted for clarity.

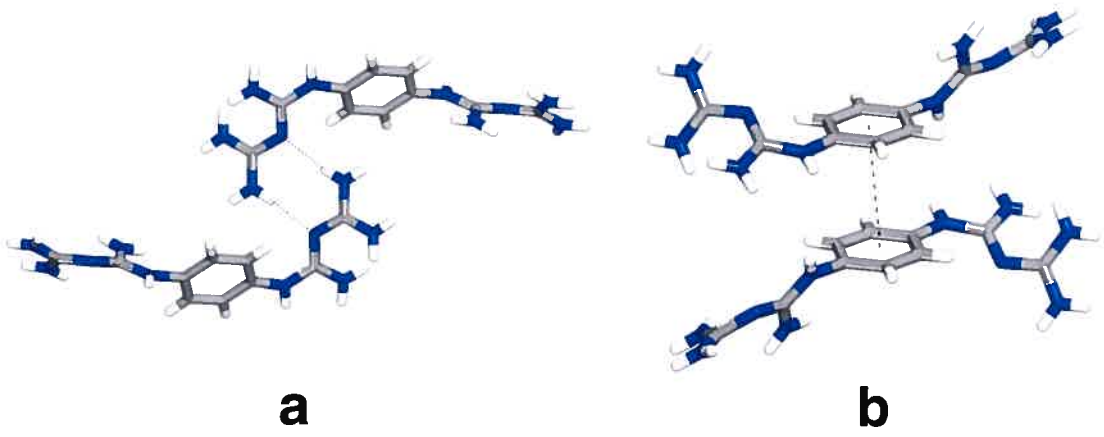

Fig. 3.4. Views of the structure of crystals of the dihydrochloride salt of bis(biguanide) **28** grown from acetone/water. a) The biguanidinium cations favor structure **II** (Scheme 1) and form hydrogen-bonded pairs. b) Addition cohesion is contributed by slightly offset face-to-face aromatic interactions. Hydrogen bonds and the aromatic interaction are represented by dotted lines, and included water molecules are omitted for simplicity. Hydrogen atoms appear in white, carbon in gray, and nitrogen in blue.

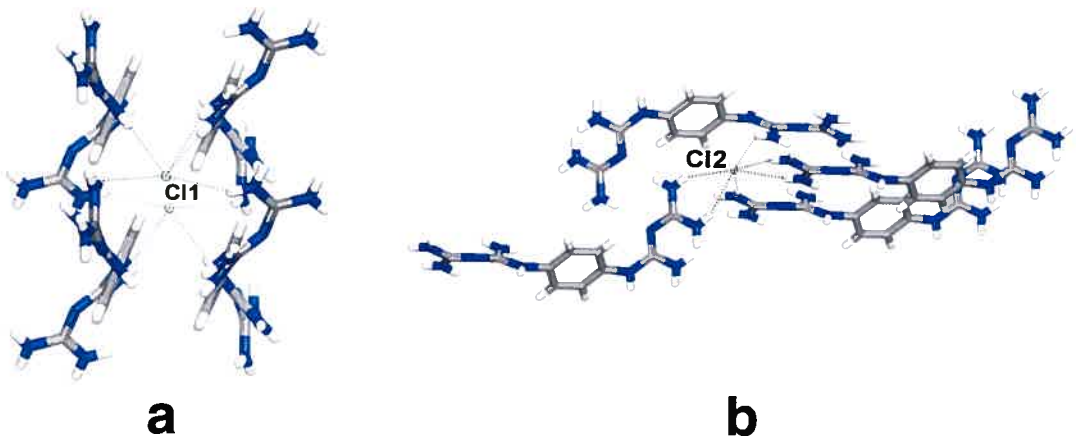

Fig. 3.5. Views of the structure of crystals of the dihydrochloride salt of bis(biguanide) **28**, showing ionic hydrogen bonds involving chloride. a) One set of chloride ions (Cl1) accepts hydrogen bonds donated by five N-H groups in four different bis(biguanidinium) dications. b) The other type of chloride (Cl2) accepts six hydrogen bonds (four involving chelation), contributed again by N-H groups in four different bis(biguanidinium) dications. In both views, hydrogen bonds are represented by broken lines. Hydrogen atoms appear in white, carbon in gray, nitrogen in blue, and chlorine in green.

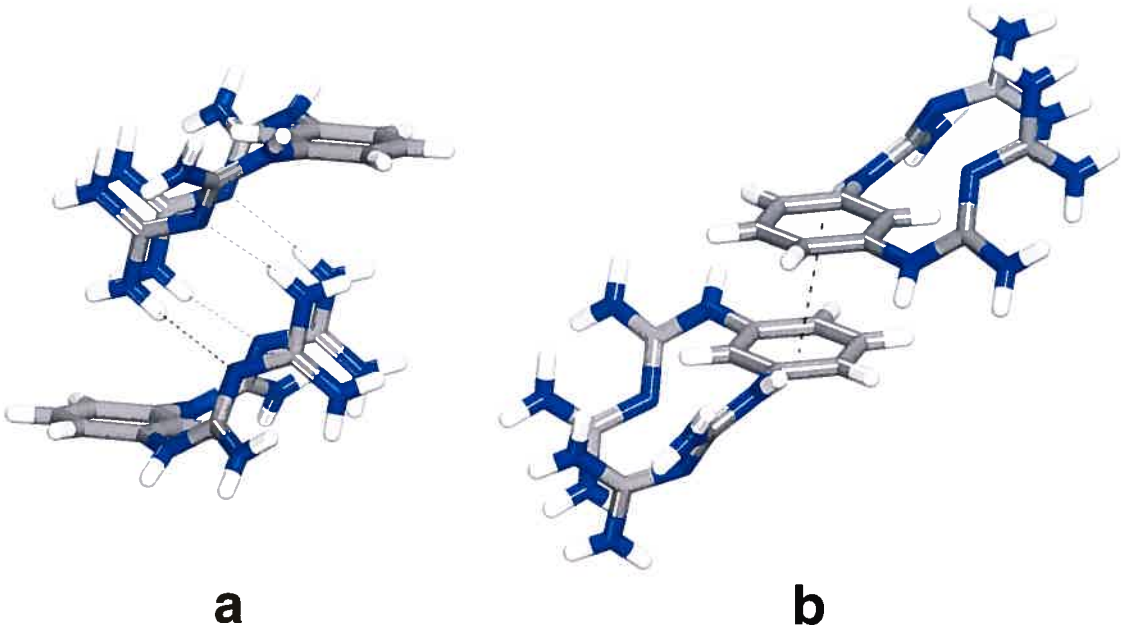

Fig. 3.6. Views of the structure of crystals of the dihydrochloride salt of bis(biguanide) **29** grown from acetone/water. a) The biguanidinium cations favor structure **II** (Scheme 1) and form hydrogen-bonded pairs. b) Addition cohesion is contributed by face-to-face aromatic interactions. Hydrogen bonds and the aromatic interaction are represented by dotted lines, and included water molecules are omitted for simplicity. Hydrogen atoms appear in white, carbon in gray, and nitrogen in blue.

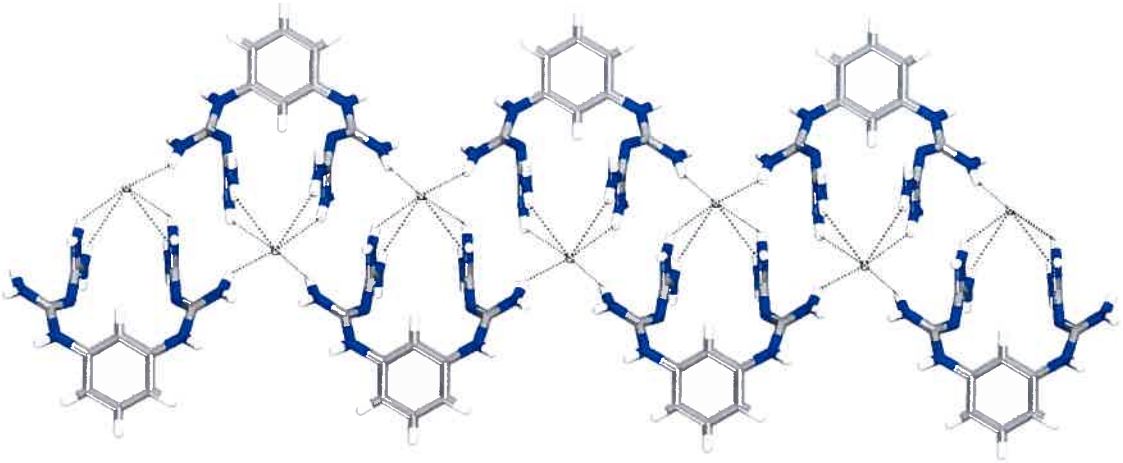

a

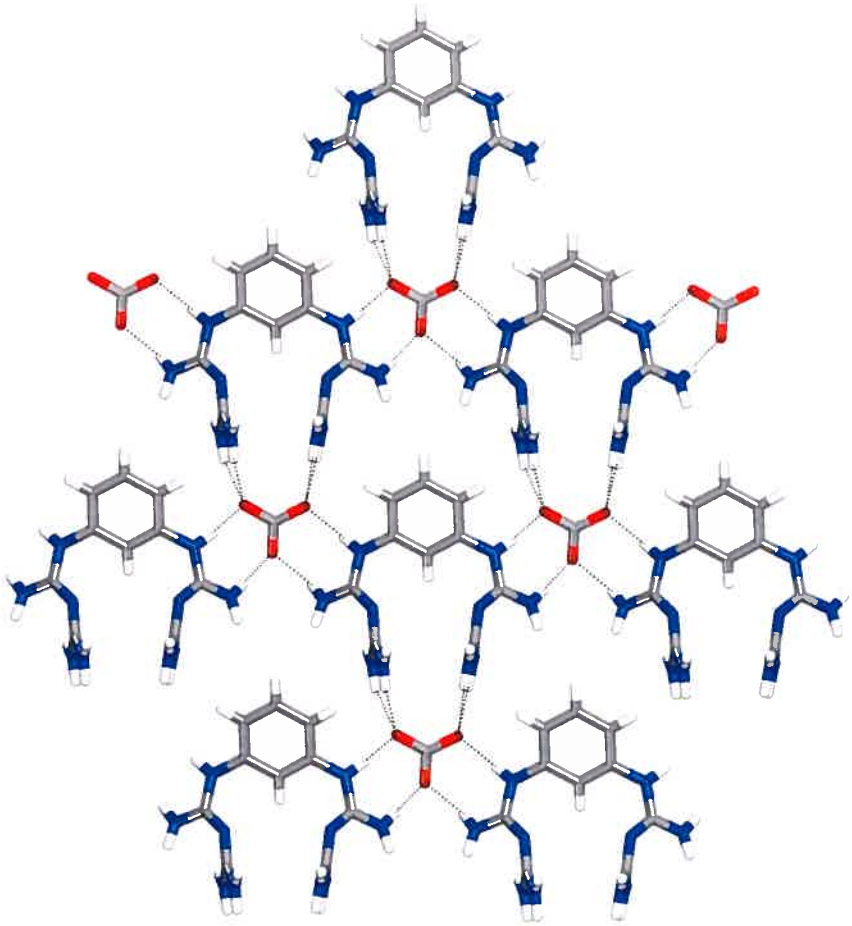

b

Fig. 3.7. a) View along the *c* axis of the structure of crystals of the dihydrochloride salt of bis(biguanide) **29** grown from acetone/water. The view shows a tape constructed by ionic hydrogen bonding involving one of the two types of chloride ions in the structure. Each bis(biguanidinium) dication adopts a pincer-like conformation that permits chelation of chloride by the simultaneous donation of four hydrogen bonds. b) View along the *c* axis of the closely related structure of crystals of the carbonate salt of bis(biguanide) **29** grown from dioxane/water. In both views, hydrogen bonds are represented by broken lines. Hydrogen atoms appear in white, carbon in gray, nitrogen in blue, oxygen in red, and chlorine in green.

3.4 Conclusions

Les biguanides ainsi que leurs sels forment des réseaux cristallins où les molécules s'associent à l'aide de ponts hydrogène selon des motifs prévisibles qui ont déjà été observés. De plus, dans le cas de sels biguanidinium, les contre-ions participent à l'architecture du réseau à l'aide de ponts hydrogène renforcés par des interactions électrostatiques. Par contre, la flexibilité des unités de reconnaissance ainsi que le grand nombre de sites pouvant former des ponts hydrogène limite la prévisibilité des structures cristallines. Dans ce cas précis, il est difficile d'évaluer avec certitude le potentiel des biguanides en tectonique moléculaire étant donné que la petite taille des espaceurs phényles n'est pas représentative des unités centrales normalement utilisées en tectonique moléculaire. Des études plus poussées utilisant des unités centrales plus volumineuses et plus rigides, comme le tétraphénylméthane (**39**), par exemple, devraient s'avérer plus pertinentes.

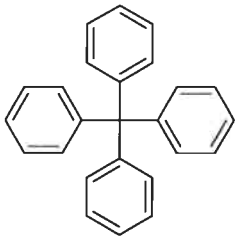

39

Références

1. a) Brown, C.J. *J. Chem. Soc. A* **1967**, 60. b) Ernst, S.R.; Cagle, F.W., Jr. *Acta Crystallogr.* **1977**, *B33*, 235. c) Pinkerton, A.A.; Schwarzenbach, D. *J. Chem. Soc., Dalton Trans.* **1978**, 989. d) Dalpiaz, A.; Ferretti, V.; Gilli, P.; Bertolasi, V. *Acta Crystallogr.* **1996**, *B52*, 509.
2. a) Ernst, S.R. *Acta Crystallogr.* **1977**, *B33*, 237. b) Hariharan, M.; Rajan, S.S.; Srinivasan, R. *Acta Crystallogr.* **1989**, *C45*, 911. c) Zhu, M.; Lu, L.; Yang, P. *Acta Crystallogr.* **2003**, *E59*, o586. d) Lu, L.; Zhang, H.; Feng, S.; Zhu, M. *Acta Crystallogr.* **2004**, *E60*, o640. e) Lu, L.; Zhang, H.; Feng, S.; Zhu, M. *Acta Crystallogr.* **2004**, *C60*, o740. f) Portalone, G.; Colapietro, M. *Acta Crystallogr.* **2004**, *E60*, o1165.

3. a) Coghi, L.; Nardelli, M.; Pelizzi, G. *Acta Crystallogr.* **1976**, *B32*, 842. b) Tada, T.; Kushi, Y.; Yoneda, Y. *Bull. Chem. Soc. Jpn.* **1982**, *55*, 1063. c) Hart, R.O.C.; Bott, S.G.; Atwood, J.L.; Cooper, S.R. *Chem. Commun.* **1992**, 894. d) Das, G.; Bharadwaj, P.K.; Ghosh, D.; Chaudhuri, B.; Banerjee, R. *Chem. Commun.* **2001**, 323. e) Bentefrit, F.; Lemoine, P.; Nguyen-Huy, D.; Morgant, G.; Viossat, B. *Acta Crystallogr.* **2003**, *C59*, m331. f) Lu, L.; Yang, P.; Qin, S.; Zhu, M. *Acta Crystallogr.* **2004**, *C60*, m219.
4. Albescu, I. *Rev. Roum. Chim.* **1973**, *18*, 820.
5. a) Mattew, M.; Kunchur, N.R. *Acta Crystallogr.* **1970**, *B26*, 2054. b) Ward, D.L.; Caughlan, C.N.; Smith, G.D. *Acta Crystallogr.* **1971**, *B27*, 1541. c) Coghi, L.; Pelizzi, G. *Acta Crystallogr.* **1975**, *B31*, 131. d) De, A. *Acta Crystallogr.* **1990**, *C46*, 1004. e) De, A. *J. Crystallogr. Spectrosc. Res.* **1990**, *20*, 279.

Chapitre 4 :

Propriétés gélifiantes des 4,6-diarylamino-1,3,5-triazine-2-carboxylates de sodium

4.1 Formation des gels

La formation des gels par le refroidissement d'une solution sursaturée est un processus similaire à la cristallisation.[1] Par contre, dans le cas de la gélation, l'aggrégation des molécules de soluté se produit plus rapidement selon une dimension, ce qui entraîne la formation de minces fibres qui s'enchevêtrent pour former un réseau qui emprisonne les molécules de solvant à l'intérieur (Figure 4.1).[2] Le gel lui-même est la conséquence macroscopique de ce phénomène, qui requiert dans certains cas de très faibles quantités d'agent gélifiant (moins de 2% poids/poids). Dans le cas de polymères, les fibres sont des chaînes liées de façon covalente,[3] tandis que les gélateurs de bas poids moléculaire forment des fibres à l'aide d'interactions non-covalentes.[4] Bien que les fibres de gélateur possèdent un certain degré d'ordre, ce ne sont pas des objets cristallins, et bien qu'il soit possible de les étudier à l'aide de la diffraction des rayons-X dans un synchrotron,[5] les techniques classiques de cristallographie ne sont d'aucune utilité.

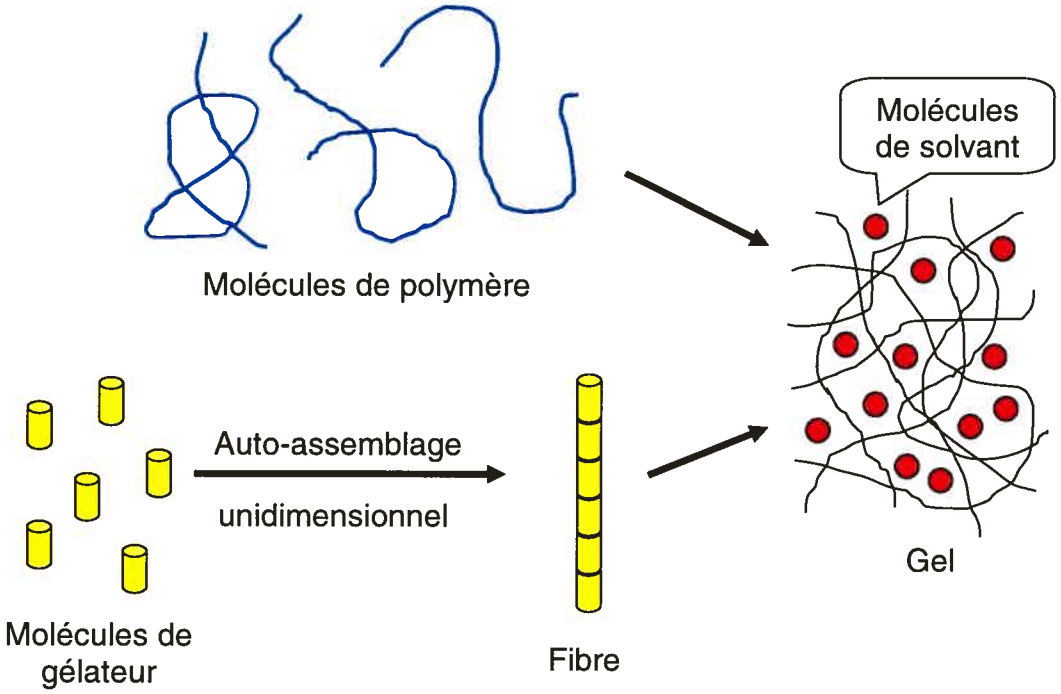

Figure 4.1 Formation des gels à partir du refroidissement de solutions sursaturées. Ci-haut, gélation par des polymères. Ci-dessous, gélation causée par des gélateurs de bas poids moléculaire. Les molécules de gélateur s'auto-assemblent de façon unidimensionnelle par des interactions non-covalentes pour former des fibres.

4.2 Les gélateurs de bas poids moléculaire

Lors du refroidissement d'une solution d'un gélateur de bas poids moléculaire, des fibres unidimensionnelles sont formées à l'aide de plusieurs types différents d'interactions non-covalentes, comme les ponts hydrogène, les interactions de van der Waals, les interactions aromatiques et la coordination aux métaux, par exemple.[6] En règle générale, la présence de groupes fonctionnels participant à au moins deux types d'interactions non-covalentes est requise pour la formation de gels.

Par exemple, les dérivés d'acides aminés **10**, **11** (voir p.8) et **40** peuvent s'associer à l'aide de ponts hydrogène et d'interactions de van der Waals.[7] D'autre part, le dérivé du sorbitol **41** peut former des ponts hydrogène et des interactions aromatiques,[8] tandis que le dialkoxyanthracène **42** s'associe par l'empilement des unités anthracène et de multiples interactions de van der Waals entre les chaînes alkyles.[9]

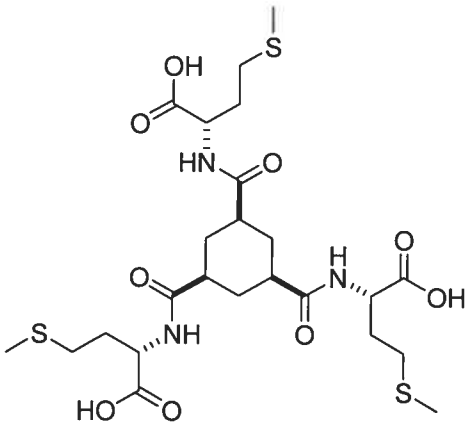

40

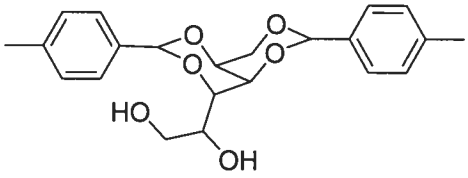

41

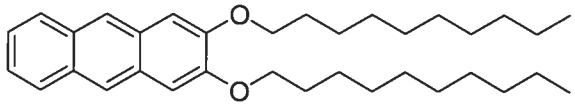

42

Bien que quelques éléments structuraux présents dans plusieurs gélateurs de bas poids moléculaire aient été identifiés, tels que la présence de groupes flexibles, un caractère amphiphile ainsi que la chiralité (qui défavorise la cristallisation), il est encore difficile de prédire si un composé donné possède la capacité de former des gels en se basant sur sa structure moléculaire.[10]

4.3 Caractérisation des gels

La méthode afin de déterminer la capacité d'un composé à former un gel repose en grande partie sur l'observation à l'œil nu. Si le refroidissement d'une solution sursaturée de composé dans un solvant donné entraîne la formation d'une masse gélatineuse qui rigidifie le solvant, il y a de fortes chances que le composé soit un gélateur. Le test de gélation est alors considéré positif s'il est possible de tenir l'échantillon à l'envers sans qu'il n'y ait fuite de solvant (Figure 4.2).[11] La phrase de Dorothy Jordon Lloyd, « *if it looks like Jell-O, it's a gel* »,[12] s'applique encore de nos jours. En variant la concentration de soluté, il est possible de mesurer la concentration minimale afin de former un gel. Plus un gélateur peut former un gel à basse concentration, plus il est efficace.

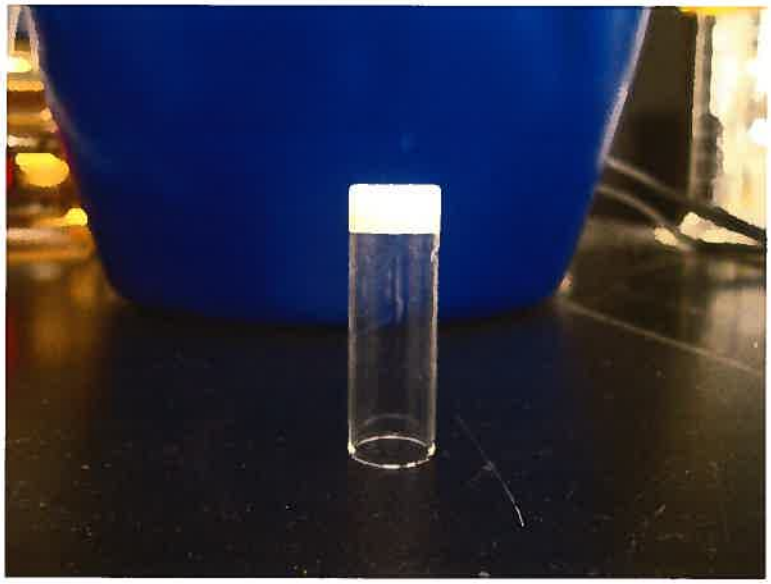

Figure 4.2 Le critère pour qu'un essai de gélation soit considéré comme réussi est que l'échantillon doit pouvoir être renversé sans qu'il n'y ait fuite de solvant ou chute de l'échantillon.

La robustesse d'un gel peut être déterminée grâce à la température de transition sol-gel (T_{gel}), qui correspond à la température où le gel redevient une solution. Deux méthodes sont couramment utilisées pour mesurer la T_{gel} : la méthode de la bille[13] et la calorimétrie différentielle à balayage (DSC, *differential scanning calorimetry*), préférablement en mode modulé.[14] La méthode de la bille (*dropping-ball*) consiste à poser une petite bille d'acier sur l'échantillon de gel et de chauffer lentement. La T_{gel}

mesurée correspond à la température où la bille tombe au fond de l'échantillon. La DSC modulée permet également de mesurer la température où la transition sol-gel se produit. Cette température a l'avantage d'être indépendante de la concentration de gélateur utilisée.

La morphologie des fibres de gélateur peut fournir quelques informations sur la structure des fibres (diamètre, présence de cavités, d'hélices, etc.). Pour ce faire, les échantillons de gel sont habituellement observés à l'aide de différentes techniques de microscopie. Les techniques de microscopie électronique à balayage (SEM, *scanning electron microscopy*)[15] et à transmission (TEM, *transmission electron microscopy*)[16] sont toutes les deux couramment utilisées, et la microscopie à force atomique (AFM, *atomic force microscopy*)[17] est un outil qui s'est ajouté récemment aux techniques disponibles. Par contre, ces trois techniques requièrent la préparation des échantillons par l'évaporation du solvant, ce qui peut potentiellement altérer la structure du réseau de fibres.

Bien que la cristallographie s'avère inefficace afin de déterminer la structure des fibres de gélateur, ces fibres diffractent toutefois les rayons-X, et des informations sur leur structure peuvent être acquises à l'aide de leur spectre de diffraction des poudres.[18] Également, en obtenant la structure cristallographique d'un gélateur cristallisé dans des conditions similaires à celles utilisées pour la formation de gels, il est possible de formuler un modèle quant à la structure au niveau moléculaire des fibres. Cette hypothèse peut ensuite être vérifiée en comparant les spectres de diffraction des poudres de l'échantillon cristallin et de l'échantillon de gel.

4.4 Objectifs

Il existe plusieurs parallèles entre les tectons et les gélateurs de bas poids moléculaire. Tous les deux peuvent s'associer afin de former des suprastructures qui possèdent un certain degré d'ordre. Ces suprastructures sont déterminées par les structures moléculaires des composés ainsi que des conditions dans lesquelles elles sont formées (température, solvant, concentration, etc.). La différence majeure réside dans le

fait que l'auto-assemblage des tectons est tridimensionnel, tandis que les gélateurs s'associent majoritairement selon une dimension. Notre objectif était donc de modifier les principes de la tectonique moléculaire afin de générer des systèmes qui s'associent en une dimension. Cette modification devrait en principe favoriser la formation de gels plutôt que de cristaux.

Dans le cadre de notre exploration des biguanides et de leurs dérivés, nous avons découvert que le sel de sodium de l'acide 4,6-bis(diphénylamino)-1,3,5-triazine-2-carboxylique (**43a**) possède la capacité de former des gels dans le DMSO à de très basses concentrations. Intrigués par ce comportement inhabituel, et par le fait que ce composé présente peu de similitude avec les gélateurs connus, nous avons cherché à synthétiser d'autres composés similaires, à étudier l'effet du contre-ion sur la formation des gels et à examiner la capacité de ces composés à gélifier d'autres solvants. Nous avons également caractérisé les gels obtenus afin d'élucider leur mécanisme de gélation, la morphologie des fibres et leur structure au niveau moléculaire.

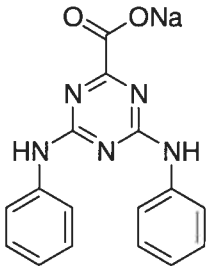

43a

4.5 Article 3 :

A New Class of Selective Low-Molecular-Weight Gelators Based on Salts of Diaminotriazinecarboxylic Acids

Olivier Lebel, Marie-Ève Perron, Thierry Maris, Sylvia F. Zalzal, Antonio Nanci, James D. Wuest. *Chemistry of Materials*, soumis pour publication.

Submitted to *Chem. Mater.*

Version of January 5, 2006

A New Class of Selective Low-Molecular-Weight Gelators Based on Salts of Diaminotriazinecarboxylic Acids

Olivier LeBel,[1,†] Marie-Ève Perron,[†] Thierry Maris,[†] Sylvia F. Zalzal,[‡] Antonio Nanci,[‡] and James D. Wuest*,[†]

[†]*Département de Chimie, Université de Montréal, Montréal, Québec H3C 3J7 Canada*

[‡]*Laboratoire de Recherche sur les Tissus Calcifiés et Biomatériaux, Faculté de Médecine Dentaire, Université de Montréal, Montréal, Québec H3C 3J7 Canada*

Author to whom correspondence may be addressed: [redacted]

Keywords: *low-molecular-weight gelators, crystal engineering, hydrogen bonding, arylaminotriazines*

Abstract

New low-molecular-weight gelators can be discovered by an approach that integrates classical methods for identifying potential gelators with strategies recently developed by crystal engineers to build porous molecular networks. This hybrid approach has yielded a potent new class of selective gelators based on salts of 4,6-diarylamino-1,3,5-triazine-2-carboxylic acids. These compounds lack the high degree of conformational flexibility and long alkyl chains typical of classical gelators, and Na^+ and DMSO play specific roles in the mechanism of gelation. Scanning electron microscopy and atomic force microscopy showed that the resulting gels consist of elemental nanofibers that are approximately 30-100 nm in width, and X-ray diffraction yielded the structure of needle-shaped crystals of a gelator obtained directly from its gel. The crystals are constructed from bilayers, with the hydrophobic aryl groups of the gelators interacting intermolecularly to form the core of the bilayers and polar triazinecarboxylate head groups aligned on the surface. The polar surfaces then stack in a process directed by the formation by multiple intermolecular hydrogen bonds and chelation of Na^+. The hybrid approach that led to the discovery of these gels promises to yield other new molecular materials at the boundary between gels and crystalline solids.

Introduction

Gels are semi-solid materials in which liquids have been immobilized by low concentrations of solutes. The broad utility of gels has made the search for new gelators a very active area of science. Despite this effort, our understanding of the formation of gels remains incomplete, and our ability to correlate the structure of molecules with their ability to form gels is poor. Typically, gelation occurs when solvent is trapped in three-dimensional networks built from suitable solutes. In gels formed by polymeric gelators, the networks arise from the entanglement and interaction of covalently bonded chains, whereas in gels formed by low-molecular-weight gelators, the networks are held together by multiple non-covalent interactions. The behavior of low-molecular-weight gelators is a subject of special interest,[1-3] in part because the networks are derived from fully-defined compounds, thereby allowing detailed structural characterization of the resulting gels.

Potentially instructive but virtually unexplored analogies exist between low-molecular-weight gelators and molecules that interact to form crystalline solid networks in which large quantities of solvent are included.[4] In both materials, solvent is trapped in networks formed reversibly by molecular association. Gelators are typically more effective and can immobilize solvent even at concentrations less than 1% by weight; however, crystalline molecular solids can also include impressive quantities of solvent, with the networks themselves constituting less than 25% by weight in the most impressive examples observed so far.[5] Moreover, porous crystalline networks assembled from suitably flexible molecules are known to be able to change their shape without losing crystallinity, placing their mechanical properties between those of gels and normal rigid solids.[6]

These intriguing analogies call for further exploration of molecular materials that lie at the boundary between gels and crystalline solids. As part of this exploration, we have begun to study the behavior of special hybrid molecules that have structures combining

features of typical gelators with those of compounds predisposed to form porous crystalline networks. In principle, this approach may allow strategies developed by crystal engineers to be used to create new classes of low-molecular-weight gelators.

A particularly promising strategy in crystal engineering is based on the controlled association of molecules that form strong interactions in multiple directions. Such molecules, which have been called tectons from the Greek word for builder,[7,8] tend to crystallize according to reliable directional preferences to form open networks related to those of gels, rather than normal close-packed structures. Tectons can be constructed conveniently by attaching sites of association to suitable molecular cores. Particularly effective sticky sites of association can be derived from 1,3,5-triazine-2,4-diamine (**44**), a compact molecule with multiple sites that can accept and donate hydrogen bonds according to dependable motifs.[5,9] Attaching aminotriazine groups to complex aromatic cores has proven to be a productive source of tectons disposed to crystallize as highly porous hydrogen-bonded networks. This suggested that we might be able to explore the boundary between gels and crystalline solids by studying chimeric low-molecular-weight arylaminotriazines incorporating the following dual features: 1) an amphiphilic structure composed of a hydrophobic aromatic domain and a polar heterocyclic head group, as frequently encountered in the field of gelation; and 2) a relatively compact and rigid structure designed to interact with neighbors according to well-established directional preferences, as typically seen in the field of crystal engineering. We have therefore begun to examine the behavior of low-molecular-weight arylaminotriazines and related compounds with these dual features. This approach has led us to discover that salts of 4,6-diarylamino-1,3,5-triazine-2-carboxylic acids (**45**) define a potent new class of selective gelators.

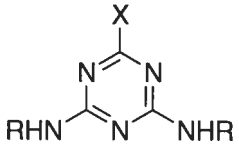

44 (X = H, R = H)

45 (X = COOH, R = aryl)

Experimental Section

Biguanides **30a-i** were prepared by published methods.[10] All other reagents were commercial products that were used without further purification. NMR spectra were recorded at 25 °C unless another temperature is specified.

1,5-Bis(4-iodophenyl)biguanide Hydrochloride (30k • HCl). 4-Iodoaniline (3.04 g, 13.9 mmol) and sodium dicyanimide (0.618 g, 6.94 mmol) were added to a mixture of aqueous HCl (1.00 M, 13.9 mL, 13.9 mmol) and C_2H_5OH (5 mL), and the mixture was heated at reflux for 12 h. The mixture was then cooled to 25 °C, and the resulting precipitate was separated by filtration and dissolved in a small amount of DMF. Toluene was added and the precipitate was filtered, washed with C_2H_5OH, and dried in air. The crude material was then purified by recrystallization from a large volume of hot H_2O. The crystals were dried under vacuum to give 1,5-bis(4-iodophenyl)biguanide hydrochloride (**30k** • HCl; 1.56 g, 2.88 mmol, 41%) as a colorless solid: mp 251-252 °C; ^{1}H NMR (400 MHz, DMSO-d_6) δ 10.21 (s, 2H), 7.64 (d, ^3J = 8.6 Hz, 4H), 7.60 (s, 4H), 7.14 (d, ^3J = 8.6 Hz, 4H); ^{13}C NMR (100 MHz, DMSO-d_6) δ 157.7, 138.9, 138.3, 124.1, 88.9; HRMS (ESI) calcd for $C_{14}H_{14}I_2N_5$ *m/e* 505.9333, found 505.9344. Anal. Calcd for $C_{14}H_{14}ClI_2N_5$: C, 31.05; H, 2.61; N, 12.93. Found: C, 31.11; H, 2.49; N, 12.63.

1,5-Bis[(4-hexyloxy)phenyl]biguanide Hydrochloride (30l • HCl). 4-Hexyloxyaniline (3.00 g, 15.5 mmol) was added to a mixture of aqueous HCl (1.00 M, 15.5 mL, 15.5 mmol) and C_2H_5OH (10 mL). Sodium dicyanimide (0.691 g, 7.76 mmol) was added, and the mixture was heated at reflux for 12 h. The mixture was then cooled to 25 °C, and the resulting precipitate was separated by filtration, washed with ethyl acetate, and dried under vacuum to yield pure 1,5-bis[(4-hexyloxy)phenyl]biguanide hydrochloride (**30l** • HCl; 2.98 g, 6.08 mmol, 78%) as a colorless solid; mp 230-231 °C; ^{1}H NMR (400 MHz, DMSO-d_6) δ 9.77 (s, 2H), 7.31 (s, 4H), 7.19 (d, ^3J = 8.9 Hz, 4H), 6.86 (d, ^3J = 8.9 Hz, 4H), 3.91 (t, ^3J = 7 Hz, 4H), 1.68 (quint, ^3J = 7 Hz, 4H), 1.40 (quint, ^3J = 7 Hz, 4H),

1.29 (m, 8H), 0.87 (t, ^3J = 7 Hz, 6H); ^{13}C NMR (100 MHz, DMSO-d_6) δ 157.9, 156.5, 131.4, 124.7, 115.4, 68.5, 31.9, 29.6, 26.1, 23.0, 14.8; HRMS (ESI) calcd for $C_{26}H_{40}N_5O_2$ *m/e* 454.3177, found 454.3174. Anal. Calcd for $C_{26}H_{40}ClN_5O_2$: C, 63.72; H, 8.23; N 14.29. Found: C, 63.45; H, 8.19; N, 14.15.

Methyl 4,6-Bis(phenylamino)-1,3,5-triazine-2-carboxylate (46a). Dimethyl oxalate (0.354 g, 3.00 mmol) and a solution of $NaOCH_3$ in CH_3OH (25% w/w, 0.01 mL, 0.04 mmol) were added to a solution of 1,5-diphenylbiguanide (**30a**; 0.253 g, 1.00 mmol) in CH_3OH (30 ml), and the mixture was heated at reflux for 12 h. The mixture was then cooled to 25 °C, and H_2O was added until a colorless precipitate formed. The precipitate was separated by filtration, washed with H_2O, and dried under vacuum to provide methyl 4,6-bis(phenylamino)-1,3,5-triazine-2-carboxylate **(46a**; 0.205 g, 0.64 mmol, 64%) as a colorless solid. The product could be used without further purification, but a sample for analysis was obtained by crystallization from toluene: mp 167-168 °C; IR (KBr) 3300-2800 (br), 1750, 1637, 1607, 1582, 1532, 1512, 1480, 1448, 1220, 1019, 757 cm^{-1}; ^{1}H NMR (400 MHz, $CDCl_3$) δ 7.79 (br s, 2H), 7.56 (br d, ^3J = 8 Hz, 4H), 7.34 (t, ^3J = 8 Hz, 4H), 7.15 (t, ^3J = 8 Hz, 2H), 3.93 (s, 3H); ^{13}C NMR (125 MHz, $CDCl_3$, 10°C) δ 164.6, 163.6, 163.4, 137.4, 129.0, 124.7, 121.4, 53.7; HRMS (ESI) calcd for $C_{17}H_{16}N_5O_2$ *m/e* 322.1298, found 322.1297. Anal. Calcd for $C_{17}H_{15}N_5O_2$: C, 63.54; H, 4.71; N. 21.79. Found: C, 63.76; H, 4.59; N, 21.39.

Methyl 4,6-bis(arylamino)-1,3,5-triazine-2-carboxylates **46b-i** were synthesized by analogous procedures.

Methyl 4,6-Bis[(4-methylphenyl)amino]-1,3,5-triazine-2-carboxylate (46b). Yield 84%: mp 156-157 °C; IR (KBr) 3400-2800 (br), 3344, 1745, 1622, 1580, 1508, 1452, 1432, 1411, 1357, 1307, 1228, 1181, 1012, 828, 815, 794 cm^{-1}; ^{1}H NMR (400 MHz, $CDCl_3$) δ 7.75 (s, 2H), 7.43 (d, ^3J = 8.4 Hz, 4H), 7.13 (d, ^3J = 8.4 Hz, 4H), 3.89 (s, 3H), 2.35 (s, 6H); ^{13}C NMR (125 MHz, $CDCl_3$, 10 °C) δ 164.5, 163.6, 163.2, 135.0, 134.1, 129.4, 121.4, 53.5, 21.0; HRMS (ESI) calcd for $C_{19}H_{20}N_5O_2$ *m/e* 350.1611, found

350.1615. Anal. Calcd for $C_{19}H_{19}N_5O_2$: C, 65.32; H, 5.48; N, 20.04. Found: C, 65.43; H, 5.36; N, 19.90.

Methyl 4,6-bis[(4-methoxyphenyl)amino]-1,3,5-triazine-2-carboxylate (46c). Yield 75%: mp 149-150 °C; IR (KBr) 3600-2800 (br), 1752, 1616, 1583, 1536, 1504, 1438, 1418, 1356, 1303, 1247, 1215, 1182, 1034, 1029, 828, 799 cm^{-1}; ^1H NMR (400 MHz, $CDCl_3$) δ 7.73 (s, 2H), 7.41 (d, ^3J = 8.3 Hz, 4H), 6.85 (d, ^3J = 8.5 Hz, 4H), 3.87 (s, 3H), 3.80 (s, 6H); ^{13}C NMR (125 MHz, $CDCl_3$, 10°C) δ 164.5, 163.7, 163.1, 156.6, 130.4, 123.0, 114.0, 55.6, 53.8; HRMS (ESI) calcd for $C_{19}H_{20}N_5O_4$ *m/e* 382.1509, found 382.1508. Anal. Calcd for $C_{19}H_{19}N_5O_4 \bullet 0.5\ H_2O$: C, 58.46; H, 5.16; N, 17.94. Found: C, 57.99; H, 5.06; N, 17.57.

Methyl 4,6-Bis[(4-cyanophenyl)amino]-1,3,5-triazine-2-carboxylate (46d). Yield 69%: mp 281-282 °C; IR (KBr) 3400-2900 (br), 3349, 3308, 2232, 1738, 1610, 1573, 1555, 1501, 1461, 1428, 1416, 1226, 1008, 833, 787 cm^{-1}; ^1H NMR (400 MHz, DMSO-d_6) δ 10.78 (br s, 2H), 7.89 (m, 4H), 7.76 (m, 4H), 3.87 (s, 3H); ^{13}C NMR (100 MHz, DMSO-d_6) δ 164.1, 163.5, 163.0, 143.0, 132.9, 120.2, 119.1, 104.6, 52.8; HRMS (ESI) calcd for $C_{19}H_{14}N_7O_2$ *m/e* 372.1203, found 372.1202. Anal. Calcd for $C_{19}H_{13}N_7O_2 \bullet 0.5\ H_2O$: C, 60.00; H, 3.71; N, 25.78. Found: C, 60.46; H, 3.43; N, 26.00.

Methyl 4,6-Bis[(4-bromophenyl)amino]-1,3,5-triazine-2-carboxylate (46e). Yield 79%: mp 168-169 °C; IR (KBr) 3600-2800 (br), 3279, 1754, 1629, 1598, 1572, 1520, 1485, 1450, 1433, 1402, 1352, 1300, 1219, 1179, 1074, 1009, 822, 788 cm^{-1}; ^1H NMR (400 MHz, DMSO-d_6) δ 10.49 (br s, 2H), 7.64 (m, 4H), 7.52 (d, ^3J = 7.4 Hz, 4H), 3.88 (s, 3H); ^{13}C NMR (100 MHz, DMSO-d_6) δ 164.1, 163.6, 163.3, 138.0, 131.3, 122.6, 115.0, 52.6; HRMS (ESI) calcd for $C_{17}H_{14}Br_2N_5O_2$ *m/e* 477.9508, found 477.9504. Anal. Calcd for $C_{17}H_{13}Br_2N_5O_2 \bullet 0.5\ H_2O$: C, 41.83; H, 2.89; N, 14.35. Found: C, 41.85; H, 2.92; N, 13.94.

Methyl 4,6-Bis[(2-methylphenyl)amino]-1,3,5-triazine-2-carboxylate (46h). Yield 59%: mp 229-230 °C; IR (KBr) 3300-2800 (br), 1752, 1620, 1616, 1575, 1525, 1460,

1442, 1395, 1357, 1221, 748 cm^{-1}; ^1H NMR (400 MHz, $CDCl_3$) δ 7.80 (d, ^3J = 7.7 Hz, 2H), 7.33 (br s, 2H), 7.19 (d, ^3J = 7.5 Hz, 2H), 7.14 (br s, 2H), 7.08 (t, ^3J = 7 Hz, 2H), 3.96 (s, 3H), 2.28 (s, 6H); ^{13}C NMR (125 MHz, $CDCl_3$, 10 °C) δ 165.0, 163.9, 163.7, 135.6, 130.6, 129.7, 126.4, 125.2, 123.6, 53.8, 18.3; HRMS (ESI) calcd for $C_{19}H_{20}N_5O_2$ *m/e* 350.1611, found 350.1610. Anal. Calcd for $C_{19}H_{19}N_5O_2$: C, 65.32; H, 5.48; N 20.04. Found: C, 65.29; H, 5.50; N 20.05.

Methyl 4,6-Bis[(3-methylphenyl)amino]-1,3,5-triazine-2-carboxylate (46i). Yield 78%: mp 138-139 °C; IR (KBr) 3300-2800 (br), 1749, 1629, 1586, 1529, 1488, 1453, 1428, 1353, 1222, 1166, 1030, 780 cm^{-1}; ^1H NMR (400 MHz, $CDCl_3$) δ 7.57 (br s, 2H), 7.36 (m, 4H), 7.23 (t, ^3J = 8 Hz, 2H), 6.96 (d, ^3J = 8 Hz, 2H), 3.98 (s, 3H), 2.33 (s, 6H); ^{13}C NMR (100 MHz, $CDCl_3$) δ 164.6, 163.6, 163.5, 138.9, 137.3, 128.8, 125.3, 121.6, 118.2, 53.6, 21.4; HRMS (ESI) calcd for $C_{19}H_{20}N_5O_2$ *m/e* 350.1611, found 350.1613. Anal. Calcd for $C_{19}H_{19}N_5O_2$: C, 65.32; H, 5.48; N, 20.04. Found: C, 65.06; H, 5.50; N, 19.82.

Methyl 4,6-Bis[(2-bromophenyl)amino]-1,3,5-triazine-2-carboxylate (46j). The crude product was filtered on a short silica pad using ethyl acetate as eluent. Yield 69%: mp 198-199 °C; IR (KBr) 3300-2800 (br), 3224, 3073, 1753, 1610, 1567, 1525, 1440, 1423, 1360, 1286, 1216, 1015, 758, 732 cm^{-1}; ^1H NMR (400 MHz, $CDCl_3$) δ 8.21 (br s, 2H), 7.76 (s, 2H), 7.59 (dd, ^3J = 8 Hz, ^4J = 1 Hz, 2H), 7.29 (m, 2H), 7.02 (dt, ^3J = 8 Hz, ^4J = 1 Hz, 2H), 4.04 (s, 3H); ^{13}C NMR (100 MHz, $CDCl_3$) δ 164.7, 164.3, 163.4, 135.3, 132.7, 127.7, 125.6, 123.7, 115.4, 53.7; HRMS (ESI) calcd for $C_{17}H_{14}Br_2N_5O_2$ *m/e* 477.9508, found 477.9506.

Methyl 4,6-Bis[(3,5-dimethylphenyl)amino]-1,3,5-triazine-2-carboxylate (46k). Yield 96%: T_g 72 °C; IR (KBr) 3400-2800 (br), 1753, 1620, 1588, 1526, 1433, 1344, 1261, 1221, 1163, 1054, 842, 793 cm^{-1}; ^1H NMR (400 MHz, $CDCl_3$) δ 7.63 (s, 2H), 7.13 (s, 4H), 6.77 (s, 2H), 3.93 (s, 3H), 2.26 (s, 12H); ^{13}C NMR (100 MHz, $CDCl_3$) δ 164.6, 163.6, 163.5, 138.6, 137.2, 126.2, 119.0, 53.5, 21.3; HRMS (ESI) calcd for $C_{21}H_{24}N_5O_2$

m/e 378.1924, found 378.1920. Anal. Calcd for $C_{21}H_{23}N_5O_2$: C, 66.83; H, 6.14; N, 18.55. Found: C, 66.86; H, 6.38; N, 18.57.

Methyl 4,6-Bis[(4-iodophenyl)amino]-1,3,5-triazine-2-carboxylate (46f). A solution of $NaOCH_3$ in CH_3OH (25% w/w, 0.80 mL, 3.5 mmol) was diluted with CH_3OH (50 mL), 1,5-bis(4-iodophenyl)biguanide hydrochloride (**30k** • HCl; 1.45 g, 2.68 mmol) was added, and the mixture was stirred at 25 °C for 15 min. Dimethyl oxalate (0.949 g, 8.04 mmol) was then added, and the mixture was heated at reflux for 12 h. The mixture was cooled to 25 °C, and H_2O was added until a white precipitate formed. The precipitate was separated by filtration, washed with H_2O, and dried under vacuum to provide methyl 4,6-bis[(4-iodophenyl)amino]-1,3,5-triazine-2-carboxylate (**46f**; 0.932 g, 1.63 mmol, 61%) as a colorless solid, which could be used without further purification: mp 129-130 °C; ^{1}H NMR (400 MHz, DMSO-d_6) δ 10.45 (s, 2H), 7.65 (br d, ^3J = 8 Hz, 4H), 7.50 (m, 4H), 3.87 (s, 3H); ^{13}C NMR (100 MHz, DMSO-d_6) δ 164.1, 163.5, 163.3, 138.5, 137.1, 122.8, 86.8, 52.6; HRMS (ESI) calcd for $C_{17}H_{14}I_2N_5O_2$ *m/e* 573.9231, found 573.9222. Anal. Calcd for $C_{17}H_{13}I_2N_5O_2$ • 0.5 H_2O: C, 35.08; H, 2.42; N, 12.03. Found: C, 35.52; H, 2.65; N, 11.42.

Methyl 4,6-bis[(4-hexyloxyphenyl)amino]-1,3,5-triazine-2-carboxylate **46g** was synthesized from 1,5-bis[(4-hexyloxy)phenyl]biguanide hydrochloride (**30l** • HCl) by an analogous procedure.

Methyl 4,6-Bis[(4-hexyloxyphenyl)amino]-1,3,5-triazine-2-carboxylate (46g). The crude product was filtered on a short silica pad using acetone as eluent. Yield 96%: mp 127-128 °C; ^{1}H NMR (400 MHz, $CDCl_3$) δ 7.74 (s, 2H), 7.43 (d, ^3J = 8.4 Hz, 4H), 6.87 (d, ^3J = 8.4 Hz, 4H), 3.97 (t, ^3J = 7 Hz, 4H), 3.94 (s, 3H), 1.80 (quint, ^3J = 7 Hz, 4H), 1.49 (m, 4H), 1.36 (m, 8H), 0.93 (t, ^3J = 7 Hz, 6H); ^{13}C NMR (125 MHz, $CDCl_3$, 10 °C) δ 164.5, 163.8, 163.1, 156.1, 130.3, 122.9, 114.5, 68.3, 53.7, 31.7, 29.3, 25.8, 22.7, 14.2; HRMS (ESI) calcd for $C_{29}H_{40}N_5O_4$ *m/e* 522.3075, found 522.3073. Anal. Calcd for $C_{29}H_{39}N_5O_4$ • 0.5 H_2O: C, 65.64; H, 7.60; N, 13.20. Found: C, 65.49; H, 7.63; N, 13.34.

4,6-Bis(phenylamino)-1,3,5-triazine-2-carboxylic acid (47a). Aqueous NaOH (1.0 M, 5.5 mL, 5.5 mmol) was added to a solution of methyl 4,6-bis(phenylamino)-1,3,5-triazine-2-carboxylate (**46a**; 0.176 g, 0.548 mmol) in C_2H_5OH (30 mL), and the mixture was heated at reflux for 3 h. The mixture was then cooled to 25 °C, and aqueous HCl (1.0 M, 10 mL 10 mmol) was added. The resulting precipitate was separated by filtration, washed successively with H_2O and acetone, and dried under vacuum to afford 4,6-bis(phenylamino)-1,3,5-triazine-2-carboxylic acid (**47a**; 0.163 g, 0.530 mmol, 97%) as a colorless solid that required no further purification: mp 275 °C (dec.); IR (KBr) 3300-2700 (br), 1700, 1657, 1610, 1592, 1561, 1498, 1450, 1381, 1341, 1318, 1235, 786, 754, 701 cm^{-1}; ^1H NMR (400 MHz, DMSO-d_6) δ 13.6 (br s, 1H), 10.24 (s, 2H), 7.75 (m, 4H), 7.32 (m, 4H), 7.06 (m, 2H); ^{13}C NMR (100 MHz, DMSO-d_6) δ 165.4, 164.9, 164.2, 138.9, 128.5, 123.1, 120.8; HRMS (ESI) calcd for $C_{16}H_{14}N_5O_2$ *m/e* 308.1142, found 308.1143. Anal. Calcd for $C_{16}H_{13}N_5O_2$: C, 62.53; H, 4.26; N, 22.79. Found: C, 62.08; H, 4.35; N, 22.34.

4,6-Bis(arylamino)-1,3,5-triazine-2-carboxylic acids **47b-k** were synthesized from the corresponding methyl esters **46b-k** by analogous procedures.

4,6-Bis[(4-methylphenyl)amino]-1,3,5-triazine-2-carboxylic acid (47b). Yield 87%: mp 276 °C (dec.); IR (KBr) 3600-2500 (br), 3089, 1695, 1633, 1699, 1546, 1509, 1427, 1376, 1336, 1319, 1235, 1185, 1083, 946, 871, 817, 793 cm^{-1}; ^1H NMR (400 MHz, DMSO-d_6) δ 13.6 (br s, 1H), 10.13 (br s, 2H), 7.59 (m, 4H), 7.12 (d, ^3J = 7.4 Hz, 4H), 2.28 (s, 6H); ^{13}C NMR (100 MHz, DMSO-d_6) δ 165.2, 164.9, 164.1, 136.2, 132.1, 128.9, 120.7, 20.4; HRMS (ESI) calcd for $C_{18}H_{18}N_5O_2$ *m/e* 336.1455, found 336.1456. Anal. Calcd for $C_{18}H_{17}N_5O_2$: C, 64.47; H, 5.11; N, 20.88. Found: C, 63.92; H, 5.11; N, 20.72.

4,6-Bis[(4-methoxyphenyl)amino]-1,3,5-triazine-2-carboxylic acid (47c). Yield 86%: mp 289 °C (dec.); IR (KBr) 3600-2600 (br), 3082, 1693, 1641, 1608, 1565, 1543, 1511, 1424, 1384, 1233, 832, 787 cm^{-1}; ^1H NMR (400 MHz, DMSO-d_6) δ 10.01 (s, 2H), 7.56 (m, 4H), 6.90 (d, ^3J = 8.3 Hz, 4H), 3.74 (s, 6H); ^{13}C NMR (100 MHz, DMSO-d_6) δ

165.0, 164.1, 164.1, 155.3, 131.7, 122.5, 113.6, 55.2; HRMS (ESI) calcd for $C_{18}H_{18}N_5O_4$ *m/e* 368.1353, found 368.1361. Anal. Calcd for $C_{18}H_{17}N_5O_4$: C, 58.85; H, 4.66; N, 19.06. Found: C, 58.70; H, 5.05; N, 19.02.

4,6-Bis[(4-cyanophenyl)amino]-1,3,5-triazine-2-carboxylic acid (47d). Yield 94%: mp 208 °C (dec.); IR (KBr) 3600-2600 (br), 3288, 1724, 1612, 1583, 1503, 1412, 1226, 1178, 834, 786 cm^{-1}; ^1H NMR (400 MHz, DMSO-d_6) δ 10.77 (s, 2H), 7.98 (m, 4H), 7.83 (d, ^3J = 7.8 Hz, 4H); ^{13}C NMR (100 MHz, DMSO-d_6) δ 165.4, 164.4, 164.2, 143.2, 133.0, 120.2, 119.2, 104.6; HRMS (ESI) calcd for $C_{18}H_{12}N_7O_2$ *m/e* 358.1046, found 358.1052. Anal. Calcd for $C_{18}H_{11}N_7O_2 \bullet H_2O$: C, 57.60; H 3.49; N, 26.12. Found: C, 57.87; H, 3.22; N, 26.35.

4,6-Bis[(4-bromophenyl)amino]-1,3,5-triazine-2-carboxylic acid (47e). Yield 95%: mp 290 °C (dec.); IR (KBr) 3500-2600 (br), 3088, 1696, 1614, 1551, 1488, 1422, 1403, 1373, 1234, 1075, 821, 768 cm^{-1}; ^1H NMR (400 MHz, DMSO-d_6) δ 13.7 (br s, 1H), 10.39 (s, 2H), 7.68 (m, 4H), 7.51 (d, ^3J = 8.4 Hz, 4H); ^{13}C NMR (100 MHz, DMSO-d_6) δ 165.3, 164.7, 164.1, 138.2, 131.3, 122.5, 114.9; HRMS (ESI) calcd for $C_{16}H_{12}Br_2N_5O_2$ *m/e* 463.9352, found 463.9349. Anal. Calcd for $C_{16}H_{11}Br_2N_5O_2 \bullet 1/2\ H_2O$: C, 40.53; H, 2.55; N, 14.77. Found: C, 40.48; H, 2.60; N, 14.57.

4,6-Bis[(4-iodophenyl)amino]-1,3,5-triazine-2-carboxylic acid (47f). Yield 85%: mp 389 °C (dec.); ^1H NMR (400 MHz, DMSO-d_6) δ 13.71 (br s, 1H), 10.38 (s, 2H), 7.68 (d, ^3J = 8.3 Hz, 4H), 7.54 (m, 4H); ^{13}C NMR (100 MHz, DMSO-d_6) δ 165.2, 164.7, 164.1, 138.7, 137.1, 122.8, 86.7; HRMS (APPI) calcd for $C_{16}H_{12}I_2N_5O_2$ *m/e* 559.9075, found 559.9098. Anal. Calcd for $C_{16}H_{11}I_2N_5O_2 \bullet H_2O$: C, 33.30; H, 2.27; N, 12.14. Found: C, 32.87; H, 2.10; N, 11.83.

4,6-Bis[(4-hexyloxyphenyl)amino]-1,3,5-triazine-2-carboxylic acid (47g). Yield 90%: mp 464 °C (dec.); ^1H NMR (400 MHz, DMSO-d_6) δ 9.98 (s, 2H), 7.52 (br s, 4H), 6.87 (d, ^3J = 9 Hz, 4H), 3.94 (t, ^3J = 7 Hz, 4H), 1.70 (quint, ^3J = 7 Hz, 4H), 1.41 (quint, ^3J = 7

Hz, 4H), 1.30 (m, 8H), 0.88 (t, ^3J = 7 Hz, 6H); ^{13}C NMR (100 MHz, DMSO-d_6) δ 165.0, 164.0, 164.0, 154.7, 131.5, 122.5, 114.2, 67.5, 31.0, 28.7, 25.2, 22.0, 13.8; HRMS (ESI) calcd for $C_{28}H_{36}N_5O_4$ *m/e* 506.2773, found 506.2785. Anal. Calcd for $C_{28}H_{37}N_5O_4 \bullet H_2O$: C, 63.98; H, 7.48; N, 13.32. Found: C, 63.40; H, 7.48; N, 13.33.

4,6-Bis[(2-methylphenyl)amino]-1,3,5-triazine-2-carboxylic acid (47h). Yield 84%: mp 230 °C (dec.); IR (KBr) 3300-2700 (br), 3099, 1695, 1641, 1619, 1536, 1462, 1397, 1335, 786, 747 cm^{-1}; ^{1}H NMR (400 MHz, DMSO-d_6) δ 13.5 (br s, 1H), 9.33 (s, 2H), 7.37 (m, 2H), 7.18 (m, 2H), 7.11 (m, 2H), 7.07 (m, 2H), 2.19 (s, 6H); ^{13}C NMR (100 MHz, DMSO-d_6) δ 165.8, 165.1, 164.9, 136.2, 132.8, 130.1, 126.2, 125.7, 125.3, 17.9; HRMS (ESI) calcd for $C_{18}H_{18}N_5O_2$ *m/e* 336.1455, found 336.1460. Anal. Calcd for $C_{18}H_{17}N_5O_2 \bullet 1/2\ H_2O$: C, 62.78; H, 5.27; N, 20.34. Found: C, 63.03; H, 5.17; N, 20.27.

4,6-Bis[(3-methylphenyl)amino]-1,3,5-triazine-2-carboxylic acid (47i). Yield 75%: mp 240 °C (dec.); IR (KBr) 3300-2700 (br), 3125, 2919, 1701, 1662, 1618, 1602, 1556, 1486, 1453, 1424, 1372, 1333, 797, 768 cm^{-1}; ^{1}H NMR (400 MHz, DMSO-d_6) δ 13.6 (br s, 1H), 10.15 (s, 2H), 7.52 (m, 4H), 7.20 (t, ^3J = 7.6 Hz, 2H), 6.88 (d, ^3J = 7.2 Hz, 2H), 2.26 (s, 6H); ^{13}C NMR (100 MHz, DMSO-d_6) δ 165.2, 164.8, 164.1, 138.7, 137.7, 128.3, 123.8, 121.2, 117.9, 21.1; HRMS (ESI) calcd for $C_{18}H_{18}N_5O_2$ *m/e* 336.1455, found 336.1454. Anal. Calcd for $C_{18}H_{17}N_5O_2 \bullet 1/4\ H_2O$: C, 63.61; H, 5.19; N, 20.61. Found: C, 63.68; H, 5.19; N, 20.63.

4,6-Bis[(2-bromophenyl)amino]-1,3,5-triazine-2-carboxylic acid (47j). Yield 58%: mp 240 °C (dec.); IR (KBr) 3500-2700 (br), 3408, 3377, 1747, 1723, 1600, 1575, 1513, 1442, 1288, 1237, 1208, 1023, 1001, 786, 746 cm^{-1}; ^{1}H NMR (400 MHz, DMSO-d_6) δ 9.50 (s, 2H), 7.64 (d, ^3J = 7.2 Hz, 2H), 7.57 (d, ^3J = 7.4 Hz, 2H), 7.32 (m, 2H), 7.13 (m, 2H); ^{13}C NMR (100 MHz, DMSO-d_6) δ 166.0, 164.9, 164.89, 136.2, 132.5, 128.2, 127.8, 127.2, 119.8; HRMS (ESI) calcd for $C_{16}H_{12}Br_2N_5O_2$ *m/e* 463.9352, found 463.9347. Anal. Calcd for $C_{16}H_{11}Br_2N_5O_2$: C, 41.32; H, 2.38; N, 15.06. Found: C, 41.11; H, 2.52; N, 14.90.

4,6-Bis[(3,5-dimethylphenyl)amino]-1,3,5-triazine-2-carboxylic acid (47k). Yield 80%: mp 143 °C (dec.); IR (KBr) 3500-2800 (br), 3193, 2922, 1693, 1657, 1622, 1597, 1568, 1539, 1374, 845 cm^{-1}; ^1H NMR (400 MHz, DMSO-d_6) δ 13.6 (br s, 1H), 10.03 (s, 2H), 7.27 (s, 4H), 6.70 (s, 2H), 2.19 (s, 12H); ^{13}C NMR (100 MHz, DMSO-d_6) δ 165.2, 164.9, 164.1, 138.6, 137.4, 124.7, 118.6, 21.0; HRMS (ESI) calcd for $C_{20}H_{22}N_5O_2$ *m/e* 364.1768, found 364.1766. Anal. Calcd for $C_{20}H_{21}N_5O_2 \bullet H_2O$: C, 62.98; H, 6.08; N, 18.36. Found: C, 63.27; H, 6.42; N, 18.48.

Sodium 4,6-Bis(arylamino)-1,3,5-triazine-2-carboxylates 43a-k. 4,6-Bis(arylamino)-1,3,5-triazine-2-carboxylic acids **47a-k** were finely ground and treated at 25 °C with aqueous NaOH (1.0 M). The resulting solids were separated by filtration, washed successively with H_2O and acetone, and dried under vacuum to give pure samples of the corresponding sodium 4,6-bis(arylamino)-1,3,5-triazine-2-carboxylates **43a-k** as colorless solids.

Evaluation of Sodium 4,6-Bis(arylamino)-1,3,5-triazine-2-carboxylates 43a-k as Gelators of DMSO. Appropriate quantities of sodium 4,6-bis(arylamino)-1,3,5-triazine-2-carboxylates **43a-k** were placed in small vials, and DMSO (1 mL) was added. The mixtures were heated at reflux for about 10 sec until homogeneous solutions were formed. The solutions were allowed to stand for 20 min at 25 °C. The vials were then turned upside down, and samples were considered successfully gelled if the solvent was completely immobilized.

Measurement of T_{gel} by Modulated Differential Scanning Calorimetry (DSC).[11] Measurements were made with a TA Instruments Q1000 calorimeter, using a 60 sec period and heating/cooling rates of 2 °C/min from -40 °C to 120 °C. The results reported were recorded after an initial cycle of melting and resolidification.

Measurement of T_{gel} by the Dropping-Ball Method.[12] A sample of gel of fixed volume (1 mL) and known concentration was placed in a standard 15 mm vial, and a

small steel ball (330 mg, 4.4 mm diameter) was suspended on top of the sample. The vial was heated in a thermostatted oil at the rate of 5 °C/min. The temperature at which the ball dropped to the bottom of the gel was recorded as T_{gel}.

Effect of Added Sodium Salts on the Ability of Sodium 4,6-Bis(arylamino)-1,3,5-triazine-2-carboxylates 43a-g to Gel DMSO. To samples of gels of fixed volume (1 mL) and known concentration, various amounts of sodium salts were added, and the mixtures were heated until homogeneous solutions were obtained. The solutions were allowed to stand for 20 min at 25 °C, and the normal criterion was then used to determine whether the resulting material was a gel.

Variable Temperature NMR Spectroscopy. ^{1}H NMR spectra of samples in DMSO-d_6 were recorded on a Bruker AMX-300 spectrometer.

Optical Microscopy. Gels were examined by putting a sample on a microscope slide and placing a cover glass over it. The samples were analyzed on a Linkam LTS 350 heating stage at 25 °C to 200 °C, using a heating rate of 10 °C/min. The samples were examined under polarized light using a BX51 Olympus microscope under dark-field conditions.

Scanning Electron Microscopy. Samples of gels formed by dissolving salts **43a-g** in DMSO (1.5-3.0 mg/mL) were spread on aluminum stubs and observed in the solvated state using a JEOL 6460 LV variable-pressure scanning electron microscope operated at 15-20 kV and 30-50 Pa. For higher-resolution imaging, similar samples were dried under vacuum and examined uncoated using a JEOL 7400F field-emission scanning electron microscope operated at 1 kV.

Atomic Force Microscopy. Gels prepared by dissolving salt **43b** in DMSO (3.0 mg/mL) were spin-cast on quartz. Imaging was carried out in tapping mode using a JEOL JSPM-5200 atomic force microscope in air or under vacuum at ~10^{-6} Torr. Super-sharp silicon tips (SSS-NCHR, Nanosensors, Neuchâtel, Switzerland) with a radius of

curvature of ~2 nm were used to minimize the tip-convolution effect. The software used for manipulating images was WSxM Version 2.2 (Nanotec Electrónica, Madrid).

Crystallization of Sodium 4,6-Bis[(4-methylphenyl)amino]-1,3,5-triazine-2-carboxylate (43b). Crystals suitable for X-ray diffraction were obtained from a gel made by dissolving salt **43b** (5 mg) in DMSO (1 mL) in a vial with a diameter of 15 mm. Tiny needles were produced when the sample was left undisturbed at 25 °C for 2 weeks.

Determination of the Structure of Sodium 4,6-Bis[(4-methylphenyl)amino]-1,3,5-triazine-2-carboxylate (43b) by X-Ray Crystallography. X-ray diffraction data were collected at 100 K with Cu Kα radiation using a Bruker SMART 6000 CCD diffractometer equipped with a rotating anode generator. The structure was solved by direct methods using SHELXS-96 or SHELXS-97 and refined with SHELXL-96 or SHELXL-97.[13] All non-hydrogen atoms were refined anisotropically, whereas hydrogen atoms were placed in ideal positions and refined as riding atoms. Salt **43b** proved to crystallize in the monoclinic space group $P2_1/c$ with $a = 15.8524(3)$ Å, $b = 10.4636(2)$ Å, $c = 15.8729(3)$ Å, $\beta = 105.0208(9)°$, $V = 2542.93(8)$ Å^3, $D_{calcd} = 1.342$ g/cm^3, and $Z = 4$. Full-matrix least-squares refinements on F^2 of 314 parameters led to final residuals $R_1 = 0.0401$ and $wR_2 = 0.0996$ for 4580 reflections with $I > 2\sigma(I)$.

Results and Discussion

Synthesis of Sodium 4,6-Diarylamino-1,3,5-triazine-2-carboxylates 43a-k. Synthesis of the principal compounds investigated is outlined in Scheme 1. Methyl 4,6-diarylamino-1,3,5-triazine-2-carboxylates **46a-k** were prepared by condensing 1,5-diarylbiguanides **30a-i**[10] and **30k-l** with excess dimethyl oxalate in CH_3OH,[14] typically

Scheme 4.1

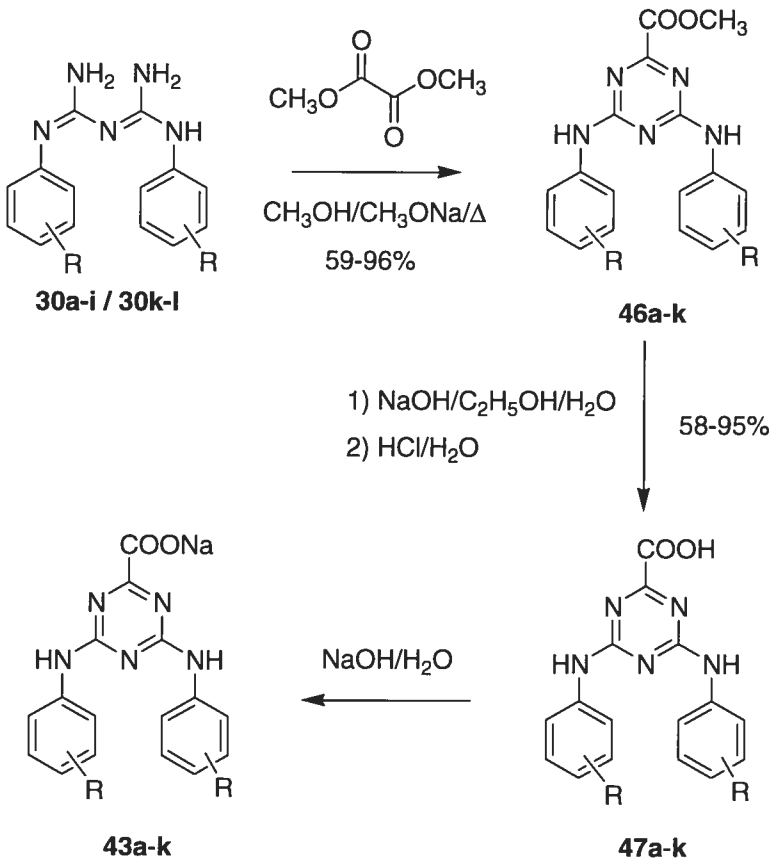

a: R = H	**e**: R = 4-Br	**h**: R = 2-CH_3
b: R = 4-CH_3	**f**: R = 4-I	**i**: R = 3-CH_3
c: R = 4-OCH_3	**g**: R = 4-OC_6H_{13}	**j**: R = 2-Br
d: R = 4-CN		**k**: R = 3,5-CH_3

with added CH_3ONa. In most cases, a catalytic amount of base was sufficient; however, when the aryl groups had strongly electron-withdrawing groups, 1 equiv of base was needed, and when the aryl groups had strongly electron-donating substituents, no base was required. Basic hydrolysis of methyl esters **46a-k**, followed by neutralization, provided the corresponding carboxylic acids **47a-k**, which were then converted into sodium salts **43a-k** by treatment with aqueous NaOH.

Selective Gelation of DMSO by Sodium 4,6-Diarylamino-1,3,5-triazine-2-carboxylates 43a-g. The simple parent compound, sodium 4,6-bis(phenylamino)-1,3,5-triazine-2-carboxylate (**43a**), and its *para*-substituted derivatives **43b-g** all proved to be

highly efficient and selective gelators of DMSO, with minimum gelator concentrations in the range 0.09-0.22% by weight (Table 4.1). In contrast, *ortho*- and *meta*-substituted analogues **43h-k** failed to gel DMSO, even in saturated solutions. Salts **43a**, **43c**, and **43e** also gelled DMF temporarily, but precipitates formed within several hours. Salts **43a-k** all have low solubility in most solvents, so potentially effective concentrations could be attained only in mixtures containing DMSO, DMF, or similar solvents. In tests with a wide range of co-solvents, gelation occurred only in mixtures containing at least 75% DMSO by volume, suggesting that DMSO plays a crucial role in inducing salts **43a-g** to form gels. Esters **46a-k**, free acids **47a-k**, and their salts with Li^+, K^+, Ag^+, NH_4^+, $Me_2NH_2^+$, Me_4N^+, and Bu_4N^+ did not gel any solvents examined, showing the importance of ionic interactions in forming the observed gels and indicating that Na^+ has a special effect. Although the aryl substituents of gelators **43a-g** have both electron-donating and electron-withdrawing substituents, the efficiency of gelation remains similar, establishing that electronic effects are not significant.

Table 4.1. Minimum gelator concentrations for salts **43a-g**.

Gelator	R	Minimum Gelator Concentration			
		mg/mL	mM	wt %	DMSO molecules / gelator molecule
43a	H	2.5	7.6	0.22	1900
43b	4-Me	2.0	5.6	0.18	2600
43c	4-OMe	2.5	6.4	0.22	2200
43d	4-CN	2.0	5.3	0.18	2700
43e	4-Br	1.0	2.1	0.09	7000
43f	4-I	1.0	1.7	0.09	8400
43g	4-OC_6H_{13}	1.5	2.8	0.13	5100

Salts **43a-g** have certain elementary structural features found in many previously identified gelators, including an apolar aryl region and a head group that is ionic and can form multiple hydrogen bonds. In other ways, however, salts **43a-g** are structurally

distinctive and define a new class of low-molecular-weight gelators. In particular, they have a notably low degree of conformational flexibility and do not require the long alkyl chains found in many other gelators. In parent salt **43a**, for example, conformational changes are limited to rotations around a total of five single bonds: two N-Ph bonds and three exocyclic C-C and C-N bonds at the 2, 4, and 6 positions of the triazine core. Few effective gelators with such low degrees of conformational mobility have ever been reported.[15] In these ways, the structures of salts **43a-g** depart significantly from those of conventional gelators and approach closely those of small rigid molecules normally preferred for engineering crystalline solids.

Stability of Gels Formed in DMSO by Sodium 4,6-Diarylamino-1,3,5-triazine-2-carboxylates 43a-g. The observed gels can be disrupted by agitation or heating, but cooling then causes the gels to reform thermoreversibly. If undisturbed, gels formed by solutions of salts **43a** and **43c-g** in DMSO are stable indefinitely, but under suitable conditions salt **43b** can be induced to crystallize slowly from its gel. Modulated differential scanning calorimetry (DSC) was used to measure the temperatures T_{gel} of sol-gel transitions for salts **43a-g** in DMSO,[11] and the results are summarized in Table 4.2. All gelators showed broad endotherms with onset temperatures as low as 30 °C and maxima typically near 70 °C. A representative thermogram, shown in Figure 4.3, reveals that the endotherms are weak and poorly defined, presumably due to the low concentrations of gelators. The corresponding exotherms could not be observed on cooling, but all gels were disrupted by heating to form transparent viscous liquids that reverted to gels when cooled. The dropping-ball method for estimating T_{gel} yielded similar results in most cases (Table 4.2).[12] Figure 4.4 provides values of T_{gel} as a function of the concentration of gelator for the representative case of parent salt **43a**. As expected, T_{gel} rises in an approximately linear manner as the concentration increases, reaching 111 °C at 8.0 mg/mL (0.7 wt %).

Table 4.2. Temperatures of sol-gel transitions (T_{gel}) for salts **43a-g** as measured by modulated differential scanning calorimetry (DSC)[11] and the dropping-ball method.[12] In the DSC measurements, the first value reported corresponds to the onset of the peak, and the second value corresponds to the maximum.

Gelator	R	[Gelator] (mg/mL)	T_{gel} (°C) (DSC)	T_{gel} (°C) (dropping ball)
43a	H	3.0	35-68	74
43b	4-Me	2.5	33-50	47
43c	4-OMe	3.0	35-65	62
43d	4-CN	2.5	30-69	25
43e	4-Br	1.5	40-68	56
43f	4-I	1.5	55-72	53
43g	4-OC_6H_{13}	2.0	40-72	47

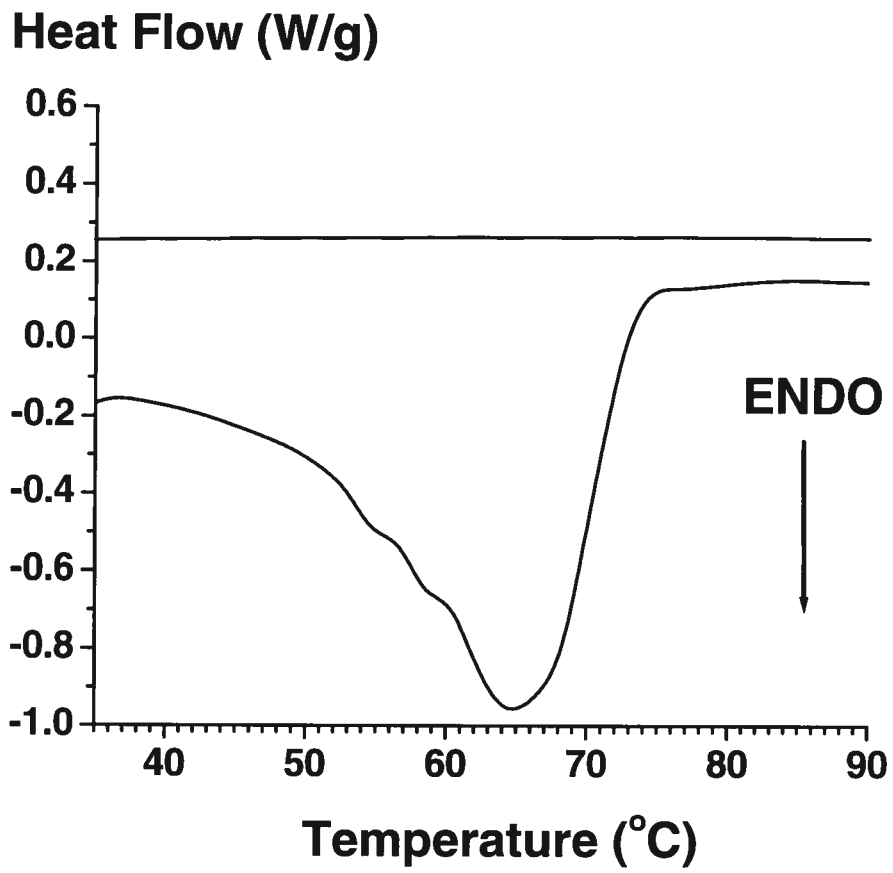

Figure 4.3. Representative thermogram, obtained by modulated differential scanning calorimetry,[11] for the gel formed by dissolving sodium 4,6-diarylamino-1,3,5-triazine-2-carboxylate **43c** in DMSO (3.0 mg/mL). Signals for reversible heat flow, irreversible heat flow, and modulated heat flow are omitted for clarity.

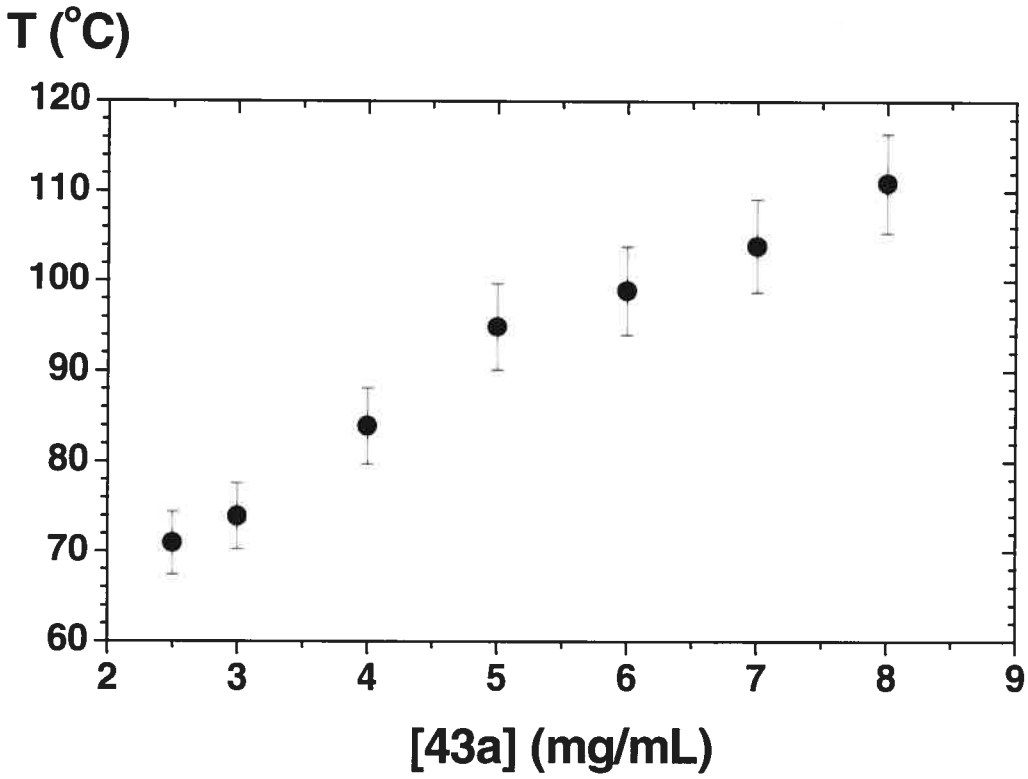

Figure 4.4. T_{gel} as a function of gelator concentration for the gel formed by dissolving sodium 4,6-diarylamino-1,3,5-triazine-2-carboxylate **43a** in DMSO, as measured by the dropping-ball method.[12]

Effect of Added Na^+ on the Stability of Gels Formed in DMSO by Sodium 4,6-Diarylamino-1,3,5-triazine-2-carboxylates 43a-g. The tolerance of the observed gels to added Na^+ was examined by measuring the minimum gelator concentrations as a function of $[Na^+]$. Figure 4.5 provides data for the representative case of parent salt **43a**. These data show that 1) substantial quantities (up to 13 equivalents) of non-basic salts such as NaI, $NaOSO_2CF_3$, and $NaBF_4$ can be added without changing the minimum gelator concentration dramatically and 2) the minimum gelator concentration increases linearly with $[Na^+]$. In contrast, more basic salts such as $NaOOCCH_3$ disrupt gelation at low concentrations, presumably by breaking hydrogen bonds between gelators or by interfering with their ionic interactions with Na^+.

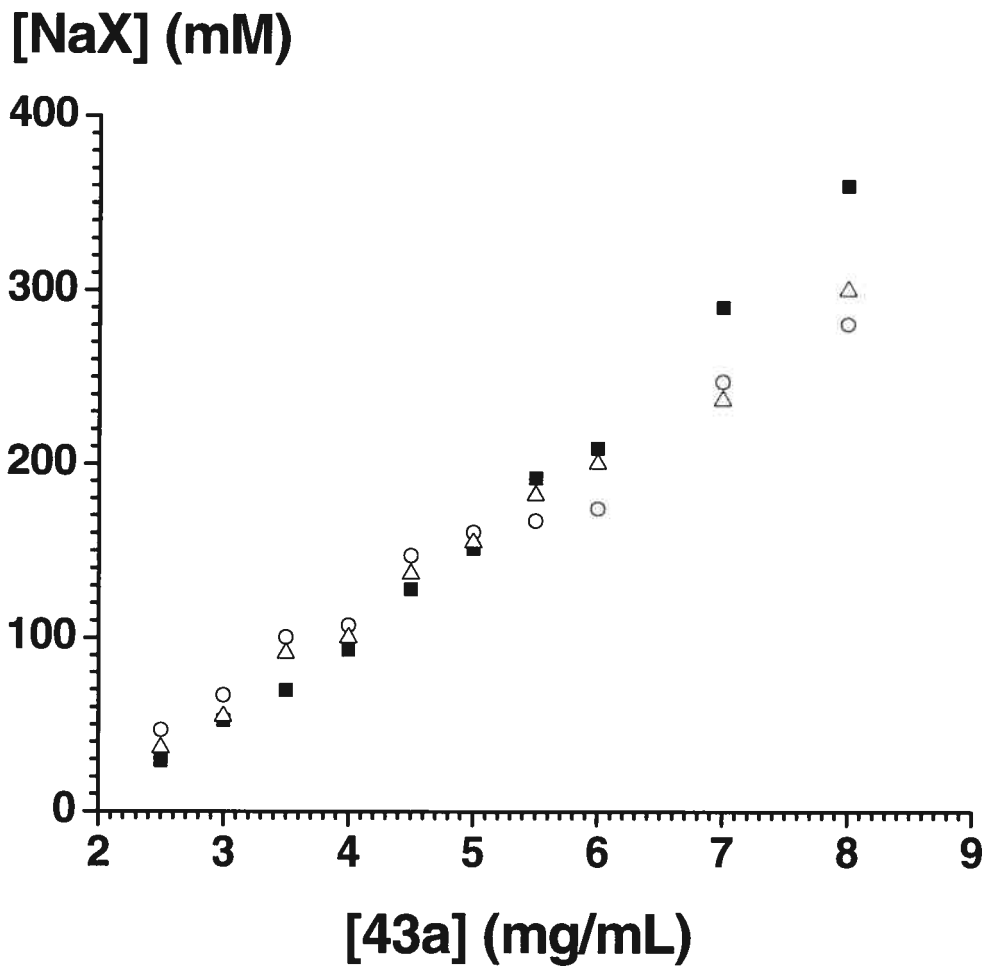

Figure 4.5. Minimum concentrations of sodium 4,6-diarylamino-1,3,5-triazine-2-carboxylate **43a** required to gel DMSO, as a function of the concentration of added NaI (○), $NaOSO_2CF_3$ (■), and $NaBF_4$ (Δ).

Spectroscopic Studies of Gels Formed in DMSO by Sodium 4,6-Diarylamino-1,3,5-triazine-2-carboxylates 43a-g. In a representative study, ^{1}H NMR spectra of samples of parent salt **43a** were recorded in DMSO-d_6 at 27 °C (below T_{gel}), 50 °C (below T_{gel}), 66 °C (near T_{gel}), and 90 °C (above T_{gel}), and the downfield regions are shown in Figure 4.6. Resolution of the aromatic peaks increased with temperature, presumably because rotation around the exocyclic C-NHAr bonds of arylaminotriazine units becomes faster.[10] Pronounced upfield shifts of the N-H signals, from δ 9.71 in the gel (both at 27 °C and 50 °C) to δ 9.37 in solution at 90 °C, are consistent with disrupted hydrogen

bonding, leading to lower ordering of the gelator at higher temperatures. Broad absorption in the N-H stretching region made complementary studies of association by FTIR spectroscopy uninformative.

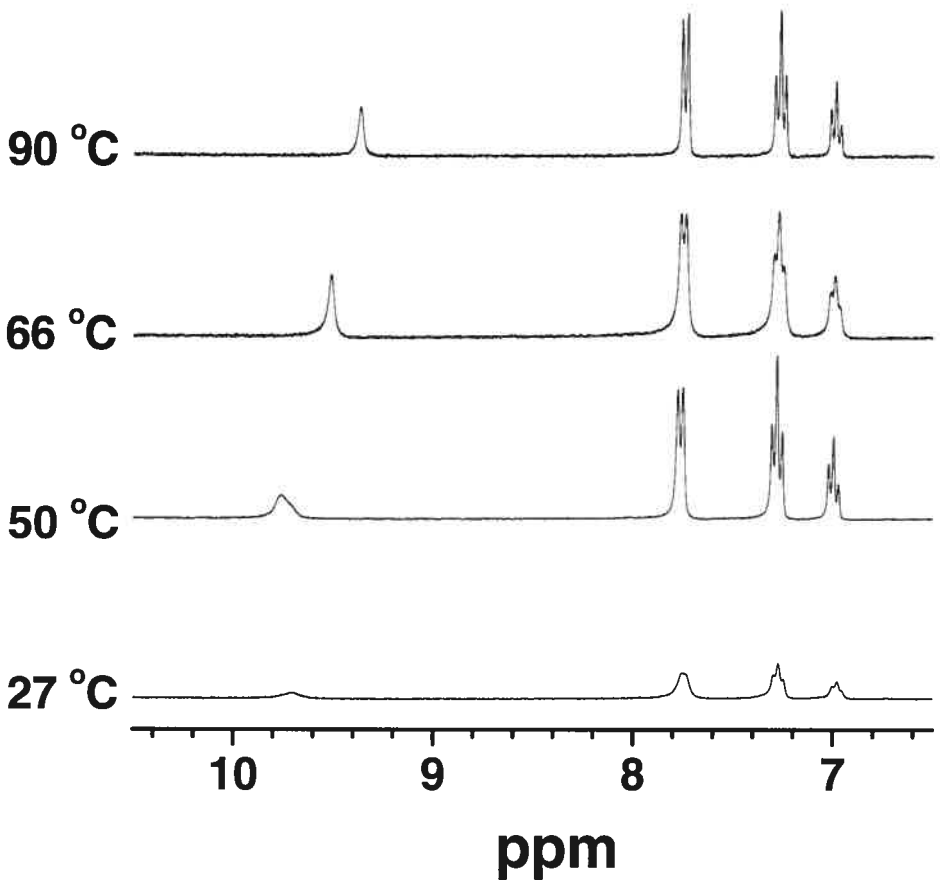

Figure 4.6. Downfield region of ^{1}H NMR spectra of sodium 4,6-diarylamino-1,3,5-triazine-2-carboxylate **43a** in DMSO-d_6 at 27 °C (below T_{gel}), 50 °C (below T_{gel}), 66 °C (near T_{gel}), and 90 °C (above T_{gel}).

Morphology of Gels Formed in DMSO by Sodium 4,6-Diarylamino-1,3,5-triazine-2-carboxylates 43a-g. The morphology of gels produced by sodium 4,6-diarylamino-1,3,5-triazine-2-carboxylates **43a-g** was examined by optical microscopy, variable-pressure scanning electron microscopy (SEM), field-emission SEM, and atomic force microscopy (AFM). Representative micrographs of samples containing parent salt **43a**

are shown in Figures 4.7-4.10, and further images are provided in the Supporting Information. The optical micrograph in Figure 4.7a corresponds to the native gel at 27 °C, and Figure 4.7b shows the appearance after extensive removal of DMSO by evaporation at 200 °C.[16] Under both conditions, the samples contain tight mats of distinct fibers, which are particularly evident on the periphery of the dried sample (Figure 4.7b). The similarity of images obtained under different conditions suggests that the creation of fibrous networks is a characteristic and persistent feature of the self-assembly of salts **43a-g** in DMSO.

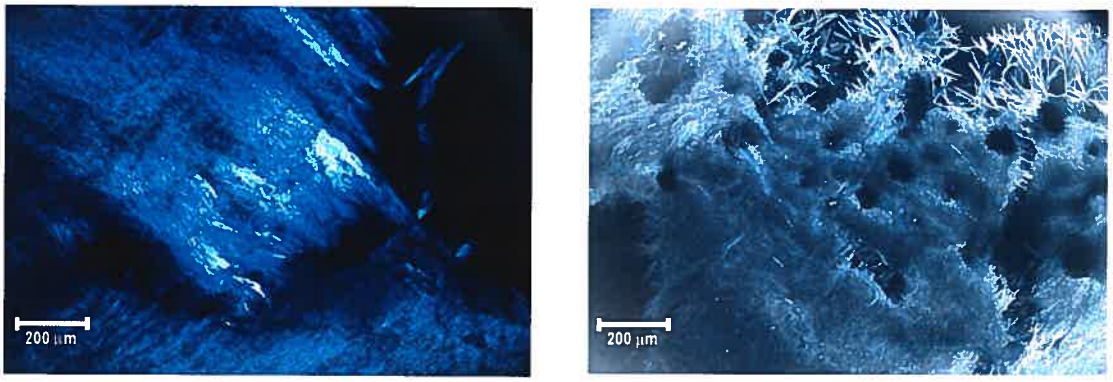

Figure 4.7. a) Dark-field optical micrograph of the native gel formed by a 3.0 mg/mL solution of sodium 4,6-diarylamino-1,3,5-triazine-2-carboxylate **43a** in DMSO at 27 °C. b) Optical micrograph showing a similar sample after extensive removal of DMSO by evaporation at 200 °C.

Additional images of gels produced by dissolving sodium 4,6-diarylamino-1,3,5-triazine-2-carboxylates **43a-g** in DMSO were obtained by variable-pressure SEM under conditions of relatively high pressure (30-50 Pa) to ensure slow evaporation of DMSO and minimal deviation of samples from their native gelled states. Figure 4.8a confirms that parent salt **43a** again forms networks of fibers under these conditions. Figure 4.8b shows the fibers at higher magnification and establishes that they are approximately 0.2 µm in width and 5 µm in length. Variable-pressure SEM micrographs of gels formed by sodium salts **43c** (3.0 mg/mL) and **43e** (1.5 mg/mL) both show similar networks of fibers.[17]

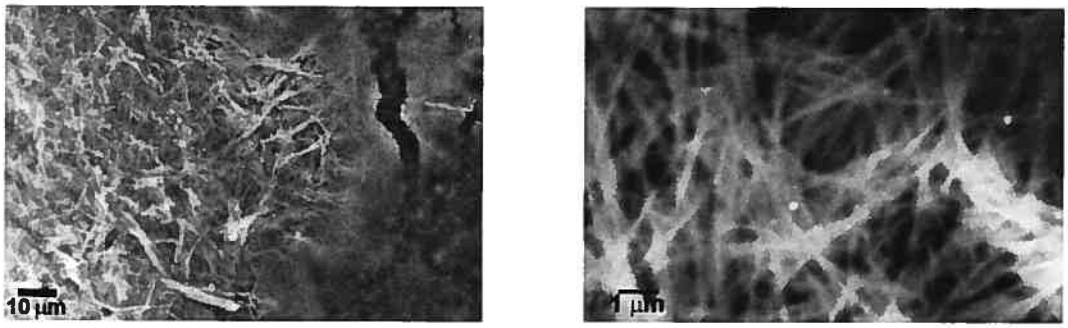

Figure 4.8. Variable-pressure scanning electron micrographs obtained at relatively high pressure (30-50 Pa), showing the fibrous network structure of the gel formed by a 3.0 mg/mL solution of sodium 4,6-diarylamino-1,3,5-triazine-2-carboxylate **43a** in DMSO at 27 °C. Micrographs a) and b) correspond to enlargements of 1000-fold and 10,000-fold, respectively.

More detailed images, obtained by field-emission SEM using uncoated samples (Figure 4.9), confirm that the basic fibrous structure is maintained when the gel is exposed to high vacuum, and they reveal that the coarse fibers shown at low resolution in Figures 4.7-4.8 are in fact spaghetti-like bundles of finer elemental fibers, with widths of about 50-100 nm. Similarly, images obtained by AFM, using samples of gel formed by sodium salt **43b** (3.0 mg/mL) spin-cast on quartz, showed bundles of small fibers approximately 30 nm in diameter (Figure 4.10).

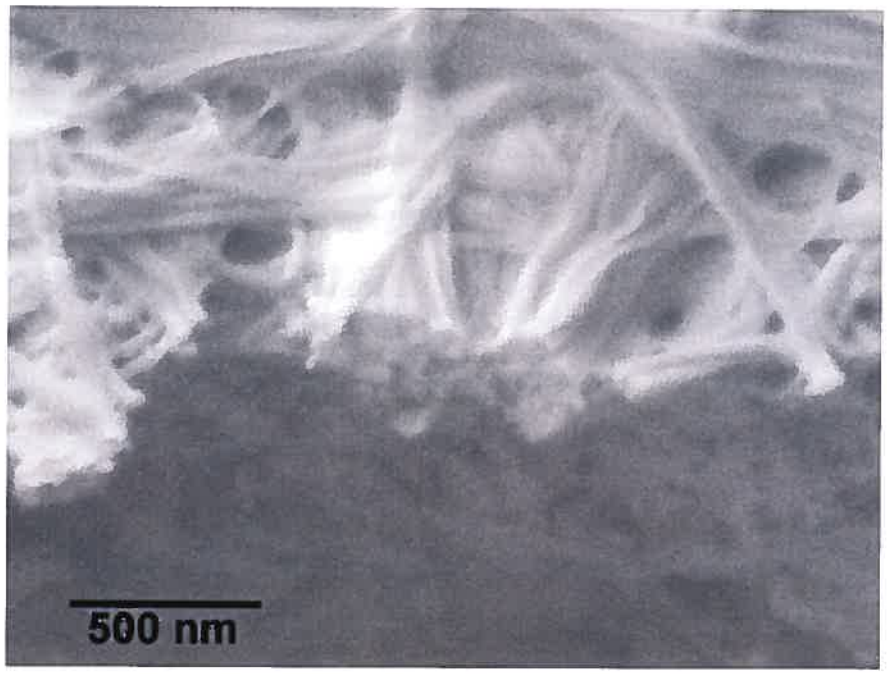

Figure 4.9. Field-emission scanning electron micrograph of an uncoated sample prepared by drying the gel formed by dissolving sodium 4,6-diarylamino-1,3,5-triazine-2-carboxylate **43a** in DMSO (3.0 mg/mL). The image reveals that the fibrous networks shown in Figures 4.7-4.8 are composed of elemental nanofibers.

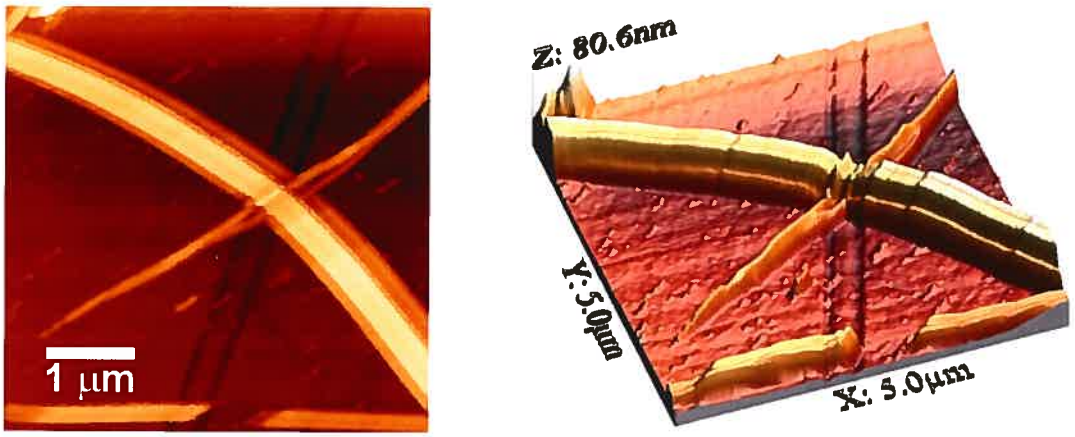

Figure 4.10. Tapping-mode atomic force micrographs of gel fibers spin-cast onto quartz from a 3.0 mg/mL solution of sodium 4,6-diarylamino-1,3,5-triazine-2-carboxylate **43b** in DMSO. The images were recorded under reduced pressure (10^{-6} Torr). Micrographs a) and b) correspond to two- and three-dimensional views of a bundle of fibers. The elemental nanofibers that compose the bundle are approximately 30 nm in diameter.

Crystallization of Sodium 4,6-Diarylamino-1,3,5-triazine-2-carboxylate 43b from DMSO and Determination of its Structure by X-Ray Diffraction. 1,5-Diphenylbiguanide (**30a**) and its monohydrochloride (**30a** • HCl) are amphiphilic molecules that have a close structural relationship to 4,6-diarylamino-1,3,5-triazine-2-carboxylic acids **47a-k**, esters **44a-k**, and salts **43a-k**. Biguanide **30a**, salt **30a** • HCl, and related compounds are known to crystallize to form networks constructed from bilayers, with hydrophobic aryl tails interacting to form the core and polar biguanide head groups aligned on the surface.[10] The bilayers then stack in a process controlled in part by multiple intermolecular hydrogen bonds formed by the biguanide units, which either interact directly (in the case of neutral biguanides) or indirectly via bridging chloride ions (in the case of biguanidinium hydrochlorides). Such molecules therefore incorporate chimeric features expected to give rise to materials near the boundary between gels and crystalline solids. Specifically, they have amphiphilic structures composed of a hydrophobic aromatic domain and a polar head group, as frequently encountered among gelators. On the other hand, they have relatively compact and rigid structures designed to associate with neighbors according to well-established directional interactions, as typically seen in molecules used to engineer crystalline solids with predictable structures.

The structures of analogues **30a** and **30a** • HCl, as well as those of other hydrogen-bonded networks derived from diaminotriazines,[5,9] strongly suggest that the elemental supramolecular nanofibers observed directly by SEM and AFM in gels formed by sodium 4,6-diarylamino-1,3,5-triazine-2-carboxylates **43a-g** are assembled analogously from bilayers held together by the combined forces of hydrogen bonding, aryl interactions, and specific coordination of Na^+. To test this hypothesis, we attempted to grow crystals of salts of 4,6-diarylamino-1,3,5-triazine-2-carboxylic acids and determine their structure. After much effort, we found that we could induce the gel prepared by dissolving sodium salt **43b** in DMSO to deposit crystals of the gelator in the form of tiny needles, which proved to be suitable for X-ray diffraction using an instrument equipped with a rotating anode source and special focusing optics. Obtaining suitable

crystals of a known gelator directly from its gel is a very unusual achievement,[3] and it makes the resulting structure particularly likely to reveal how the gel itself is organized.

Crystals of salt **43b** were found to belong to the monoclinic space group $P2_1/c$ and to correspond to an inclusion compound of composition **43b** • 2 DMSO. Views of the structure appear in Figures 4.11-4.14. Like analogous 1,5-diarylbiguanides and their salts, salt **43b** favors a conformation **I** in which both aryl substituents are directed away from the polar head group, rather than alternatives **II** or **III** (Figure 4.11). The aryl

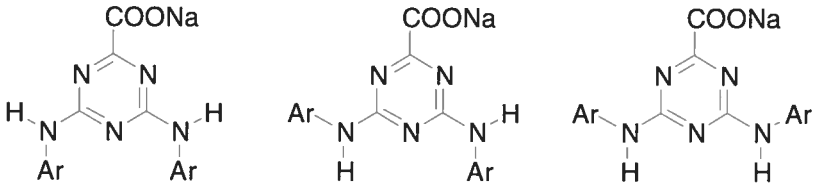

groups in conformation **I** are too far apart to interact intramolecularly, but their orientation enhances the amphiphilic nature of compound **43b** and favors the assembly of bilayers characteristic of analogous biguanides and their salts. As expected, the observed C-N bond lengths are similar to those found in other aminotriazines, the carboxylate group lies close to the plane of the triazine ring (dihedral angle 8.1(1)°), hybridization of the exocyclic N atoms is sp^2, and the N-H and N-Ar bonds in each -NHAr group lie close to the plane of the triazine ring. One of the aryl substituents is essentially coplanar, whereas the other forms an angle of 41.4(1)° with the triazine ring.

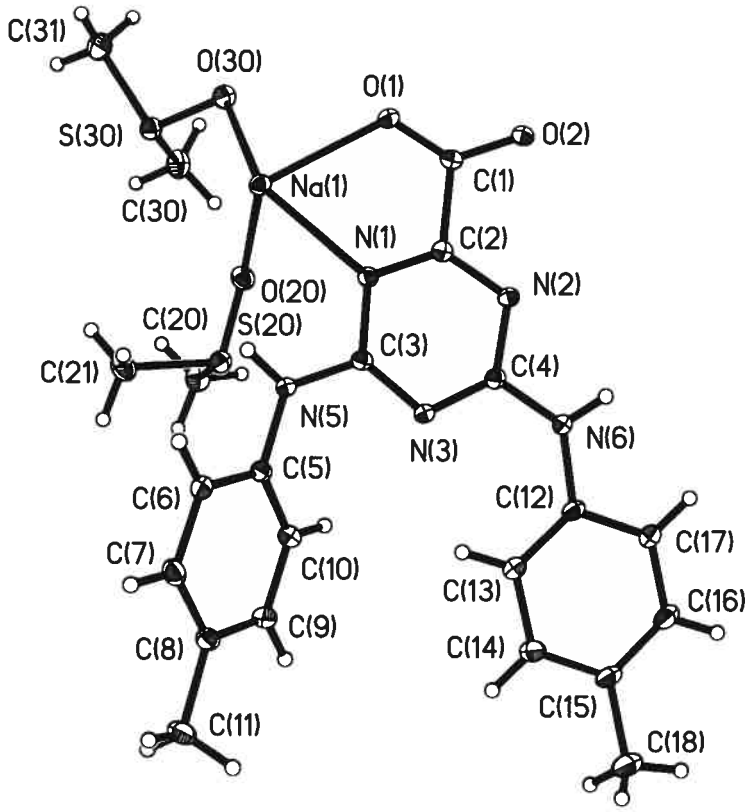

Figure 4.11. View of the structure of sodium 4,6-bis[(4-methylphenyl)amino]-1,3,5-triazine-2-carboxylate (**43b**) when crystallized from the gel it forms in DMSO. Displacement ellipsoids are drawn at the 30% probability level, and hydrogen atoms are represented by spheres of arbitrary radius.

Figure 4.12 confirms that the structure of salt **43b** can be considered to consist of bilayers with polar surfaces and hydrophobic interiors featuring intermolecular aryl interactions similar to those observed in related biguanides and biguanidinium salts.[10] An additional view of the aryl interactions is provided by Figure 4.13. Similar compact arrangements of aryl groups can presumably be attained with the parent salt **43a** and the other *para*-substituted derivatives **43c-g**, but not with *ortho*- and *meta*-substituted analogues. This accounts for the failure of compounds **43h-k** to serve as gelators.

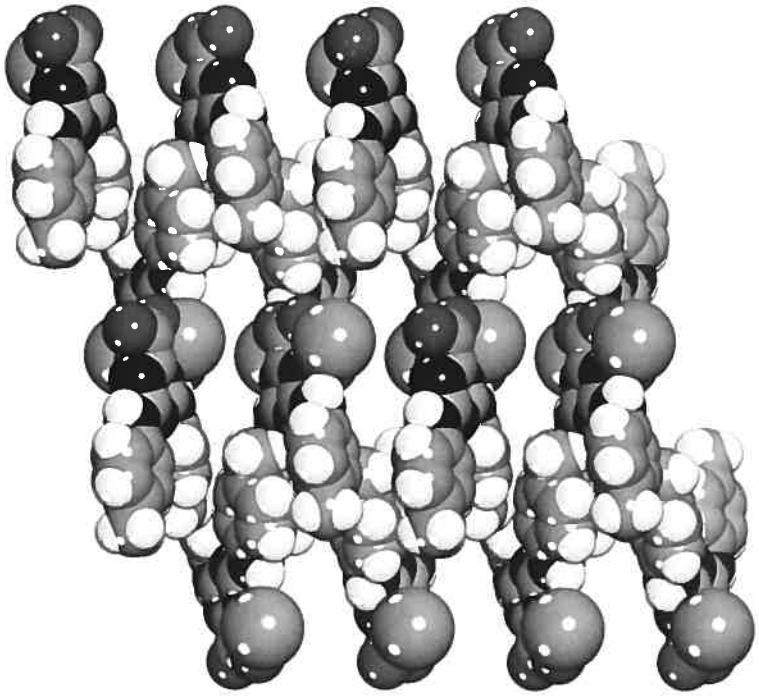

Figure 4.12. View along the *b* axis of the structure of crystals of sodium 4,6-bis[(4-methylphenyl)amino]-1,3,5-triazine-2-carboxylate (**43b**) as obtained from its gel in DMSO. The image reveals distinct bilayers in the *bc* plane, with hydrophobic aryl cores and polar triazinecarboxylate head groups. The view shows a 1 × 1 × 2 array of unit cells with atoms represented by spheres of van der Waals radii. Atoms of hydrogen appear in white, carbon and sodium in light gray, oxygen in dark gray, and nitrogen in black. Molecules of DMSO have been omitted for clarity.

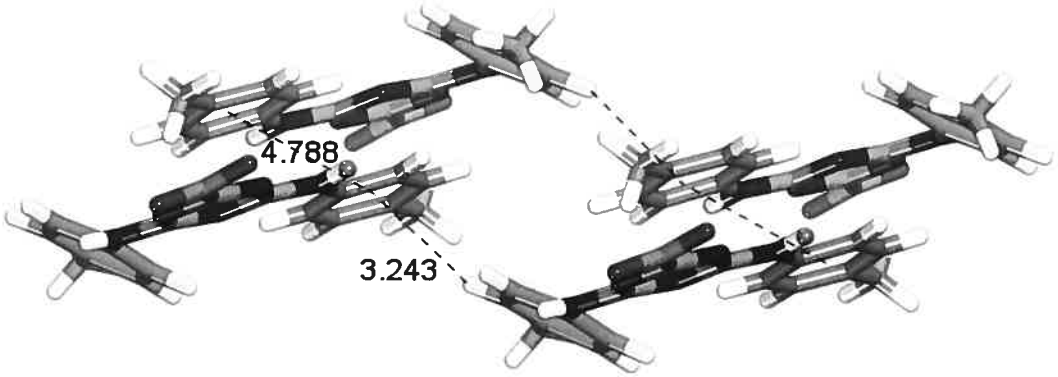

Figure 4.13. View along the *a* axis of the structure of crystals of sodium 4,6-bis[(4-methylphenyl)amino]-1,3,5-triazine-2-carboxylate (**43b**) as obtained from its gel in DMSO. The image provides a detailed view of aromatic interactions in the bilayers. In each molecule, the aryl group closest to the plane of the triazine ring participates in a face-to-face aromatic interaction with the corresponding aryl group of a neighboring molecule. The aryl group that lies out of the plane of the triazine ring engages in an edge-to-face aromatic interaction with the other aryl group of another molecule. Center-to-center and H-to-center distances for the aromatic interactions are shown in Å, and molecules of DMSO have been omitted for clarity.

The bilayers lie perpendicular to the *a* axis, and their polar surfaces stack along the *a* axis in a process directed by the formation of multiple hydrogen bonds and coordination of Na^+ (Figure 4.14). Each Na^+ bridges two molecules of salt **43b**, which serve as bidentate ligands in which Na^+ is chelated by an O atom provided by COO^- and by an adjacent N atom of the triazine ring. In addition, each Na^+ binds two molecules of DMSO (Figure 4.14b). Each carboxylate group interacts with two Na^+ ions and simultaneously accepts an intermolecular hydrogen bond donated by a nearby -NHAr group. The donors are the -NHAr groups with aryl substituents that lie closest to the plane of the triazine ring, and the other -NHAr group of each molecule does not participate in hydrogen bonding. In the resulting structure, the multi-point binding of Na^+, the particular geometry of its chelation, and the inclusion of coordinated DMSO help explain why gelation is selective and occurs only 1) significant quantities of DMSO are present and 2) suitable 4,6-diarylamino-1,3,5-triazine-2-carboxylates are in the form of their Na^+ salts.

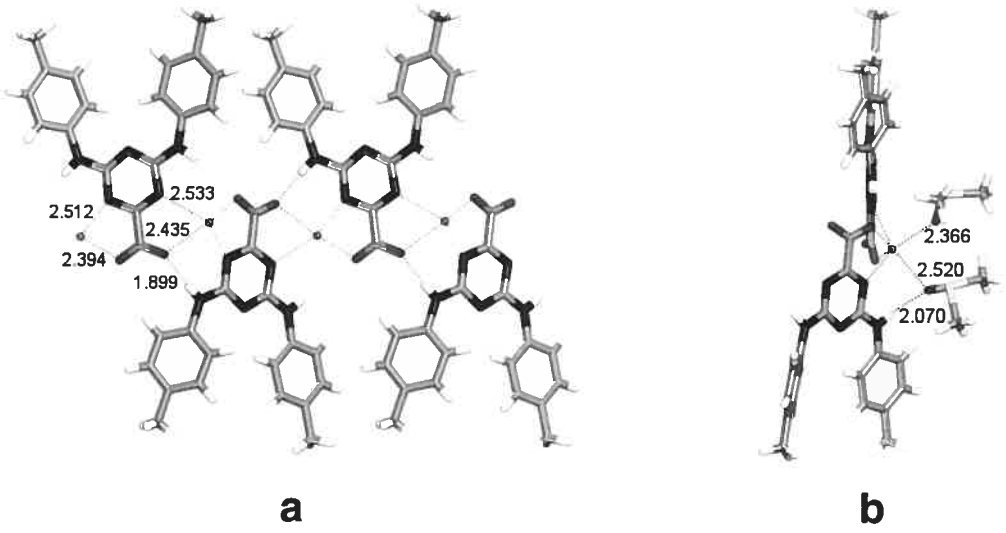

Figure 4.14. a) View along the *c* axis of the structure of crystals of sodium 4,6-bis[(4-methylphenyl)amino]-1,3,5-triazine-2-carboxylate (**43b**) as obtained from its gel in DMSO. The image shows how the polar triazinecarboxylate head groups interact by forming hydrogen bonding and chelating Na^+. The view establishes that these interactions are confined primarily to the *ab* plane. Important O-Na, N-Na, and O···H distances are shown in Å. b) View along the *b* axis, showing how the included molecules of DMSO are bound by hydrogen bonding and coordination to Na^+. Key O-Na and O···H distances are given in Å.

When previous studies of gelation have reported structural studies using single-crystal X-ray diffraction, the crystals investigated have typically been those of gelators grown under conditions where gelation does not occur, or they have been those of non-gelators with related structures. Although such studies are of interest, they do not necessarily reveal the true structure of the gels. In contrast, we have solved the structure of a gelator crystallized directly from its gel. Moreover, the gross structural features observed, including the amphiphilic nature of salt **43b**, its organization in bilayers, and the intermolecular association of its polar head group by hydrogen bonding and ionic interactions, are closely analogous to those observed in a series of related structures. Finally, the observed structure accounts persuasively for every characteristic feature of the gels, including 1) the failure of *ortho*- and *meta*-substituted analogues **43h-k** to serve as gelators; 2) the selective gelation of DMSO; and 3) the need for Na^+ salts of 4,6-diarylamino-1,3,5-triazine-2-carboxylates. The ability of the observed structure to account for these features suggests that the crystals and the native gel have closely similar architectures.

Unfortunately, we were unable to establish an unambiguous correlation between the structure of salt **43b**, as determined by single-crystal X-ray diffraction, and that of its gel, as revealed by studies using X-ray powder diffraction under various conditions. In the native gel, low crystallinity and scattering from retained DMSO prevented us from obtaining useful data, whereas dried samples gave inconsistent powder diffraction patterns, presumably because molecules of DMSO critical for maintaining crystallinity were lost. Nevertheless, features that appear in the structure of sodium 4,6-diarylamino-1,3,5-triazine-2-carboxylate **43b** account neatly for the characteristic morphology of the gels formed by all salts **43a-g**. In particular, growth of crystals with the characteristic bilayer structure shown in Figure 4.12 may be relatively slow in the *a* and *b* directions, which are especially rich in sites for hydrogen bonding, coordination of Na^+, and interaction with DMSO. Figure 4.14 reveals that the aryl groups are largely confined to the *ab* plane, making the corresponding surface one of high energy in DMSO and favoring the formation of fibers by rapid growth along *c*. As a result, we suggest that the elemental nanofibers observed by field-emission SEM and AFM have a similar internal

structure and that their characteristic morphology results logically from the need to minimize surfaces most weakly solvated by DMSO. The widths of the nanofibers (which correspond to slow growth along the *a* and *b* axes) are equivalent to approximately 50 unit cells, and their lengths (which result from fast growth along the *c* axis) typically exceed 1000 unit cells. Partial desolvation of the polar surfaces perpendicular to the *c* axis should create potential points of junction where the fibers can associate by hydrogen bonding and coordination of Na^+, leading to the formation of cross links and aggregation in bundles, as shown in Figures 4.9-4.10. These correlations give further support to the notion that the structures of the crystal and the gels are closely related.

Conclusions

Our work demonstrates how new low-molecular-weight gelators can be discovered by an approach that integrates classical methods for identifying potential gelators with strategies recently developed by crystal engineers to build porous molecular networks. This hybrid approach has yielded a new class of gelators based on salts of diaminotriazinecarboxylic acids. These compounds do not require the high degree of conformational flexibility and long alkyl chains found in many other gelators, and their mechanism of gelation shows a selective dependence on Na^+ and DMSO. We have acquired a detailed understanding of the morphology and underlying molecular structure of the resulting gels by using a combination of microscopy and X-ray diffraction, which has allowed us to solve the structure of crystals of a gelator obtained directly from its gel. The hybrid approach that led to the discovery of these gelators promises to yield other new molecular materials at the boundary between gels and crystalline solids.

Acknowledgments. We are grateful to the Natural Sciences and Engineering Research Council of Canada, the Ministère de l'Éducation du Québec, the Canada Foundation for Innovation, and the Canada Research Chairs Program for financial support. In addition, we thank Prof. Jurgen Sygusch for providing access to a Bruker SMART 6000 CCD diffractometer equipped with a rotating anode. We are also grateful to Dr. Alexandra

Furtos for obtaining mass spectra and to Dr. Ji-Hyun (Daniel) Yi for recording AFM images.

Supporting Information Available: Additional SEM and AFM images and further crystallographic details, including ORTEP drawings and tables of crystallographic data, atomic coordinates, anisotropic thermal parameters, and bond lengths and angles for sodium 4,6-bis[(4-methylphenyl)amino]-1,3,5-triazine-2-carboxylate (**43b**). This material is available free of charge via the Internet at http://pubs.acs.org.

Notes and References

(1) Sangeetha, N. M.; Maitra, U. *Chem. Soc. Rev.* **2005**, *34*, 821-836. Estroff, L. A.; Hamilton, A. D. *Chem. Rev.* **2004**, *104*, 1201-1217. van Esch, J. H.; Feringa, B. L. *Angew. Chem., Int. Ed.* **2000**, *39*, 2263-2266. Abdallah, D. J.; Weiss, R. G. *Adv. Mater.* **2000**, *12*, 1237-1247. Terech, P.; Weiss. R. G. *Chem. Rev.* **1997**, *97*, 3133-3159.

(2) For recent studies of low-molecular-weight gelators, see: Shirakawa, M.; Fujita, N.; Shinkai, S. *J. Am. Chem. Soc.* **2005**, *127*, 4164-4165. Mohmeyer, N.; Schmidt, H.-W. *Chem. Eur. J.* **2005**, *11*, 863-872. Moniruzzaman, M.; Sundararajan, P. R. *Langmuir* **2005**, *21*, 3802-3807. Bhuniya, S.; Park, S. M.; Kim, B. H. *Org. Lett.* **2005**, *7*, 1741-1744. Suzuki, M.; Sato, T.; Kurose, A.; Shirai, H.; Hanabusa, K. *Tetrahedron Lett.* **2005**, *46*, 2741-2745. Trivedi, D. R.; Ballabh, A.; Dastidar, P. *J. Mater. Chem.* **2005**, *15*, 2606-2614. Griffiths, P. C.; Côte, M.; James, R.; Rogueda, P. G.; Morgan, I. R.; Knight, D. W. *Chem. Commun.* **2005**, 3998-4000. Brosse, N.; Barth, D.; Jamart-Grégoire, B. *Tetrahedron Lett.* **2004**, *45*, 9521-9524. van Bommel, K. J. C.; van der Pol, C.; Muizebelt, I.; Friggeri, A.; Heeres, A.; Meetsma, A.; Feringa, B. L.; van Esch, J. *Angew. Chem., Int. Ed.* **2004**, *43*, 1663-1667. Čaplar, V.; Žinić, M.; Pozzo, J.-L.;

Fages, F.; Mieden-Gundert, G.; Vögtle, F. *Eur. J. Org. Chem.* **2004**, 4048-4059. George, M.; Snyder, S. L.; Terech, P.; Glinka, C. J.; Weiss, R. G. *J. Am. Chem. Soc.* **2003**, *125*, 10275-10283. Babu, P.; Sangeetha, N. M.; Vijaykumar, P.; Maitra, U.; Rissanen, K.; Raju, A. R. *Chem. Eur. J.* **2003**, *9*, 1922-1932. Wang, G.; Hamilton, A. D. *Chem. Commun.* **2003**, 310-311. Hashimoto, M.; Ujiie, S.; Mori, A. *Adv. Mater.* **2003**, *15*, 797-800. Maji, S. K.; Malik, S.; Drew, M. G. B.; Nandi, A. K.; Banerjee, A. *Tetrahedron Lett.* **2003**, *44*, 4103-4107. Schmidt, R.; Adam, F. B.; Michel, M.; Schmutz, M.; Decher, G.; Mésini, P. J. *Tetrahedron Lett.* **2003**, *44*, 3171-3174.

(3) Kumar, D. K.; Jose, D. A.; Das, A.; Dastidar, P. *Chem. Commun.* **2005**, 4059-4061.

(4) For previous work that reports initial exploration of the relationship between designing gels and engineering porous crystalline solids, see: Kumar, D. K.; Jose, D. A.; Dastidar, P.; Das, A. *Chem. Mater.* **2004**, *16*, 2332-2335. Carr, A. J.; Melendez, R.; Geib, S. J.; Hamilton, A. D. *Tetrahedron Lett.* **1998**, *39*, 744-7450.

(5) Malek, N.; Maris, T.; Simard, M.; Wuest, J. D. *J. Am. Chem. Soc.* **2005**, *127*, 5910-5916. Fournier, J.-H.; Maris, T.; Wuest, J. D. *J. Org. Chem.* **2004**, *69*, 1762-1775.

(6) Saied, O.; Maris, T.; Wuest, J. D. *J. Am. Chem. Soc.* **2003**, *125*, 14956-14957.

(7) Simard, M.; Su, D.; Wuest, J. D. *J. Am. Chem. Soc.* **1991**, *113*, 4696-4697.

(8) Wuest, J. D. *Chem. Commun.* **2005**, 5830-5837.

(9) Laliberté, D.; Maris, T.; Demers, E.; Helzy, F.; Arseneault, M.; Wuest, J. D. *Cryst. Growth Des.* **2005**, *5*, 1451-1456. Demers, E.; Maris, T.; Wuest, J. D. *Cryst. Growth Des.* **2005**, *5*, 1227-1235. Laliberté, D.; Maris, T.; Wuest, J. D. *J. Org. Chem.* **2004**, *69*, 1776-1787. Laliberté, D.; Maris, T.; Sirois, A.; Wuest, J. D. *Org. Lett.* **2003**, *5*, 4787-4790. Sauriat-Dorizon, H.; Maris, T.; Wuest, J. D.; Enright, G. D. *J. Org. Chem.* **2003**, *68*, 240-246. Brunet, P.; Demers, E.; Maris,

T.; Enright, G. D.; Wuest, J. D. *Angew. Chem., Int. Ed.* **2003**, *42*, 5303-5306. Le Fur, E.; Demers, E.; Maris, T.; Wuest, J. D. *Chem. Commun.* **2003**, 2966-2967.

(10) LeBel, O.; Maris, T.; Duval, H.; Wuest, J. D. *Can. J. Chem.* **2005**, *83*, 615-626.

(11) Reading, M.; Luget, A.; Wilson, R. *Thermochim. Acta* **1994**, *238*, 295-307.

(12) Takahashi, A.; Sakai, M.; Kato, T. *Polymer J.* **1980**, *12*, 335-341.

(13) Sheldrick, G. M. SHELXS-97, Program for the Solution of Crystal Structures and SHELXL-97, Program for the Refinement of Crystal Structures; Universität Göttingen: Germany, 1997.

(14) Overberger, C. J.; Shapiro, S. L. *J. Am. Chem. Soc.* **1954**, *76*, 93-96.

(15) For selected examples, see: Yoza, K.; Ono, Y.; Yoshihara, K.; Akao, T.; Shinmori, H.; Takeuchi, M.; Shinkai, S.; Reinhoudt, D. N. *Chem. Commun.* **1998**, 907-908. Vassilev, V. P.; Simanek, E. E.; Wood, M. R.; Wong, C.-H. *Chem. Commun.* **1998**, 1865-1866. Hanabusa, K.; Matsumoto, Y.; Miki, T.; Koyama, T.; Shirai, H. *Chem. Commun.* **1994**, 1401-1402.

(16) Analysis by ^{1}H NMR spectroscopy confirmed that sodium 4,6-diarylamino-1,3,5-triazine-2-carboxylates did not decompose during the formation of xerogels.

(17) For additional images, see the Supporting Information.

4.6 Conclusions

Les 4,6-bis(arylamino)-1,3,5-triazine-2-carboxylates de sodium représentent une nouvelle classe de gélateurs de bas poids moléculaire possédant des éléments structuraux et un mode d'association différents de ceux des gélateurs connus. Nos gélateurs se sont avérés d'une grande efficacité malgré le fait qu'ils peuvent seulement former des gels dans le DMSO ou des mélanges de solvants contenant du DMSO. Des études de microscopie ont démontré que ces composés forment des faisceaux de minces fibres d'un diamètre d'environ 25 à 30 nm. La structure cristallographique de l'un des gélateurs nous a également permis de proposer un modèle de l'assemblage au niveau moléculaire de ces fibres où les molécules forment des rubans par chélation au Na^+. Par la suite, ces rubans s'empilent pour former des bicouches à l'aide d'interactions aromatiques. Le fait que seuls les composés substitués en position 4- des groupes phényles et que seuls les sels de sodium forment des gels appuient cette hypothèse. Bien que l'aspect fondamental de ces gels ait été en grande partie l'objectif principal de cette étude, plusieurs applications pourraient découler de ce projet. Étant donné leur grande tolérance à la présence de sels de sodium, nos gels pourraient être utiles comme électrolytes semi-solides.[9,19] Il serait également possible de fonctionnaliser les groupes phényles afin d'élaborer des systèmes fonctionnels où l'auto-assemblage des molécules génère de nouveaux matériaux partiellement ordonnés, comme des matériaux photochromiques, par exemple.[20]

Références

1. Bradford, S.C. *Biochem. J.* **1921**, *15*, 553.
2. a) Hanabusa, K.; Yamada, M.; Kimura, M.; Shirai, H. *Angew. Chem. Int. Ed. Engl.* **1996**, *35*, 1949. b) van Esch, J.; De Feyter, S.; Kellogg, R.M.; De Schryver, F.; Feringa, B.L. *Chem. Eur. J.* **1997**, *3*, 1238. c) de Loos, M.; van Esch, J.; Kellogg, R.M.; Feringa, B.L. *Angew. Chem. Int. Ed.* **2001**, *40*, 613. d) Mieden-Gundert, G.; Klein, L.; Fischer, M.; Vögtle, F.; Heuze, K.; Pozzo, J.-L.; Vallier, M.; Fages, F. *Angew. Chem. Int. Ed.* **2001**, *40*, 3164.
3. Voir par exemple : Osada, Y. *Adv. Mater.* **1991**, *3*, 107.

4. a) Terech, P.; Weiss, R.G. *Chem. Rev.* **1997**, *97*, 3133. b) Abdallah, D.J.; Weiss, R.G. *Adv. Mater.* **2000**, *12*, 1237. c) Estroff, L.A.; Hamilton, A.D. *Chem. Rev.* **2004**, *104*, 1201.
5. Feringa, B.L., conversation privée.
6. a) Menger, F.M.; Caran, K.L. *J. Am. Chem. Soc.* **2000**, *122*, 11679. b) Makarevic, J.; Jokic, M.; Peric, B.; Tomisic, V.; Kojic-Prodic, B.; Zinic, M. *Chem. Eur. J.* **2001**, *7*, 3328. c) Suzuki, M.; Nakajima, Y.; Yumoto, M.; Kimura, M.; Shirai, H.; Hanabusa, K. *Langmuir* **2003**, *19*, 8622.
7. van Bommel, K.J.C.; van der Pol, C.; Muizebelt, I.; Friggeri, A.; Heeres, A.; Meetsma, A.; Feringa, B.L.; van Esch, J. *Angew. Chem. Int. Ed.* **2004**, *43*, 1663.
8. Mohmeyer, N.; Wang, P.; Schmidt, H.-W.; Zakeeruddin, S.M.; Grätzel, M. *J. Mater. Chem.* **2004**, *14*, 1905.
9. Placin, F.; Desvergne, J.-P.; Lassègues, J.-C. *Chem. Mater.* **2001**, *13*, 117.
10. Voir par exemple : a) Jokic, M.; Makarevic, J.; Zinic, M. *J. Chem. Soc., Chem. Commun.* **1995**, 1723. b) Ishi, T.; Ono, Y.; Shinkai, S. *Chem. Lett.* **2000**, 808. c) Gronwald, O.; Shinkai, S. *J. Chem. Soc. Perkin Trans. 2* **2001**, 1933. d) Makarevic, J.; Jokic, M.; Peric, B.; Tomisic, V.; Kojic-Prodic, B.; Zinic, M. *Chem. Eur. J.* **2001**, *7*, 3328.
11. Hanabusa, K.; Matsumoto, Y.; Miki, T.; Koyama, T.; Shirai, H. *J. Chem. Soc., Chem. Commun.* **1994**, 1401.
12. Jordon Lloyd, D. *Colloid Chemistry*; Alexander, J., Ed.; The Chemical Catalog Co.: New York, 1926.
13. Takahashi, A.; Sakai, M.; Kato, T. *Polymer J.* **1980**, *12*, 335-341.
14. Reading, M.; Luget, A.; Wilson, R. *Thermochim. Acta* **1994**, *238*, 295-307.
15. a) Wang, G.; Hamilton, A.D. *Chem. Eur. J.* **2002**, *8*, 1954. b) Maji, S.K.; Malik, S.; Drew, M.G.B.; Nandi, A.K.; Banerjee, A. *Tetrahedron Lett.* **2003**, *44*, 4103.
16. a) Ikeda, A.; Sonoda, K.; Ayabe, M.; Tamaru, S.; Nakashima, T.; Kimizuka, N.; Shinkai, S. *Chem. Lett.* **2001**, 1154. b) Suzuki, M.; Yumoto, M.; Kimura, M.; Shirai, H.; Hanabusa, K. *New J. Chem.* **2002**, *26*, 817.
17. Voir par exemple : Shirakawa, M.; Fujita, N.; Shinkai, S. *J. Am. Chem. Soc.* **2005**, *127*, 4164.

18. a) Luo, X.; Li, C.; Liang, Y. *Chem. Commun.* **2000**, 2091. b) Makarevic, J.; Jokic, M.; Raza, Z.; Stefanic, Z.; Kojic-Prodic, B.; Zinic, M. *Chem. Eur. J.* **2003**, *9*, 5567. c) Sugiyasu, K.; Numata, M.; Fujita, N.; Park, S.M.; Yun, Y.J.; Kim, B.H.; Shinkai, S. *Chem. Commun.* **2004**, 1996. d) Trivedi, D.R.; Ballabh, A.; Dastidar, P.; Ganguly, B. *Chem. Eur. J.* **2004**, *10*, 5311.
19. Hanabusa, K.; Hiratsuka, K.; Kimura, M.; Shirai, H. *Chem. Mater.* **1999**, *11*, 649.
20. Sangeetha, N.M.; Maitra, U. *Chem. Soc. Rev.* **2005**, *34*, 821.

Chapitre 5 :

Vers la conception de matériaux moléculaires amorphes auto-assemblés

5.1 L'état solide amorphe

Dans la majorité des cas, lorsqu'un composé en phase liquide ou gazeuse se solidifie, le solide obtenu est cristallin. Toutefois, un refroidissement très rapide peut entraîner la formation d'un solide à l'aspect vitreux. Ces solides sont amorphes, isotropes, existent dans un état de non-équilibre thermodynamique et ne présentent pas d'ordre positionnel ou directionnel à grande échelle.[1]

Il existe certains composés capables de former des phases vitreuses qui sont stables à la température de la pièce. Lorsqu'ils sont suffisamment chauffés, certaines parties des molécules commencent à se mouvoir. À l'échelle macroscopique, ceci se traduit par la présence d'une transition vitreuse où le solide s'amollit pour atteindre un état caoutchoutique. On appelle la température où le changement de phase se produit la température de transition vitreuse (T_g).[1] En principe, ces transitions sont réversibles mais leur réversibilité dépend de la vitesse de refroidissement car la cristallisation peut compétitionner et dans certains cas favoriser la formation de cristaux.

La majorité des polymères présentent des températures de transition vitreuse en raison de leur flexibilité, du grand nombre de conformations différentes qu'ils peuvent adopter et de leur difficulté à former des structures ordonnées en raison de leur grande taille, de leur dispersité et de leur composition hétérogène.[2] Par contre, ce genre de comportement est moins fréquent chez les petites molécules.[3] En particulier, la capacité de former des phases vitreuses stables à la température de la pièce et de participer dans une transition vitreuse réversible est une propriété rare pour des petites molécules.

5.2 Les verres moléculaires ou matériaux moléculaires amorphes

Les verres moléculaires, aussi appelés matériaux moléculaires amorphes, sont des petites molécules possédant une T_g et capables de former spontanément des phases vitreuses stables à température ambiante.[4] Généralement, cette capacité de former des phases solides amorphes découle du fait que ces composés sont stériquement encombrés, s'empilent mal et possèdent des éléments de dissymétrie moléculaire qui

font en sorte que les molécules ont de la difficulté à former des phases ordonnées périodiques, comme des cristaux.[4]

La classe de verres moléculaires la plus connue, les composés « π-starburst », sont des molécules polyaromatiques ramifiées, comme les composés **48**,[5] **49**[6] ou **50**.[7] Il existe aussi certains calixarènes et resorcinarènes, tels les composés **51**[8] ou **52**,[9] exhibant des T_g. Tous ces composés ont certaines caractéristiques en commun : ils possèdent des formes défavorisant l'empilement compact, une liberté conformationnelle ainsi que peu de groupes pouvant former des interactions non-covalentes fortes. La cristallisation de ces composés est donc défavorisée, bien que toutefois possible.

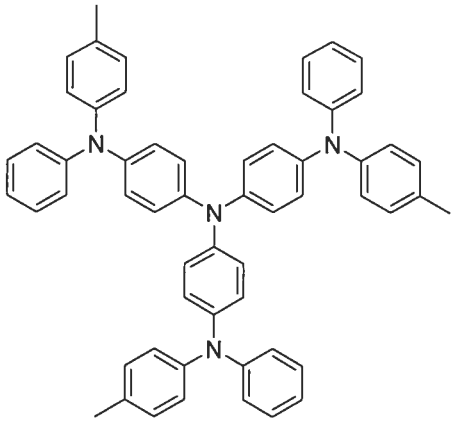

48

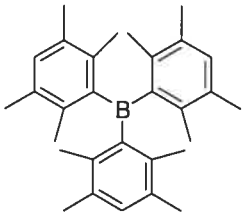

49

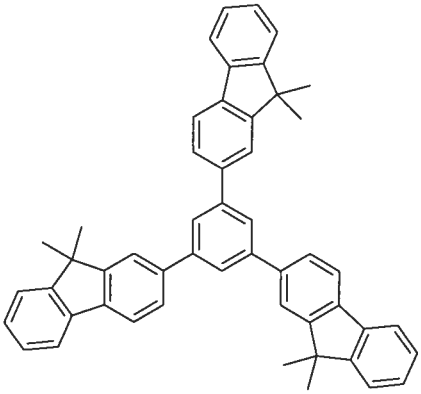

50

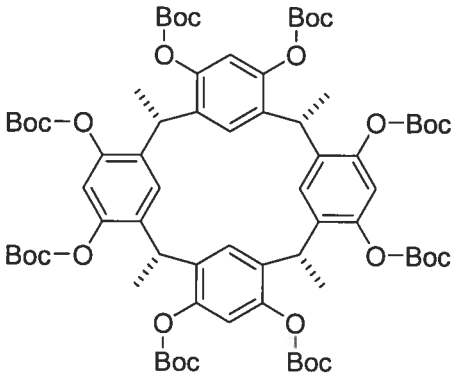

51

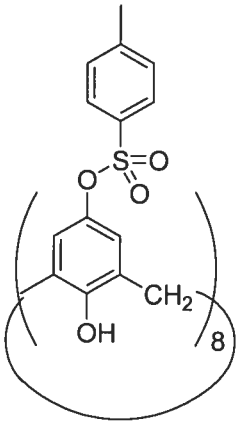

52

5.3 Utilité des verres moléculaires

Les verres moléculaires ont la capacité de former des solides amorphes et d'aspect vitreux, donc ils sont des candidats idéaux pour toutes les applications

impliquant des couches minces, car ils peuvent être déposés soit par déposition de vapeur soit à partir d'une solution (impression à jet d'encre ou *spin-coating*, par exemple).[10] Une des utilités des couches minces réside dans la fabrication de dispositifs comme des diodes organiques électroluminescentes (OLED, *organic light-emitting diode*) ou des cellules photovoltaïques.[11] Le fait que plusieurs de ces composés possèdent un centre polyaromatique fait en sorte qu'ils sont d'excellents candidats pour ce genre d'application. Certains autres verres moléculaires possèdent des groupes fonctionnels pouvant être clivés ou polymérisés par simple irradiation, ce qui en fait de bons candidats pour la nanolithographie.[12] L'ajout d'un groupe fonctionnel capable de photoisomérisation permet de générer des matériaux photochromiques.[13] Étant donné que les verres moléculaires, contrairement aux polymères, possèdent une composition moléculaire définie, ils sont plus faciles à purifier et à caractériser, de qui en fait des candidats potentiels pour n'importe quelle application utilisant des polymères. Par contre, la robustesse des verres moléculaires connus est de loin inférieure à celle des polymères, ce qui limite présentement leur utilisation.

5.4 Méthodes de caractérisation

Les méthodes pour caractériser les verres moléculaires sont rares, et il est jusqu'à présent impossible de déterminer leur structure au niveau moléculaire à l'état amorphe. Afin de déterminer le comportement thermique des composés, la DSC reste la méthode la plus fiable.[14] Comme les transitions vitreuses sont des transitions de phase de deuxième ordre, elles sont généralement de faible énergie et peuvent s'étaler sur 15 °C. Le signal sur une courbe de DSC est donc un glissement plutôt qu'un pic. Étant donné leur faible énergie, ces transitions sont souvent difficiles à observer. Il est nécessaire d'effectuer plusieurs cycles de chauffage/refroidissement ou encore d'utiliser la DSC modulée. La DSC permet d'également d'observer si le composé peut cristalliser lorsqu'on le chauffe. En effet, plusieurs verres moléculaires peuvent passer de la phase caoutchoutique à la phase cristalline lorsqu'on leur fournit suffisamment d'énergie.[15] Afin de confirmer la présence l'état amorphe, la diffraction des poudres peut être utilisée.[6,16] Dans le cas d'un composé amorphe, le spectre de diffraction des poudres présente des pics élargis de faible intensité. Dans l'éventualité où des monocristaux sont

obtenus, la diffraction des rayons-X peut être utilisée pour élucider leur structure cristallographique.[17] Bien que cette technique n'apporte aucune information sur l'arrangement des molécules en phase amorphe, elle est parfois utile afin de rationnaliser la capacité du composé de former des solides amorphes. La morphologie des couches minces peut être étudiée par microscopie à force atomique.[18] Finalement, les propriétés mécaniques des solides amorphes peuvent être étudiées à l'aide de plusieurs techniques rhéologiques.[19]

5.5 Objectifs

Durant notre étude des biguanides et des triazinecarboxylates, nous avons observé que le 1,5-bis(3,5-diméthylphényl)biguanide (**30i**) et son produit de condensation avec l'oxalate de diméthyle, le 4,6-bis[(3,5-diméthylphényl)amino]-1,3,5-triazine-2-carboxylate de méthyle (**46k**), subissaient des transitions vitreuses à de relativement basses températures (37 °C et 75 °C, respectivement). Étrangement, aucun autre

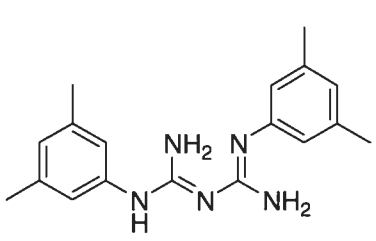

30i

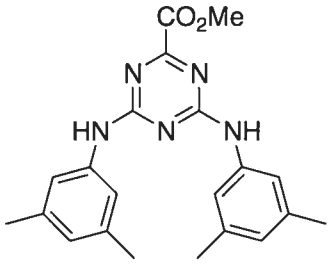

46k

composé parmi tous ceux rapportés dans ces deux études n'a exhibé un tel comportement. De plus, aucun de ces deux composés ne cristallise lorsque chauffé, et tous les deux passent de la phase caoutchoutique à la phase vitreuse lorsque refroidis lentement. Intrigués par la propension de ces composés à former des solides amorphes malgré leur capacité à s'auto-assembler à l'aide de ponts hydrogène, nous avons cherché à vérifier la présence de ponts hydrogène dans l'état amorphe. À l'aide de la synthèse de quelques dérivés et d'études de diffraction des rayons-X et de spectroscopie infrarouge, nous avons cherché à établir le rôle de l'auto-assemblage dans la formation de phases amorphes par cette famille de composés, ainsi que leur stabilité.

5.6 Article 4 :

The Dark Side of Crystal Engineering: Creating Glasses from Small Symmetric Molecules that Form Multiple Hydrogen Bonds.

Olivier Lebel, Thierry Maris, Marie-Ève Perron, Eric Demers, James D. Wuest. *Journal of the American Chemical Society*, soumis pour publication.

Submitted to *J. Am. Chem. Soc.*
Version 1 of April 27, 2006

The Dark Side of Crystal Engineering: Creating Glasses from Small Symmetric Molecules that Form Multiple Hydrogen Bonds

Olivier LeBel,[1] Thierry Maris, Marie-Ève Perron, Eric Demers, and James D. Wuest*

Département de Chimie, Université de Montréal, Montréal, Québec H3C 3J7 Canada

Author to whom correspondence may be addressed:

Keywords: *low-molecular-weight glasses, amorphous molecular materials, crystal engineering, hydrogen bonding, arylaminotriazines*

Amorphous molecular materials (molecular glasses) are a prime source of isotropic thin films for use in optoelectronic devices.[1-2] Molecular glasses are most commonly derived from polymers, although compounds of low molecular weight can also exist in amorphous forms with high glass transition temperatures (T_g > 25 °C).[1-2] Because such glasses are derived from small molecules, they offer the advantage of working with materials of precise mass, well-defined composition, high purity, and good processability. However, small molecules tend to reach thermodynamic equilibrium quickly, thereby converting their amorphous forms into ordered crystalline phases. Few low-molecular-weight glasses can forestall this process indefinitely, especially at temperatures between T_g and their melting point.

Regrettably, there are few reliable guidelines for identifying new small molecules that will form long-lived glasses. Current efforts to design such glasses are based on relatively crude principles, such as inhibiting crystallization by incorporating long alkyl chains and bulky substituents, lowering symmetry, avoiding planarity, increasing molecular size, selecting awkward globular shapes, reducing intermolecular cohesion, and favoring multiple conformations.[3] Recent research in crystal engineering has provided deeper understanding of how molecular crystals can be created by design, thereby raising the possibility of using this understanding not to favor crystallization but to thwart it. For example, crystal engineers have established that hydrogen bonding provides strong directional cohesion that can favor crystallization according to established patterns; at the same time, however, hydrogen bonding creates an opportunity to inhibit crystallization 1) by inducing molecules to aggregate unproductively in ways that preclude effective packing and crystallization; and 2) by slowing diffusion and reorientation in the glassy state. At present, long-lived glasses made from small molecules that engage in hydrogen bonding are particularly rare, and the role of hydrogen bonding in these materials is not clear.[4] In this paper, we report the results of an initial exploration of the "dark side" of crystal engineering, in which structural features and directional interactions that normally favor crystallization are subverted to work against it.

In exploring the supramolecular chemistry of biguanides and aminotriazines, we noted that both 1,5-bis(3,5-dimethylphenyl)biguanide (**30i** = 1,5-dimexylbiguanide)[5,6] and methyl 4,6-bis(mexylamino)-1,3,5-triazine-2-carboxylate (**46k**)[7] form glasses with high

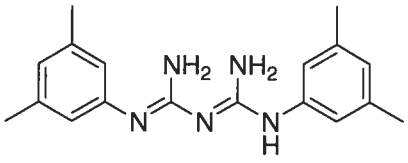

30i

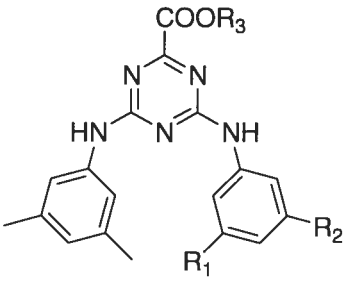

46k ($R_1 = R_2 = R_3 = Me$)
53a ($R_1 = R_2 = H$, $R_3 = Me$)
53b ($R_1 = R_3 = Me$, $R_2 = H$)
53c ($R_1 = R_2 = Me$, $R_3 = Et$)
53d ($R_1 = R_2 = Me$, $R_3 = n$-Pr)
53e ($R_1 = R_2 = Me$, $R_3 = n$-Bu)

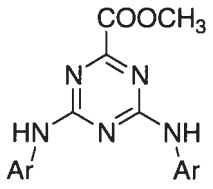

46a (Ar = Ph)
46b (Ar = 4-MePh)
46i (Ar = 3-MePh)
46h (Ar = 2-MePh)

T_g (37 and 75 °C, respectively), as measured by modulated differential scanning calorimetry (mDSC).[8] These glasses result even when melts are cooled slowly, and they do not show a propensity to crystallize, despite the small size of the molecules, their high symmetry, their low degree of flexibility, and their conspicuous ability to form hydrogen bonds. To identify the structural elements that underlie this surprising behavior, we examined the properties of aminotriazine **46k** and related compounds in detail.

Neither simple bis(phenylamino)triazine **46a**[7] nor its methyl-substituted derivatives **46b** and **46h-i**[7] formed glasses when melted and cooled under similar conditions, so the mexyl group appears to play a crucial role in inhibiting crystallization. Monomexyl derivatives **53a-b**, prepared from mexyldicyandiamide by standard methods,[5,7] yielded glasses with T_g = 51 and 38 °C, respectively, establishing that a single mexyl group suffices to block crystallization. Not surprisingly, the lower symmetry of derivatives **53a-b** leads to lower values of T_g. Esters **53c-e**, prepared from dimexyl compound **46k** by transesterification, also yielded glasses, and their values of T_g (62, 58, and 54 °C, respectively) decreased as expected as the length of the alkyl chain increased.

In addition, we examined the behavior of derivatives **54a-b**, in which the carbomethoxy group of bis(mexylamino)triazine **46k** has been replaced by other substituents of similar

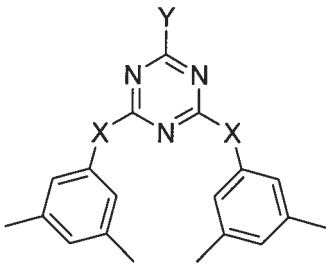

54a (X = NH, Y = OMe)
54b (X = NH, Y = NHMe)
54c (X = O, Y = OMe)

size. Compounds **54a-b**, which were prepared from cyanuric chloride by classic methods,[9] both formed glasses (T_g = 54 and 94 °C, respectively). In sharp contrast, very close analogue **54c**, which cannot self-associate by hydrogen bonding, did not produce a glass under similar conditions. Together, these observations suggest that the mexyl group and hydrogen bonding are both essential and must act in concert to forestall crystallization, even though strong directional association in small, symmetric, and relatively inflexible molecules normally promotes crystallization.

To probe this unusual behavior, we crystallized bis(mexylamino)triazine **46k** from $CHCl_3$ and solved its structure by X-ray crystallography. The crystals were found to belong to the monoclinic space group C2/c and to correspond to an inclusion compound of composition **46k** • 1 $CHCl_3$ • 1 H_2O. Approximately 39% of the volume of the crystals is accessible to guests, as measured by standard methods.[10] The failure of compound **46k** to yield a close-packed structure without included guests helps provide the free volume typically associated with molecular glasses,[1-2] and it reflects inherent structural problems that disfavor normal crystallization. Like related diarylbiguanides and bis(arylamino)triazines,[5,7] compound **46k** crystallizes in an amphiphilic conformation with a lipophilic aryl region and a polar triazinecarboxylate head group that forms multiple hydrogen bonds (Figure 5.1). Such conformations naturally favor

structures consisting of bilayers with interdigitated aryl groups (Figure 5.2),[5,7] but the mexyl groups of compound **46k** can be seen to inhibit efficient packing. In particular, no aromatic interactions involving aryl groups are present, and the closest distance between the centers of aromatic rings is 4.84(1) Å.

FT-IR spectra of solutions of bis(mexylamino)triazine **46k** (CH_2Cl_2) show an N-H stretch at 3403 cm^{-1}, which shifts to 3346 cm^{-1} in the glassy state and to 3359 cm^{-1} in crystals, thereby confirming that compound **46k** forms hydrogen-bonded aggregates in the glass. This aggregation does not appear to involve the carbonyl group, which gives rise to similar bands in solution (1747 cm^{-1}) and in the glassy state (1751 cm^{-1}), whereas stretching occurs at 1738 cm^{-1} in crystals. We conclude that crystallization of the observed glasses is thwarted by self-association of aminotriazine units directed by hydrogen bonding, which leads to the formation of aggregates with reduced mobility and particular structural features that cannot be accommodated in closely packed structures.

Our observations are noteworthy because they demonstrate that long-lived glasses can be made from families of small molecules with properties that would normally promote rapid crystallization, including high symmetry, low flexibility, and participation in multiple strong intermolecular interactions. Systematic structural variations, in conjunction with crystallographic and spectroscopic analyses, show explicitly how crystallization can be forestalled by hydrogen bonding, when properly combined with the effect of a group specifically selected to block close packing.

Acknowledgments. We are grateful to the Natural Sciences and Engineering Research Council of Canada, the Ministère de l'Éducation du Québec, the Canada Foundation for Innovation, and the Canada Research Chairs Program for financial support.

Supporting Information Available: Experimental procedures for making compounds **53a-e** and **54a-c**; characterization of compounds **53a-e** and **54a-c**; representative mDSC traces for compound **46k**; and crystallographic details for compound **46k**, including

ORTEP drawings and tables of crystallographic data, atomic coordinates, anisotropic thermal parameters, and bond lengths and angles. This material is available free of charge via the Internet at http://pubs.acs.org.

Notes and References

(1) Fuhrman, T.; Salbeck, J. *Adv. Photochem.* **2002**, *27*, 83-166.

(2) Shirota, Y. *J. Mater. Chem.* **2005**, *15*, 75-93. Strohriegel, P.; Grazulevicius, J. V. *Adv. Mater.* **2002**, *14*, 1439-1452.

(3) Miao, Q.; Chi, X.; Xiao, S.; Zeis, R.; Lefenfeld, M.; Siegrist, T.; Steigerwald, M. L.; Nuckolls, C. *J. Am. Chem. Soc.* **2006**, *128*, 1340-1345. Aujard, I.; Baltaze, J.-P.; Baudin, J.-B.; Cogné, E.; Ferrage, F.; Jullien, L.; Perez, É.; Prévost, V.; Qian, L. M.; Ruel, O. *J. Am. Chem. Soc.* **2001**, *123*, 8177-8188. Wang, S.; Oldham, W. J., Jr.; Hudack, R. A., Jr.; Bazan, G. C. *J. Am. Chem. Soc.* **2000**, *122*, 5695-5709. Shirota, Y. *J. Mater. Chem.* **2000**, *10*, 1-25.

(4) Baran, J.; Davydova, N. A.; Pietrasko, A. *J. Mol. Struct.* **2005**, *744-747*, 301-305. Dirama, T. E.; Carri, G. A.; Sokolov, A. P. *J. Chem. Phys.* **2005**, *122*, 114505. Boils, D.; Perron, M.-È.; Monchamp, F.; Duval, H.; Maris, T.; Wuest, J. D. *Macromolecules* **2004**, *37*, 7351-7357. Takahashi, A.; Mallia, V. A.; Tamaoki, N. *J. Mater. Chem.* **2003**, *13*, 1582-1587. Boileau, S.; Bouteiller, L.; Foucat, E.; Lacoudre, N. *J. Mater. Chem.* **2002**, *12*, 195-199. Chelli, R.; Cardini, G.; Procacci, P.; Righini, R.; Califano, S. *J. Chem. Phys.* **2002**, *116*, 6205-6215. Kim, S.-J.; Karis, T. E. *J. Mater. Res.* **1995**, *10*, 2128-2136. Naito, K. *Chem. Mater.* **1994**, *6*, 2343-2350.

(5) Lebel, O.; Maris, T.; Duval, H.; Wuest, J. D. *Can. J. Chem.* **2005**, *83*, 615-625.

(6) 1,3-Dimethylphenyl can be abbreviated by mexyl (Ryu, D. H.; Corey, E. J. *J. Am. Chem. Soc.* **2005**, *127*, 5384-5387).

(7) Lebel, O.; Perron, M.-È.; Maris, T.; Zalzal, S. F.; Nanci, A.; Wuest, J. D. *Chem. Mater.* **2006**, submitted for publication (copy provided).

(8) Reading, M.; Luget, A.; Wilson, R. *Thermochim. Acta* **1994**, *238*, 295-307.

(9) Thurston, J. T.; Schaefer, F. C.; Dudley, J. R.; Holm-Hansen, D. *J. Am. Chem. Soc.* **1951**, *73*, 2992-2996. Dudley, J. R.; Thurston, J. T.; Schaefer, F. C.; Holm-Hansen, D.; Hull, C. J.; Adams, P. *J. Am. Chem. Soc.* **1951**, *73*, 2986-2990.

(10) Spek, A. L. *PLATON, A Multipurpose Crystallographic Tool*; Utrecht University: Utrecht, The Netherlands, 2001. van der Sluis, P.; Spek, A. L. *Acta Crystallogr.* **1990**, *A46*, 194-201.

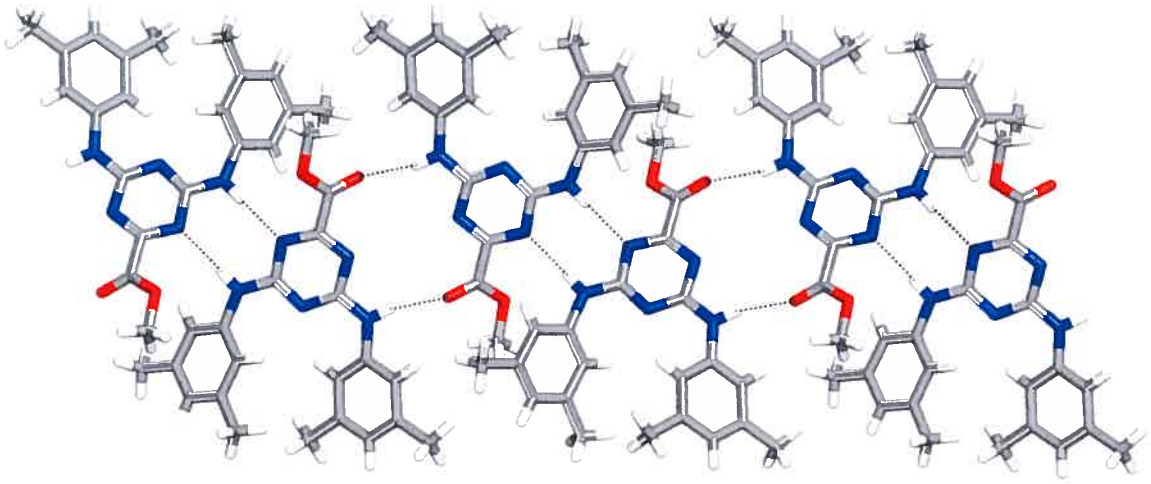

Figure 5.1. View of the structure of crystals of methyl 4,6-bis(mexylamino)-1,3,5-triazine-2-carboxylate (**46k**) grown from $CHCl_3$. The view shows how molecules of compound **46k** adopt an amphiphilic conformation and form hydrogen bonds with two neighbors to define tapes that lie along the *ac* diagonal. Hydrogen bonds are represented by dotted lines. Carbon atoms are shown in gray, hydrogen atoms in white, nitrogen atoms in blue, and oxygen atoms in red.

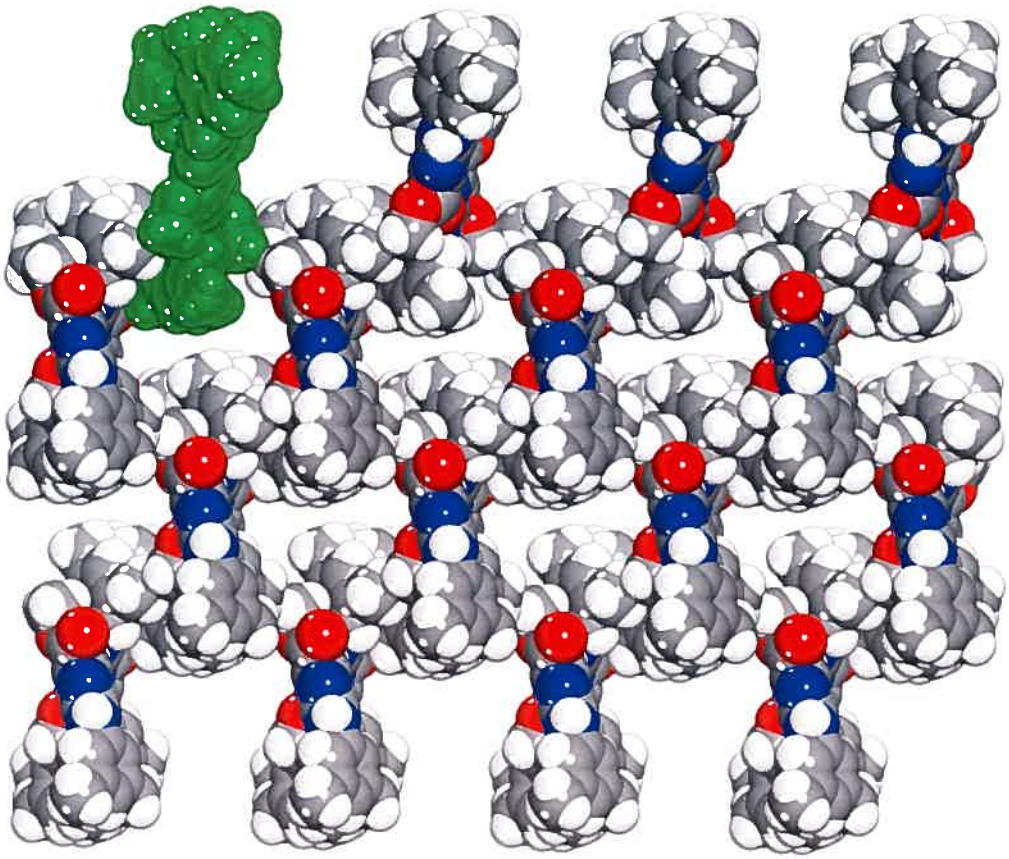

Figure 5.2. View along the *ac* diagonal showing a truncated 2 × 4 × 1 array of unit cells in the structure of bis(mexylamino)triazine **46k**. The views shows how the characteristic hydrogen-bonded tapes that lie along the *ac* diagonal (Figure 5.1) are packed along the *b* axis. For clarification, the cross section of one tape is depicted in green, and guest molecules are omitted. Carbon atoms are shown in gray, hydrogen atoms in white, nitrogen atoms in blue, and oxygen atoms in red.

5.7 Conclusions

Nous avons synthétisé de nouveaux dérivés dans cette famille de composés, dont plusieurs possèdent la propriété de former spontanément des phases amorphes. Cette propriété n'est donc pas limitée aux composés **30i** et **46k** (voir p.133). De tous les nouveaux composés décrits, seul l'analogue **54c**, qui ne peut pas s'auto-associer à l'aide de ponts hydrogène, n'est pas un verre moléculaire, ce qui tend à démontrer l'importance de l'auto-assemblage dans la formation de phases amorphes pour ces composés.

Par ailleurs, nous avons démontré que la présence d'un seul groupe 3,5-diméthylphényle suffit à prévenir la cristallisation. Nous avons également établi que 1) la diminution du degré de symétrie et 2) l'augmentation de la flexibilité d'un composé résultent tous deux en une diminution de la température de transition vitreuse.

Les études de DSC nous ont permis d'étudier le comportement thermique de ces composés. Les phases amorphes formées par les verres moléculaires que nous avons synthétisés se sont avérées extrêmement stables et se forment spontanément, sont réversibles et aucune cristallisation n'est observée lors du chauffage.

Le composé **46k** (voir p.133) a été cristallisé dans le chloroforme, et sa structure cristallographique a été déterminée. Nous avons observé que les molécules de **46k** forment des chaînes unidimensionnelles assemblées à l'aide de ponts hydrogène. Ces chaînes s'empilent de façon décalée les unes sur les autres à l'aide de contacts de van der Waals. Cet empilement n'est toutefois pas optimal et laisse 39% du volume du cristal disponible à des molécules de solvant. Cet espace est occupé par des molécules de chloroforme et d'eau. Une comparaison des spectres infrarouge des monocristaux du composé **46k** avec le solide amorphe correspondant et un échantillon en solution nous a permis d'établir qu'un degré significatif d'association par ponts hydrogène est présent dans la phase amorphe, bien que le motif exact des suprastructures résultantes soit inconnu.

Ces études nous ont permis de confirmer le rôle et la présence d'auto-assemblage à l'aide de ponts hydrogène dans la formation de phases amorphes. Cependant, plusieurs questions restent encore sans réponse, tel que 1) quel est le rôle du groupe fonctionnel en position 2- du cycle triazine dans la formation de phases amorphes, 2) quel est le mécanisme par lequel le solide vitreux passe à l'état caoutchoutique et 3) est-ce que la formation et le bris des ponts hydrogène sont impliqués dans la transition vitreuse? Le prochain objectif de ce projet consiste à accroître notre compréhension des éléments structuraux responsables de la formation de solides amorphes en synthétisant une vaste gamme de dérivés portant différents groupes fonctionnels en position 2- du cycle triazine. Cette étude pourrait nous permettre d'identifier les groupes fonctionnels qui favorisent la formation de solides amorphes ainsi que d'établir le mécanisme par lequel ces verres moléculaires passent de l'état vitreux à l'état caoutchoutique.

Références

1. Tilley, R. *Understanding Solids: the Science of Materials*; John Wiley & Sons, **2004**.
2. a) Fréchet, J.M.J.; Wilson, C.G. *Proc. Microcircuit Eng.* **1982**, 260. b) Fréchet, J.M.J.; Eichler, E.; Ito, H.; Wilson, C.G. *Polymer* **1983**, *24*, 995.
3. a) Plazek, D.J.; Magill, J.H. *J. Chem. Phys.* **1966**, *45*, 3038. b) Greet, R.J.; Turnbull, D. *J. Chem. Phys.* **1966**, *46*, 1243.
4. Shirota, Y. *J. Mater. Chem.* **2000**, *10*, 1.
5. Shirota, Y.; Kobata, T.; Noma, N. *Chem. Lett.* **1989**, 1145.
6. Kinoshita, M.; Kita, H.; Shirota, Y. *Adv. Funct. Mater.* **2002**, *12*, 780.
7. Kreger, K.; Jandke, M.; Strohriegl, P. *Synth. Metals* **2001**, *119*, 163.
8. Young-Gil, K.; Kim, J.B.; Fujigaya, T.; Shibasaki, Y.; Ueda, M. *J. Mater. Chem.* **2002**, *12*, 53.
9. Nakayama, T.; Ueda, M. *J. Mater. Chem.* **1999**, *9*, 697.
10. a) Brown, A.R.; Pomp, A.; Hart, C.M.; de Leeuw, D.M.; Klassen, D.B.M.; Havinga, E.E.; Herwig, P.; Müllen, K. *J. Appl. Phys.* **1996**, *79*, 2136. b) Chang, S.-C.; Liu, J.; Bharathan, J.; Yang, Y.; Onohara, J.; Kido, J. *Adv. Mater.* **1999**, *11*, 734.

11. Strohriegl, P.; Grazulevicius, J.V. *Adv. Mater.* **2002**, *14*, 1439.
12. Tsuchiya, K.; Chang, S.W.; Felix, N.M.; Ueda, M.; Ober, C.K. *J. Photopolym. Sci. Technol.* **2005**, *18*, 431.
13. Shirota, Y. *J. Mater. Chem.* **2005**, *15*, 75.
14. Higuchi, A.; Inada, H.; Kobata, T.; Shirota, Y. *Adv. Mater.* **1991**, *3*, 549.
15. Shirota, Y.; Kobata, T.; Noma, N. *Chem. Lett.* **1989**, 1145.
16. Doi, H.; Kinoshita, M.; Okumoto, K.; Shirota, Y. *Chem. Mater.* **2003**, *15*, 1080.
17. a) Ueta, E.; Nakano, H.; Shirota, Y. *Chem. Lett.* **1994**, 2397. b) Inada, H.; Ohnishi, K.; Nomura, S.; Higuchi, A.; Nakano, H.; Shirota, Y. *J. Mater. Chem.* **1994**, *4*, 171. c) Sakai, J.; Kageyama, H.; Nomura, S.; Nakano, H.; Shirota, Y. *Mol. Cryst. Liq. Cryst.* **1997**, *296*, 445.
18. Han, E.-M.; Do, L.-M.; Fujihara, M.; Inada, H.; Shirota, Y. *J. Appl. Phys.* **1996**, *80*, 3297.
19. a) Sehramm, G. *A Practical Approach to Rheology and Rheometry*; HAAKE, Paramus, **1994**. b) Boils, D.; Perron, M.-È.; Monchamp, F.; Duval, H.; Maris, T.; Wuest, J.D. *Macromolecules* **2004**, *37*, 7351.

Chapitre 6 :

Conclusions et perspectives

6.1 Conclusions

Le premier objectif des travaux résumés dans cette thèse était d'établir des procédures de synthèse, de purification et de caractérisation simples et faciles d'usage dans la chimie des arylbiguanides et des diarylbiguanides. Le travail décrit au chapitre 2 démontre des procédures simples d'usage afin de synthétiser ces dérivés, ainsi que des méthodes spectroscopiques permettant la caractérisation des produits obtenus. Nous avons également étudié les aspects structuraux des diarylbiguanides à l'état cristallin à l'aide du 1,5-diphénylbiguanide (**30a**) et de son sel d'hydrochlorure. Malgré des différences conformationnelles, les deux composés, qui ont un caractère amphiphile, forment des structures où des domaines hydrophobes et des domaines polaires sont disposés en alternance. Dans les deux cas, l'échafaudage cristallin est maintenu par des interactions aromatiques et des ponts hydrogène. Dans le cas du chlorure de 1,5-diphénylbiguanidinium, les ions chlorure jouent un rôle pontant dans la structure.

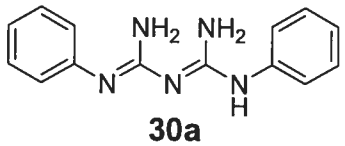

30a

Nous avons ensuite tenté au chapitre 3 d'évaluer le potentiel des biguanides et de leurs sels comme groupements de reconnaissance en génie cristallin. Pour ce faire, nous avons étudié les structures cristallographiques de composés modèles basés sur le 1,4-phénylènebis(biguanide) (**28**) et le 1,3-phénylènebis(biguanide) (**29**). Dans toutes les structures étudiées, les molécules s'associent à l'aide de ponts hydrogène. Dans le cas des sels de biguanidinium correspondants, les contre-ions participent au réseau cristallin en formant des ponts hydrogène renforcés par des interactions électrostatiques. Bien que des molécules de solvant soient incluses dans le réseau cristallin dans chaque cas, le pourcentage occupé par le solvant est faible et aucun canal n'a été observé. De plus, la flexibilité des groupes de reconnaissance et la variété des motifs de reconnaissance possibles limitent la prévisibilité des structures cristallographiques obtenues.

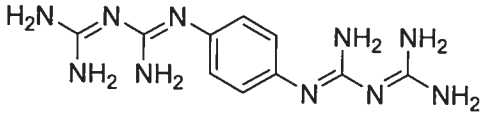

28

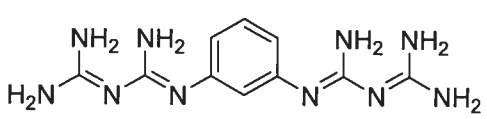

29

À l'intérieur du chapitre 4, nous avons discuté de l'utilisation des 1,5-diarylbiguanides synthétisés au chapitre 2 comme précurseurs synthétiques afin de générer des dérivés d'acides 4,6-diarylamino-1,3,5-triazine-2-carboxyliques. Nous avons également étudié les propriétés de leurs sels de sodium en tant que gélateurs de bas poids moléculaire. En effet, ces composés possèdent la capacité de former des gels à très basse concentration dans le DMSO en générant des réseaux de fibres qui s'assemblent à l'aide de liens non-covalents. Nous avons étudié la morphologie de ces fibres et nous avons formulé un modèle expliquant leur auto-association à l'aide d'une étude structure-fonction à partir d'une série de dérivés ainsi que de la structure cristallographique de l'un des composés. Dans cette structure cristallographique, les molécules de gélateur s'associent à l'aide de la coordination aux ions sodium et d'interactions aromatiques des groupes aryles pour former des bicouches.

La recherche rapportée au chapitre 5 traite de la synthèse et de la caractérisation de dérivés 4,6-diarylamino-1,3,5-triazine et 4,6-diaryloxy-1,3,5-triazine portant des groupes 3,5-diméthylphényles. Certains de ces composés possèdent la capacité de former spontanément et réversiblement des phases solides amorphes d'une grande stabilité. La structure cristallographique de l'un des verres moléculaires, en conjonction avec une étude comparative par spectroscopie infrarouge des cristaux, du solide amorphe et d'un échantillon en solution, nous a permis de vérifier la présence d'auto-assemblage par ponts hydrogène à l'état amorphe. De plus, la synthèse de composés similaires incapables d'auto-assemblage ont confirmé l'importance des ponts hydrogène dans la formation de solides amorphes. Nous avons formulé l'hypothèse que les molécules s'associent à l'aide de ponts hydrogène pour former des rubans qui s'empilent de façon désordonnée dans l'état amorphe. Cependant, il nous est impossible de prouver cette hypothèse.

Ces études démontrent le potentiel des biguanides à la fois comme précurseurs et comme cibles synthétiques en chimie supramoléculaire. Nous avons également démontré comment les leçons apprises dans le cadre de la tectonique moléculaire

peuvent nous aider à élaborer des systèmes auto-assemblés dans d'autres états solides d'un moindre degré d'organisation.

6.2 Perspectives et recherches futures

6.2.1 Nouveaux agents antibactériens potentiels

Étant donné que plusieurs biguanides possèdent des activités biologiques diverses, dans la plupart des cas une activité antimicrobienne,[1] il serait intéressant de cribler les biguanides qui ont été synthétisés dans le cadre des présentes études pour évaluer leurs propriétés antibactériennes potentielles. Il est envisageable que l'un de ces dérivés possède une activité comparable à celles des composés commerciaux tels la chlorhexidine ou le poly(hexaméthylènebiguanide).

6.2.2 Biguanides comme groupes de reconnaissance en tectonique moléculaire

Bien que les biguanides ne soient pas des groupes de reconnaissance très prévisibles, ils comportent toutefois certains avantages. Étant donné que les biguanides peuvent soit s'auto-associer, former des sels avec des acides ou coordonner des métaux, il serait possible de générer plusieurs structures cristallines utilisant divers modes d'association à partir d'un seul tecton. De plus, ces composés sont habituellement solubles dans l'eau, ce qui apporterait une toute nouvelle dimension à la tectonique moléculaire. Cependant, afin de générer des réseaux poreux, il serait crucial de contrebalancer la flexibilité des groupes de reconnaissance à l'aide d'unités centrales rigides. Les tectons **55**, **56** et **57**, qui possèdent des unités centrales rigides comme le tétraphénylméthane,[2] le 9,9'-spirobifluorène[3] ou l'hexaphénylbenzène,[4] pourraient s'avérer des cibles synthétiques intéressantes.

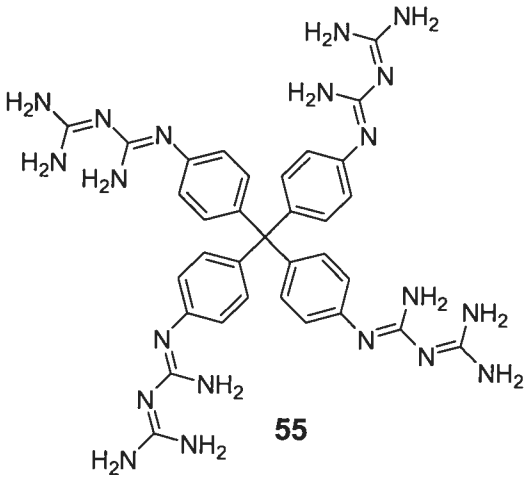

55

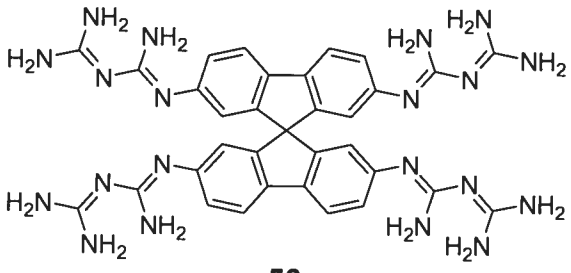

56

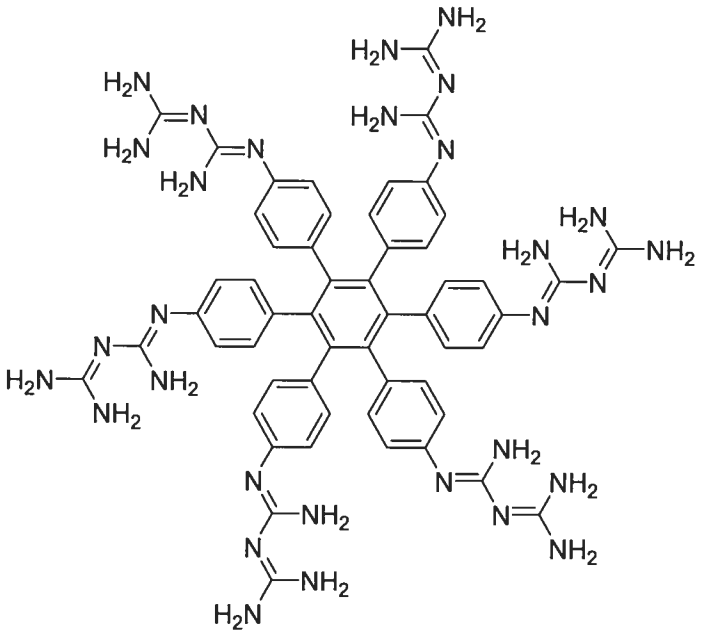

57

6.2.3 Sels d'acides pyrimidine-2-carboxyliques

Étant donné que les sels de sodium de certains dérivés d'acides 1,3,5-triazine-2-carboxyliques forment des gels à l'aide de la coordination au sodium, il serait facile à tester si les sels de sodium de dérivés de l'acide pyrimidine-2-carboxylique (**58**)[5]

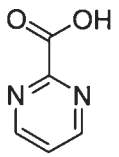

58

possèdent des propriétés similaires. Dans ce cas, en plus de fonctionnaliser le cycle pyrimidine dans les positions 4- et 6-, il serait également possible d'ajouter des groupes fonctionnels divers dans la position 5-, ce qui est impossible dans le cas des triazines (Figure 6.1). Des études comparatives pourraient être effectuées afin de déterminer quel motif de substitution engendre les gélateurs les plus efficaces.

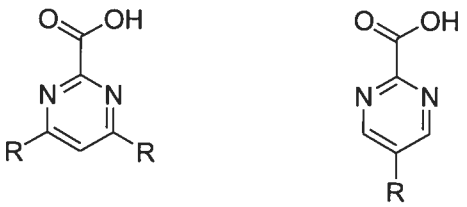

Figure 6.1 Divers motifs de substitution possibles pour les acides pyrimidine-2-carboxyliques.

6.2.4 Gélateurs photochromiques

Une plus grande compréhension de certains éléments structuraux présents dans les gélateurs de bas poids moléculaire a entraîné récemment la conception de gélateurs fonctionnels. Par exemple, il existe quelques cas dans la littérature de gélateurs pouvant s'isomériser lorsqu'irradiés.[6] De tels gélateurs possèdent un mécanisme intrinsèque permettant de moduler leur efficacité de gélation à l'aide d'un signal externe. Étant donné que les 4,6-diarylamino-1,3,5-triazine-2-carboxylates de sodium peuvent porter divers substituants en position 4- des groupes aryles sans perdre leur propriétés gélifiantes, il serait envisageable de greffer des groupes capables de photoisomérisation. Des triazines portant des groupes azobenzène telles que les composés **59** ou **60** pourraient subir une isomérisation *cis-trans* induite photochimiquement (Figure 6.2). Il est fort probable que l'isomère *cis* possède une efficacité de gélation inférieure à l'isomère *trans*

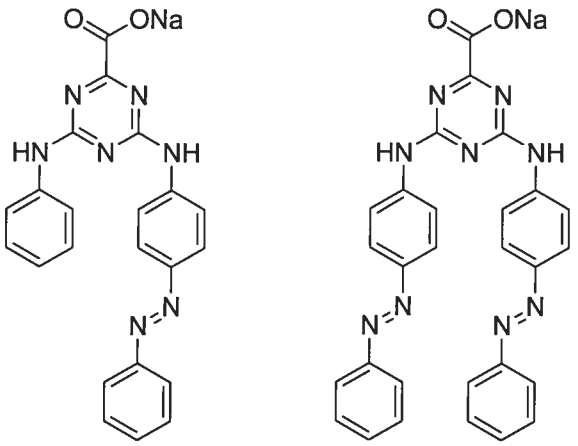

59 **60**

causée par l'encombrement stérique accru. Cette propriété pourrait potentiellement résulter en des gélateurs où la formation de gels peut être contrôlée à l'aide de stimuli externes. Ces gélateurs seraient simples et peu coûteux à synthétiser.

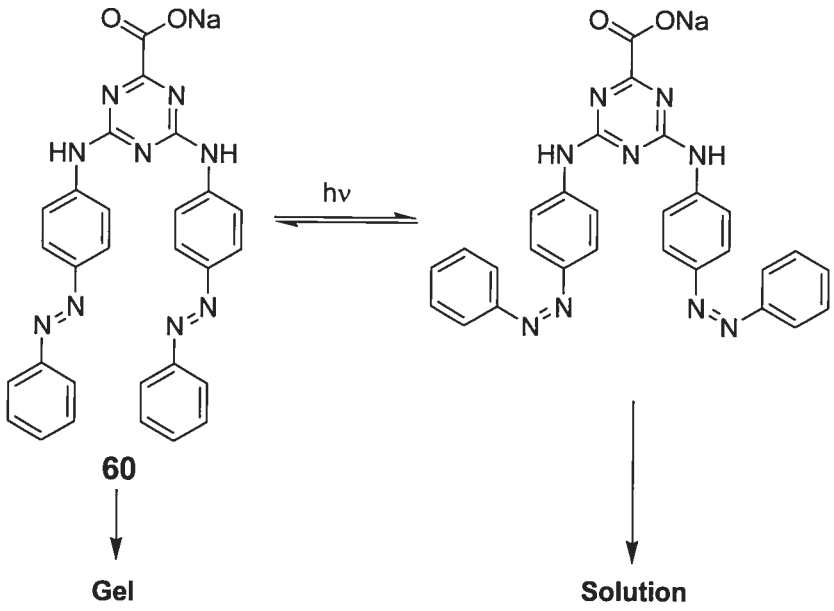

Figure 6.2 Isomérisation *cis-trans* du composé **60** contrôlée photochimiquement. Dans la forme *cis*, l'encombrement stérique causé par les groupes phényles devrait prévenir la gélation en défavorisant l'assemblage en bicouches.

6.2.5 Électrolytes semi-solides

Des gélateurs de bas poids moléculaires ont fait l'objet d'études dans le but de rigidifier des solutions d'électrolytes.[7] La présence d'un squelette semi-solide permet de limiter les déversements en cas de bris tout en conservant une vitesse de diffusion similaire à celle d'une solution. Les gélateurs décrits au chapitre 4 présentent toutes les caractéristiques requises afin de rigidifier des électrolytes : ils peuvent gélifier des solvants polaires, ils peuvent tolérer de grandes quantités d'ions et ils peuvent supporter de hautes températures. Il serait donc intéressant de vérifier si ces composés possèdent la capacité de rigidifier des solutions d'électrolytes sans perte d'efficacité ou déformation du gel.

6.2.6 Utilisation des gélateurs dans des dispositifs opto-électroniques

Étant donné que les fibres formées par les molécules de gélateur présentent un certain degré d'ordre unidimensionnel, il serait envisageable d'utiliser les fibres de gélateur dans des dispositifs comme les cellules photovoltaïques,[8] les transistors à effet de champ[9] ou les diodes électroluminescentes organiques (OLED, *organic light-emitting diode*).[10] De récentes études ont démontré la possibilité d'utiliser les gels dans des

dispositifs opto-électroniques en utilisant des gélateurs comme le dérivé du tétrathiafulvalène **61**[11] ou en utilisant le tétracène **62** comme dopant dans un gel du composé **42**, par exemple.[12]

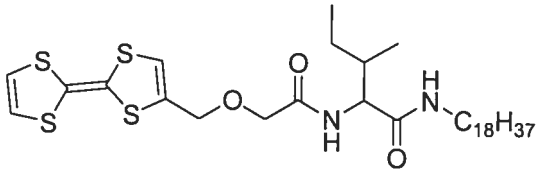

61

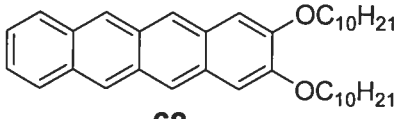

62

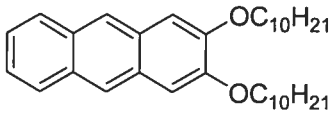

42

Bien entendu, les gélateurs décrits au chapitre 4 ne possèdent aucun groupe fonctionnel pouvant participer efficacement au transport d'électrons, mais il serait possible de concevoir des gélateurs portant des groupes fonctionnels semiconducteurs tels que les composés **63** ou **64** dont les fibres pourraient être impliquées dans la fabrication de dispositifs.

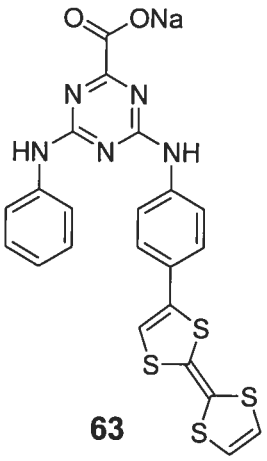

63

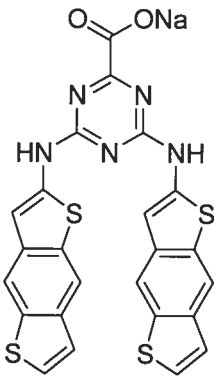

64

6.2.7 Verres moléculaires auto-assemblés

Nous avons effectué la synthèse de plusieurs dérivés 4,6-bis[(3,5-diméthylphényl)amino]-1,3,5-triazine portant différents groupes fonctionnels en position 2-, dont les composés **65** et **66**, qui ne possèdent pas de T_g, et les composés **67**, **68** et **69** qui sont tous les trois des verres moléculaires avec des T_g de 97, 41 et 87 °C, respectivement. Nous sommes présentement en train de tenter de corréler les différents éléments structuraux de ces composés avec leur capacité à former des phases amorphes

et leur T_g. Des études morphologiques de couches minces de certains de ces composés à l'aide de microscopie à force atomique (AFM) sont également en cours.

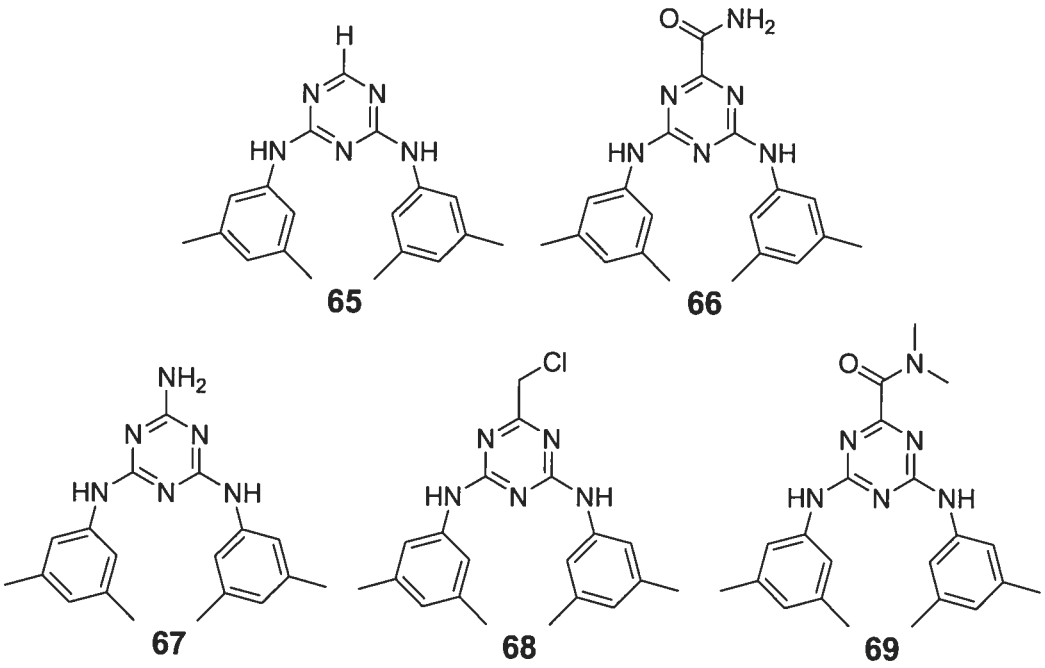

6.2.8 Stratégies visant à prévenir la cristallisation

Il serait également intéressant de vérifier si les verres moléculaires présentés au chapitre 5 pourraient potentiellement servir de point de départ vers des stratégies générales visant à générer des verres moléculaires à partir d'une unité centrale donnée par simple ajout de groupes fonctionnels en périphérie. Un point de départ potentiel pour de telles études serait d'utiliser les unités centrales couramment utilisées en tectonique moléculaire et y greffer des groupes 4,6-bis[(3,5-diméthylphényl)amino]-1,3,5-triazin-2-yles (Figure 6.3).

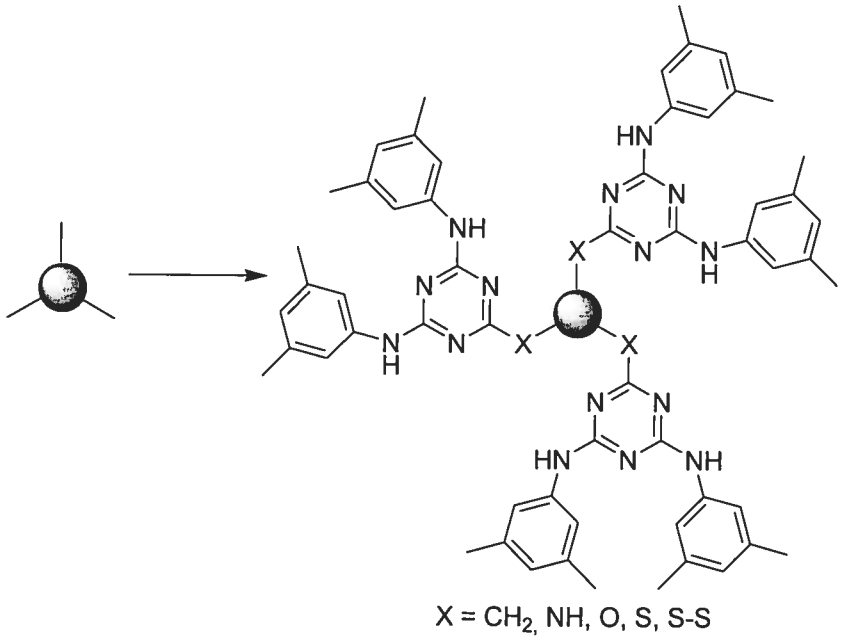

Figure 6.3 Fonctionnalisation des unités centrales utilisées en tectonique moléculaire par des unités 4,6-bis[(3,5-diméthylphényl)amino]-1,3,5-triazin-2-yles afin de générer des matériaux moléculaires amorphes auto-assemblés.

Il serait également intéressant d'étudier l'effet sur les propriétés mécaniques des composés du remplacement des groupes 4,6-diamino-1,3,5-triazin-2-yles des tectons par de simples groupes 3,5-diméthylphényles qui sont isostériques mais incapables d'auto-assemblage (Figure 6.4).

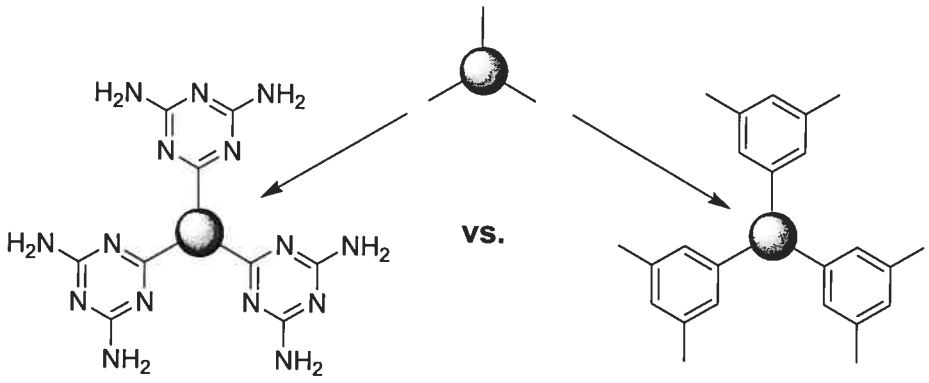

Figure 6.4 Remplacement des unités 4,6-diamino-1,3,5-triazin-2-yle utilisées en tectonique moléculaire par des unités 3,5-diméthylphényle isostériques mais dépourvues de sites pouvant participer à la formation de ponts hydrogène.

6.2.8 Matériaux amorphes auto-assemblés fonctionnels

S'il s'avère possible de générer des verres moléculaires capables de s'auto-assembler par simple fonctionnalisation d'unités centrales à l'aide de groupes stratégiquement choisis, l'étape suivante consisterait à tenter de générer des matériaux fonctionnels par cette stratégie. En effet, il serait intéressant d'utiliser des unités centrales connues pour leurs propriétés opto-électroniques et d'y greffer en périphérie des groupes leur conférant la capacité de former des phases amorphes stables et de s'auto-assembler à l'aide de ponts hydrogène. De telles unités centrales pourraient inclure des composés transporteurs d'électrons ou de trous comme le tris(8-hydroxyisoquinolato)aluminium (**70**)[13] ou la triphénylamine (**71**),[10a] des semiconducteurs comme le pentacène (**72**)[14] ou des composés photochromiques comme le 1,2-bis(2-méthylthién-3-yl)-3,3,4,4,5,5-hexafluoropentène (**73**).[15] Dans le cas où des verres moléculaires seraient obtenus, il serait intéressant d'incorporer ces composés dans des dispositifs et de comparer leur efficacité avec celle des composés connus afin de mesurer l'effet de l'auto-assemblage sur la performance des dispositifs.

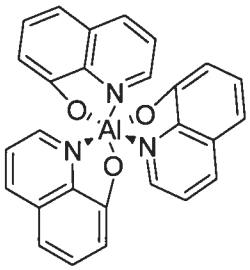

70

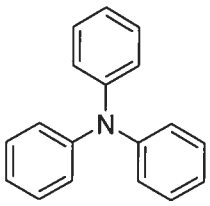

71

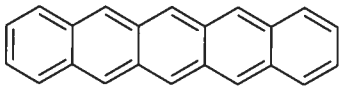

72

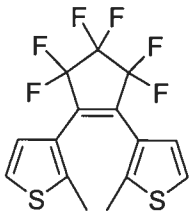

73

Références

1. a) Jôno, K.; Uemura, T.; Kuno, M.; Higashide, E. *Yakugaku Zasshi* **1985**, *105*, 751. b) Tsubouchi, H.; Ohguro, K.; Yasumura, K.; Ishikawa, H.; Kikuchi, M. *Bioorg. Med. Chem. Lett.* **1997**, *7*, 1721.
2. a) Brunet, P.; Simard, M.; Wuest, J.D. *J. Am. Chem. Soc.* **1997**, *119*, 2737. b) Fournier, J.-H.; Maris, T.; Wuest, J.D.; Guo, W.; Galoppini, E. *J. Am. Chem. Soc.* **2003**, *125*, 1002.
3. Fournier, J.-H.; Maris, T.; Wuest, J.D. *J. Org. Chem.* **2004**, *69*, 1762.

4. a) Maly, K.E.; Gagnon, E.; Maris, T.; Wuest, J.D. *Cryst. Growth Des.* **2006**, ASAP. b) Maly, K.E.; Gagnon, E.; Maris, T.; Wuest, J.D. *J. Am. Chem. Soc.*, soumis pour publication.
5. Holland, A. *Chem. Ind.* **1954**, 786.
6. a) Murata, K.; Aoki, M.; Nishi, T.; Ikeda, A.; Shinkai, S. *Org. Biomol. Chem.* **2003**, *1*, 2744. b) de Jong, J.J.D.; Lucas, L.N.; Kellogg, R.M.; van Esch, J.H.; Feringa, B.L. *Science* **2004**, *304*, 278.
7. a) Hanabusa, K.; Hiratsuka, K.; Kimura, M.; Shirai, H. *Chem. Mater.* **1999**, *11*, 649. b) Placin, F.; Desvergne, J.-P.; Lassègues, J.-C. *Chem. Mater.* **2001**, *13*, 117.
8. a) O'Regan, B.; Grätzel, M. *Nature* **1991**, *353*, 737. b) Kubo, W.; Kitamura, T.; Hanabusa, K.; Wada, Y.; Yanagida, S. *Chem. Commun.* **2002**, 374. c) Mohmeyer, N.; Wang, P.; Schmidt, H.-W.; Zakeeruddin, S.M.; Grätzel, M. *J. Mater. Chem.* **2004**, *14*, 1905.
9. Katz, H.E.; Bao, Z.; Gilat, S.L. *Acc. Chem. Res.* **2001**, *34*, 359.
10. a) Tang, C.W.; Van Slyke, S.A. *Appl. Phys. Lett.* **1987**, *51*, 913. b) Burroughes, J.H.; Bradley, D.D.C.; Brown, A.R.; Marks, R.N.; Mackay, K.; Friend, R.H.; Burn, P.L.; Holmes, A.B. *Nature* **1990**, *347*, 539.
11. Kitamura, T.; Nakaso, S.; Mizoshita, N.; Tochigi, Y.; Shimomura, T.; Moriyama, M.; Ito, K.; Kato, T. *J. Am. Chem. Soc.* **2005**, *127*, 14769.
12. Del Guerzo, A.; Olive, A.G.L.; Reichwagen, J.; Hopf, H.; Desvergne, J.-P. *J. Am. Chem. Soc.* **2005**, *127*, 17984.
13. Borsenberger, P.M.; O'Regan, M.B. *Chem. Phys.* **1995**, *200*, 257.
14. Voir par exemple : Würthner, F. *Angew. Chem., Int. Ed.* **2001**, *40*, 1037.
15. Nakamura, S.; Irie, M. *J. Org. Chem.* **1988**, *53*, 6136.

Annexe 1 :

Information supplémentaire de l'article 1

Submitted to *Can. J. Chem.*
Revised Version of February 23, 2005

Supporting Information

A Practical Guide to Arylbiguanides: Synthesis and Structural Characterization

Olivier LeBel, Thierry Maris, Hugues Duval, and James D. Wuest

Département de Chimie, Université de Montréal, Montréal, Québec H3C 3J7 Canada

Contents

(30e), 1,5-bis(4-cyanophenyl)-biguanide (30f), bis(2-bromophenyl)biguanide (30g), 1,5-bis(4-bromophenyl)-biguanide (30h), 1,5-bis(3,5-dimethylphenyl)biguanide (30i), and 1,5-bis(2,4,6-trimethylphenyl)biguanide (30j) (A1-10-A1-13)

4) **Crystal and molecular structure of the hydrochloride salt of 1,5-diphenylbiguanide (30a • HCl) (A1-15-A1-22)**
5) **Crystal and molecular structure of 1,5-diphenylbiguanide (30a) (A1-23-A1-32)**

1) Variable-temperature ^{1}H NMR spectra of 1,5-diphenylbiguanide hydrochloride (30a • HCl) and 1,5-diphenylbiguanide (30a)

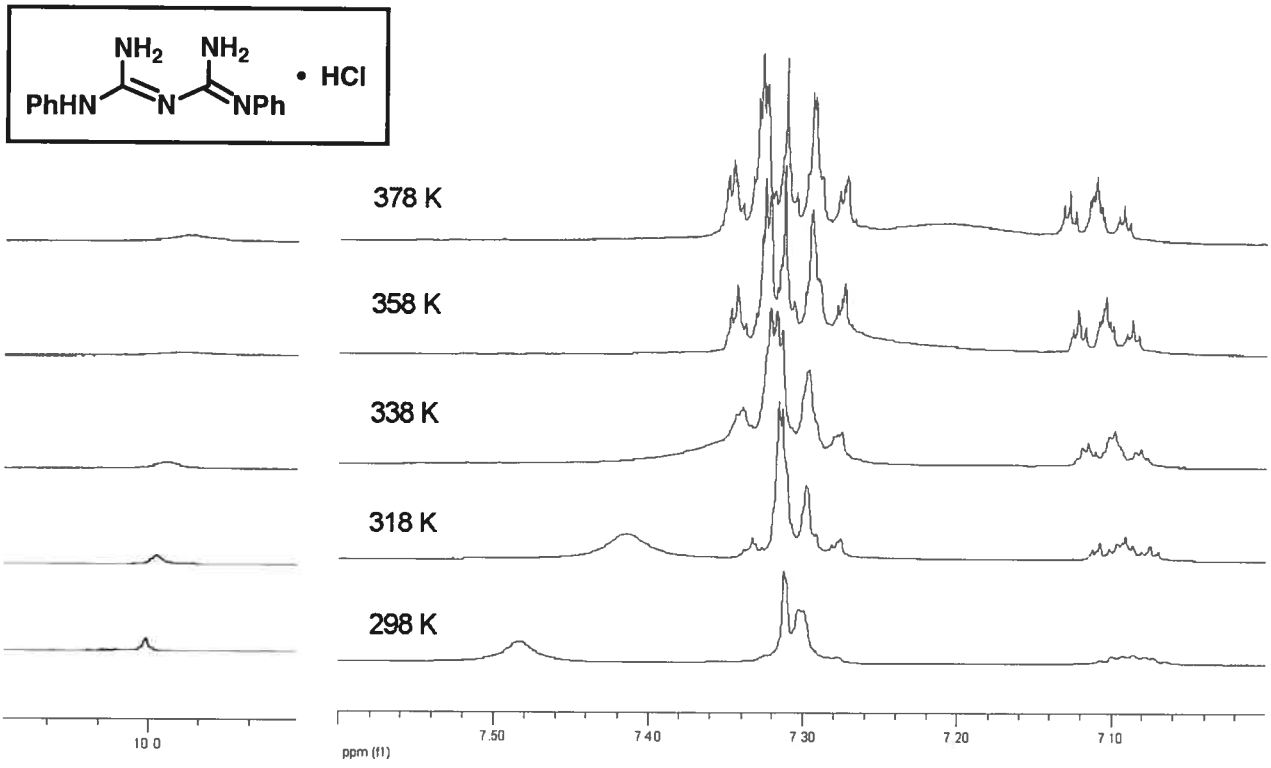

Figure A1-1. ^{1}H NMR spectra of 1,5-diphenylbiguanide hydrochloride (**30a** • HCl) at variable temperatures (DMSO-d_6, 400 MHz).

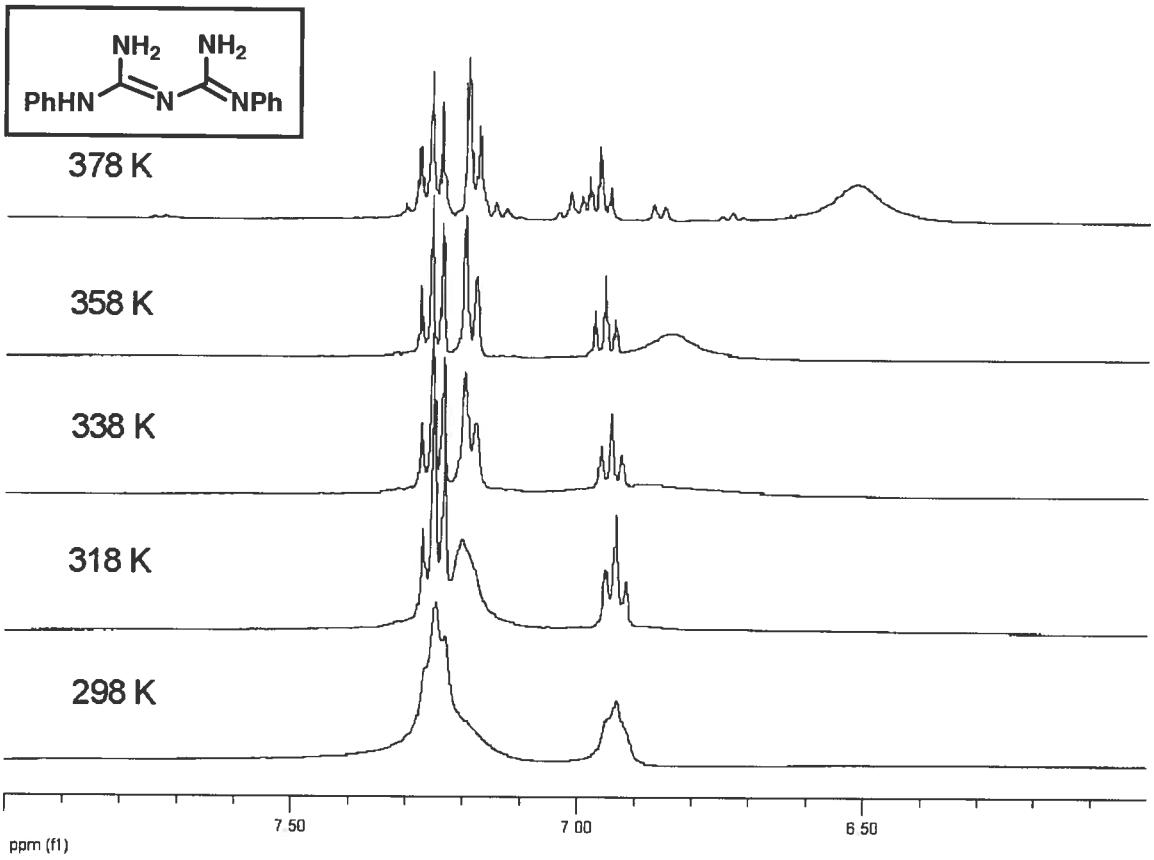

Figure A1-2. ^{1}H NMR spectra of 1,5-diphenylbiguanide (**30a**) at variable temperatures (DMSO-d_6, 400 MHz).

2) Synthesis and characterization of the monohydrochloride salts of 1,5-bis(2-methylphenyl)biguanide (30b), 1,5-bis(3-methylphenyl)biguanide (30c), 1,5-bis(4-methylphenyl)biguanide (30d), 1,5-bis(4-methoxyphenyl)biguanide (30e), 1,5-bis(4-cyanophenyl)biguanide (30f), 1,5-bis(2-bromophenyl)biguanide (30g), 1,5-bis(4-bromophenyl)biguanide (30h), 1,5-bis(3,5-dimethylphenyl)biguanide (30i), and 1,5-bis(2,4,6-trimethylphenyl)biguanide (30j)

Monohydrochloride salts of biguanides **30b-j** were prepared by the method used to make the monohydrochloride salt of 1,5-diphenylbiguanide (**30a**), as described in the Experimental Section of the published manuscript.

1,5-Bis(2-methylphenyl)biguanide (30b) • HCl

Yield 67%, mp 269 to 270 °C. IR (KBr) 3340 (m), 3296 (m), 3247 (m), 3181 (m), 1646 (s), 1607 (s), 1572 (m), 1520 (s), 1456 (m), 1382 (m), 1286 (w), 1256 (m), 1116 (m), 743 (m), 713 (m), 663 (m) cm^{-1}. ^1H NMR (300 MHz, DMSO-d_6) δ: 9.31 (s, 2H), 7.40 (s, 4H), 7.20 (m, 2H), 7.11 (m, 4H), 2.19 (s, 6H). ^{13}C NMR (75 MHz, DMSO-d_6) δ: 158.4, 136.6, 133.5, 131.3, 127.0, 126.7, 126.6, 18.7. Anal. calcd. for $C_{16}H_{20}ClN_5$: C 60.47, H 6.34, N 22.04; found: C, 60.44, H 6.46, N 22.23.

1,5-Bis(3-methylphenyl)biguanide (30c) • HCl

Yield 49%, mp 209 to 210 °C. IR (KBr) 3302 (m), 3181 (m), 3087 (m), 2950 (w), 1610 (s), 1583 (s), 1519 (s), 1484 (s), 1443 (m), 1371 (m), 1281 (m), 1262 (m), 1168 (m), 1089 (m), 1067 (m), 787 (w), 765 (m), 729 (m), 688 (m) cm^{-1}. ^1H NMR (300 MHz, DMSO-d_6) δ: 9.91 (s, 2H), 7.44 (s, 4H), 7.17 (t, ^3J = 8.4 Hz, 2H), 7.10 (m, 4H), 6.89 (d, ^3J = 8.4 Hz, 2H), 2.22 (s, 6H); ^{13}C NMR (75 MHz, DMSO-d_6) δ: 157.6, 138.9, 138.7,

129.5, 125.7, 123.0, 119.7, 21.9. Anal. calcd. for $C_{16}H_{20}ClN_5 \cdot 1/4\ H_2O$: C 59.62, H 6.41, N 21.73; found: C 59.68, H 6.21, N 21.84.

1,5-Bis(4-methylphenyl)biguanide (30d) • HCl

Yield 71%, mp 243 to 244 °C (lit. (1) mp 231 to 234 °C). IR (KBr) 3346 (m), 3302 (m), 3186 (m), 3115 (m), 1629 (s), 1580 (s), 1530 (s), 1506 (s), 1410 (m), 1377 (m), 1286 (w), 1256 (m), 814 (m), 779 (w), 716 (m), 507 (w) cm^{-1}. ^1H NMR (400 MHz, DMSO-d_6) δ: 9.88 (s, 2H), 7.38 (s, 4H), 7.17 (d, ^3J = 8.4 Hz, 4H), 7.09 (d, ^3J = 8.4 Hz, 4H), 2.24 (s, 6H). ^{13}C NMR (75 MHz, DMSO-d_6) δ: 157.7, 136.2, 134.1, 130.1, 122.6, 21.3. Anal. calcd. for $C_{16}H_{20}ClN_5$: C 60.47, H 6.34, N 22.04; found: C 60.54, H 6.45, N, 22.28.

1,5-Bis(4-methoxyphenyl)biguanide (30e) • HCl

Yield 60%, mp 231 to 232 °C (lit. (1) mp 222 °C, lit. (42) mp 256 °C). IR (KBr) 3346 (s), 3302 (s), 3197 (m), 3115 (m), 2967 (m), 2917 (m), 1651 (m), 1613 (m), 1585 (s), 1533 (s), 1514 (m), 1503 (s), 1248 (m), 1234 (m), 1171 (m), 1048 (m), 823 (m) cm^{-1}. ^1H NMR (300 MHz, DMSO-d_6) δ: 9.58 (s, 2H), 7.23 (s, 4H), 7.19 (d, ^3J = 8.9 Hz, 4H), 6.88 (d, ^3J = 8.9 Hz, 4H), 3.72 (s, 6H). ^{13}C NMR (75 MHz, DMSO-d_6) δ: 158.0, 157.1, 131.5, 124.7, 114.9, 56.1. Anal. calcd. for $C_{16}H_{20}ClN_5O_2$: C 54.94, H 5.76, N 20.02; found: C 54.96, H 5.82, N 20.11.

1,5-Bis(4-cyanophenyl)biguanide (30f) • HCl

Yield 68%, mp 263 to 264 °C. IR (KBr) 3456 (m), 3384 (m), 3297 (s), 3186 (s), 3072 (s), 2990 (s), 2890 (s), 2214 (s), 2181 (m), 1643 (s), 1621 (s), 1604 (s), 1572 (s), 1547 (s), 1519 (s), 1489 (s), 1424 (s), 1410 (s), 1377 (s), 1306 (s), 1257 (s), 1175 (s), 1059 (m), 831 (s), 757 (m), 729 (m), 702 (m), 546 (m), 529 (w) cm^{-1}. ^1H NMR (300 MHz, DMSO-d_6) δ: 10.76 (s, 2H), 7.90 (s, 4H), 7.77 (d, ^3J = 8.7 Hz, 4H), 7.51 (d, ^3J =

8.7 Hz, 4H). ^{13}C NMR (75 MHz, DMSO-d_6) δ: 157.7, 143.4, 134.1, 121.6, 119.8, 106.4. Anal. calcd. for $C_{16}H_{14}ClN_7$ • 1/2 H_2O: C 55.10, H 4.33, N 28.11; found: C 55.31, H 4.39, N 28.17.

1,5-Bis(2-bromophenyl)biguanide (30g) • HCl

Yield 63%, mp 265 to 266 °C. IR (KBr) 3307 (s), 3230 (s), 3170 (s), 1640 (s), 1600 (s), 1566 (s), 1511 (s), 1437 (s), 1385 (m), 1286 (m), 1072 (m), 1045 (m), 1023 (m), 746 (m), 713 (m), 663 (m), 642 (w) cm^{-1}. ^{1}H NMR (300 MHz, DMSO-d_6) δ: 9.35 (s, 2H), 7.70 (s, 4H), 7.62 (d, ^3J = 8.0 Hz, 2H), 7.42 (d, ^3J = 8.0 Hz, 2H), 7.30 (t, ^3J = 8.0 Hz, 2H), 7.12 (t, ^3J = 8.0 Hz, 2H); ^{13}C NMR (75 MHz, DMSO-d_6) δ: 158.3, 136.5, 133.6, 128.9, 128.7, 128.3, 119.5. Anal. calcd. for $C_{14}H_{14}Br_2ClN_5$: C 37.57, H 3.15, N 15.65; found: C 37.67, H 3.06, N 15.67.

1,5-Bis(4-bromophenyl)biguanide (30h) • HCl

Yield 54%, mp 251 to 253 °C (lit. (2) mp 259 °C). IR (KBr) 3296 (s), 3181 (s), 3109 (m), 2972 (s), 1648 (m), 1626 (s), 1572 (m), 1525 (s), 1486 (s), 1404 (m), 1377 (m), 1248 (m), 1067 (s), 817 (m), 722 (m) cm^{-1}. ^{1}H NMR (300 MHz, DMSO-d_6) δ: 10.19 (s, 2H), 7.58 (s, 4H), 7.48 (d, ^3J = 8.1 Hz, 4H), 7.25 (d, ^3J = 8.1 Hz, 4H). ^{13}C NMR (75 MHz, DMSO-d_6) δ: 157.7, 138.2, 132.5, 124.3, 116.9. Anal. calcd. for $C_{14}H_{14}Br_2ClN_5$: C 37.57, H 3.15, N 15.65; found: C 37.54, H 3.07, N 15.62.

1,5-Bis(3,5-dimethylphenyl)biguanide (30i) • HCl

Yield 68%, mp 234 to 235 °C. IR (KBr) 3401 (w), 3307 (m), 3186 (m), 1640 (s), 1599 (s), 1525 (s), 1465 (m), 1374 (m), 1322 (w), 1182(m), 836 (m) cm^{-1}. ^{1}H NMR (300 MHz, DMSO-d_6) δ: 9.85 (s, 2H), 7.41 (s, 4H), 6.91 (s, 4H), 6.72 (s, 2H), 2.18 (s, 12H);

^{13}C NMR (75 MHz, DMSO-d_6) δ: 157.5, 138.7, 138.6, 126.5, 120.3, 21.8. Anal. calcd. for $C_{18}H_{24}ClN_5$: C 62.51, H 6.99, N 20.25; found: C 62.65, H 7.24, N 20.59.

1,5-Bis(2,4,6-trimethylphenyl)biguanide (30j) • HCl

Yield 69%, mp 262 to 263 °C. IR (KBr) 3347 (m), 3303 (m), 3187 (m), 1647 (m), 1611 (s), 1581 (s), 1517 (s), 1482 (m), 1438 (w), 1378 (m), 1235 (m), 1158 (w), 1065 (w), 1032 (w), 840 (w), 725 (w), 686 (w) cm^{-1}. ^{1}H NMR (300 MHz, DMSO-d_6) δ: 8.95 (bs, 2H), 7.29 (bs, 2H), 6.88 (bs, 4H), 6.72 (bs, 2H), 2.20 (s, 6H), 2.14 (bs, 6H), 1.80 (bs, 6H). ^{13}C NMR (75 MHz, DMSO-d_6) δ: 158.6, 136.6, 129.7, 128.8, 21.4, 18.7. Anal. calcd. for $C_{20}H_{28}ClN_5$: C 64.24, H 7.55, N 18.73; found: C 64.11, H 7.83, N 18.65.

References

1. F. H. S. Curd and F. L. Rose. J. Chem. Soc. 729 (1946).

2. A. B. Sen and P. R. Singh. J. Ind. Chem. Soc. **39**, 41 (1962).

3) Synthesis and characterization of 1,5-bis(2-methylphenyl)biguanide (30b), 1,5-bis(3-methylphenyl)biguanide (30c), 1,5-bis(4-methylphenyl)biguanide (30d), 1,5-bis(4-methoxyphenyl)biguanide (30e), 1,5-bis(4-cyanophenyl)biguanide (30f), bis(2-bromophenyl)biguanide (30g), 1,5-bis(4-bromophenyl)biguanide (30h), 1,5-bis(3,5-dimethylphenyl)biguanide (30i), and 1,5-bis(2,4,6-trimethylphenyl)-biguanide (30j)

Biguanides **30b-j** were prepared by the method used to make 1,5-diphenylbiguanide (**30a**), as described in the Experimental Section of the published manuscript.

1,5-Bis(2-methylphenyl)biguanide (30b)

Yield 96%, mp 174 to 175 °C (dec.). IR (KBr) 3457 (m), 3374 (m), 3237 (m), 3171 (m), 2968 (s), 2913 (s), 1610 (s), 1591 (s), 1550 (s), 1478 (m), 1454 (m), 1390 (s), 1251 (s), 1188 (w), 1043 (m), 747 (m) cm^{-1}. ^1H NMR (300 MHz, DMSO-d_6) δ: 7.14 (d, ^3J = 7.2 Hz, 2H), 7.07 (m, 4H), 6.88 (t, ^3J = 7.8 Hz, 2H), 9-5 (bs, 5H), 2.14 (s, 6H). ^{13}C NMR (75 MHz, DMSO-d_6) δ: 154.6, 145.2, 131.3, 131.1, 127.3, 124.0, 123.2, 18.9. FAB-MS (3-nitrobenzyl alcohol) *m/e*: 282, 265, 175, 150, 133; MAB-HR-MS calcd. for $C_{16}H_{19}N_5$ *m/e*: 281.1640; found: 281.1645. Anal. calcd. for $C_{16}H_{19}N_5 \cdot 1/3\ H_2O$: C 66.87, H 6.90, N 24.37; found: C 66.83, H 6.84, N 24.39.

1,5-Bis(3-methylphenyl)biguanide (30c)

Yield 86%, mp 114 to 115 °C (dec.). IR (KBr) 3440 (w), 3351 (m), 3236 (s), 3104 (m), 2972 (m), 2917 (m), 1613 (s), 1591 (s), 1525 (s), 1481 (m), 1374 (s), 1349 (s), 1259 (s), 1163 (m), 754 (m), 735 (m), 683 (m), 595 (m) cm^{-1}. ^1H NMR (300 MHz, DMSO-d_6) δ:

7.12 (t, ^3J = 8.1 Hz, 2H), 6.97 (m, 4H), 6.73 (d, ^3J = 7.2 Hz, 2H), 9-5 (bs, 5H), 2.26 (s, 6H). ^{13}C NMR (75 MHz, DMSO-d_6) δ: 156.3, 146.1, 138.8, 129.5, 123.0, 119.5, 22.1. FAB-MS (3-nitrobenzyl alcohol) *m/e*: 282, 265, 175, 150, 133. FAB-HR-MS (3-nitrobenzyl alcohol) calcd. for $C_{16}H_{20}N_5$ *m/e*: 282.1719; found: 282.1731. Anal. calcd. for $C_{16}H_{19}N_5$: C 68.30, H 6.81, N 24.89; found: C 68.29, H 6.95, N, 25.23.

1,5-Bis(4-methylphenyl)biguanide (30d)

Yield 99%, mp 184 to 185 °C (dec.) (lit. (1) mp 187 °C). IR (KBr) 3439 (m), 3351 (m), 3225 (s), 3109 (m), 1621 (s), 1591 (s), 1541 (s), 1522 (s), 1503 (s), 1380 (m), 1352 (s), 1283 (m), 1240 (s), 812 (m), 738 (m), 680 (m), 606 (w), 513 (m) cm^{-1}. ^{1}H NMR (300 MHz, DMSO-d_6) δ: 7.04 (m, 8H), 9-5 (bs, 5H), 2.23 (s, 6H). ^{13}C NMR (75 MHz, DMSO-d_6) δ: 156.5, 143.9, 130.9, 130.2, 122.4, 21.3; FAB-MS (3-nitrobenzyl alcohol) *m/e*: 282, 265, 175, 150, 133. FAB-HR-MS (3-nitrobenzyl alcohol) calcd. for $C_{16}H_{20}N_5$ *m/e*: 282.1719; found: 282.1709. Anal. calcd. for $C_{16}H_{19}N_5$: C 68.30, H 6.81, N 24.89; found: C 68.30, H 6.93, N 25.21.

1,5-Bis(4-methoxyphenyl)biguanide (30e)

Yield 96%, mp 143 to 144 °C (dec.). IR (KBr) 3439 (m), 3351 (m), 3241 (m), 3126 (m), 2994 (m), 2835 (m), 1615 (s), 1591 (s), 1530 (s), 1497 (s), 1456 (m), 1437 (m), 1377 (m), 1349 (m), 1286 (m), 1237 (m), 1176 (m), 1102 (w), 1034 (m), 820 (m), 770 (w), 672 (w) cm^{-1}. ^{1}H NMR (300 MHz, DMSO-d_6) δ: 7.05 (bs, 4H), 6.83 (d, ^3J = 8.4 Hz, 4H), 9-5 (bs, 5H), 3.70 (s, 6H). ^{13}C NMR (75 MHz, DMSO-d_6) δ: 157.0, 155.2, 138.9, 123.9, 115.0, 56.0. FAB-MS (3-nitrobenzyl alcohol) *m/e*: 314, 297, 191, 166, 149; FAB-HR-MS (3-nitrobenzyl alcohol) calcd. for $C_{16}H_{20}N_5O_2$ *m/e*: 314.1617; found: 314.1607. Anal. calcd. for $C_{16}H_{19}N_5O_2$: C 61.33, H 6.11, N 22.35; found: C 61.30, H 6.19, N 22.47.

1,5-Bis(4-cyanophenyl)biguanide (30f)

Yield 92%, mp 189 to 190 °C (dec.) (lit. (2) mp 203 to 204 °C). IR (KBr) 3467 (m), 3362 (m), 3181 (m), 2978 (w), 2219 (s), 1681 (s), 1648 (s), 1569 (s), 1492 (s), 1423 (m), 1355 (m), 1289 (m), 1253 (m), 1171 (m), 1056 (m), 935 (w), 864 (m), 831 (w), 713 (w), 548 (m) cm^{-1}. ^1H NMR (300 MHz, DMSO-d_6) δ: 9.1 (bs, 1H), 7.64 (d, ^3J = 8.4 Hz, 4H), 7.38 (bs, 4H), 7.0 (bs, 4H). ^{13}C NMR (75 MHz, DMSO-d_6) δ: 156.2, 150.9, 133.9, 122.5, 120.6, 103.4. MAB-MS (N_2) *m/e*: 303, 160, 143, 118. FAB-HR-MS (3-nitrobenzyl alcohol) calcd. for $C_{16}H_{14}N_7$ *m/e*: 304.1311; found: 304.1307. Anal. calcd. for $C_{16}H_{13}N_7 \cdot 1/8\ C_6H_{14}$: C 64.05, H 4.73, N 31.22; found: C 64.02, H 4.90, N 31.45.

1,5-Bis(2-bromophenyl)biguanide (30g)

Yield 99%, mp 142 to 144 °C (dec.). IR (KBr) 3450 (m), 3379 (m), 3285 (m), 3120 (m), 1618 (s), 1511 (s), 1410 (s), 1355 (m), 1289 (m), 1253 (w), 1234 (w), 1020 (m), 931 (w), 740 (m), 653 (w) cm^{-1}. ^1H NMR (300 MHz, $CDCl_3$) δ: 8.46 (bs, 1H), 7.56 (d, ^3J = 7 Hz, 2H), 7.26 (t, ^3J = 7 Hz, 2H), 7.16 (m, 2H), 6.88 (t, ^3J = 7 Hz, 2H), 6.5 (bs, 4H). ^{13}C NMR (75 MHz, DMSO-d_6) δ: 152.3, 146.7, 133.4, 129.2, 125.3, 124.1, 118.8. FAB-MS (3-nitrobenzyl alcohol) *m/e*: 412, 410. FAB-HR-MS (3-nitrobenzyl alcohol) calcd. for $C_{14}H_{14}Br_2N_5$ *m/e*: 409.9616; found: 409.9604. Anal. calcd. for $C_{14}H_{13}Br_2N_5 \cdot 1/12\ PhCH_3$: C 41.83, H 3.29, N 16.72; found: C 41.63, H 3.24, N 17.00.

1,5-Bis(4-bromophenyl)biguanide (30h)

Yield 93%, mp 135 to 136 °C (dec.). IR (KBr) 3439 (w), 3351 (m), 3203 (m), 3093 (m), 2967 (s), 2895 (m), 1618 (s), 1591 (s), 1519 (s), 1481 (s), 1377 (s), 1349 (s), 1234 (s), 1064 (s), 1004 (m), 864 (m), 814 (m), 798 (m), 732 (w), 694 (m), 663 (w), 617 (w), 502 (m) cm^{-1}. ^1H NMR (300 MHz, $CDCl_3$) δ: 7.43 (d, ^3J = 8.1 Hz, 4H), 6.97 (d, ^3J = 8.1 Hz, 4H), 5.6 (bs, 5H). ^{13}C NMR (75 MHz, DMSO-d_6) δ: 155.9, 146.0, 132.3, 124.5, 113.7. FAB-MS (3-nitrobenzyl alcohol) *m/e*: 412, 410. FAB-HR-MS (3-nitrobenzyl alcohol)

calcd. for $C_{14}H_{13}Br_2N_5$ *m/e*: 408.9538; found: 408.9527. Anal. calcd. for $C_{14}H_{13}Br_2N_5$ • 1/2 $PhCH_3$: C 45.98, H 3.75, N 15.32; found: C 45.65, H 3.68, N 15.59.

1,5-Bis(3,5-dimethylphenyl)biguanide (30i)

Yield 85%, mp 166 to 167 °C (dec.), Tg 37.15 °C. IR (KBr) 3462 (m), 3385 (m), 3303 (m), 3132 (m), 3022 (m), 2912 (m), 2858 (m), 1640 (s), 1599 (s), 1541 (s), 1467 (s), 1393(s), 1305 (s), 1177 (m), 843 (m) cm^{-1}. ^1H NMR (300 MHz, $CDCl_3$) δ: 6.76 (s, 6H), 5.7 (bs, 5H), 2.31 (s, 12H). ^{13}C NMR (75 MHz, $CDCl_3$) δ: 157.3, 143.8, 139.6, 126.1, 121.9, 21.7. FAB-MS (3-nitrobenzyl alcohol) *m/e*: 310, 189, 164, 147. MAB-HR-MS (N_2) calcd. for $C_{18}H_{23}N_5$ *m/e*: 309.1953; found: 309.1964. Anal. calcd. for $C_{18}H_{23}N_5$ • 1/8 C_2H_5OH: C 69.55, H 7.60, N 22.22; found: C 69.39, H 7.82, N 22.46.

1,5-Bis(2,4,6-trimethylphenyl)biguanide (30j)

Yield 92%, mp 219 to 220 °C (dec.). IR (KBr) 3490 (w), 3457 (m), 3396 (m), 3347 (m), 2907 (m), 1662 (m), 1610 (s), 1555 (s), 1473 (m), 1369 (m), 1298 (w), 1237 (m), 1153 (w), 1029 (w), 1010 (w), 922 (w), 843 (w), 785 (w), 719 (w) cm^{-1}. ^1H NMR (300 MHz, $CDCl_3$) δ: 6.91 (s, 4H), 4.7 (bs, 5 H), 2.29 (s, 6H), 2.25 (s, 12H). ^{13}C NMR (75 MHz, $CDCl_3$) δ: 157.6, 138.1, 134.7, 133.7, 129.4, 21.3, 18.6. MAB-HR-MS (N_2) calcd. for $C_{20}H_{27}N_5$ *m/e*: 337.2266; found: 337.2280. Anal. calcd. for $C_{20}H_{27}N_5$: C 71.18, H 8.06, N 20.75; found: C 71.25, H 8.32, N 20.95.

References

1. F. H. S. Curd and F. L. Rose. J. Chem. Soc. 729 (1946).

2. Ashley, J. N.; Berg, S. S.; MacDonald, R. D. J. Chem. Soc. 4525 (1960).

Université de Montréal

CRYSTAL AND MOLECULAR STRUCTURE OF

C14 H16 Cl N5 COMPOUND (JIW794)

Equipe WUEST

Département de chimie, Université de Montréal,

C.P. 6128, Succ. Centre-Ville, Montréal, Québec, H3C 3J7 (Canada)

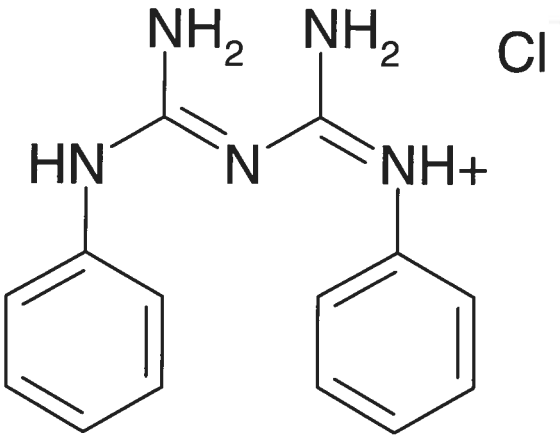

30a • HCl

Structure solved and refined in the Laboratory of X-Ray Diffraction, Université de Montréal by Dr. Thierry Maris

Table A1-1. Crystal data and structure refinement for C14 H16 Cl N5.

Identification code	JIW794
Empirical formula	C14 H16 Cl N5
Formula weight	289.77
Temperature	293(2)K
Wavelength	1.54178 Å
Crystal system	Monoclinic
Space group	$P2_1/n$
Unit cell dimensions	a = 9.627(5) Å α = 90° b = 4.9751(5) Å β = 95.79(2)° c = 35.2533(5) Å γ = 90°
Volume	1679.9(9)Å^3
Z	4
Density (calculated)	1.146 Mg/m^3
Absorption coefficient	1.994 mm^{-1}
F(000)	608
Crystal size	0.35 x 0.08 x 0.08 mm
Theta range for data collection	2.52 to 66.39°
Index ranges	$-11 \leq h \leq 11$, $-5 \leq k \leq 5$, $-41 \leq \ell \leq 41$
Reflections collected	12693
Independent reflections	2854 [R_{int} = 0.0385]
Absorption correction	Semi-empirical from equivalents
Max. and min. transmission	0.85680 and 0.5420
Refinement method	Full-matrix least-squares on F^2
Data / restraints / parameters	2854 / 0 / 215
Goodness-of-fit on F^2	1.069
Final R indices [I>2sigma(I)]	R_1 = 0.0587, wR_2 = 0.1790
R indices (all data)	R_1 = 0.0676, wR_2 = 0.1874
Largest diff. peak and hole	0.325 and -0.273 e/Å^3

Description of structure determination and refinement procedure

X-ray crystallographic data for compound **6a** • HCl were collected from a single crystal sample, which was mounted on a loop fiber. Data were collected at T = 293 K using a Bruker Platform diffractometer, equipped with a Bruker SMART 2K Charged-Coupled Device (CCD) Area Detector using the program SMART and normal-focus sealed-tube-source graphite-monochromated Cu-Kα radiation. The crystal-to-detector distance was 4.908 cm, and the data collection was carried out in 512 x 512 pixel mode, utilizing 4 x 4 pixel binning.

The initial unit cell parameters were determined by a least-squares fit of the angular setting of strong reflections, collected by a 9.0 degree scan in 30 frames over four different parts of the reciprocal space (120 frames total). One complete sphere of data was collected, to better than 0.8 Å resolution. Upon completion of the data collection, the first 101 frames were recollected in order to improve the decay correction analysis.

All non-hydrogen atoms were treated as anisotropic. All hydrogen atoms were located from the difference Fourier map and were refined with restraints on distances. Once the refinement was completed, the structure was subjected to the ADDSYM routine implemented in Platon to check for possible missed symmetry.

Table A1-2. Atomic coordinates (x 10^4) and equivalent isotropic displacement parameters (Å^2 x 10^3) for C14 H16 Cl N5.

U_{eq} is defined as one third of the trace of the orthogonalized Uij tensor.

	x	y	z	U_{eq}
C(1)	5928(2)	4191(5)	1819(1)	77(1)
Cl(1)	9830(1)	4898(1)	2176(1)	93(1)
N(1)	4633(2)	3894(5)	1643(1)	87(1)
C(2)	3474(2)	4359(5)	1820(1)	81(1)
N(2)	2297(2)	4976(5)	1588(1)	95(1)
C(3)	2180(2)	5239(5)	1166(1)	84(1)
N(3)	6986(2)	2998(5)	1645(1)	85(1)
C(4)	2996(3)	7127(7)	981(1)	103(1)
N(4)	6315(2)	5641(6)	2146(1)	99(1)
C(5)	2855(3)	7331(9)	574(1)	122(1)
N(5)	3363(2)	4168(7)	2210(1)	98(1)
C(6)	1914(4)	5742(9)	344(1)	120(1)
C(7)	1098(4)	3935(8)	523(1)	126(1)
C(8)	1224(3)	3641(8)	937(1)	109(1)
C(9)	6957(2)	1691(5)	1268(1)	78(1)
C(10)	7953(3)	-331(6)	1223(1)	104(1)
C(11)	8033(4)	-1495(8)	847(1)	133(1)
C(12)	7164(5)	-654(8)	520(1)	121(1)
C(13)	6199(3)	1318(7)	569(1)	109(1)
C(14)	6085(3)	2510(7)	938(1)	97(1)

Table A1-3. Hydrogen coordinates (x 10^4) and isotropic displacement parameters (Å^2 x 10^3) for C14 H16 Cl N5.

	x	y	z	U_{eq}
H(4)	3615	8247	1126	129(11)
H(5)	3409	8549	457	158(14)
H(6)	1839	5877	80	127(10)
H(7)	447	2903	375	160(14)
H(8)	673	2397	1050	103(9)
H(10)	8542	-933	1431	90(7)
H(11)	8686	-2838	818	155(13)
H(12)	7245	-1390	280	130(10)
H(13)	5599	1878	360	124(10)
H(14)	5428	3856	960	114(9)
H(52)	3920(30)	3280(50)	2343(7)	90(8)
H(51)	2620(40)	4260(50)	2287(8)	98(8)
H(41)	5790(30)	6470(50)	2255(7)	82(8)

H(42)	7200(40)	5960(60)	2208(9)	116(9)
H(3)	7740(30)	3200(50)	1765(7)	97(8)
H(2)	1640(50)	5010(60)	1685(10)	117(11)

Table A1-4. Anisotropic parameters ($Å^2$ x 10^3) for C14 H16 Cl N5.

The anisotropic displacement factor exponent takes the form:

$$-2\pi^2 [h^2 a^{*2} U_{11} + ... + 2 h k a^* b^* U_{12}]$$

	U11	U22	U33	U23	U13	U12
C(1)	42(1)	131(2)	59(1)	4(1)	10(1)	2(1)
Cl(1)	42(1)	163(1)	74(1)	-1(1)	9(1)	-10(1)
N(1)	42(1)	156(2)	64(1)	-5(1)	8(1)	8(1)
C(2)	44(1)	135(2)	65(1)	3(1)	9(1)	4(1)
N(2)	41(1)	174(2)	70(1)	12(1)	11(1)	13(1)
C(3)	48(1)	138(2)	67(1)	7(1)	6(1)	19(1)
N(3)	38(1)	145(2)	71(1)	-9(1)	7(1)	0(1)
C(4)	77(2)	141(2)	90(2)	16(2)	4(1)	4(2)
N(4)	45(1)	179(2)	75(1)	-26(1)	14(1)	-3(1)
C(5)	98(2)	176(3)	93(2)	37(2)	13(2)	23(2)
N(5)	43(1)	185(2)	67(1)	16(1)	12(1)	9(1)
C(6)	109(3)	175(3)	78(2)	11(2)	14(2)	49(2)
C(7)	108(2)	162(3)	100(2)	-22(2)	-23(2)	20(2)
C(8)	72(2)	155(3)	98(2)	7(2)	-2(1)	-1(2)
C(9)	49(1)	113(2)	76(1)	0(1)	19(1)	-7(1)
C(10)	84(2)	125(2)	106(2)	14(2)	23(2)	21(2)
C(11)	149(3)	126(3)	132(3)	-14(2)	52(3)	34(2)
C(12)	137(3)	133(2)	98(2)	-27(2)	40(2)	-5(2)
C(13)	98(2)	158(3)	74(2)	-8(2)	15(1)	-9(2)
C(14)	74(1)	143(2)	74(1)	-9(1)	10(1)	15(2)

Table A1-5. Bond lengths [Å] and angles [°] for C14 H16 Cl N5

C(1)-N(1)	1.343(3)	C(6)-C(7)	1.387(5)
C(1)-N(3)	1.375(3)	C(7)-C(8)	1.459(4)
C(1)-N(4)	1.378(3)	C(9)-C(10)	1.410(4)
N(1)-C(2)	1.351(3)	C(9)-C(14)	1.423(3)
C(2)-N(2)	1.364(3)	C(10)-C(11)	1.457(5)
C(2)-N(5)	1.394(3)	C(11)-C(12)	1.417(5)
N(2)-C(3)	1.487(3)	C(12)-C(13)	1.374(5)
C(3)-C(8)	1.406(4)	C(13)-C(14)	1.445(4)
C(3)-C(4)	1.423(4)	N(1)-C(1)-N(3)	116.26(19)
N(3)-C(9)	1.479(3)	N(1)-C(1)-N(4)	127.1(2)
C(4)-C(5)	1.433(4)	N(3)-C(1)-N(4)	116.6(2)
C(5)-C(6)	1.397(5)	C(1)-N(1)-C(2)	122.68(18)

N(1)-C(2)-N(2)	115.9(2)	C(6)-C(7)-C(8)	121.8(3)
N(1)-C(2)-N(5)	126.3(2)	C(3)-C(8)-C(7)	120.0(3)
N(2)-C(2)-N(5)	117.7(2)	C(10)-C(9)-C(14)	117.7(2)
C(2)-N(2)-C(3)	126.5(2)	C(10)-C(9)-N(3)	117.5(2)
C(8)-C(3)-C(4)	118.1(2)	C(14)-C(9)-N(3)	124.5(2)
C(8)-C(3)-N(2)	120.2(2)	C(9)-C(10)-C(11)	118.9(3)
C(4)-C(3)-N(2)	121.7(2)	C(12)-C(11)-C(10)	122.8(3)
C(1)-N(3)-C(9)	129.96(18)	C(13)-C(12)-C(11)	117.4(3)
C(3)-C(4)-C(5)	120.2(3)	C(12)-C(13)-C(14)	121.3(3)
C(6)-C(5)-C(4)	122.1(3)	C(9)-C(14)-C(13)	121.8(3)
C(7)-C(6)-C(5)	117.8(3)		

Table A1-6. Torsion angles [°] for C14 H16 Cl N5.

N(3)-C(1)-N(1)-C(2)	163.4(2)	C(5)-C(6)-C(7)-C(8)	-1.2(5)
N(4)-C(1)-N(1)-C(2)	-19.2(4)	C(4)-C(3)-C(8)-C(7)	0.4(4)
C(1)-N(1)-C(2)-N(2)	156.1(3)	N(2)-C(3)-C(8)-C(7)	179.0(2)
C(1)-N(1)-C(2)-N(5)	-26.4(4)	C(6)-C(7)-C(8)-C(3)	0.8(5)
N(1)-C(2)-N(2)-C(3)	-1.4(4)	C(1)-N(3)-C(9)-C(10)	-152.7(3)
N(5)-C(2)-N(2)-C(3)	-179.1(3)	C(1)-N(3)-C(9)-C(14)	33.7(4)
C(2)-N(2)-C(3)-C(8)	122.5(3)	C(14)-C(9)-C(10)-C(11)	-0.7(4)
C(2)-N(2)-C(3)-C(4)	-58.9(4)	N(3)-C(9)-C(10)-C(11)	-174.7(3)
N(1)-C(1)-N(3)-C(9)	8.3(4)	C(9)-C(10)-C(11)-C(12)	1.0(5)
N(4)-C(1)-N(3)-C(9)	-169.4(2)	C(10)-C(11)-C(12)-C(13)	-1.0(6)
C(8)-C(3)-C(4)-C(5)	-1.3(4)	C(11)-C(12)-C(13)-C(14)	0.7(5)
N(2)-C(3)-C(4)-C(5)	-179.8(2)	C(10)-C(9)-C(14)-C(13)	0.3(4)
C(3)-C(4)-C(5)-C(6)	0.9(5)	N(3)-C(9)-C(14)-C(13)	174.0(2)
C(4)-C(5)-C(6)-C(7)	0.4(5)	C(12)-C(13)-C(14)-C(9)	-0.4(5)

Table A1-7. Bond lengths [Å] and angles [°] related to the hydrogen bonding for C14 H16 Cl N5.

D-H	..A	d(D-H)	d(H..A)	d(D..A)	<DHA
N(5)-H(52)	CL1#1	0.81(3)	2.59(3)	3.385(3)	166(2)
N(5)-H(51)	CL1#2	0.80(3)	2.69(4)	3.410(3)	152(3)
N(4)-H(41)	N(5)	0.78(3)	2.60(3)	2.966(4)	111(2)
N(4)-H(41)	CL1#3	0.78(3)	2.74(2)	3.456(3)	153(2)
N(4)-H(42)	CL1	0.87(4)	2.60(4)	3.396(3)	152(3)
N(3)-H(3)	CL1	0.80(3)	2.51(3)	3.296(2)	166(2)
N(2)-H(2)	CL1#2	0.75(4)	2.58(4)	3.308(2)	165(4)

Symmetry transformations used to generate equivalent atoms:

#1 -x+3/2,y-1/2,-z+1/2 #2 x-1,y,z #3 -x+3/2,y+1/2,-z+1/2

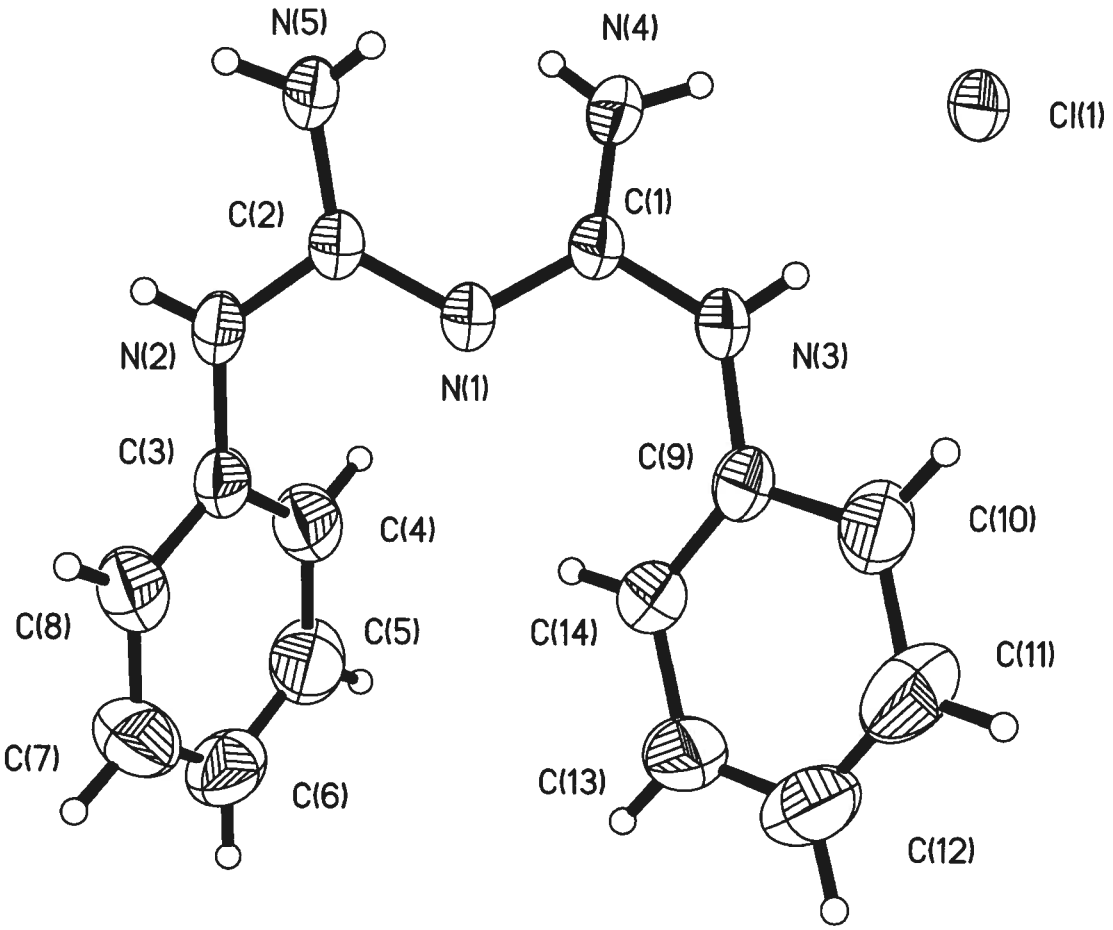

ORTEP view of the C14 H16 Cl N5 compound with the numbering scheme adopted. Ellipsoids drawn at 30% probability level. Hydrogens represented by sphere of arbitrary size.

REFERENCES

SAINT (1999) Release 6.06; Integration Software for Single Crystal Data.
Bruker AXS Inc., Madison, WI 53719-1173.

Sheldrick, G.M. (1996). SADABS, Bruker Area Detector Absorption Corrections.
Bruker AXS Inc., Madison, WI 53719-1173.

Sheldrick, G.M. (1997). SHELXS97, Program for the Solution of Crystal Structures. Univ. of Gottingen, Germany.

Sheldrick, G.M. (1997). SHELXL97, Program for the Refinement of Crystal Structures. Univ. of Gottingen, Germany.

SHELXTL (1997) Release 5.10; The Complete Software Package for Single Crystal Structure Determination. Bruker AXS Inc., Madison, WI 53719-1173.

SMART (1999) Release 5.059; Bruker Molecular Analysis Research Tool.
Bruker AXS Inc., Madison, WI 53719-1173.

Spek, A.L. (2000). PLATON, Molecular Geometry Program, 2000 version.
University of Utrecht, Utrecht, Holland.

XPREP (1997) Release 5.10; X-Ray Data Preparation and Reciprocal Space Exploration Program. Bruker AXS Inc., Madison, WI 53719-1173.

Université de Montréal

CRYSTAL AND MOLECULAR STRUCTURE OF

C14 H15 N5 COMPOUND (JIW810)

Equipe WUEST

Département de chimie, Université de Montréal,

C.P. 6128, Succ. Centre-Ville, Montréal, Québec, H3C 3J7 (Canada)

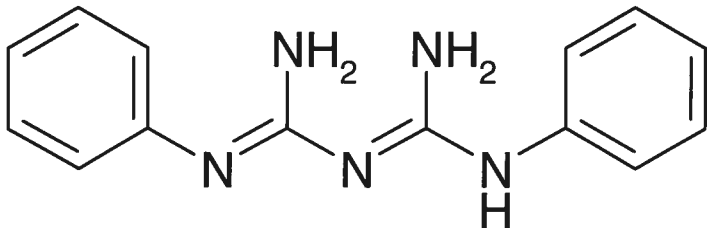

30a

Structure solved and refined in the Laboratory of X-Ray Diffraction, Université de Montréal by Dr. Thierry Maris

Table A1-8. Crystal data and structure refinement for C14 H15 N5.

Identification code	JIW810
Empirical formula	C14 H15 N5
Formula weight	253.31
Temperature	100(2)K
Wavelength	1.54178 Å
Crystal system	Monoclinic
Space group	Pc
Unit cell dimensions	a = 9.0317(3) Å α = 90° b = 6.3945(2) Å β = 99.588(2)° c = 22.5874(8) Å γ = 90°
Volume	1286.27(7)Å^3
Z	4
Density (calculated)	1.308 g/cm^3
Absorption coefficient	0.663 mm^{-1}
F(000)	536
Crystal size	0.20 x 0.12 x 0.03 mm
Theta range for data collection	3.97 to 71.96°
Index ranges	$-11 \leq h \leq 11$, $-7 \leq k \leq 7$, $-27 \leq \ell \leq 27$
Reflections collected	7271
Independent reflections	2530 [R_{int} = 0.035]
Absorption correction	Semi-empirical from equivalents
Max. and min. transmission	1.0000 and 0.7000
Refinement method	Full-matrix least-squares on F^2
Data / restraints / parameters	2530 / 470 / 343
Goodness-of-fit on F^2	1.024
Final R indices [I>2sigma(I)]	R_1 = 0.0673, wR_2 = 0.1525
R indices (all data)	R_1 = 0.0745, wR_2 = 0.1551

Absolute structure parameter	Not refined (see text next page)
Largest diff. peak and hole	0.321 and -0.327 e/Å^3

Description of structure determination and refinement procedure

X-ray crystallographic data for compound **6a** were collected from a single crystal sample, which was mounted on a loop fiber. Data were collected at T = 100 K using a Bruker Platform diffractometer, equipped with a Bruker SMART 2K Charged-Coupled Device (CCD) Area Detector using the program SMART and normal-focus sealed-tube -ource graphite-monochromated Cu-Kα radiation. The crystal-to-detector distance was 4.908 cm, and the data collection was carried out in 512 x 512 pixel mode, utilizing 4 x 4 pixel binning.

The initial unit cell parameters were determined by a least-squares fit of the angular setting of strong reflections, collected by a 9.0 degree scan in 30 frames over four different parts of the reciprocal space (120 frames total). One complete sphere of data was collected, to better than 0.8 Å resolution. Upon completion of the data collection, the first 101 frames were recollected in order to improve the decay correction analysis.

All non-hydrogen atoms were treated as anisotropic. All hydrogen atoms were located from the difference Fourier map but were refined as riding atoms (C-H distance of 0.95 Å, N-H distance of 0.88 Å) because the data to parameter ratio (7.4 without refining hydrogen) was not sufficient to allow full refinement of both coordinates and atomic thermal displacement parameters of hydrogen atoms. As no elements heavier than oxygen are present, the Friedel pairs were merged and the absolute structure could not be determined. Once the refinement was completed, the structure was subjected to the ADDSYM routine implemented in Platon to check for possible missed symmetry.

Table A1-9. Atomic coordinates (x 10^4) and equivalent isotropic displacement parameters ($Å^2$ x 10^3) for C14 H15 N5.

U_{eq} is defined as one third of the trace of the orthogonalized Uij tensor.

	x	y	z	U_{eq}
N(1)	2462(5)	10997(7)	5942(2)	29(1)
N(2)	1873(5)	9199(7)	6749(2)	28(1)
N(3)	3993(5)	8273(7)	6331(2)	29(1)
N(4)	5797(5)	5783(7)	6643(2)	29(1)
N(5)	3843(5)	6288(7)	7230(2)	26(1)
C(1)	3258(6)	11396(9)	5471(3)	28(1)
C(2)	3665(6)	9785(9)	5097(2)	25(1)
C(3)	4532(6)	10314(9)	4659(2)	28(1)
C(4)	4963(6)	12305(10)	4571(2)	30(1)
C(5)	4508(6)	13914(9)	4927(3)	30(1)
C(6)	3690(6)	13470(9)	5365(3)	28(1)
C(7)	2810(6)	9413(9)	6362(2)	27(1)
C(8)	4444(6)	6740(8)	6751(2)	26(1)
C(9)	4642(7)	4857(8)	7643(2)	25(1)
C(10)	5920(6)	5408(9)	8040(2)	26(1)
C(11)	6662(6)	3924(9)	8426(3)	27(1)
C(12)	6171(6)	1886(9)	8420(2)	26(1)
C(13)	4883(6)	1322(9)	8044(2)	27(1)
C(14)	4080(6)	2806(9)	7657(3)	30(1)
N(21)	7941(5)	-685(7)	7078(2)	25(1)
N(22)	6655(5)	1088(7)	6280(2)	27(1)
N(23)	9171(5)	1988(7)	6686(2)	23(1)
N(24)	10649(5)	4462(7)	6387(2)	27(1)
N(25)	8262(5)	3983(7)	5801(2)	26(1)
C(21)	9150(6)	-1179(8)	7532(2)	23(1)
C(22)	9871(6)	368(9)	7919(2)	25(1)
C(23)	11118(6)	-206(9)	8351(2)	26(1)
C(24)	11546(6)	-2319(9)	8433(3)	27(1)
C(25)	10713(6)	-3814(9)	8085(2)	22(1)
C(26)	9565(6)	-3291(8)	7645(2)	23(1)
C(27)	7930(6)	858(8)	6665(2)	22(1)
C(28)	9253(6)	3543(8)	6264(3)	25(1)
C(29)	8710(6)	5517(9)	5404(2)	23(1)
C(30)	9699(6)	5019(9)	5020(2)	25(1)
C(31)	10077(6)	6479(9)	4633(3)	29(1)
C(32)	9538(6)	8532(9)	4642(2)	24(1)
C(33)	8490(6)	9015(9)	5020(2)	25(1)
C(34)	8064(7)	7517(9)	5393(3)	31(1)

Table A1-10. Hydrogen coordinates ($\times 10^4$) and isotropic displacement parameters ($Å^2 \times 10^3$) for C14 H15 N5.

	x	y	z	U_{eq}
H(1)	1690	11806	5973	35
H(2A)	2020	8204	7022	33
H(2B)	1102	10050	6734	33
H(4A)	6258	4862	6899	34
H(4B)	6174	6113	6320	34
H(2)	3357	8382	5142	30
H(3)	4829	9236	4414	33
H(4)	5563	12610	4274	36
H(5)	4774	15322	4860	36
H(6)	3404	14573	5603	33
H(10)	6288	6802	8047	31
H(11)	7530	4322	8701	33
H(12)	6723	876	8675	31
H(13)	4530	-77	8045	32
H(14)	3167	2428	7407	36
H(21A)	7120	-1440	7060	29
H(22A)	6577	2070	6004	32
H(22B)	5888	258	6302	32
H(24A)	10909	5412	6142	32
H(24B)	11280	4099	6710	32
H(22)	9524	1773	7890	30
H(23)	11676	843	8589	32
H(24)	12390	-2705	8722	32
H(25)	10952	-5249	8156	27
H(26)	9029	-4361	7408	27
H(30)	10115	3654	5026	30
H(31)	10711	6104	4354	35
H(32)	9875	9582	4398	29
H(33)	8077	10382	5016	30
H(34)	7341	7830	5641	38

Table A1-11. Anisotropic parameters ($Å^2$ x 10^3) for C14 H15 N5.

The anisotropic displacement factor exponent takes the form:

$$-2\pi^2 [h^2 a^{*2} U_{11} + ... + 2 h k a^* b^* U_{12}]$$

	U11	U22	U33	U23	U13	U12
N(1)	25(2)	31(2)	29(2)	3(2)	-1(2)	-3(2)
N(2)	25(2)	29(2)	27(2)	3(2)	-2(2)	-4(2)
N(3)	25(2)	28(2)	33(2)	8(2)	-2(2)	3(2)
N(4)	28(2)	31(2)	25(2)	-2(2)	-2(2)	-1(2)
N(5)	24(2)	26(2)	29(2)	4(2)	3(2)	-5(2)
C(1)	25(2)	29(2)	28(2)	3(2)	4(2)	-4(2)
C(2)	23(2)	26(3)	26(2)	5(2)	1(2)	4(2)
C(3)	32(3)	27(3)	24(2)	-1(2)	2(2)	8(2)
C(4)	30(3)	33(3)	26(3)	8(2)	3(2)	1(2)
C(5)	27(3)	29(3)	33(3)	1(2)	2(2)	5(2)
C(6)	28(3)	24(2)	29(3)	1(2)	2(2)	4(2)
C(7)	23(2)	28(3)	27(2)	9(2)	2(2)	-2(2)
C(8)	24(2)	25(2)	26(2)	-2(2)	-1(2)	-2(2)
C(9)	30(2)	23(2)	20(2)	5(2)	1(2)	2(2)
C(10)	24(2)	26(3)	24(2)	-2(2)	-2(2)	-3(2)
C(11)	27(2)	25(2)	28(2)	1(2)	-1(2)	2(2)
C(12)	25(2)	25(2)	25(3)	5(2)	0(2)	6(2)
C(13)	26(3)	29(3)	25(3)	5(2)	7(2)	7(2)
C(14)	31(3)	30(3)	26(3)	3(2)	-2(2)	-5(2)
N(21)	26(2)	23(2)	24(2)	0(2)	4(2)	0(2)
N(22)	26(2)	24(2)	29(2)	4(2)	2(2)	-4(2)
N(23)	24(2)	23(2)	18(2)	1(2)	-6(2)	-1(2)
N(24)	23(2)	28(2)	27(2)	2(2)	0(2)	-1(2)
N(25)	24(2)	25(2)	27(2)	6(2)	4(2)	5(2)
C(21)	24(2)	21(2)	23(2)	5(2)	1(2)	-3(2)
C(22)	17(2)	29(3)	26(2)	-5(2)	-3(2)	-2(2)
C(23)	24(2)	27(3)	26(2)	3(2)	1(2)	-2(2)
C(24)	26(3)	28(3)	26(3)	8(2)	1(2)	6(2)
C(25)	21(2)	23(2)	23(2)	4(2)	6(2)	0(2)
C(26)	17(2)	25(2)	27(2)	1(2)	3(2)	-2(2)
C(27)	26(2)	19(2)	22(2)	-2(2)	6(2)	-2(2)
C(28)	27(2)	24(2)	24(2)	2(2)	6(2)	-5(2)
C(29)	23(2)	28(2)	17(2)	1(2)	2(2)	-1(2)
C(30)	26(2)	21(2)	26(2)	1(2)	2(2)	5(2)
C(31)	31(3)	28(3)	25(2)	-1(2)	-2(2)	2(2)
C(32)	20(2)	27(3)	25(2)	5(2)	4(2)	-7(2)
C(33)	30(3)	24(3)	20(2)	3(2)	0(2)	0(2)
C(34)	33(3)	33(3)	28(3)	-3(2)	3(2)	4(2)

Table A1-12. Bond lengths [Å] and angles [°] for C14 H15 N5

N(1)-C(7)	1.388(7)	C(6)-C(1)-C(2)	118.2(5)
N(1)-C(1)	1.402(7)	C(3)-C(2)-C(1)	118.4(5)
N(2)-C(7)	1.322(7)	C(4)-C(3)-C(2)	122.5(5)
N(3)-C(7)	1.305(7)	C(3)-C(4)-C(5)	119.0(5)
N(3)-C(8)	1.377(6)	C(6)-C(5)-C(4)	120.5(5)
N(4)-C(8)	1.424(7)	C(5)-C(6)-C(1)	121.3(5)
N(5)-C(8)	1.320(7)	N(3)-C(7)-N(2)	126.7(5)
N(5)-C(9)	1.416(7)	N(3)-C(7)-N(1)	117.7(5)
C(1)-C(6)	1.415(8)	N(2)-C(7)-N(1)	115.5(5)
C(1)-C(2)	1.419(8)	N(5)-C(8)-N(3)	127.2(5)
C(2)-C(3)	1.402(7)	N(5)-C(8)-N(4)	121.9(5)
C(3)-C(4)	1.356(8)	N(3)-C(8)-N(4)	110.6(5)
C(4)-C(5)	1.408(8)	C(10)-C(9)-C(14)	119.1(5)
C(5)-C(6)	1.359(8)	C(10)-C(9)-N(5)	122.7(5)
C(9)-C(10)	1.385(8)	C(14)-C(9)-N(5)	118.1(5)
C(9)-C(14)	1.408(8)	C(11)-C(10)-C(9)	119.8(5)
C(10)-C(11)	1.384(8)	C(12)-C(11)-C(10)	121.5(5)
C(11)-C(12)	1.376(8)	C(13)-C(12)-C(11)	119.6(5)
C(12)-C(13)	1.369(8)	C(12)-C(13)-C(14)	120.3(5)
C(13)-C(14)	1.407(7)	C(13)-C(14)-C(9)	119.5(5)
N(21)-C(27)	1.357(6)	C(27)-N(21)-C(21)	125.6(5)
N(21)-C(21)	1.403(7)	C(27)-N(23)-C(28)	120.5(4)
N(22)-C(27)	1.331(6)	C(28)-N(25)-C(29)	115.3(5)
N(23)-C(27)	1.328(7)	N(21)-C(21)-C(22)	121.3(5)
N(23)-C(28)	1.387(6)	N(21)-C(21)-C(26)	119.9(5)
N(24)-C(28)	1.376(7)	C(22)-C(21)-C(26)	118.6(5)
N(25)-C(28)	1.289(7)	C(21)-C(22)-C(23)	118.7(5)
N(25)-C(29)	1.433(7)	C(24)-C(23)-C(22)	120.7(5)
C(21)-C(22)	1.406(7)	C(25)-C(24)-C(23)	118.6(5)
C(21)-C(26)	1.413(7)	C(26)-C(25)-C(24)	121.7(5)
C(22)-C(23)	1.410(7)	C(25)-C(26)-C(21)	121.2(5)
C(23)-C(24)	1.409(8)	N(23)-C(27)-N(22)	126.6(5)
C(24)-C(25)	1.378(8)	N(23)-C(27)-N(21)	117.5(5)
C(25)-C(26)	1.353(7)	N(22)-C(27)-N(21)	115.9(5)
C(29)-C(30)	1.381(7)	N(25)-C(28)-N(24)	124.0(5)
C(29)-C(34)	1.404(8)	N(25)-C(28)-N(23)	127.1(5)
C(30)-C(31)	1.360(8)	N(24)-C(28)-N(23)	108.6(5)
C(31)-C(32)	1.401(8)	C(30)-C(29)-C(34)	120.6(5)
C(32)-C(33)	1.410(7)	C(30)-C(29)-N(25)	121.0(5)
C(33)-C(34)	1.373(8)	C(34)-C(29)-N(25)	118.3(5)
		C(31)-C(30)-C(29)	120.2(5)
C(7)-N(1)-C(1)	124.4(5)	C(30)-C(31)-C(32)	120.6(5)
C(7)-N(3)-C(8)	120.8(5)	C(31)-C(32)-C(33)	118.9(5)
C(8)-N(5)-C(9)	116.6(5)	C(34)-C(33)-C(32)	120.2(5)
N(1)-C(1)-C(6)	119.4(5)	C(33)-C(34)-C(29)	119.2(5)
N(1)-C(1)-C(2)	122.4(5)		

Table A1-13. Torsion angles [°] for C14 H15 N5.

C(7)-N(1)-C(1)-C(6)	-132.5(6)	C(27)-N(21)-C(21)-C(22	51.1(7)
C(7)-N(1)-C(1)-C(2)	46.8(8)	C(27)-N(21)-C(21)-C(26)	-135.2(5)
N(1)-C(1)-C(2)-C(3)	-176.5(5)	N(21)-C(21)-C(22)-C(23)	-177.4(5)
C(6)-C(1)-C(2)-C(3)	2.9(8)	C(26)-C(21)-C(22)-C(23)	8.8(8)
C(1)-C(2)-C(3)-C(4)	-1.6(9)	C(21)-C(22)-C(23)-C(24)	-6.1(8)
C(2)-C(3)-C(4)-C(5)	-0.9(9)	C(22)-C(23)-C(24)-C(25)	-0.4(8)
C(3)-C(4)-C(5)-C(6)	2.2(9)	C(23)-C(24)-C(25)-C(26)	4.2(8)
C(4)-C(5)-C(6)-C(1)	-0.8(9)	C(24)-C(25)-C(26)-C(21)	-1.4(8)
N(1)-C(1)-C(6)-C(5)	177.7(5)	N(21)-C(21)-C(26)-C(25)	-179.1(5)
C(2)-C(1)-C(6)-C(5)	-1.7(8)	C(22)-C(21)-C(26)-C(25)	-5.3(8)
C(8)-N(3)-C(7)-N(2)	-4.5(9)	C(28)-N(23)-C(27)-N(22)	-2.7(8)
C(8)-N(3)-C(7)-N(1)	176.9(4)	C(28)-N(23)-C(27)-N(21)	177.8(5)
C(1)-N(1)-C(7)-N(3)	2.9(8)	C(21)-N(21)-C(27)-N(23)	0.7(7)
C(1)-N(1)-C(7)-N(2)	-175.9(5)	C(21)-N(21)-C(27)-N(22)	-178.8(5)
C(9)-N(5)-C(8)-N(3)	-170.7(5)	C(29)-N(25)-C(28)-N(24)	0.7(8)
C(9)-N(5)-C(8)-N(4)	2.2(7)	C(29)-N(25)-C(28)-N(23)	-173.3(5)
C(7)-N(3)-C(8)-N(5)	-3.4(8)	C(27)-N(23)-C(28)-N(25)	-5.2(8)
C(7)-N(3)-C(8)-N(4)	-177.0(5)	C(27)-N(23)-C(28)-N(24)	-179.9(5)
C(8)-N(5)-C(9)-C(10)	76.2(7)	C(28)-N(25)-C(29)-C(30)	75.4(7)
C(8)-N(5)-C(9)-C(14)	-105.4(6)	C(28)-N(25)-C(29)-C(34)	-107.6(6)
C(14)-C(9)-C(10)-C(11)	2.7(9)	C(34)-C(29)-C(30)-C(31)	1.1(9)
N(5)-C(9)-C(10)-C(11)	-179.0(5)	N(25)-C(29)-C(30)-C(31)	178.1(5)
C(9)-C(10)-C(11)-C(12)	1.0(9)	C(29)-C(30)-C(31)-C(32)	3.6(9)
C(10)-C(11)-C(12)-C(13)	-3.0(9)	C(30)-C(31)-C(32)-C(33)	-5.8(9)
C(11)-C(12)-C(13)-C(14)	1.3(8)	C(31)-C(32)-C(33)-C(34)	3.2(8)
C(12)-C(13)-C(14)-C(9)	2.3(8)	C(32)-C(33)-C(34)-C(29)	1.4(9)
C(10)-C(9)-C(14)-C(13)	-4.3(9)	C(30)-C(29)-C(34)-C(33)	-3.6(9)
N(5)-C(9)-C(14)-C(13)	177.3(5)	N(25)-C(29)-C(34)-C(33)	179.3(5)

Table A1-14. Bond lengths [Å] and angles [°] related to the hydrogen bonding for C14 H15 N5.

D-H	..A	d(D-H)	d(H..A)	d(D..A)	<DHA
N(2)-H(2A)	N(5)	0.88	2.04	2.677(6)	128
N(2)-H(2B)	N(23)#1	0.88	2.13	3.007(6)	177.3

Symmetry transformations used to generate equivalent atoms:

#1 x-1,y+1,z

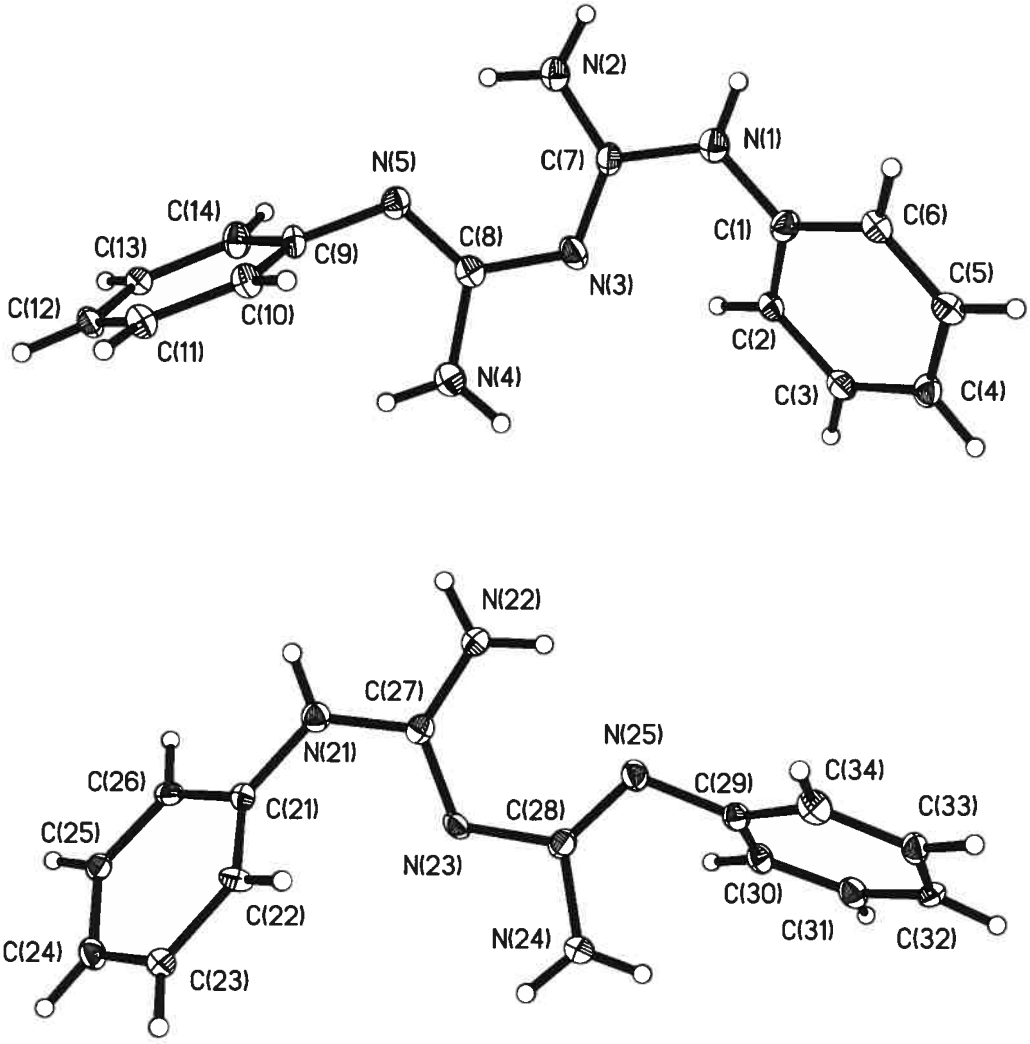

ORTEP view of the C14 H15 N5 compound with the numbering scheme adopted. Ellipsoids drawn at 30% probability level. Hydrogen atoms are represented by sphere of arbitrary size.

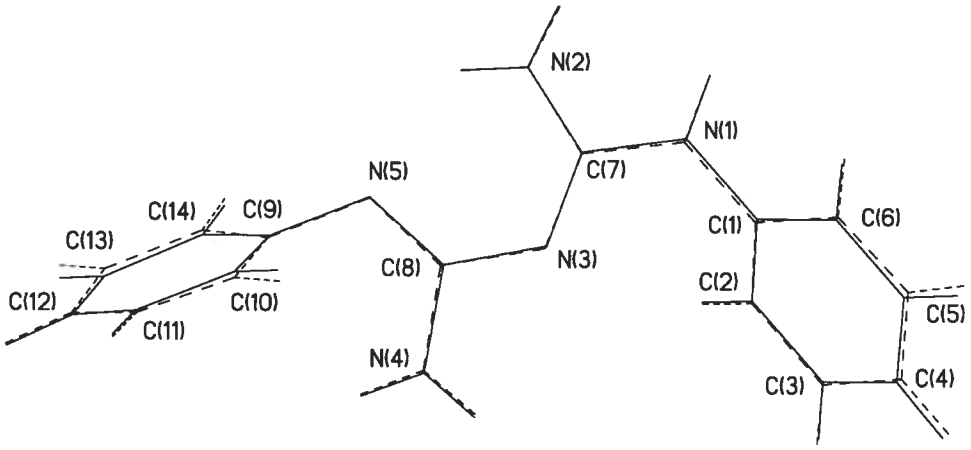

View of the two symmetry-independent molecules, overlapped to reveal their similar conformations. Only labeling of the first molecule is shown. Add 20 to the number in the labels for the atoms of the first molecule to get the corresponding label in the second molecule.

REFERENCES

Flack, H.D. (1983). Acta Cryst. A39, 876-881.

Flack, H.D. and Schwarzenbach, D. (1988). Acta Cryst. A44, 499-506.

International Tables for Crystallography (1992). Vol. C. Tables 4.2.6.8 and
6.1.1.4, Dordrecht: Kluwer Academic Publishers.

SAINT (1999) Release 6.06; Integration Software for Single Crystal Data.
Bruker AXS Inc., Madison, WI 53719-1173.

Sheldrick, G.M. (1996). SADABS, Bruker Area Detector Absorption Corrections.
Bruker AXS Inc., Madison, WI 53719-1173.

Sheldrick, G.M. (1997). SHELXS97, Program for the Solution of Crystal Structures. Univ. of Gottingen, Germany.

Sheldrick, G.M. (1997). SHELXL97, Program for the Refinement of Crystal Structures. Univ. of Gottingen, Germany.

SHELXTL (1997) Release 5.10; The Complete Software Package for Single Crystal Structure Determination. Bruker AXS Inc., Madison, WI 53719-1173.

SMART (1999) Release 5.059; Bruker Molecular Analysis Research Tool.
Bruker AXS Inc., Madison, WI 53719-1173.

Spek, A.L. (2000). PLATON, Molecular Geometry Program, 2000 version.
University of Utrecht, Utrecht, Holland.

XPREP (1997) Release 5.10; X-Ray Data Preparation and Reciprocal Space Exploration Program. Bruker AXS Inc., Madison, WI 53719-1173.

Annexe 2 :

Information supplémentaire de l'article 2

Submitted to *Can. J. Chem.*
Version of March 18, 2006

Supporting Information

Hydrogen-Bonded Networks in Crystals Built from Bis(biguanides) and Their Salts

Olivier Lebel, Thierry Maris, and James D. Wuest

Département de Chimie, Université de Montréal, Montréal, Québec H3C 3J7 Canada

Contents

Université de Montréal

CRYSTAL AND MOLECULAR STRUCTURE OF

C10 H18 N10 O COMPOUND (JIW845)

Equipe WUEST

Département de chimie, Université de Montréal,

C.P. 6128, Succ. Centre-Ville, Montréal, Québec, H3C 3J7 (Canada)

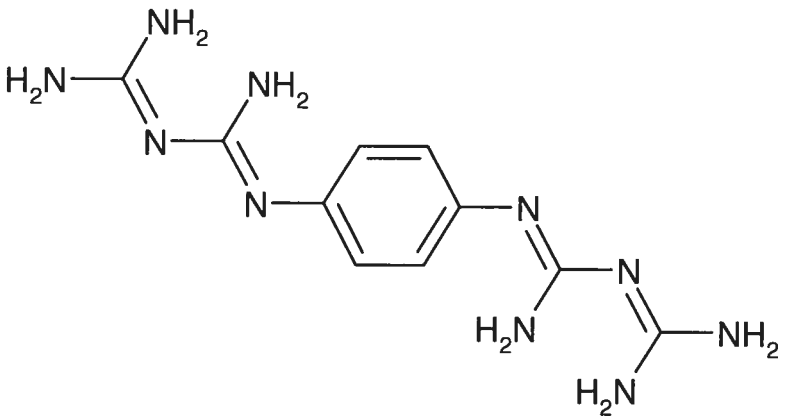

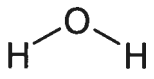

Structure solved and refined in the Laboratory of X-Ray Diffraction, Université de Montréal by Dr. Thierry Maris

Table A2-1. Crystal data and structure refinement for C10 H18 N10 O.

Identification code	JIW845
Empirical formula	C10 H18 N10 O
Formula weight	294.34
Temperature	100(2)K
Wavelength	1.54178 Å
Crystal system	Triclinic
Space group	P-1
Unit cell dimensions	a = 10.0311(16) Å α = 88.090(7)° b = 10.8820(18) Å β = 87.280(7)° c = 21.127(3) Å γ = 62.735(6)°
Volume	2047.5(6)Å^3
Z	6
Density (calculated)	1.432 Mg/m^3
Absorption coefficient	0.863 mm^{-1}
F(000)	936
Crystal size	0.20 x 0.07 x 0.01 mm
Theta range for data collection	2.09 to 58.01°
Index ranges	$-10 \leq h \leq 10$, $-11 \leq k \leq 11$, $-23 \leq \ell \leq 23$
Reflections collected	34030
Independent reflections	6951 [R_{int} = 0.070]
Absorption correction	Semi-empirical from equivalents
Max. and min. transmission	0.9914 and 0.8463
Refinement method	Full-matrix least-squares on F^2
Data / restraints / parameters	6951 / 514 / 588
Goodness-of-fit on F^2	1.012
Final R indices [I>2sigma(I)]	R_1 = 0.0600, wR_2 = 0.0903
R indices (all data)	R_1 = 0.1294, wR_2 = 0.1012

Largest diff. peak and hole 0.318 and -0.360 e/Å^3

The crystals used were very thin needles that did not diffract well (only up to $2\theta = 58$ degrees). Three different data sets were collected from different samples. No reliable unit cell could be found with conventional indexing routines, so the crystals were indexed using a special program called "cell_now" (Sheldrick, 2004), which gave a C-centered monoclinic cell. This program indicated that the crystals appeared to be non-merohedrally twinned, with two twin components present. We used the capacity for integrating data from twinned samples implemented in the new version of Saint. Integration of the data processed well and gave good results with reasonable statistics. However, direct methods failed to solve the structure. After three tests, we abandoned the suggested monoclinic C-centered cell, and we attempted to use the primitive triclinic unit cell that has the following reduced dimensions:

a = 10.0311(16) Å	α = 88.090(7)°
b = 10.8820(18) Å	β = 87.280(7)°
c = 21.127(3) Å	γ = 62.735(6)°

Integrations using this new cell gave better data, and direct methods succeeded in solving the structure, giving four symmetry-independent molecules. Further analysis with the module "Addsym" from the "Platon" program (Spek, 2004) did not find any missing symmetry, confirming that the structure is actually triclinic and not monoclinic. The triclinic cell has a metric (dimensions) giving accidentally an apparent C-centered monoclinic "super-cell," as found in the initial indexation. With the triclinic unit cell, the twin law between the two domains is a 180 degree rotation around an arbitrary axis that is close to the crystallographic *c*-axis:

Domain 2 is rotated from first domain by 179.7 degrees about reciprocal axis 0.001 -0.002 1.000 and real axis -0.110 0.026 1.000

Twin law to convert hkl from first to domain 1:

-0.997	-0.006	0.001
0.007	-1.003	-0.004
-0.220	0.051	1.000

Data processing with Twinabs, the equivalent of the Sadabs program but written specifically for twinned samples (Sheldrick, 2001), gave the following statistics:

Maximum 2-theta = 116.01 deg.
34030 data
10867 data (3455 unique) involve component 1 only, mean I/sigma 3.0
10903 data (3449 unique) involve component 2 only, mean I/sigma 2.9

12260 data (3497 unique) involve 2 components, mean I/sigma 4.3

All non-H atoms were refined by full-matrix least squares with anisotropic displacement parameters. Hydrogen atoms were located from the difference Fourier map and then refined with restraints on distances. The ratio between the two components refined to 0.488, a value close to 0.5. Final residuals after complete refinement were:

Final R indices [$I > 2\sigma(I)$]	$R_1 = 0.0600$	$wR_2 = 0.0903$
R indices (all data)	$R_1 = 0.1294$	$wR_2 = 0.1012$

Table A2-2. Atomic coordinates (x 10^4) and equivalent isotropic displacement parameters ($Å^2$ x 10^3) for C10 H18 N10 O.

U_{eq} is defined as one third of the trace of the orthogonalized Uij tensor.

	x	y	z	U_{eq}
C(1)	9600(20)	-3136(19)	5361(8)	23(5)
N(1)	9810(14)	-4151(14)	5773(6)	27(4)
C(2)	10612(19)	-2308(18)	4532(8)	23(5)
N(2)	8247(15)	-2035(14)	5388(6)	27(4)
C(3)	9337(17)	-576(18)	3794(7)	20(4)
N(3)	10786(14)	-3281(14)	4993(6)	19(4)
C(4)	9420(18)	626(19)	3934(7)	28(5)
N(4)	11937(14)	-2280(14)	4379(6)	32(4)
C(5)	9329(17)	1567(17)	3467(8)	24(5)
N(5)	9349(15)	-1524(14)	4275(6)	23(4)
C(6)	9136(17)	1330(18)	2840(7)	21(4)
N(6)	9191(14)	2260(14)	2365(6)	22(4)
C(7)	9028(18)	134(19)	2698(7)	26(5)
N(7)	6840(15)	2668(14)	1961(6)	31(4)
C(8)	9128(18)	-805(17)	3173(8)	24(5)
N(8)	8204(14)	3578(14)	1448(6)	22(4)
C(9)	8160(20)	2764(17)	1943(8)	25(5)
N(9)	10848(15)	2720(15)	1444(6)	33(4)
C(10)	9500(20)	3520(18)	1231(8)	23(5)
N(10)	9446(14)	4318(15)	727(6)	30(4)
C(11)	4177(19)	13286(18)	3742(7)	22(5)
N(11)	3653(14)	14264(14)	4209(6)	31(4)
C(12)	3690(20)	11980(17)	2998(7)	22(5)
N(12)	5638(14)	12777(13)	3582(6)	23(4)
C(13)	5189(17)	10539(18)	2176(8)	21(4)
N(13)	3211(14)	12939(14)	3495(6)	22(4)
C(14)	4757(17)	11048(17)	1569(8)	25(5)
N(14)	2568(14)	11627(14)	2861(6)	31(4)
C(15)	4981(18)	10150(19)	1065(7)	27(5)
N(15)	4986(14)	11465(13)	2685(6)	20(4)
C(16)	5696(17)	8731(18)	1146(8)	21(4)
N(16)	5883(14)	7781(14)	640(6)	23(4)
C(17)	6135(17)	8219(17)	1747(8)	23(4)
N(17)	7887(15)	8151(15)	220(6)	33(4)
C(18)	5917(17)	9115(18)	2250(7)	22(4)
N(18)	7392(14)	6567(14)	-267(6)	21(4)
C(19)	6960(18)	7543(18)	217(8)	24(5)
N(19)	4939(15)	6744(14)	-338(6)	27(4)
C(20)	6430(20)	6147(18)	-461(7)	23(5)
N(20)	6989(14)	5053(15)	-862(6)	33(4)
C(21)	8850(20)	3445(18)	-2134(8)	27(5)
N(21)	8401(15)	4313(15)	-2639(6)	34(4)
C(22)	8500(20)	1903(18)	-1457(8)	27(5)

N(22)	10049(15)	3395(14)	-1849(6)	29(4)
C(23)	9752(18)	815(19)	-550(8)	20(4)
N(23)	8093(14)	2786(14)	-1975(6)	24(4)
C(24)	8973(17)	1381(17)	28(8)	23(5)
N(24)	7599(15)	1257(15)	-1387(6)	34(4)
C(25)	9206(18)	561(19)	562(7)	23(5)
N(25)	9580(15)	1682(14)	-1083(6)	23(4)
C(31)	4810(20)	6786(18)	2966(7)	23(5)
N(31)	4861(14)	5824(15)	2552(6)	33(4)
C(32)	6030(20)	7393(18)	3740(8)	25(5)
N(32)	3534(14)	7977(14)	3003(6)	27(4)
C(33)	4969(17)	9148(18)	4509(7)	22(5)
N(33)	6056(15)	6479(14)	3273(6)	23(4)
C(34)	4413(17)	9084(17)	5113(8)	22(5)
N(34)	7503(14)	7057(13)	3879(6)	25(4)
C(35)	4449(17)	9930(18)	5603(7)	25(5)
N(35)	4824(14)	8329(14)	4019(6)	24(4)
O(1)	3496(11)	5582(13)	5604(5)	29(3)
O(2)	8980(12)	4964(12)	2710(5)	28(3)
O(3)	5550(12)	5416(12)	999(5)	31(3)

Table A2-3. Hydrogen coordinates (x 10^4) and isotropic displacement parameters (Å^2 x 10^3) for C10 H18 N10 O.

	x	y	z	U_{eq}
H(1A)	10695	-4877	5795	33
H(1B)	9060	-4096	6025	33
H(2A)	7558	-2018	5666	32
H(2B)	8043	-1330	5127	32
H(4)	9542	800	4359	33
H(4A)	11969	-1697	4087	39
H(4B)	12757	-2844	4573	39
H(5)	9397	2379	3571	29
H(7)	8886	-33	2274	31
H(7A)	6630	2233	2278	37
H(7B)	6204	3041	1654	37
H(8)	9052	-1615	3073	28
H(9A)	10957	2148	1764	40
H(9B)	11638	2761	1265	40
H(10A)	10281	4288	560	36
H(10B)	8579	4872	564	36
H(11A)	2702	14637	4335	38
H(11B)	4269	14516	4382	38
H(12A)	6040	12148	3286	28
H(12B)	6197	13072	3773	28
H(14)	4304	12018	1492	30
H(14A)	2717	11042	2556	38
H(14B)	1708	11990	3079	38
H(15)	4631	10530	658	32
H(17)	6592	7249	1822	27
H(17A)	7773	8740	518	40
H(17B)	8598	7955	-77	40
H(18)	6282	8731	2654	26
H(19A)	4509	7493	-107	32
H(19B)	4394	6385	-490	32
H(20A)	7946	4660	-980	40
H(20B)	6392	4739	-1003	40
H(21A)	7616	4412	-2846	41
H(21B)	8891	4780	-2761	41
H(22A)	10400	2864	-1512	35
H(22B)	10481	3893	-2000	35
H(24)	8284	2336	48	28
H(24A)	7741	657	-1076	41
H(24B)	6881	1445	-1654	41
H(25)	8643	946	942	28
H(31A)	5691	5046	2498	39
H(31B)	4064	5985	2339	39

H(32A)	3467	8643	3247	33
H(32B)	2762	8091	2782	33
H(34)	4000	8465	5202	27
H(34A)	7682	7495	4181	30
H(34B)	8256	6406	3665	30
H(35)	4065	9860	6016	29
H(1X)	2600(140)	5900(300)	5440(120)	250
H(1Y)	3500(300)	5000(300)	5930(90)	250
H(2X)	9100(300)	4110(90)	2710(150)	250
H(2Y)	8040(120)	5500(200)	2840(150)	250
H(3X)	6410(180)	4800(200)	1170(140)	250
H(3Y)	5400(300)	6300(300)	870(150)	250

Table A2-4. Anisotropic parameters ($Å^2$ x 10^3) for C10 H18 N10 O.

The anisotropic displacement factor exponent takes the form:

$$-2\pi^2 [h^2 a^{*2} U_{11} + ... + 2 h k a^* b^* U_{12}]$$

	U11	U22	U33	U23	U13	U12
C(1)	25(11)	23(12)	20(11)	-6(9)	-8(9)	-11(10)
N(1)	21(8)	31(9)	23(8)	9(7)	-5(6)	-6(7)
C(2)	25(11)	28(12)	19(11)	-7(9)	7(9)	-14(10)
N(2)	23(8)	30(9)	23(8)	7(6)	4(6)	-10(7)
C(3)	16(10)	31(11)	11(10)	2(9)	-1(8)	-10(9)
N(3)	16(8)	28(8)	10(7)	1(7)	0(6)	-8(7)
C(4)	32(11)	37(12)	14(10)	2(9)	-1(8)	-16(10)
N(4)	23(8)	36(9)	34(8)	13(7)	-3(7)	-11(7)
C(5)	23(10)	24(11)	27(10)	-3(8)	-3(9)	-13(9)
N(5)	23(8)	26(9)	19(8)	5(7)	-6(7)	-10(7)
C(6)	16(10)	24(12)	16(10)	0(9)	-7(8)	-2(9)
N(6)	27(8)	25(9)	16(8)	2(7)	-4(7)	-13(7)
C(7)	34(12)	37(12)	8(10)	-6(9)	-3(8)	-18(10)
N(7)	27(9)	41(10)	25(8)	15(7)	-5(7)	-16(8)
C(8)	29(12)	25(12)	17(11)	-4(9)	-2(9)	-12(10)
N(8)	20(8)	33(9)	15(8)	8(7)	0(6)	-15(7)
C(9)	29(13)	23(13)	15(11)	-1(9)	2(10)	-7(11)
N(9)	21(8)	45(10)	32(9)	15(7)	-3(7)	-15(8)
C(10)	23(12)	31(13)	9(11)	-7(9)	-2(9)	-8(11)
N(10)	21(8)	42(9)	22(8)	14(7)	-3(7)	-11(7)
C(11)	24(11)	26(12)	14(10)	5(9)	1(9)	-10(10)
N(11)	28(8)	35(9)	30(8)	-10(7)	0(7)	-13(7)
C(12)	29(11)	22(12)	13(10)	7(9)	-10(9)	-10(10)
N(12)	24(8)	28(8)	16(8)	-5(6)	-1(6)	-9(7)
C(13)	17(10)	25(11)	22(10)	0(9)	5(8)	-10(9)
N(13)	22(8)	30(9)	16(8)	-2(7)	-1(6)	-13(7)
C(14)	18(10)	23(11)	28(11)	3(8)	1(9)	-5(9)
N(14)	24(8)	42(9)	25(8)	-9(7)	3(7)	-13(7)
C(15)	25(11)	33(12)	16(10)	4(9)	-6(8)	-7(10)
N(15)	20(8)	22(8)	16(8)	-5(6)	1(6)	-7(7)
C(16)	12(10)	30(11)	22(10)	-3(9)	3(8)	-9(9)
N(16)	23(8)	26(9)	17(8)	-4(7)	2(7)	-10(7)
C(17)	26(11)	23(11)	20(10)	2(8)	2(8)	-12(9)
N(17)	35(9)	41(9)	27(8)	-14(7)	9(7)	-20(8)
C(18)	18(11)	34(11)	9(9)	2(8)	-3(8)	-9(9)
N(18)	21(8)	26(9)	17(8)	-3(7)	-1(6)	-11(7)
C(19)	14(10)	27(12)	25(11)	1(9)	-8(9)	-5(9)
N(19)	21(8)	30(8)	25(8)	-8(6)	-4(7)	-8(7)
C(20)	27(12)	24(12)	11(10)	1(9)	0(9)	-5(10)
N(20)	26(8)	44(10)	34(9)	-14(8)	0(7)	-19(7)
C(21)	32(12)	27(12)	18(11)	-3(9)	-2(9)	-10(10)
N(21)	32(8)	43(9)	32(8)	10(7)	-7(7)	-21(7)

C(22)	30(12)	31(12)	26(11)	-4(9)	10(9)	-20(10)
N(22)	28(8)	35(9)	26(8)	8(7)	-6(7)	-18(7)
C(23)	17(10)	32(12)	19(10)	0(9)	-6(8)	-18(9)
N(23)	26(8)	31(9)	19(8)	9(7)	-5(6)	-16(7)
C(24)	23(11)	22(11)	25(10)	0(9)	1(9)	-11(9)
N(24)	32(8)	44(9)	29(8)	16(7)	-15(7)	-20(7)
C(25)	18(11)	36(12)	15(10)	0(9)	2(8)	-12(10)
N(25)	26(8)	33(9)	14(8)	6(7)	-6(7)	-16(7)
C(31)	30(12)	24(12)	8(10)	-4(9)	5(9)	-6(10)
N(31)	28(8)	34(9)	30(8)	-9(7)	-6(7)	-8(7)
C(32)	26(11)	27(12)	22(11)	3(9)	-9(9)	-11(10)
N(32)	25(8)	34(9)	19(8)	-2(7)	-10(6)	-9(7)
C(33)	17(10)	32(12)	12(10)	-2(9)	-2(8)	-7(9)
N(33)	23(8)	25(8)	19(8)	-3(6)	-7(6)	-8(7)
C(34)	21(10)	27(12)	21(10)	0(9)	0(8)	-14(9)
N(34)	18(8)	28(9)	22(8)	-8(6)	-2(6)	-4(7)
C(35)	21(10)	30(12)	16(10)	2(8)	-2(8)	-5(9)
N(35)	23(8)	32(9)	13(8)	-7(7)	0(7)	-9(7)
O(1)	28(8)	39(9)	21(8)	-4(6)	-2(6)	-16(7)
O(2)	28(8)	40(9)	19(7)	2(6)	-3(6)	-17(7)
O(3)	27(8)	40(10)	26(8)	4(6)	-11(6)	-15(7)

Table A2-5. Bond lengths [Å] and angles [°] for C10 H18 N10 O.

C(1)-N(1)	1.328(19)	C(25)-C(23)#1	1.38(2)
C(1)-N(3)	1.335(18)	C(31)-N(33)	1.330(19)
C(1)-N(2)	1.340(19)	C(31)-N(32)	1.343(18)
C(2)-N(5)	1.293(18)	C(31)-N(31)	1.369(19)
C(2)-N(4)	1.367(17)	C(32)-N(35)	1.300(18)
C(2)-N(3)	1.37(2)	C(32)-N(34)	1.395(18)
C(3)-C(8)	1.39(2)	C(32)-N(33)	1.415(19)
C(3)-C(4)	1.39(2)	C(33)-C(34)	1.381(19)
C(3)-N(5)	1.420(19)	C(33)-C(35)#2	1.38(2)
C(4)-C(5)	1.37(2)	C(33)-N(35)	1.443(18)
C(5)-C(6)	1.40(2)	C(34)-C(35)	1.42(2)
C(6)-C(7)	1.40(2)	C(35)-C(33)#2	1.38(2)
C(6)-N(6)	1.418(19)		
N(6)-C(9)	1.306(19)	N(1)-C(1)-N(3)	117.1(16)
C(7)-C(8)	1.38(2)	N(1)-C(1)-N(2)	115.8(15)
N(7)-C(9)	1.369(19)	N(3)-C(1)-N(2)	127.0(17)
N(8)-C(10)	1.330(18)	N(5)-C(2)-N(4)	124.7(17)
N(8)-C(9)	1.361(19)	N(5)-C(2)-N(3)	123.8(16)
N(9)-C(10)	1.322(19)	N(4)-C(2)-N(3)	111.5(16)
C(10)-N(10)	1.338(19)	C(8)-C(3)-C(4)	118.9(16)
C(11)-N(13)	1.324(18)	C(8)-C(3)-N(5)	119.0(16)
C(11)-N(12)	1.338(17)	C(4)-C(3)-N(5)	121.9(15)
C(11)-N(11)	1.375(18)	C(1)-N(3)-C(2)	119.5(15)
C(12)-N(15)	1.310(17)	C(5)-C(4)-C(3)	121.2(16)
C(12)-N(14)	1.391(18)	C(4)-C(5)-C(6)	119.9(16)
C(12)-N(13)	1.409(18)	C(2)-N(5)-C(3)	117.8(14)
C(13)-C(18)	1.38(2)	C(7)-C(6)-C(5)	119.1(15)
C(13)-C(14)	1.39(2)	C(7)-C(6)-N(6)	122.6(15)
C(13)-N(15)	1.441(18)	C(5)-C(6)-N(6)	118.0(16)
C(14)-C(15)	1.41(2)	C(9)-N(6)-C(6)	119.9(14)
C(15)-C(16)	1.38(2)	C(8)-C(7)-C(6)	120.2(15)
C(16)-C(17)	1.38(2)	C(7)-C(8)-C(3)	120.6(16)
C(16)-N(16)	1.458(19)	C(10)-N(8)-C(9)	121.1(15)
N(16)-C(19)	1.304(18)	N(6)-C(9)-N(8)	122.7(16)
C(17)-C(18)	1.41(2)	N(6)-C(9)-N(7)	126.2(16)
N(17)-C(19)	1.366(19)	N(8)-C(9)-N(7)	110.8(15)
N(18)-C(20)	1.327(19)	N(9)-C(10)-N(8)	127.1(16)
N(18)-C(19)	1.403(19)	N(9)-C(10)-N(10)	115.8(16)
N(19)-C(20)	1.347(18)	N(8)-C(10)-N(10)	117.1(15)
C(20)-N(20)	1.364(18)	N(13)-C(11)-N(12)	126.4(16)
C(21)-N(23)	1.292(19)	N(13)-C(11)-N(11)	117.9(15)
C(21)-N(22)	1.346(19)	N(12)-C(11)-N(11)	115.7(16)
C(21)-N(21)	1.350(19)	N(15)-C(12)-N(14)	122.0(15)
C(22)-N(25)	1.297(19)	N(15)-C(12)-N(13)	127.4(15)
C(22)-N(24)	1.376(18)	N(14)-C(12)-N(13)	110.6(15)
C(22)-N(23)	1.38(2)	C(18)-C(13)-C(14)	116.7(16)
C(23)-C(25)#1	1.38(2)	C(18)-C(13)-N(15)	122.6(15)
C(23)-N(25)	1.409(19)	C(14)-C(13)-N(15)	120.6(16)
C(23)-C(24)	1.415(19)	C(11)-N(13)-C(12)	119.7(14)
C(24)-C(25)	1.37(2)	C(13)-C(14)-C(15)	121.0(16)

C(16)-C(15)-C(14)	121.6(15)	C(25)#1-C(23)-N(25)	120.8(16)
C(12)-N(15)-C(13)	117.0(14)	C(25)#1-C(23)-C(24)	118.7(15)
C(17)-C(16)-C(15)	117.5(15)	N(25)-C(23)-C(24)	120.1(16)
C(17)-C(16)-N(16)	119.6(16)	C(21)-N(23)-C(22)	119.5(15)
C(15)-C(16)-N(16)	122.7(15)	C(25)-C(24)-C(23)	120.6(15)
C(19)-N(16)-C(16)	117.2(15)	C(24)-C(25)-C(23)#1	120.6(15)
C(16)-C(17)-C(18)	120.8(16)	C(22)-N(25)-C(23)	117.5(14)
C(13)-C(18)-C(17)	122.1(15)	N(33)-C(31)-N(32)	126.2(16)
C(20)-N(18)-C(19)	120.1(14)	N(33)-C(31)-N(31)	116.9(16)
N(16)-C(19)-N(17)	123.6(17)	N(32)-C(31)-N(31)	116.8(16)
N(16)-C(19)-N(18)	125.0(16)	N(35)-C(32)-N(34)	126.1(15)
N(17)-C(19)-N(18)	111.3(15)	N(35)-C(32)-N(33)	125.1(16)
N(18)-C(20)-N(19)	126.8(16)	N(34)-C(32)-N(33)	108.6(15)
N(18)-C(20)-N(20)	116.9(16)	C(34)-C(33)-C(35)#2	117.7(15)
N(19)-C(20)-N(20)	116.2(16)	C(34)-C(33)-N(35)	118.9(16)
N(23)-C(21)-N(22)	127.9(17)	C(35)#2-C(33)-N(35)	123.3(15)
N(23)-C(21)-N(21)	117.5(17)	C(31)-N(33)-C(32)	119.0(15)
N(22)-C(21)-N(21)	114.7(17)	C(33)-C(34)-C(35)	121.1(15)
N(25)-C(22)-N(24)	123.7(17)	C(33)#2-C(35)-C(34)	121.2(15)
N(25)-C(22)-N(23)	126.0(16)	C(32)-N(35)-C(33)	119.1(14)
N(24)-C(22)-N(23)	110.3(16)		

Symmetry transformations used to generate equivalent atoms:

#1 -x+2,-y,-z #2 -x+1,-y+2,-z+1

Table A2-6. Torsion angles [°] for C10 H18 N10 O.

N(1)-C(1)-N(3)-C(2)	175.8(15)	C(14)-C(15)-C(16)-C(17)	2(2)
N(2)-C(1)-N(3)-C(2)	-9(3)	C(14)-C(15)-C(16)-N(16)	177.3(15)
N(5)-C(2)-N(3)-C(1)	-25(3)	C(17)-C(16)-N(16)-C(19)	-106.0(18)
N(4)-C(2)-N(3)-C(1)	155.6(14)	C(15)-C(16)-N(16)-C(19)	79(2)
C(8)-C(3)-C(4)-C(5)	-1(3)	C(15)-C(16)-C(17)-C(18)	-3(2)
N(5)-C(3)-C(4)-C(5)	-176.6(15)	N(16)-C(16)-C(17)-C(18)	-177.6(14)
C(3)-C(4)-C(5)-C(6)	1(3)	C(14)-C(13)-C(18)-C(17)	-4(2)
N(4)-C(2)-N(5)-C(3)	1(2)	N(15)-C(13)-C(18)-C(17)	-178.8(15)
N(3)-C(2)-N(5)-C(3)	-178.9(16)	C(16)-C(17)-C(18)-C(13)	3(2)
C(8)-C(3)-N(5)-C(2)	109.9(17)	C(16)-N(16)-C(19)-N(17)	-1(2)
C(4)-C(3)-N(5)-C(2)	-75(2)	C(16)-N(16)-C(19)-N(18)	173.7(14)
C(4)-C(5)-C(6)-C(7)	0(2)	C(20)-N(18)-C(19)-N(16)	23(2)
C(4)-C(5)-C(6)-N(6)	-174.1(15)	C(20)-N(18)-C(19)-N(17)	-161.5(15)
C(7)-C(6)-N(6)-C(9)	53(2)	C(19)-N(18)-C(20)-N(19)	14(2)
C(5)-C(6)-N(6)-C(9)	-132.4(16)	C(19)-N(18)-C(20)-N(20)	-170.4(15)
C(5)-C(6)-C(7)-C(8)	-1(2)	N(22)-C(21)-N(23)-C(22)	0(3)
N(6)-C(6)-C(7)-C(8)	173.6(15)	N(21)-C(21)-N(23)-C(22)	-179.1(14)
C(6)-C(7)-C(8)-C(3)	0(3)	N(25)-C(22)-N(23)-C(21)	2(3)
C(4)-C(3)-C(8)-C(7)	1(3)	N(24)-C(22)-N(23)-C(21)	-177.1(15)
N(5)-C(3)-C(8)-C(7)	176.4(15)	C(25)#1-C(23)-C(24)-C(25)	-3(3)
C(6)-N(6)-C(9)-N(8)	-175.0(15)	N(25)-C(23)-C(24)-C(25)	-175.8(14)
C(6)-N(6)-C(9)-N(7)	11(3)	C(23)-C(24)-C(25)-C(23)#1	3(3)
C(10)-N(8)-C(9)-N(6)	24(2)	N(24)-C(22)-N(25)-C(23)	-5(3)
C(10)-N(8)-C(9)-N(7)	-161.1(15)	N(23)-C(22)-N(25)-C(23)	175.4(15)
C(9)-N(8)-C(10)-N(9)	0(3)	C(25)#1-C(23)-N(25)-C(22)	98(2)
C(9)-N(8)-C(10)-N(10)	177.5(16)	C(24)-C(23)-N(25)-C(22)	-89.0(19)
N(12)-C(11)-N(13)-C(12)	-3(2)	N(32)-C(31)-N(33)-C(32)	8(3)
N(11)-C(11)-N(13)-C(12)	177.6(14)	N(31)-C(31)-N(33)-C(32)	-175.5(14)
N(15)-C(12)-N(13)-C(11)	-8(2)	N(35)-C(32)-N(33)-C(31)	19(2)
N(14)-C(12)-N(13)-C(11)	172.6(14)	N(34)-C(32)-N(33)-C(31)	-165.3(14)
C(18)-C(13)-C(14)-C(15)	3(2)	C(35)#2-C(33)-C(34)-C(35)	0(3)
N(15)-C(13)-C(14)-C(15)	178.6(15)	N(35)-C(33)-C(34)-C(35)	-176.3(14)
C(13)-C(14)-C(15)-C(16)	-3(3)	C(33)-C(34)-C(35)-C(33)#2	0(3)
N(14)-C(12)-N(15)-C(13)	2(2)	N(34)-C(32)-N(35)-C(33)	2(3)
N(13)-C(12)-N(15)-C(13)	-177.5(15)	N(33)-C(32)-N(35)-C(33)	177.1(15)
C(18)-C(13)-N(15)-C(12)	-97.6(18)	C(34)-C(33)-N(35)-C(32)	-119.0(17)
C(14)-C(13)-N(15)-C(12)	87.6(19)	C(35)#2-C(33)-N(35)-C(32)	65(2)

Symmetry transformations used to generate equivalent atoms:

#1 -x+2,-y,-z #2 -x+1,-y+2,-z+1

Table A2-7. Bond lengths [Å] and angles [°] related to the hydrogen bonding for C10 H18 N10 O.

D-H	..A	d(D-H)	d(H..A)	d(D..A)	<DHA
N(1)-H(1A)	N(34)#3	0.88	2.33	3.167(18)	158.0
N(1)-H(1B)	N(13)#4	0.88	2.25	3.056(17)	153.1
N(2)-H(2B)	N(5)	0.88	2.13	2.700(17)	121.7
N(2)-H(2A)	N(13)#4	0.88	2.28	3.083(17)	151.9
N(4)-H(4A)	N(32)#5	0.88	2.65	3.319(18)	133.2
N(7)-H(7A)	N(15)#6	0.88	2.29	3.057(17)	145.7
N(9)-H(9A)	N(6)	0.88	2.09	2.682(17)	123.9
N(10)-H(10B)	N(18)	0.88	2.42	3.177(18)	144.1
N(10)-H(10A)	N(18)#7	0.88	2.15	2.984(17)	158.6
N(11)-H(11A)	N(3)#8	0.88	2.59	3.310(18)	139.2
N(11)-H(11B)	O(1)#2	0.88	2.20	2.986(16)	149.0
N(12)-H(12A)	N(15)	0.88	2.05	2.685(17)	128.5
N(12)-H(12B)	O(1)#2	0.88	2.13	2.944(16)	152.8
N(17)-H(17B)	N(10)#7	0.88	2.72	3.412(18)	136.9
N(19)-H(19A)	N(16)	0.88	2.26	2.785(18)	117.9
N(19)-H(19B)	O(3)#9	0.88	2.24	3.009(18)	145.2
N(20)-H(20A)	N(22)	0.88	2.62	3.406(18)	149.3
N(20)-H(20B)	O(3)#9	0.88	2.03	2.846(17)	153.6
N(21)-H(21A)	N(31)#9	0.88	2.66	3.340(18)	135.3
N(21)-H(21B)	O(2)#7	0.88	2.28	3.064(16)	147.7
N(22)-H(22A)	N(25)	0.88	1.99	2.616(17)	126.7
N(22)-H(22B)	O(2)#7	0.88	2.12	2.941(15)	154.7
N(31)-H(31B)	N(21)#9	0.88	2.68	3.340(18)	132.5
N(31)-H(31B)	N(23)#9	0.88	2.12	2.944(18)	155.5
N(31)-H(31A)	N(7)	0.88	2.58	3.332(19)	144.0
N(32)-H(32A)	N(35)	0.88	2.09	2.684(17)	124.0
N(32)-H(32B)	N(23)#9	0.88	2.36	3.124(17)	146.1
N(34)-H(34A)	N(5)#10	0.88	2.38	3.061(18)	134.5
N(34)-H(34B)	O(2)	0.88	2.47	3.228(16)	144.9
N(34)-H(34B)	N(1)#3	0.88	2.62	3.167(18)	121.3
O(1)-H(1X)	N(3)#11	0.9(2)	1.9(2)	2.779(17)	171
O(1)-H(1Y)	N(33)#4	0.9(2)	2.2(3)	3.112(17)	170
O(2)-H(2X)	N(6)	0.9(2)	2.2(1)	2.966(17)	159
O(2)-H(2Y)	N(33)	0.9(2)	2.0(2)	2.845(17)	169
O(3)-H(3X)	N(8)	0.9(2)	1.8(3)	2.689(18)	175
O(3)-H(3Y)	N(16)	0.9(2)	2.0(3)	2.816(18)	159

Symmetry transformations used to generate equivalent atoms:

#1 -x+2,-y,-z	#2 -x+1,-y+2,-z+1	#3 -x+2,-y,-z+1
#4 -x+1,-y+1,-z+1	#5 x+1,y-1,z	#6 x,y-1,z
#7 -x+2,-y+1,-z	#8 x-1,y+2,z	#9 -x+1,-y+1,-z
#10 x,y+1,z	#11 x-1,y+1,z	

Table A2-8

Least-squares planes (x,y,z in crystal coordinates) and deviations from them (* indicates atom used to define plane)

1) N1 C1 N2 N3 C2 N4 N5

```
  4.2695 (0.0512) x + 8.2148 (0.0308) y + 14.3091 (0.0608) z = 9.1878
(0.0709)

 *    -0.1480 (0.0094)  N1
 *     0.0082 (0.0143)  C1
 *     0.3705 (0.0092)  N2
 *    -0.1330 (0.0118)  N3
 *    -0.0687 (0.0139)  C2
 *     0.3017 (0.0090)  N4
 *    -0.3307 (0.0094)  N5

 Rms deviation of fitted atoms =    0.2336
```

2) C3 C4 C5 C6 C7 C8

```
  8.6298 (0.0313) x - 0.4011 (0.0672) y - 2.5946 (0.1289) z = 7.0891
(0.0590)

 Angle to previous plane (with approximate esd) = 87.62 ( 0.44 )

 *     0.0075 (0.0114)  C3
 *    -0.0056 (0.0119)  C4
 *    -0.0009 (0.0119)  C5
 *     0.0053 (0.0113)  C6
 *    -0.0033 (0.0118)  C7
 *    -0.0031 (0.0121)  C8

 Rms deviation of fitted atoms =    0.0048
```

3) N6 C9 N7 C10 N9 N10

```
  1.3234 (0.0493) x + 8.6414 (0.0229) y + 11.9439 (0.0873) z = 5.7673
(0.0527)

 Angle to previous plane (with approximate esd) = 68.09 ( 0.49 )

 *     0.2261 (0.0093)  N6
 *     0.0217 (0.0142)  C9
 *    -0.2148 (0.0089)  N7
 *     0.1403 (0.0122)  N8
 *     0.0009 (0.0147)  C10
 *    -0.2565 (0.0093)  N9
 *     0.0824 (0.0096)  N10
```

```
Rms deviation of fitted atoms =   0.1647
```

4) N11 C11 N12 N13 C12 N14 N15

0.3423 (0.0518) x + 7.4281 (0.0259) y - 13.6896 (0.0619) z = 4.9008 (0.0561)

Angle to previous plane (with approximate esd) = 74.85 (0.26)

*	0.0578	(0.0091)	N11
*	-0.0109	(0.0140)	C11
*	-0.1205	(0.0087)	N12
*	0.0355	(0.0117)	N13
*	0.0203	(0.0132)	C12
*	-0.0922	(0.0085)	N14
*	0.1100	(0.0088)	N15

Rms deviation of fitted atoms = 0.0758

5) C13 C14 C15 C16 C17 C18

9.7984 (0.0126) x + 4.6295 (0.0565) y - 3.5162 (0.1211) z = 9.2127 (0.0641)

Angle to previous plane (with approximate esd) = 81.07 (0.45)

*	-0.0147	(0.0114)	C13
*	0.0116	(0.0119)	C14
*	-0.0078	(0.0120)	C15
*	0.0069	(0.0117)	C16
*	-0.0102	(0.0117)	C17
*	0.0141	(0.0115)	C18

Rms deviation of fitted atoms = 0.0113

6) N16 C19 N17 N18 C20 N19 N20

- 0.9613 (0.0605) x + 6.6873 (0.0312) y - 13.9232 (0.0768) z = 4.1153 (0.0558)

Angle to previous plane (with approximate esd) = 88.31 (0.48)

*	-0.3683	(0.0096)	N16
*	-0.0420	(0.0147)	C19
*	0.2718	(0.0095)	N17
*	-0.0632	(0.0117)	N18
*	0.0191	(0.0142)	C20
*	0.3909	(0.0096)	N19
*	-0.2082	(0.0092)	N20

Rms deviation of fitted atoms = 0.2425

7) N21 N22 C21 N23 C22 N24 N25

2.8625 (0.0510) x - 5.9202 (0.0325) y - 12.2692 (0.0806) z = 3.1041 (0.0443)

Angle to previous plane (with approximate esd) = 78.43 (0.30)

*	-0.0154	(0.0090)	N21
*	0.0313	(0.0091)	N22
*	0.0080	(0.0148)	C21
*	-0.0140	(0.0118)	N23
*	-0.0105	(0.0146)	C22
*	0.0287	(0.0089)	N24
*	-0.0283	(0.0091)	N25

Rms deviation of fitted atoms = 0.0214

8) C23 C24 C25 C23#1 C24#1 C25#1

9.4321 (0.0291) x + 6.9548 (0.0735) y + 6.2158 (0.1658) z = 9.4321 (0.0291)

Angle to previous plane (with approximate esd) = 86.90 (0.52)

*	-0.0095	(0.0095)	C23
*	0.0096	(0.0096)	C24
*	-0.0097	(0.0098)	C25
*	0.0095	(0.0095)	C23#1
*	-0.0096	(0.0096)	C24#1
*	0.0097	(0.0098)	C25#1

Rms deviation of fitted atoms = 0.0096

9) N31 C31 N32 N33 C32 N34 N35

4.6531 (0.0395) x + 7.7091 (0.0357) y - 13.9023 (0.0593) z = 3.3366 (0.0450)

Angle to previous plane (with approximate esd) = 66.60 (0.50)

*	-0.1320	(0.0089)	N31
*	0.0103	(0.0144)	C31
*	0.2828	(0.0091)	N32
*	-0.0741	(0.0116)	N33
*	-0.0308	(0.0143)	C32
*	0.2021	(0.0087)	N34
*	-0.2582	(0.0090)	N35

Rms deviation of fitted atoms = 0.1738

10) C33 C34 C35 C33#2 C34#2 C35#2

6.6442 (0.0693) x - 3.5387 (0.0935) y + 5.6881 (0.1749) z = 2.6275 (0.1536)

Angle to previous plane (with approximate esd) = 75.08 (0.55)

```
 *     0.0016 (0.0095)   C33
 *    -0.0017 (0.0095)   C34
 *     0.0017 (0.0095)   C35
 *    -0.0016 (0.0095)   C33#2
 *     0.0017 (0.0095)   C34#2
 *    -0.0017 (0.0095)   C35#2

 Rms deviation of fitted atoms =    0.0017
```

11) N1 C1 N2 N3

```
  5.8437 (0.0637) x + 7.0951 (0.0678) y + 15.2144 (0.1200) z = 11.5651
(0.0716)

 Angle to previous plane (with approximate esd) = 75.55 ( 0.62 )

 *     0.0064 (0.0043)   N1
 *    -0.0205 (0.0138)   C1
 *     0.0070 (0.0048)   N2
 *     0.0071 (0.0048)   N3

 Rms deviation of fitted atoms =    0.0119
```

12) N3 C2 N4 N5

```
  1.5811 (0.0789) x + 7.4960 (0.0645) y + 15.1791 (0.1162) z = 6.8256
(0.0923)

 Angle to previous plane (with approximate esd) = 28.87 ( 0.88 )

 *    -0.0003 (0.0043)   N3
 *     0.0008 (0.0137)   C2
 *    -0.0003 (0.0043)   N4
 *    -0.0003 (0.0051)   N5

 Rms deviation of fitted atoms =    0.0005
```

13) N10 C10 N9 N8

```
  2.7823 (0.0768) x + 8.5040 (0.0604) y + 13.5070 (0.1460) z = 7.2858
(0.0782)

 Angle to previous plane (with approximate esd) =  8.78 ( 1.23 )

 *    -0.0036 (0.0043)   N10
 *     0.0119 (0.0142)   C10
 *    -0.0041 (0.0049)   N9
 *    -0.0041 (0.0049)   N8

 Rms deviation of fitted atoms =    0.0069
```

14) N8 C9 N6 N7

```
 - 0.6906 (0.0807) x + 7.6892 (0.0655) y + 11.8267 (0.1368) z = 3.8889
(0.0806)

 Angle to previous plane (with approximate esd) = 21.00 ( 1.03 )

 *     0.0087 (0.0043)  N8
 *    -0.0283 (0.0139)  C9
 *     0.0106 (0.0052)  N6
 *     0.0091 (0.0045)  N7

 Rms deviation of fitted atoms =    0.0164
```

15) N11 N12 C11 N13

1.0067 (0.0757) x + 7.3950 (0.0650) y - 14.3510 (0.1290) z = 4.8756 (0.1477)

Angle to previous plane (with approximate esd) = 78.39 (0.55)

*	-0.0001 (0.0041)	N11
*	-0.0001 (0.0046)	N12
*	0.0003 (0.0135)	C11
*	-0.0001 (0.0048)	N13

Rms deviation of fitted atoms = 0.0001

16) N13 C12 N14 N15

- 0.5354 (0.0785) x + 6.9568 (0.0683) y - 13.8383 (0.1224) z = 3.9914 (0.1320)

Angle to previous plane (with approximate esd) = 9.20 (1.22)

*	0.0011 (0.0042)	N13
*	-0.0036 (0.0130)	C12
*	0.0011 (0.0039)	N14
*	0.0014 (0.0049)	N15

Rms deviation of fitted atoms = 0.0021

17) N20 C20 N19 N18

0.9350 (0.0767) x + 6.2560 (0.0737) y - 16.5282 (0.1110) z = 5.2320 (0.0783)

Angle to previous plane (with approximate esd) = 14.18 (1.14)

*	0.0070 (0.0041)	N20
*	-0.0231 (0.0136)	C20
*	0.0080 (0.0047)	N19
*	0.0081 (0.0048)	N18

Rms deviation of fitted atoms = 0.0134

18) N18 C19 N17 N16

- 3.6300 (0.0776) x + 5.0817 (0.0818) y - 12.8682 (0.1263) z = 1.0041 (0.1109)

Angle to previous plane (with approximate esd) = 29.39 (0.93)

```
*    -0.0073 (0.0044)  N18
*     0.0235 (0.0141)  C19
*    -0.0074 (0.0045)  N17
*    -0.0088 (0.0053)  N16

Rms deviation of fitted atoms =   0.0136
```

19) N21 N22 C21 N23

2.6711 (0.0753) x - 5.9904 (0.0731) y - 12.5452 (0.1438) z = 2.9721 (0.0907)

Angle to previous plane (with approximate esd) = 74.02 (0.63)

* -0.0016 (0.0043) N21
* -0.0018 (0.0049) N22
*   0.0053 (0.0145) C21
* -0.0019 (0.0052) N23

Rms deviation of fitted atoms = 0.0031

20) N23 C22 N24 N25

3.1021 (0.0767) x - 5.7092 (0.0774) y - 12.2452 (0.1326) z = 3.3371 (0.0781)

Angle to previous plane (with approximate esd) = 2.59 (1.46)

*   0.0010 (0.0045) N23
* -0.0031 (0.0143) C22
*   0.0010 (0.0044) N24
*   0.0012 (0.0054) N25

Rms deviation of fitted atoms = 0.0018

21) N31 N32 C31 N33

5.4736 (0.0642) x + 6.5145 (0.0699) y - 14.9711 (0.1205) z = 2.6301 (0.0991)

Angle to previous plane (with approximate esd) = 72.06 (0.58)

*   0.0049 (0.0042) N31
*   0.0055 (0.0048) N32
* -0.0160 (0.0139) C31
*   0.0056 (0.0048) N33

Rms deviation of fitted atoms = 0.0092

22) N33 C32 N34 N35

2.9272 (0.0735) x + 7.7292 (0.0596) y - 14.3611 (0.1203) z = 2.0867 (0.1146)

Angle to previous plane (with approximate esd) = 20.90 (1.00)

* -0.0066 (0.0043) N33
*   0.0218 (0.0141) C32
* -0.0068 (0.0044) N34

```
*    -0.0084 (0.0055)  N35

Rms deviation of fitted atoms =   0.0126
```

Symmetry transformations used to generate equivalent atoms:

#1 -x+2,-y, -z #2 -x+1,-y+2, -z+1

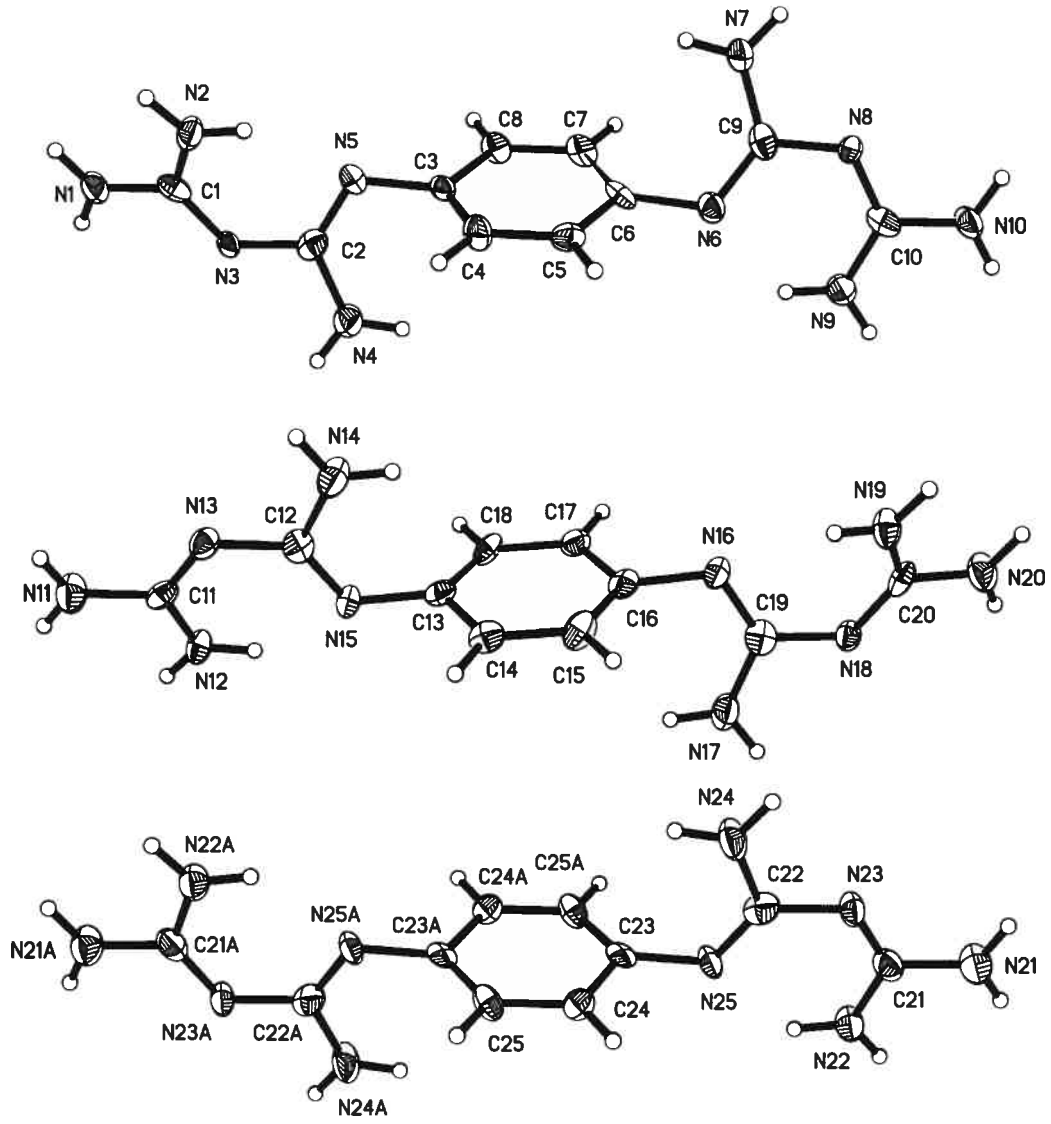

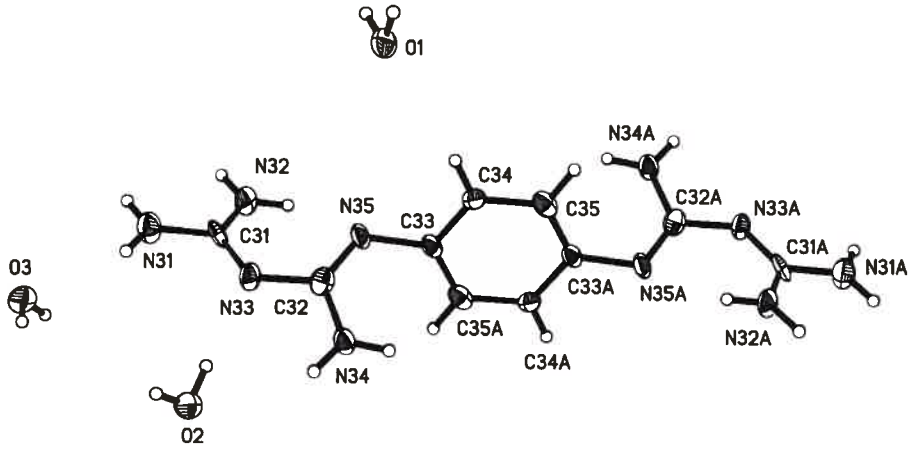

Figure A2-1. ORTEP view of the C10 H18 N10 O compound (**28**) with the numbering scheme adopted. Ellipsoids are drawn at the 50% probability level. Hydrogen atoms are represented by a sphere of arbitrary size.

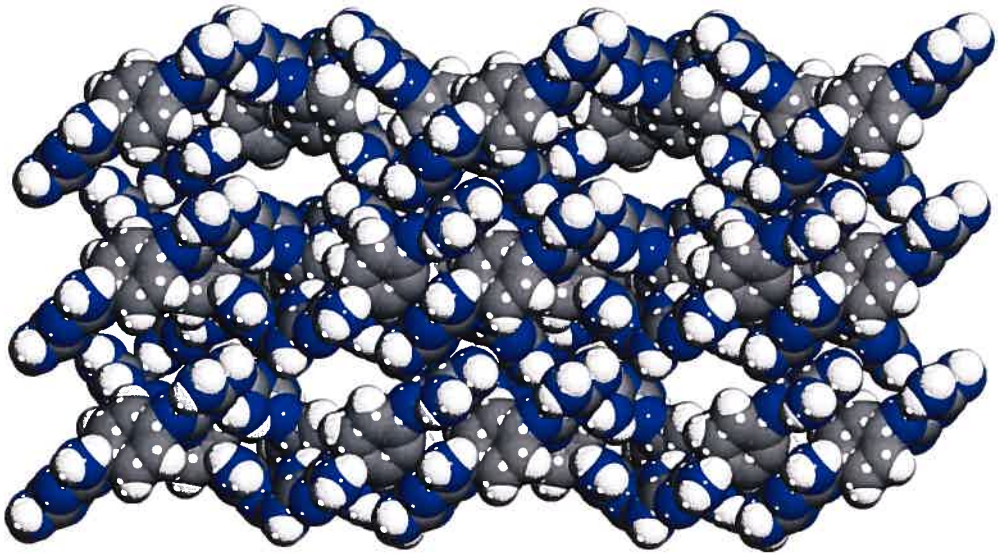

Figure A2-2. View along the *a* axis of the structure of crystals of 1,4-phenylenebis(biguanide) (**28**) grown from water, showing a 1 × 2 × 2 array of unit cells with atoms represented by spheres of van der Waals radii. Hydrogen atoms appear in white, carbon in gray, and nitrogen in blue. Guest molecules of water are omitted for clarity.

Université de Montréal

CRYSTAL AND MOLECULAR STRUCTURE OF

C10 H20 Cl2 N10 O COMPOUND (JIW811)

Equipe WUEST

Département de chimie, Université de Montréal,

C.P. 6128, Succ. Centre-Ville, Montréal, Québec, H3C 3J7 (Canada)

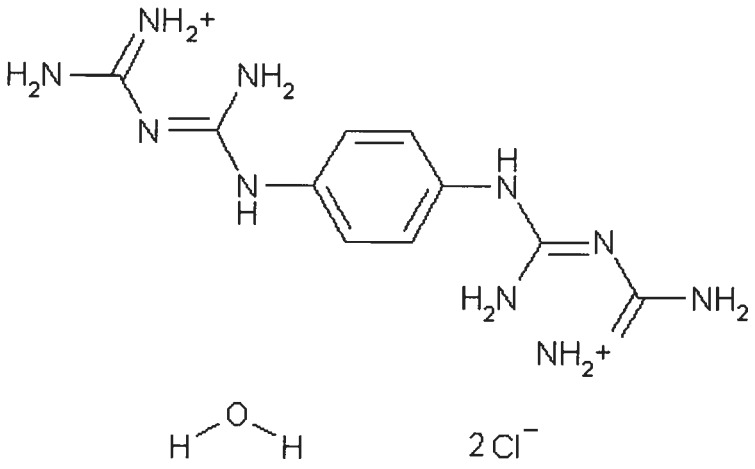

Structure solved and refined in the Laboratory of X-Ray Diffraction, Université de Montréal by Dr. Thierry Maris

Table A2-9. Crystal data and structure refinement for C10 H20 Cl2 N10 O.

Identification code	JIW811
Empirical formula	C10 H20 Cl2 N10 O
Formula weight	367.26
Temperature	293(2)K
Wavelength	1.54178 Å
Crystal system	Triclinic
Space group	P-1
Unit cell dimensions	a = 5.8749(8) Å α = 105.66(3)° b = 12.036(5) Å β = 95.65(3)° c = 13.084(5) Å γ = 102.12(2)°
Volume	859.1(5)Å^3
Z	2
Density (calculated)	1.420 g/cm^3
Absorption coefficient	3.591 mm^{-1}
F(000)	384
Crystal size	0.25 x 0.25 x 0.15 mm
Theta range for data collection	3.56 to 70.01°
Index ranges	$-7 \leq h \leq 7$, $-14 \leq k \leq 14$, $-15 \leq \ell \leq 15$
Reflections collected	6433
Independent reflections	3241 [R_{int} = 0.000]
Absorption correction	Analytical
Max. and min. transmission	0.6100 and 0.4600
Refinement method	Full-matrix least-squares on F^2
Data / restraints / parameters	3241 / 3 / 217
Goodness-of-fit on F^2	1.105
Final R indices [I>2sigma(I)]	R_1 = 0.0456, wR_2 = 0.1109

R indices (all data)	R_1 = 0.0463, wR_2 = 0.1110
Largest diff. peak and hole	0.323 and -0.396 e/Å^3

Table A2-10. Atomic coordinates (x 10^4) and equivalent isotropic displacement parameters (Å^2 x 10^3) for C10 H20 Cl2 N10 O.

U_{eq} is defined as one third of the trace of the orthogonalized Uij tensor.

	Occ.	x	y	z	U_{eq}
Cl(1)	1	362(1)	3025(1)	2641(1)	35(1)
Cl(2)	1	9545(1)	7688(1)	2094(1)	36(1)
C(1)	1	6450(3)	9100(2)	6631(2)	29(1)
C(2)	1	6016(3)	8279(2)	5616(2)	28(1)
C(3)	1	3990(3)	8153(2)	4902(2)	24(1)
C(4)	1	2454(4)	8865(2)	5215(2)	30(1)
C(5)	1	2928(4)	9704(2)	6229(2)	30(1)
C(6)	1	4890(3)	9801(2)	6937(2)	27(1)
C(10)	1	4170(3)	10682(2)	8767(1)	22(1)
N(10)	1	5470(3)	10668(2)	7982(1)	28(1)
C(11)	1	3738(3)	11864(2)	10441(2)	25(1)
N(11)	1	2204(3)	9815(2)	8590(1)	32(1)
N(12)	1	5081(3)	11530(2)	9700(1)	28(1)
N(13)	1	1357(3)	11716(2)	10220(1)	31(1)
N(14)	1	4774(3)	12382(2)	11451(1)	33(1)
C(20)	1	4189(3)	6390(2)	3391(1)	24(1)
N(20)	1	3399(3)	7368(2)	3851(1)	29(1)
C(21)	1	6747(3)	5204(2)	3625(2)	26(1)
N(21)	1	3512(3)	5941(2)	2323(1)	33(1)
N(22)	1	5397(3)	5948(2)	4012(1)	28(1)
N(23)	1	7861(4)	5251(2)	2799(2)	38(1)
N(24)	1	6989(4)	4402(2)	4106(2)	38(1)
O(1)	0.50	3169(6)	4450(3)	13(2)	41(1)
O(2)	0.50	8391(7)	4232(3)	128(3)	47(1)

Table A2-11. Hydrogen coordinates (x 10^4) and isotropic displacement parameters ($Å^2$ x 10^3) for C10 H20 Cl2 N10 O.

	Occ.	x	y	z	U_{eq}
H(1)	1	7797	9181	7110	34
H(2)	1	7072	7815	5414	33
H(4)	1	1094	8782	4744	36
H(5)	1	1917	10196	6424	36
H(10)	1	6750	11220	8113	34
H(11A)	1	1410	9771	9102	38
H(11B)	1	1733	9302	7964	38
H(13A)	1	591	11957	10729	38
H(13B)	1	621	11382	9571	38
H(14A)	1	6275	12497	11620	40
H(14B)	1	3948	12604	11940	40
H(20)	1	2380	7529	3430	35
H(21A)	1	3869	5301	1979	39
H(21B)	1	2720	6293	1982	39
H(23A)	1	8719	4762	2591	45
H(23B)	1	7726	5771	2472	45
H(24A)	1	7855	3921	3884	45
H(24B)	1	6281	4355	4643	45
H(1A)	0.50	2418	3839	-561	250
H(1B)	0.50	4533	4938	5	250
H(2A)	0.50	7735	3470	-229	250
H(2B)	0.50	9874	4347	-4	250

Table A2-12. Anisotropic parameters ($Å^2$ x 10^3) for C10 H20 Cl2 N10 O.

The anisotropic displacement factor exponent takes the form:

$$-2\pi^2 [h^2 a^{*2} U_{11} + ... + 2 h k a^* b^* U_{12}]$$

	U11	U22	U33	U23	U13	U12
Cl(1)	33(1)	33(1)	35(1)	-2(1)	6(1)	16(1)
Cl(2)	33(1)	38(1)	39(1)	21(1)	-2(1)	4(1)
C(1)	25(1)	28(1)	31(1)	6(1)	2(1)	7(1)
C(2)	27(1)	27(1)	28(1)	3(1)	3(1)	13(1)
C(3)	23(1)	26(1)	26(1)	8(1)	7(1)	9(1)
C(4)	32(1)	33(1)	29(1)	11(1)	2(1)	15(1)
C(5)	31(1)	33(1)	28(1)	8(1)	9(1)	13(1)
C(6)	27(1)	27(1)	27(1)	6(1)	9(1)	6(1)
C(10)	24(1)	26(1)	18(1)	7(1)	2(1)	8(1)
N(10)	29(1)	28(1)	23(1)	4(1)	7(1)	3(1)
C(11)	23(1)	23(1)	30(1)	7(1)	5(1)	6(1)
N(11)	32(1)	33(1)	28(1)	5(1)	9(1)	5(1)
N(12)	27(1)	32(1)	21(1)	1(1)	4(1)	5(1)
N(13)	29(1)	39(1)	25(1)	4(1)	7(1)	13(1)
N(14)	33(1)	43(1)	22(1)	2(1)	6(1)	13(1)
C(20)	24(1)	26(1)	22(1)	7(1)	5(1)	6(1)
N(20)	35(1)	29(1)	25(1)	6(1)	0(1)	16(1)
C(21)	28(1)	20(1)	27(1)	3(1)	3(1)	5(1)
N(21)	40(1)	31(1)	25(1)	4(1)	2(1)	12(1)
N(22)	36(1)	31(1)	22(1)	6(1)	8(1)	16(1)
N(23)	49(1)	33(1)	42(1)	16(1)	26(1)	20(1)
N(24)	48(1)	36(1)	42(1)	17(1)	21(1)	26(1)
O(1)	51(2)	41(2)	35(2)	17(1)	6(1)	12(2)
O(2)	59(2)	53(2)	39(2)	25(2)	11(2)	15(2)

Table A2-13. Bond lengths [Å] and angles [°] for C10 H20 Cl2 N10 O

C(1)-C(2)	1.387(3)	C(4)-C(3)-N(20)	116.24(17)
C(1)-C(6)	1.388(3)	C(2)-C(3)-N(20)	124.51(17)
C(2)-C(3)	1.393(3)	C(3)-C(4)-C(5)	120.68(18)
C(3)-C(4)	1.388(3)	C(6)-C(5)-C(4)	119.74(18)
C(3)-N(20)	1.404(3)	C(5)-C(6)-C(1)	120.12(18)
C(4)-C(5)	1.394(3)	C(5)-C(6)-N(10)	121.56(18)
C(5)-C(6)	1.370(3)	C(1)-C(6)-N(10)	118.21(18)
C(6)-N(10)	1.436(3)	N(12)-C(10)-N(10)	115.64(17)
C(10)-N(12)	1.337(2)	N(12)-C(10)-N(11)	125.65(17)
C(10)-N(10)	1.337(2)	N(10)-C(10)-N(11)	118.49(17)
C(10)-N(11)	1.337(3)	C(10)-N(10)-C(6)	124.95(17)
C(11)-N(14)	1.320(3)	N(14)-C(11)-N(12)	118.39(17)
C(11)-N(12)	1.341(2)	N(14)-C(11)-N(13)	117.39(17)
C(11)-N(13)	1.364(2)	N(12)-C(11)-N(13)	124.22(18)
C(20)-N(22)	1.313(2)	C(10)-N(12)-C(11)	121.65(17)
C(20)-N(21)	1.340(2)	N(22)-C(20)-N(21)	126.48(18)
C(20)-N(20)	1.366(2)	N(22)-C(20)-N(20)	119.09(17)
C(21)-N(24)	1.310(3)	N(21)-C(20)-N(20)	114.34(17)
C(21)-N(23)	1.325(3)	C(20)-N(20)-C(3)	130.10(16)
C(21)-N(22)	1.349(2)	N(24)-C(21)-N(23)	118.47(18)
		N(24)-C(21)-N(22)	117.83(18)
C(2)-C(1)-C(6)	120.49(18)	N(23)-C(21)-N(22)	123.69(18)
C(1)-C(2)-C(3)	119.71(18)	C(20)-N(22)-C(21)	122.29(16)
C(4)-C(3)-C(2)	119.22(18)		

Table A2-14. Torsion angles [°] for C10 H20 Cl2 N10 O.

C(6)-C(1)-C(2)-C(3)	-0.4(3)	C(1)-C(6)-N(10)-C(10)	-119.0(2)
C(1)-C(2)-C(3)-C(4)	0.9(3)	N(10)-C(10)-N(12)-C(11)	161.11(18)
C(1)-C(2)-C(3)-N(20)	178.75(18)	N(11)-C(10)-N(12)-C(11)	-24.3(3)
C(2)-C(3)-C(4)-C(5)	0.4(3)	N(14)-C(11)-N(12)-C(10)	157.59(18)
N(20)-C(3)-C(4)-C(5)	-177.67(18)	N(13)-C(11)-N(12)-C(10	-23.1(3)
C(3)-C(4)-C(5)-C(6)	-2.1(3)	N(22)-C(20)-N(20)-C(3)	12.5(3)
C(4)-C(5)-C(6)-C(1)	2.6(3)	N(21)-C(20)-N(20)-C(3)	-170.80(19)
C(4)-C(5)-C(6)-N(10)	178.78(19)	C(4)-C(3)-N(20)-C(20)	-163.1(2)
C(2)-C(1)-C(6)-C(5)	-1.3(3)	C(2)-C(3)-N(20)-C(20)	18.9(3)
C(2)-C(1)-C(6)-N(10)	-177.66(18)	N(21)-C(20)-N(22)-C(21)	21.6(3)
N(12)-C(10)-N(10)-C(6)	176.64(17)	N(20)-C(20)-N(22)-C(21)	-162.14(18)
N(11)-C(10)-N(10)-C(6)	1.7(3)	N(24)-C(21)-N(22)-C(20)	-149.0(2)
C(5)-C(6)-N(10)-C(10)	64.8(3)	N(23)-C(21)-N(22)-C(20)	32.0(3)

Table A2-15. Bond lengths [Å] and angles [°] related to the hydrogen bonding for C10 H20 Cl2 N10 O.

D-H	..A	d(D-H)	d(H..A)	d(D..A)	<DHA
N(10)-H(10)	Cl(2)#1	0.86	2.38	3.1992(19)	160.3
N(11)-H(11B)	Cl(1)#2	0.86	2.67	3.307(2)	131.5
N(11)-H(11A)	N(13)	0.86	2.41	2.843(3)	111.7
N(11)-H(11A)	N(13)#3	0.86	2.56	3.282(3)	142.2
N(13)-H(13A)	Cl(1)#4	0.86	2.52	3.304(2)	152.6
N(13)-H(13B)	N(11)	0.86	2.39	2.843(3)	113.0
N(13)-H(13B)	Cl(2)#5	0.86	2.71	3.313(2)	128.7
N(14)-H(14A)	Cl(1)#6	0.86	2.49	3.328(2)	163.5
N(14)-H(14B)	Cl(1)#4	0.86	2.47	3.2755(19)	155.6
N(20)-H(20)	Cl(2)#7	0.86	2.37	3.2209(19)	171.4
N(21)-H(21A)	O(1)	0.86	2.46	3.033(4)	125.1
N(21)-H(21B)	O(2)#8	0.86	2.64	3.227(4)	126.5
N(21)-H(21B)	Cl(2)#7	0.86	2.75	3.493(2)	145.7
N(23)-H(23A)	Cl(1)#9	0.86	2.49	3.285(2)	153.5
N(23)-H(23B)	Cl(2)	0.86	2.53	3.294(2)	148.8
N(24)-H(24B)	N(22)#10	0.86	2.18	3.033(3)	173.6
N(24)-H(24A)	Cl(1)#9	0.86	2.48	3.280(2)	154.3
O(1)-H(1A)	Cl(2)#8	0.89	2.32	3.216(4)	177.5
O(1)-H(1B)	O(1)#8	0.89	1.40	2.285(7)	170.9
O(2)-H(2A)	N(12)#11	0.89	2.49	3.289(4)	149.0
O(2)-H(2B)	O(2)#12	0.89	1.86	2.470(7)	124.0

Symmetry transformations used to generate equivalent atoms:

#1 -x+2,-y+2,-z+1	#2 -x,-y+1,-z+1	#3 -x,-y+2,-z+2
#4 x,y+1,z+1	#5 -x+1,-y+2,-z+1	#6 x+1,y+1,z+1
#7 x-1,y,z	#8 -x+1,-y+1,-z	#9 x+1,y,z
#10 -x+1,-y+1,-z+1	#11 x,y-1,z-1	#12 -x+2,-y+1,-z

Table A2-16

Least-squares planes (x,y,z in crystal coordinates) and deviations from them (* indicates atom used to define plane)

1) N10 C10 N11 N12 C11 N13 N14

```
 - 1.8267 (0.0058) x + 11.0502 (0.0067) y - 7.6818 (0.0064) z = 4.3486
(0.0087)

 *    0.3088 (0.0012)  N10
 *   -0.0406 (0.0015)  C10
 *   -0.5035 (0.0013)  N11
 *    0.0127 (0.0015)  N12
 *    0.0581 (0.0016)  C11
 *    0.4994 (0.0013)  N13
 *   -0.3350 (0.0013)  N14

 Rms deviation of fitted atoms =   0.3198
```

2) C1 C2 C3 C4 C5 C6

```
  2.4169 (0.0049) x + 8.8230 (0.0084) y - 8.2403 (0.0093) z = 4.1230
(0.0086)

 Angle to previous plane (with approximate esd) = 42.41 ( 0.07 )

 *    0.0002 (0.0014)  C1
 *    0.0075 (0.0014)  C2
 *   -0.0047 (0.0014)  C3
 *   -0.0057 (0.0015)  C4
 *    0.0134 (0.0015)  C5
 *   -0.0107 (0.0014)  C6

 Rms deviation of fitted atoms =   0.0082
```

3) N20 C20 N21 N22 C21 N23 N24

```
  3.7324 (0.0035) x + 6.9475 (0.0063) y - 0.4025 (0.0161) z = 5.9125
(0.0052)

 Angle to previous plane (with approximate esd) = 39.01 ( 0.08 )

 *    0.3203 (0.0013)  N20
 *   -0.0463 (0.0016)  C20
 *   -0.5677 (0.0015)  N21
 *    0.0728 (0.0016)  N22
 *    0.0751 (0.0017)  C21
 *    0.5571 (0.0014)  N23
```

```
*    -0.4113 (0.0014)  N24

Rms deviation of fitted atoms =    0.3620
```

4) N10 C10 N11 N12

```
 - 3.6887 (0.0054) x + 9.9756 (0.0088) y - 5.8450 (0.0128) z = 3.9671
(0.0143)

 Angle to previous plane (with approximate esd) = 87.84 ( 0.06 )

 *    -0.0084 (0.0005)  N10
 *     0.0268 (0.0015)  C10
 *    -0.0093 (0.0005)  N11
 *    -0.0091 (0.0005)  N12

 Rms deviation of fitted atoms =    0.0155
```

5) N12 C11 N13 N14

```
 - 0.2146 (0.0064) x + 11.7071 (0.0068) y - 5.7343 (0.0139) z = 7.8256
(0.0171)

 Angle to previous plane (with approximate esd) = 39.16 ( 0.09 )

 *     0.0012 (0.0005)  N12
 *    -0.0035 (0.0016)  C11
 *     0.0012 (0.0005)  N13
 *     0.0011 (0.0005)  N14

 Rms deviation of fitted atoms =    0.0020
```

6) N20 C20 N21 N22

```
  4.4343 (0.0048) x + 5.6807 (0.0121) y - 4.9760 (0.0137) z = 3.7821
(0.0078)

 Angle to previous plane (with approximate esd) = 51.12 ( 0.10 )

 *    -0.0053 (0.0005)  N20
 *     0.0176 (0.0016)  C20
 *    -0.0059 (0.0005)  N21
 *    -0.0063 (0.0006)  N22

 Rms deviation of fitted atoms =    0.0101
```

7) N22 C21 N23 N24

```
  3.6432 (0.0056) x + 4.0584 (0.0144) y + 5.0712 (0.0161) z = 6.4130
(0.0046)

 Angle to previous plane (with approximate esd) = 45.46 ( 0.11 )

 *     0.0016 (0.0006)  N22
 *    -0.0048 (0.0017)  C21
 *     0.0017 (0.0006)  N23
 *     0.0016 (0.0005)  N24
```

```
Rms deviation of fitted atoms =    0.0028
```

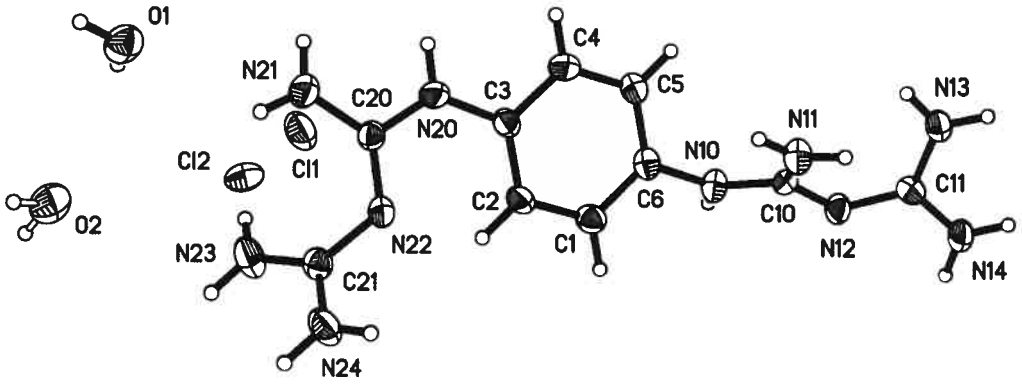

Figure A2-3. ORTEP view of the C10 H20 Cl2 N10 O compound (**28** • 2HCl) with the numbering scheme adopted. Ellipsoids are drawn at the 50% probability level. Hydrogen atoms are represented by a sphere of arbitrary size.

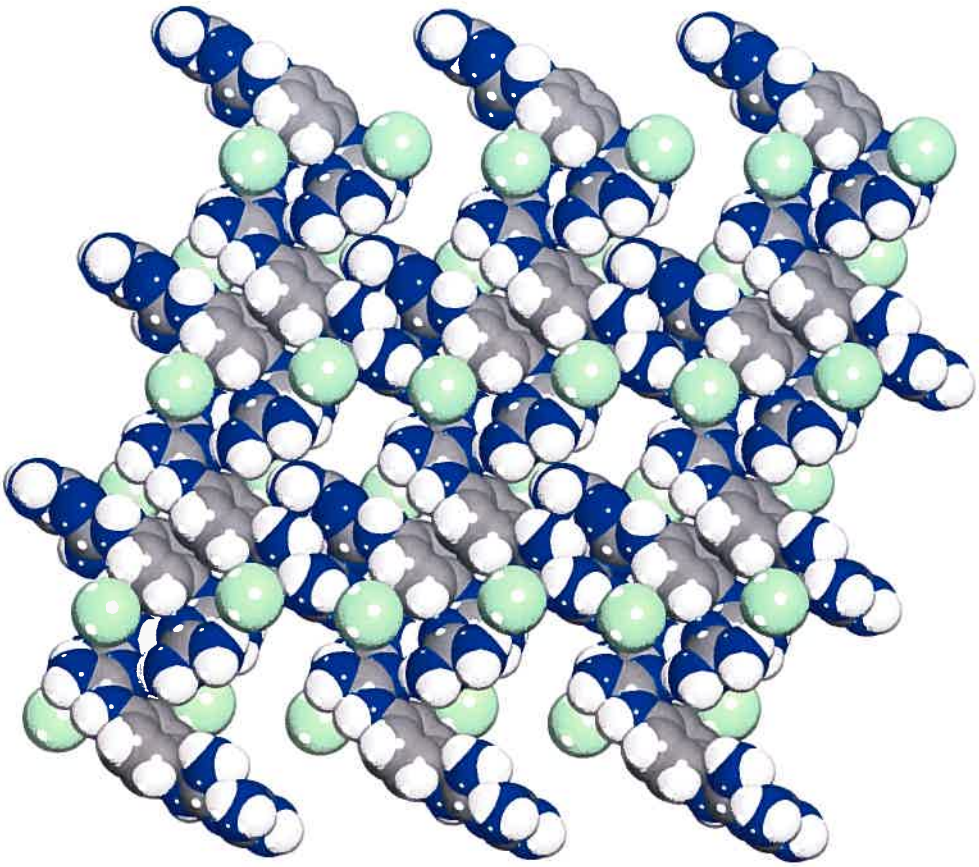

Figure A2-4. View along the *a* axis of the structure of crystals of 1,4-phenylenebis(biguanidinium) dichloride (**28** • 2HCl) grown from acetone/water, showing a 1 × 3 × 3 array of unit cells with atoms represented by spheres of van der Waals radii. Hydrogen atoms appear in white, carbon in gray, nitrogen in blue, and chlorine in green. Guest molecules of water are omitted for clarity.

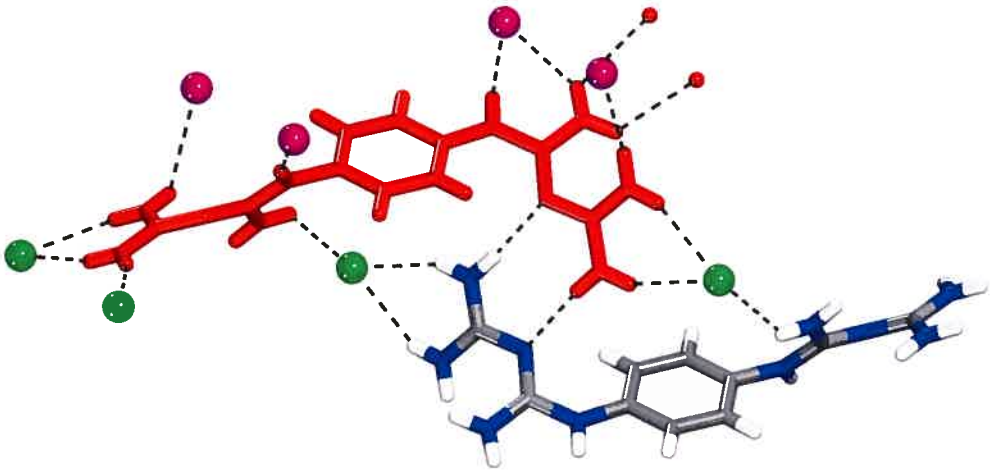

Figure A2-5. View of a 1,4-phenylenebis(biguanidinium) dication (**28** • $2H^+$) (red) surrounded by four chloride ions of type 1 (green), four chloride ions of type 2 (purple), two molecules of water (red), and a neighboring hydrogen-bonded 1,4-phenylenebis(biguanidinium) dication (with hydrogen atoms in white, carbon in gray, and nitrogen in blue).

Université de Montréal

CRYSTAL AND MOLECULAR STRUCTURE OF

C10 H24 Cl2 N10 O3 COMPOUND (JIW814)

Equipe WUEST

Département de chimie, Université de Montréal,

C.P. 6128, Succ. Centre-Ville, Montréal, Québec, H3C 3J7 (Canada)

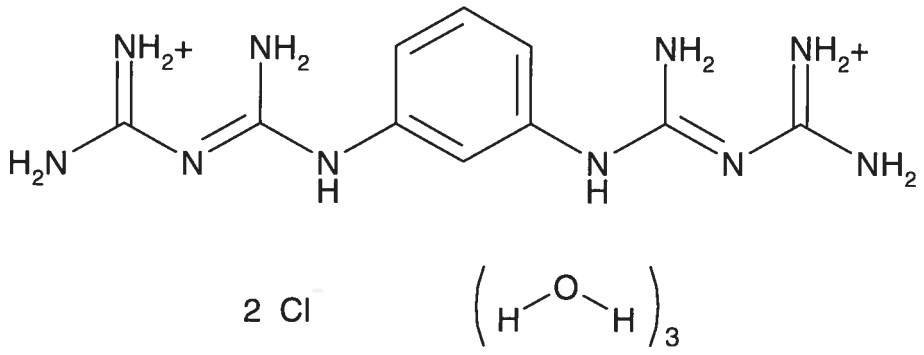

Structure solved and refined in the Laboratory of X-Ray Diffraction, Université de Montréal by Dr. Thierry Maris

Table A2-17. Crystal data and structure refinement for C10 H24 Cl2 N10 O3.

Identification code	JIW814
Empirical formula	C10 H24 Cl2 N10 O3
Formula weight	403.29
Temperature	100(2)K
Wavelength	1.54178 Å
Crystal system	Triclinic
Space group	P-1
Unit cell dimensions	a = 9.3537(3) Å α = 82.983(2)° b = 9.6015(3) Å β = 71.193(2)° c = 11.4402(4) Å γ = 73.759(2)°
Volume	933.19(5)Å^3
Z	2
Density (calculated)	1.435 g/cm^3
Absorption coefficient	3.437 mm^{-1}
F(000)	424
Crystal size	0.40 x 0.35 x 0.25 mm
Theta range for data collection	4.08 to 70.00°
Index ranges	$-11 \leq h \leq 11$, $-11 \leq k \leq 11$, $-12 \leq \ell \leq 14$
Reflections collected	4610
Independent reflections	3545 [R_{int} = 0.029]
Absorption correction	Semi-empirical from equivalents
Max. and min. transmission	0.4230 and 0.1860
Refinement method	Full-matrix least-squares on F^2
Data / restraints / parameters	3017 / 0 / 226
Goodness-of-fit on F^2	1.058
Final R indices [I>2sigma(I)]	R_1 = 0.0745, wR_2 = 0.2142

R indices (all data)	R_1 = 0.0818, wR_2 = 0.2351
Largest diff. peak and hole	0.913 and -0.626 e/Å^3

Table A2-18. Atomic coordinates (x 10^4) and equivalent isotropic displacement parameters (Å^2 x 10^3) for C10 H24 Cl2 N10 O3.

U_{eq} is defined as one third of the trace of the orthogonalized Uij tensor.

	Occ.	x	y	z	U_{eq}
C(1)	1	6877(4)	10347(4)	834(3)	15(1)
Cl(1)	1	3083(1)	3052(1)	611(1)	18(1)
Cl(2)	1	2337(1)	3800(1)	5328(1)	22(1)
N(1)	1	7520(4)	10292(3)	-392(3)	19(1)
C(2)	1	6404(4)	11806(4)	2476(3)	15(1)
N(2)	1	5905(4)	9525(3)	1403(3)	20(1)
C(3)	1	8598(4)	11413(4)	3316(3)	17(1)
N(3)	1	7328(4)	11179(3)	1438(3)	16(1)
C(4)	1	9480(4)	12261(4)	3516(3)	18(1)
N(4)	1	4843(4)	12321(4)	2748(3)	21(1)
C(5)	1	10953(4)	11594(4)	3644(3)	18(1)
N(5)	1	7056(4)	12096(3)	3285(3)	17(1)
C(6)	1	11560(4)	10098(4)	3540(3)	16(1)
N(6)	1	11287(4)	7742(3)	3300(3)	17(1)
C(7)	1	10669(5)	9267(4)	3325(3)	18(1)
N(7)	1	11549(4)	5444(3)	2782(3)	19(1)
C(8)	1	9183(4)	9925(4)	3228(3)	15(1)
N(8)	1	10744(4)	7465(3)	1530(3)	17(1)
C(9)	1	11149(4)	6861(4)	2535(3)	16(1)
N(9)	1	8987(4)	6084(4)	1594(3)	21(1)
C(10)	1	10000(4)	6872(4)	988(3)	16(1)
N(10)	1	10228(4)	7155(3)	-222(3)	19(1)
O(1)	1	3839(3)	6383(3)	4369(3)	27(1)
O(2)	1	5316(4)	8991(4)	4057(3)	41(1)
O(3)	1	5518(5)	5481(4)	1957(3)	45(1)

Table A2-19. Hydrogen coordinates (x 10^4) and isotropic displacement parameters (Å^2 x 10^3) for C10 H24 Cl2 N10 O3.

	Occ.	x	y	z	U_{eq}
H(1A)	1	7299	9716	-813	28
H(1B)	1	8165	10832	-778	28
H(2A)	1	5691	8952	973	30
H(2B)	1	5475	9553	2210	30
H(4)	1	9082	13284	3564	21
H(4A)	1	4370	12251	2214	31
H(4B)	1	4296	12728	3459	31
H(5)	1	11548	12164	3803	22
H(5A)	1	6481	12758	3833	21
H(6)	1	12571	9649	3615	20
H(6A)	1	11804	7337	3827	20
H(7A)	1	11560	4828	2267	29
H(7B)	1	11803	5120	3461	29
H(8)	1	8570	9353	3100	18
H(9A)	1	8778	5933	2399	31
H(9B)	1	8531	5719	1186	31
H(10A)	1	10846	7713	-625	29
H(10B)	1	9760	6785	-615	29
H(1X)	1	3620(60)	5550(30)	4690(30)	41
H(1Y)	1	4280(60)	6270(50)	3561(10)	41
H(2X)	1	5930(50)	8100(20)	4090(60)	61
H(2Y)	1	5910(50)	9610(40)	3950(60)	61
H(3X)	1	5900(70)	5990(50)	1280(30)	67
H(3Y)	1	5160(70)	4840(50)	1720(50)	67

Table A2-20. Anisotropic parameters ($Å^2$ x 10^3) for C10 H24 Cl2 N10 O3.

The anisotropic displacement factor exponent takes the form:

$$-2\pi^2 [h^2 a^{*2} U_{11} + ... + 2 h k a^* b^* U_{12}]$$

	U11	U22	U33	U23	U13	U12
C(1)	19(2)	16(2)	10(2)	5(2)	-9(1)	0(2)
Cl(1)	23(1)	20(1)	13(1)	0(1)	-8(1)	-6(1)
Cl(2)	29(1)	21(1)	13(1)	1(1)	-6(1)	-5(1)
N(1)	27(2)	21(2)	9(2)	-1(1)	-5(1)	-8(1)
C(2)	20(2)	15(2)	13(2)	2(2)	-6(1)	-6(2)
N(2)	30(2)	20(2)	11(2)	-3(1)	-5(1)	-8(1)
C(3)	18(2)	28(2)	5(2)	4(2)	-5(1)	-7(2)
N(3)	23(2)	17(1)	9(2)	2(1)	-6(1)	-6(1)
C(4)	24(2)	20(2)	10(2)	0(2)	-3(1)	-10(2)
N(4)	19(2)	30(2)	15(2)	-5(2)	-7(1)	-5(1)
C(5)	23(2)	23(2)	11(2)	-2(2)	-4(1)	-10(2)
N(5)	19(2)	20(2)	11(2)	-8(1)	-5(1)	2(1)
C(6)	18(2)	26(2)	8(2)	4(2)	-7(1)	-7(2)
N(6)	22(2)	20(2)	11(2)	2(1)	-10(1)	-5(1)
C(7)	25(2)	23(2)	6(2)	1(2)	-4(1)	-10(2)
N(7)	30(2)	17(1)	12(2)	-2(1)	-11(1)	-3(1)
C(8)	21(2)	19(2)	9(2)	-2(2)	-5(1)	-9(2)
N(8)	25(2)	19(2)	8(2)	0(1)	-7(1)	-6(1)
C(9)	17(2)	22(2)	11(2)	6(2)	-6(1)	-9(2)
N(9)	27(2)	25(2)	14(2)	1(1)	-10(1)	-10(1)
C(10)	17(2)	16(2)	13(2)	-1(2)	-6(1)	0(1)
N(10)	26(2)	26(2)	10(2)	-1(1)	-7(1)	-11(2)
O(1)	25(2)	21(1)	40(2)	2(1)	-14(1)	-6(1)
O(2)	35(2)	59(2)	21(2)	-3(2)	-12(1)	6(2)
O(3)	57(2)	38(2)	32(2)	4(2)	0(2)	-18(2)

Table A2-21. Bond lengths [Å] and angles [°] for C10 H24 Cl2 N10 O3

C(1)-N(2)	1.330(5)	N(3)-C(2)-N(4)	124.8(3)
C(1)-N(1)	1.337(5)	N(3)-C(2)-N(5)	118.7(3)
C(1)-N(3)	1.344(5)	N(4)-C(2)-N(5)	116.1(3)
C(2)-N(3)	1.320(5)	C(8)-C(3)-C(4)	120.5(3)
C(2)-N(4)	1.347(5)	C(8)-C(3)-N(5)	120.9(3)
C(2)-N(5)	1.353(5)	C(4)-C(3)-N(5)	118.5(3)
C(3)-C(8)	1.383(5)	C(2)-N(3)-C(1)	122.4(3)
C(3)-C(4)	1.392(5)	C(3)-C(4)-C(5)	119.4(3)
C(3)-N(5)	1.418(5)	C(6)-C(5)-C(4)	120.5(3)
C(4)-C(5)	1.394(6)	C(2)-N(5)-C(3)	124.8(3)
C(5)-C(6)	1.393(5)	C(5)-C(6)-C(7)	119.4(3)
C(6)-C(7)	1.394(5)	C(9)-N(6)-C(7)	125.4(3)
N(6)-C(9)	1.346(5)	C(8)-C(7)-C(6)	120.2(3)
N(6)-C(7)	1.416(5)	C(8)-C(7)-N(6)	122.0(3)
C(7)-C(8)	1.391(5)	C(6)-C(7)-N(6)	117.6(3)
N(7)-C(9)	1.327(4)	C(3)-C(8)-C(7)	120.0(3)
N(8)-C(10)	1.334(5)	C(10)-N(8)-C(9)	122.6(3)
N(8)-C(9)	1.341(5)	N(7)-C(9)-N(8)	124.7(4)
N(9)-C(10)	1.341(5)	N(7)-C(9)-N(6)	117.2(3)
C(10)-N(10)	1.336(5)	N(8)-C(9)-N(6)	117.9(3)
		N(8)-C(10)-N(10)	117.1(3)
N(2)-C(1)-N(1)	119.3(3)	N(8)-C(10)-N(9)	124.0(3)
N(2)-C(1)-N(3)	123.2(3)	N(10)-C(10)-N(9)	118.8(3)
N(1)-C(1)-N(3)	117.4(3)		

Table A2-22. Torsion angles [°] for C10 H24 Cl2 N10 O3.

N(4)-C(2)-N(3)-C(1)	-34.3(6)	C(5)-C(6)-C(7)-N(6)	-176.3(3)
N(5)-C(2)-N(3)-C(1)	152.8(3)	C(9)-N(6)-C(7)-C(8)	41.9(5)
N(2)-C(1)-N(3)-C(2)	-33.0(5)	C(9)-N(6)-C(7)-C(6)	-142.5(4)
N(1)-C(1)-N(3)-C(2)	151.1(3)	C(4)-C(3)-C(8)-C(7)	-0.7(5)
C(8)-C(3)-C(4)-C(5)	-0.9(5)	N(5)-C(3)-C(8)-C(7)	-176.6(3)
N(5)-C(3)-C(4)-C(5)	175.2(3)	C(6)-C(7)-C(8)-C(3)	1.4(5)
C(3)-C(4)-C(5)-C(6)	1.7(5)	N(6)-C(7)-C(8)-C(3)	176.9(3)
N(3)-C(2)-N(5)-C(3)	-20.3(5)	C(10)-N(8)-C(9)-N(7)	32.5(6)
N(4)-C(2)-N(5)-C(3)	166.1(3)	C(10)-N(8)-C(9)-N(6)	-153.2(3)
C(8)-C(3)-N(5)-C(2)	-45.1(5)	C(7)-N(6)-C(9)-N(7)	-168.2(3)
C(4)-C(3)-N(5)-C(2)	138.8(4)	C(7)-N(6)-C(9)-N(8)	17.2(5)
C(4)-C(5)-C(6)-C(7)	-1.0(5)	C(9)-N(8)-C(10)-N(10)	-152.2(4)
C(5)-C(6)-C(7)-C(8)	-0.6(5)	C(9)-N(8)-C(10)-N(9)	31.5(6)

Table A2-23. Bond lengths [Å] and angles [°] related to the hydrogen bonding for C10 H24 Cl2 N10 O3.

D-H	..A	d(D-H)	d(H..A)	d(D..A)	<DHA
N(1)-H(1A)	Cl(1)#1	0.88	2.75	3.463(3)	138.8
N(1)-H(1B)	N(8)#2	0.88	2.12	2.979(4)	166.6
N(2)-H(2A)	Cl(1)#1	0.88	2.57	3.317(3)	143.9
N(2)-H(2B)	O(2)	0.88	2.08	2.913(5)	156.6
N(4)-H(4A)	Cl(1)#3	0.88	2.44	3.272(3)	157.5
N(4)-H(4B)	Cl(2)#3	0.88	2.44	3.305(3)	168.6
N(5)-H(5A)	O(1)#4	0.88	2.21	2.977(4)	145.5
N(6)-H(6A)	O(1)#5	0.88	2.12	2.940(4)	154.9
N(7)-H(7A)	Cl(1)#5	0.88	2.49	3.280(3)	149.1
N(7)-H(7B)	Cl(2)#5	0.88	2.47	3.336(3)	168.8
N(9)-H(9B)	Cl(1)#1	0.88	2.88	3.540(3)	132.9
N(9)-H(9A)	Cl(2)#6	0.88	2.49	3.340(3)	163.6
N(10)-H(10B)	Cl(1)#1	0.88	2.62	3.329(3)	138.6
N(10)-H(10A)	N(3)#2	0.88	2.16	3.028(4)	169.0
O(1)-H(1X)	Cl(2)	0.89(3)	2.25(2)	3.102(3)	161(5)
O(1)-H(1Y)	O(3)	0.89(3)	1.94(2)	2.803(5)	164(5)
O(2)-H(2X)	Cl(2)#6	0.89(3)	2.27(2)	3.121(4)	160(6)
O(3)-H(3X)	Cl(1)#1	0.89(3)	2.26(2)	3.142(3)	170(5)
O(3)-H(3Y)	N(4)#7	0.89(3)	2.60(4)	3.233(5)	128(4)

Symmetry transformations used to generate equivalent atoms:

#1 -x+1,-y+1,-z #2 -x+2,-y+2,-z #3 x,y+1,z
#4 -x+1,-y+2,-z+1 #5 x+1,y,z #6 -x+1,-y+1,-z+1
#7 x,y-1,z

Table A2-24

Least-squares planes (x,y,z in crystal coordinates) and deviations from them
(* indicates atom used to define plane)

1) N1 N2 C1 N3

```
 - 6.0291 (0.0138) x + 5.2552 (0.0154) y - 3.1806 (0.0216) z = 1.0061
(0.0259)

 *    -0.0066 (0.0009)  N1
 *    -0.0070 (0.0010)  N2
 *     0.0204 (0.0028)  C1
 *    -0.0068 (0.0010)  N3

 Rms deviation of fitted atoms =    0.0118
```

2) N3 C2 N4 N5

```
  1.8210 (0.0189) x + 8.4970 (0.0087) y - 3.9565 (0.0211) z = 10.2526
(0.0228)

 Angle to previous plane (with approximate esd) = 54.78 ( 0.16 )

 *     0.0121 (0.0010)  N3
 *    -0.0344 (0.0030)  C2
 *     0.0116 (0.0010)  N4
 *     0.0108 (0.0009)  N5

 Rms deviation of fitted atoms =    0.0199
```

3) N6 C9 N7 N8

```
  7.8912 (0.0096) x + 1.4958 (0.0191) y - 2.6604 (0.0211) z = 9.1780
(0.0232)

 Angle to previous plane (with approximate esd) = 70.29 ( 0.17 )

 *     0.0089 (0.0010)  N6
 *    -0.0283 (0.0030)  C9
 *     0.0097 (0.0010)  N7
 *     0.0097 (0.0010)  N8

 Rms deviation of fitted atoms =    0.0163
```

4) N8 C10 N9 N10

```
  4.9086 (0.0153) x - 6.2587 (0.0138) y - 0.3389 (0.0237) z = 0.5556
(0.0255)
```

```
Angle to previous plane (with approximate esd) = 52.55 ( 0.18 )

*    -0.0063 (0.0010)  N8
*     0.0187 (0.0030)  C10
*    -0.0064 (0.0010)  N9
*    -0.0060 (0.0009)  N10

Rms deviation of fitted atoms =   0.0108
```

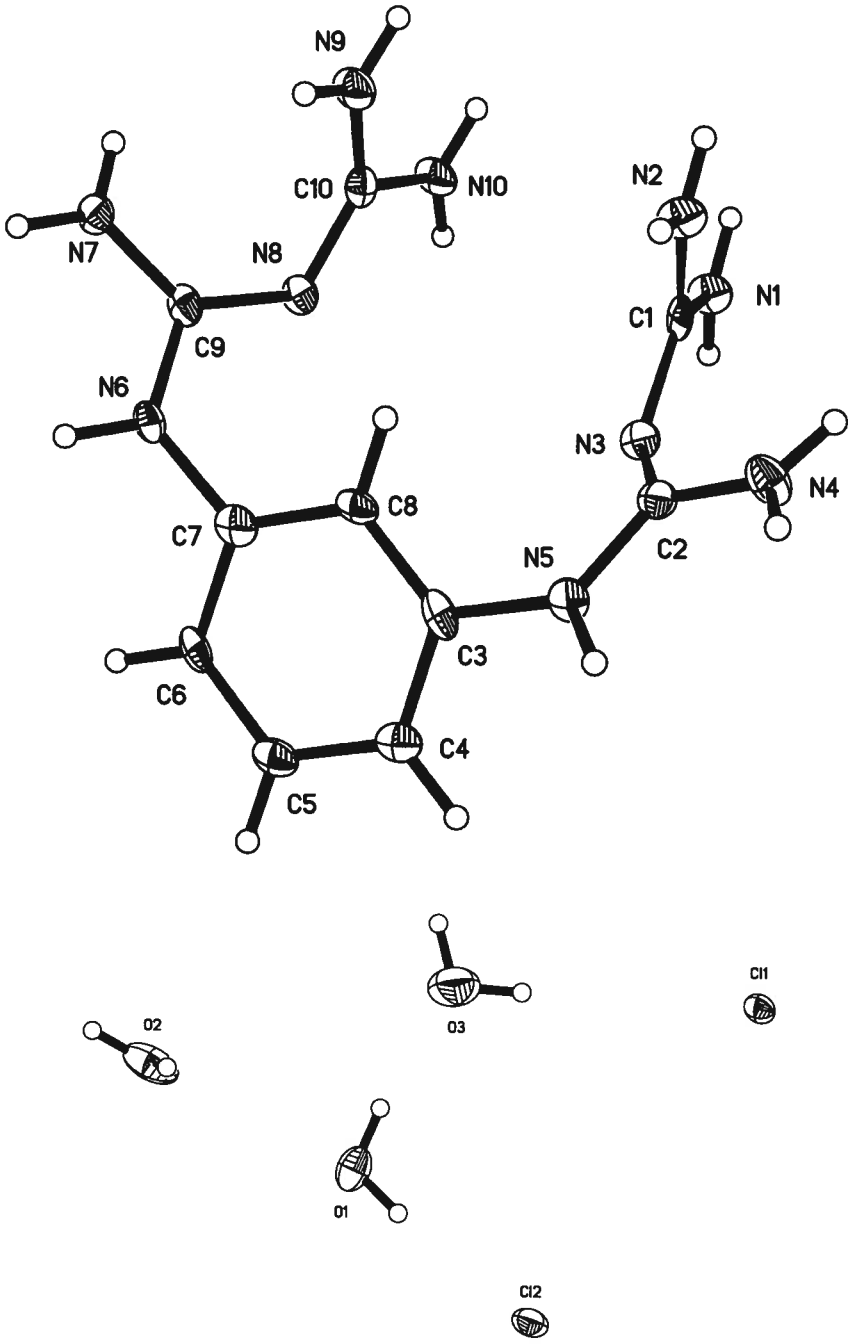

Figure A2-6. ORTEP view of the C10 H24 Cl2 N10 O3 compound (**29** • 2HCl) with the numbering scheme adopted. Ellipsoids are drawn at the 50% probability level. Hydrogens atoms are represented by a sphere of arbitrary size.

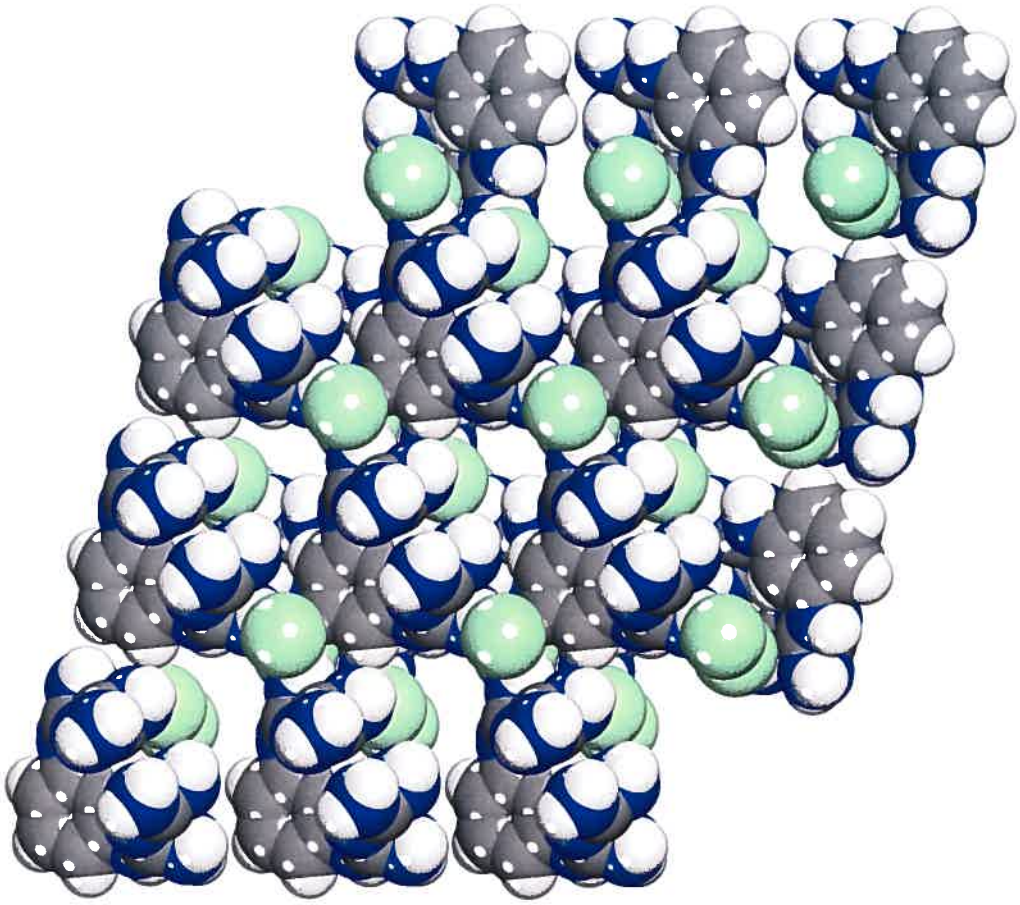

Figure A2-7. View along the *c* axis of the structure of crystals of 1,3-phenylenebis(biguanidinium) dichloride (**29** • 2HCl) grown from acetone/water, showing a 3 × 3 × 1 array of unit cells with atoms represented by spheres of van der Waals radii. Hydrogen atoms appear in white, carbon in gray, nitrogen in blue, and chlorine in green. Guest molecules of water are omitted for clarity.

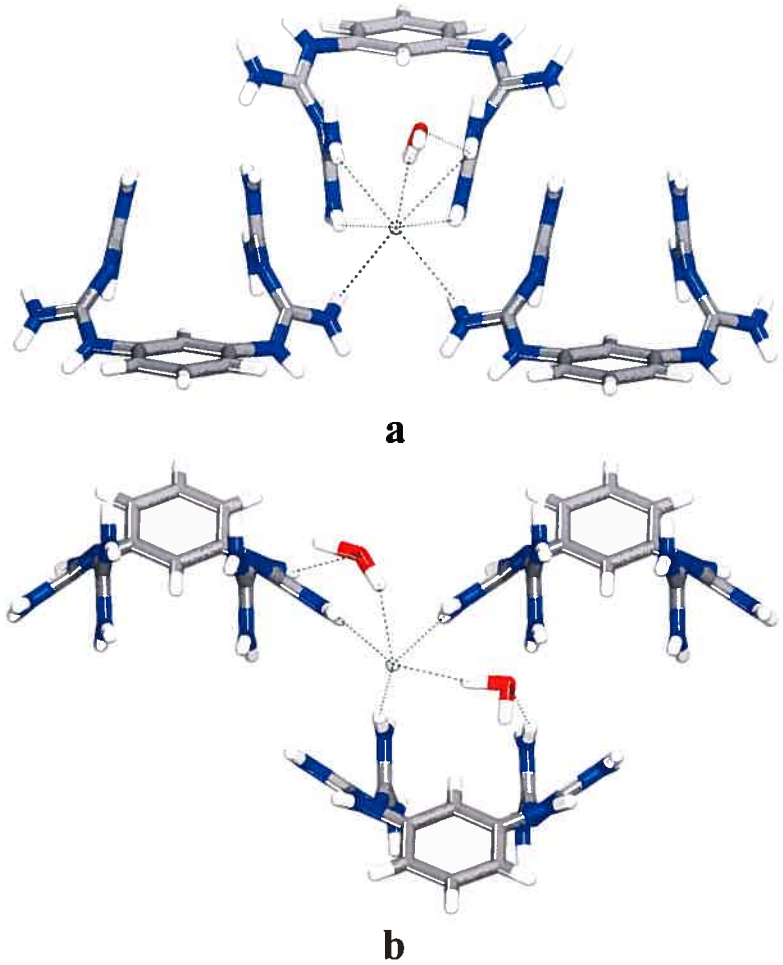

Figure A2-8. Detailed views showing interactions in the structure of crystals of 1,3-phenylenebis(biguanidinium) dichloride (**29** • 2HCl) grown from acetone/water. **a**) View showing how the bis(biguanidinium) dications adopt a pincer-like conformation that permits chelation of one type of chloride by the formation of four N-H···Cl hydrogen bonds. The chloride ion and the chelating dication are further linked by a bridging molecule of water. The chloride ion accepts two additional hydrogen bonds donated by $-NH_2$ groups in two neighboring bis(biguanidinium) dications. In this way, ionic hydrogen bonds involving chloride link the bis(biguanidinium) dications into tapes. **b**) View showing ionic N-H···Cl hydrogen bonds involving the second type of chloride ion, which bridges the tapes shown in Fig. 7a by interacting with $-NH_2$ groups from three different bis(biguanidinium) dications. Two of these dications belong to the same tape, and the third dication belongs to a neighboring tape. Bridging molecules of water are also present. In both views, hydrogen bonds are represented by broken lines. Hydrogen atoms appear in white, carbon in gray, nitrogen in blue, oxygen in red, and chlorine in green.

Université de Montréal

CRYSTAL AND MOLECULAR STRUCTURE OF

C13 H24 N10 O5 COMPOUND (JIW865)

Equipe WUEST

Département de chimie, Université de Montréal,

C.P. 6128, Succ. Centre-Ville, Montréal, Québec, H3C 3J7 (Canada)

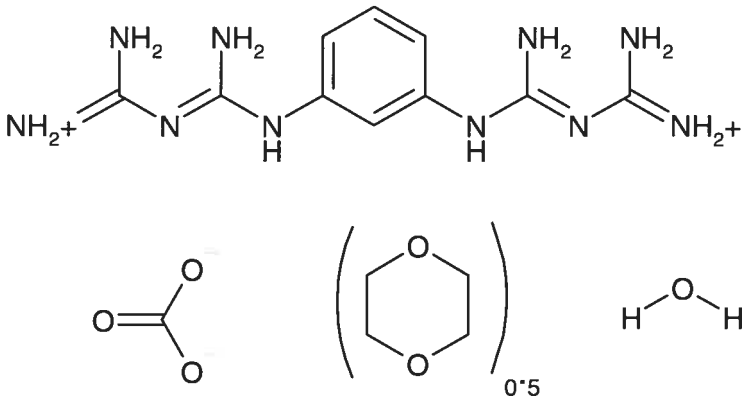

Structure solved and refined in the Laboratory of X-Ray Diffraction, Université de Montréal by Dr. Thierry Maris

Table A2-25. Crystal data and structure refinement for C13 H24 N10 O5.

Identification code	JIW865
Empirical formula	C13 H24 N10 O5
Formula weight	400.42
Temperature	100(2)K
Wavelength	1.54178 Å
Crystal system	Triclinic
Space group	P-1
Unit cell dimensions	a = 9.9072(3) Å α = 77.297(2)° b = 10.1769(3) Å β = 67.906(2)° c = 11.0195(5) Å γ = 65.826(2)°
Volume	936.32(6)Å^3
Z	2
Density (calculated)	1.420 Mg/m^3
Absorption coefficient	0.947 mm^{-1}
F(000)	424
Crystal size	0.25 x 0.20 x 0.15 mm
Theta range for data collection	4.34 to 72.03°
Index ranges	$-12 \leq h \leq 12$, $-12 \leq k \leq 12$, $-13 \leq \ell \leq 13$
Reflections collected	10733
Independent reflections	3557 [R_{int} = 0.029]
Absorption correction	Semi-empirical from equivalents
Max. and min. transmission	0.8710 and 0.7976
Refinement method	Full-matrix least-squares on F^2
Data / restraints / parameters	3526 / 5 / 259
Goodness-of-fit on F^2	0.942
Final R indices [I>2sigma(I)]	R_1 = 0.0487, wR_2 = 0.1277

R indices (all data)	R_1 = 0.0699, wR_2 = 0.1357
Largest diff. peak and hole	0.397 and -0.479 e/Å^3

Table A2-26. Atomic coordinates (x 10^4) and equivalent isotropic displacement parameters (Å^2 x 10^3) for C13 H24 N10 O5.

U_{eq} is defined as one third of the trace of the orthogonalized Uij tensor.

	x	y	z	U_{eq}
N(1)	4531(2)	-262(2)	3111(2)	17(1)
N(2)	5053(2)	-2390(2)	2352(2)	20(1)
N(3)	2508(2)	-1087(2)	3688(2)	17(1)
N(4)	633(2)	-2086(2)	4249(2)	21(1)
N(5)	1913(2)	-1718(2)	2067(2)	22(1)
N(6)	347(2)	4276(2)	2565(2)	20(1)
N(7)	-1456(2)	4658(2)	1589(2)	22(1)
N(8)	-739(2)	2545(2)	2995(2)	18(1)
N(9)	-1090(2)	1712(2)	1331(2)	23(1)
N(10)	-1880(2)	871(2)	3482(2)	20(1)
C(1)	2402(3)	1985(2)	2876(2)	17(1)
C(2)	1518(3)	3424(2)	3150(2)	18(1)
C(3)	1844(3)	4067(3)	3949(2)	20(1)
C(4)	3032(3)	3249(3)	4488(2)	22(1)
C(5)	3883(3)	1817(3)	4248(2)	20(1)
C(6)	3572(3)	1182(2)	3445(2)	18(1)
C(7)	3995(3)	-1242(2)	3014(2)	17(1)
C(8)	1721(3)	-1647(2)	3311(2)	18(1)
C(9)	-614(3)	3789(3)	2355(2)	18(1)
C(10)	-1244(2)	1736(2)	2590(2)	18(1)
O(20)	237(2)	2799(2)	7941(2)	33(1)
O(21)	2305(2)	775(2)	7871(2)	27(1)
O(22)	1741(2)	2463(2)	9149(2)	24(1)
C(20)	1422(3)	2013(3)	8319(2)	19(1)
O(40)	3532(2)	-47(2)	159(2)	36(1)
O(30)	5660(2)	4987(2)	958(2)	23(1)
C(30)	5164(3)	3849(3)	952(2)	23(1)
C(31)	6142(3)	5597(3)	-370(2)	24(1)

Table A2-27. Hydrogen coordinates (x 10^4) and isotropic displacement parameters ($Å^2$ x 10^3) for C13 H24 N10 O5.

	x	y	z	U_{eq}
H(1A)	5541	-531	2960	20
H(2A)	4785	-3111	2341	24
H(2B)	6016	-2424	1927	24
H(4A)	65	-2415	4034	25
H(4B)	486	-2048	5081	25
H(5A)	1332	-2051	1873	26
H(5B)	2623	-1433	1434	26
H(6)	241	5187	2322	24
H(7A)	-2161	4426	1473	27
H(7B)	-1305	5462	1200	27
H(9A)	-1409	1130	1119	27
H(9B)	-670	2277	717	27
H(10A)	-1959	839	4309	24
H(10B)	-2225	327	3248	24
H(1)	2209	1554	2307	21
H(3)	1262	5052	4123	24
H(4)	3259	3683	5030	27
H(5)	4681	1268	4632	24
H(40A)	2890(30)	498(14)	-290(20)	43
H(40B)	3741(3)	554(11)	457(10)	43
H(30A)	4804	3434	1863	27
H(30B)	6059	3072	434	27
H(31A)	7053	4851	-912	28
H(31B)	6466	6400	-379	28

Table A2-28. Anisotropic parameters ($Å^2$ x 10^3) for C13 H24 N10 O5.

The anisotropic displacement factor exponent takes the form:

$$-2\,\pi^2\,[\,h^2\,a^{*2}\,U_{11} + \ldots + 2\,h\,k\,a^*\,b^*\,U_{12}\,]$$

	U11	U22	U33	U23	U13	U12
N(1)	13(1)	12(1)	25(1)	-2(1)	-8(1)	-3(1)
N(2)	17(1)	15(1)	29(1)	-5(1)	-5(1)	-6(1)
N(3)	19(1)	13(1)	19(1)	0(1)	-5(1)	-7(1)
N(4)	22(1)	20(1)	23(1)	0(1)	-7(1)	-11(1)
N(5)	21(1)	24(1)	24(1)	-1(1)	-9(1)	-12(1)
N(6)	19(1)	10(1)	31(1)	3(1)	-10(1)	-5(1)
N(7)	22(1)	14(1)	32(1)	2(1)	-12(1)	-7(1)
N(8)	16(1)	14(1)	25(1)	-1(1)	-6(1)	-5(1)
N(9)	31(1)	18(1)	21(1)	0(1)	-10(1)	-11(1)
N(10)	23(1)	19(1)	22(1)	-1(1)	-7(1)	-12(1)
C(1)	18(1)	16(1)	19(1)	-2(1)	-4(1)	-8(1)
C(2)	16(1)	16(1)	20(1)	1(1)	-5(1)	-6(1)
C(3)	19(1)	13(1)	26(1)	-3(1)	-4(1)	-5(1)
C(4)	25(1)	20(1)	23(1)	-6(1)	-8(1)	-7(1)
C(5)	23(1)	17(1)	21(1)	2(1)	-9(1)	-8(1)
C(6)	18(1)	14(1)	20(1)	1(1)	-4(1)	-8(1)
C(7)	20(1)	14(1)	17(1)	2(1)	-9(1)	-4(1)
C(8)	16(1)	9(1)	24(1)	-2(1)	-6(1)	1(1)
C(9)	14(1)	15(1)	20(1)	-2(1)	-3(1)	-2(1)
C(10)	11(1)	13(1)	26(1)	-3(1)	-7(1)	1(1)
O(20)	28(1)	15(1)	65(1)	3(1)	-29(1)	-6(1)
O(21)	22(1)	21(1)	42(1)	-13(1)	-9(1)	-6(1)
O(22)	30(1)	18(1)	25(1)	-3(1)	-10(1)	-8(1)
C(20)	19(1)	15(1)	23(1)	0(1)	-4(1)	-9(1)
O(40)	34(1)	41(1)	39(1)	11(1)	-20(1)	-19(1)
O(30)	26(1)	23(1)	21(1)	1(1)	-8(1)	-12(1)
C(30)	24(1)	20(1)	23(1)	0(1)	-6(1)	-10(1)
C(31)	27(1)	23(1)	22(1)	2(1)	-6(1)	-13(1)

Table A2-29. Bond lengths [Å] and angles [°] for C13 H24 N10 O5

N(1)-C(7)	1.346(3)	C(9)-N(6)-C(2)	124.53(19)
N(1)-C(6)	1.424(3)	C(9)-N(8)-C(10)	123.0(2)
N(2)-C(7)	1.338(3)	C(6)-C(1)-C(2)	119.6(2)
N(3)-C(7)	1.336(3)	C(1)-C(2)-C(3)	120.0(2)
N(3)-C(8)	1.348(3)	C(1)-C(2)-N(6)	120.9(2)
N(4)-C(8)	1.335(3)	C(3)-C(2)-N(6)	119.0(2)
N(5)-C(8)	1.326(3)	C(4)-C(3)-C(2)	119.3(2)
N(6)-C(9)	1.345(3)	C(5)-C(4)-C(3)	121.0(2)
N(6)-C(2)	1.416(3)	C(4)-C(5)-C(6)	119.8(2)
N(7)-C(9)	1.337(3)	C(5)-C(6)-C(1)	120.3(2)
N(8)-C(9)	1.336(3)	C(5)-C(6)-N(1)	119.9(2)
N(8)-C(10)	1.339(3)	C(1)-C(6)-N(1)	119.6(2)
N(9)-C(10)	1.342(3)	N(3)-C(7)-N(2)	124.7(2)
N(10)-C(10)	1.321(3)	N(3)-C(7)-N(1)	118.4(2)
C(1)-C(6)	1.396(3)	N(2)-C(7)-N(1)	116.5(2)
C(1)-C(2)	1.396(3)	N(5)-C(8)-N(4)	118.5(2)
C(2)-C(3)	1.396(3)	N(5)-C(8)-N(3)	123.7(2)
C(3)-C(4)	1.391(3)	N(4)-C(8)-N(3)	117.7(2)
C(4)-C(5)	1.378(3)	N(8)-C(9)-N(7)	125.4(2)
C(5)-C(6)	1.385(3)	N(8)-C(9)-N(6)	118.1(2)
O(20)-C(20)	1.282(3)	N(7)-C(9)-N(6)	116.3(2)
O(21)-C(20)	1.281(3)	N(10)-C(10)-N(8)	117.8(2)
O(22)-C(20)	1.291(3)	N(10)-C(10)-N(9)	118.2(2)
O(30)-C(30)	1.433(3)	N(8)-C(10)-N(9)	124.0(2)
O(30)-C(31)	1.439(3)	O(21)-C(20)-O(20)	120.3(2)
C(30)-C(31)#1	1.508(3)	O(21)-C(20)-O(22)	119.4(2)
C(31)-C(30)#1	1.508(3)	O(20)-C(20)-O(22)	120.4(2)
		C(30)-O(30)-C(31)	108.52(17)
C(7)-N(1)-C(6)	124.40(18)	O(30)-C(30)-C(31)#1	110.87(19)
C(7)-N(3)-C(8)	121.79(19)	O(30)-C(31)-C(30)#1	111.05(18)

Symmetry transformations used to generate equivalent atoms:

#1 -x+1,-y+1,-z

Table A2-30. Torsion angles [°] for C13 H24 N10 O5.

C(6)-C(1)-C(2)-C(3)	2.3(3)	C(8)-N(3)-C(7)-N(2)	-32.1(3)
C(6)-C(1)-C(2)-N(6)	178.6(2)	C(8)-N(3)-C(7)-N(1)	155.4(2)
C(9)-N(6)-C(2)-C(1)	38.4(3)	C(6)-N(1)-C(7)-N(3)	-24.9(3)
C(9)-N(6)-C(2)-C(3)	-145.4(2)	C(6)-N(1)-C(7)-N(2)	162.1(2)
C(1)-C(2)-C(3)-C(4)	-1.4(3)	C(7)-N(3)-C(8)-N(5)	-35.6(3)
N(6)-C(2)-C(3)-C(4)	-177.7(2)	C(7)-N(3)-C(8)-N(4)	147.8(2)
C(2)-C(3)-C(4)-C(5)	-0.2(3)	C(10)-N(8)-C(9)-N(7)	26.5(3)
C(3)-C(4)-C(5)-C(6)	0.9(3)	C(10)-N(8)-C(9)-N(6)	-158.8(2)
C(4)-C(5)-C(6)-C(1)	0.1(3)	C(2)-N(6)-C(9)-N(8)	16.2(3)
C(4)-C(5)-C(6)-N(1)	175.0(2)	C(2)-N(6)-C(9)-N(7)	-168.5(2)
C(2)-C(1)-C(6)-C(5)	-1.7(3)	C(9)-N(8)-C(10)-N(10)	-154.9(2)
C(2)-C(1)-C(6)-N(1)	-176.63(19)	C(9)-N(8)-C(10)-N(9)	27.8(3)
C(7)-N(1)-C(6)-C(5)	141.6(2)	C(31)-O(30)-C(30)-C(31)#1	-57.8(3)
C(7)-N(1)-C(6)-C(1)	-43.5(3)	C(30)-O(30)-C(31)-C(30)#1	57.9(3)

Symmetry transformations used to generate equivalent atoms:

#1 -x+1,-y+1,-z

Table A2-31. Bond lengths [Å] and angles [°] related to the hydrogen bonding for C13 H24 N10 O5.

D-H	..A	d(D-H)	d(H..A)	d(D..A)	<DHA
N(1)-H(1A)	O(21)#2	0.88	1.91	2.761(2)	162.2
N(2)-H(2A)	O(30)#3	0.88	2.40	3.105(2)	137.5
N(2)-H(2B)	O(22)#2	0.88	2.08	2.956(2)	177.4
N(4)-H(4A)	O(20)#4	0.88	2.44	3.153(3)	138.8
N(4)-H(4B)	N(8)#4	0.88	2.15	3.005(3)	162.6
N(5)-H(5A)	O(20)#4	0.88	1.92	2.772(2)	161.4
N(5)-H(5B)	O(40)	0.88	2.00	2.830(3)	157.3
N(6)-H(6)	O(20)#5	0.88	1.89	2.759(3)	170.9
N(7)-H(7A)	O(30)#6	0.88	2.25	3.061(2)	152.3
N(7)-H(7B)	O(22)#5	0.88	1.95	2.788(3)	158.0
N(9)-H(9A)	O(21)#4	0.88	2.35	3.058(3)	138.1
N(9)-H(9B)	O(22)#7	0.88	2.42	3.179(3)	144.9
N(9)-H(9B)	N(7)	0.88	2.51	2.933(3)	110.1
N(10)-H(10A)	N(3)#4	0.88	2.11	2.982(3)	169.9
N(10)-H(10B)	O(21)#4	0.88	1.88	2.713(2)	156.7
O(40)-H(40A)	O(22)#7	0.88(1)	1.950(11)	2.727(2)	145.8(12)
O(40)-H(40A)	O(21)#7	0.88(1)	2.243(13)	3.013(3)	145(2)
O(40)-H(40B)	O(40)#8	0.88(1)	2.379(4)	2.835(4)	112.7(3)

Symmetry transformations used to generate equivalent atoms:

```
#1 -x+1,-y+1,-z     #2 -x+1,-y,-z+1     #3 x,y-1,z
#4 -x,-y,-z+1       #5 -x,-y+1,-z+1     #6 x-1,y,z
#7 x,y,z-1          #8 -x+1,-y,-z
```

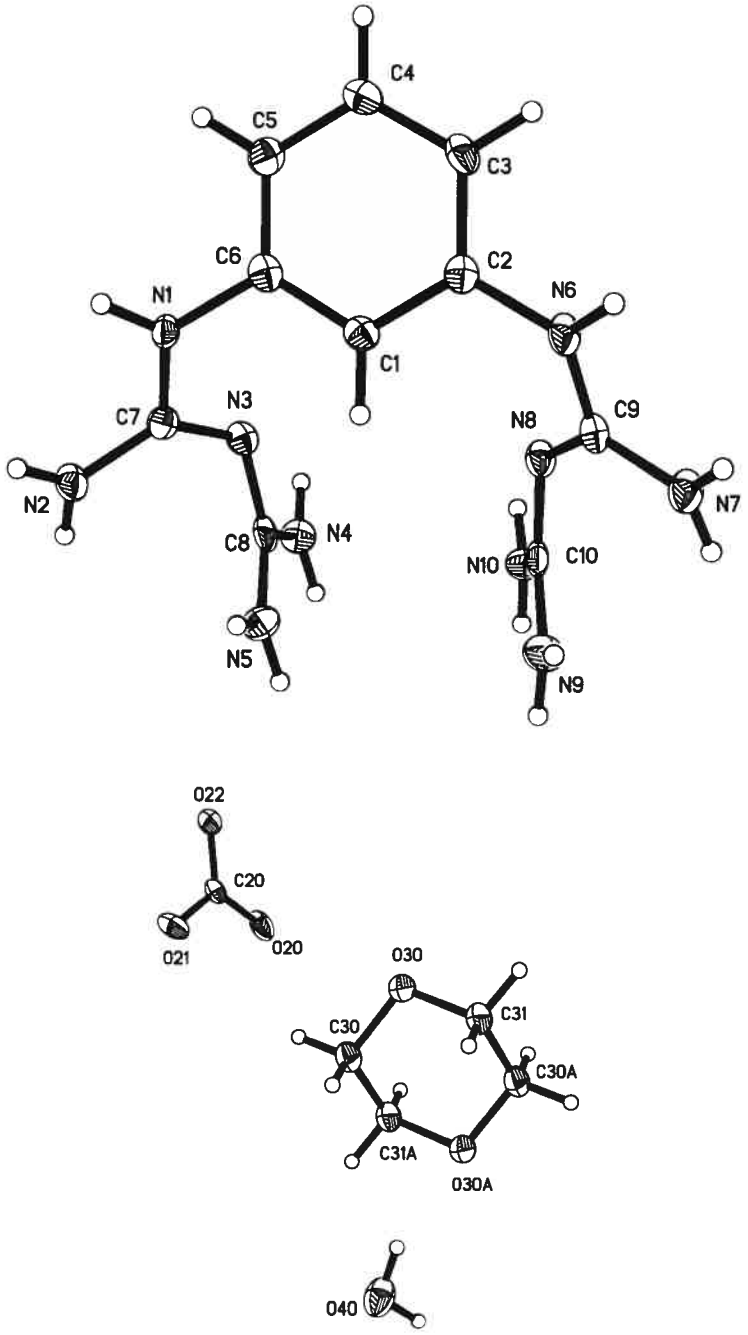

Figure A2-9. ORTEP view of the C13 H24 N10 O5 compound (**29** • H_2CO_3) with the numbering scheme adopted. Ellipsoids are drawn at the 50% probability level. Hydrogens atoms are represented by a sphere of arbitrary size.

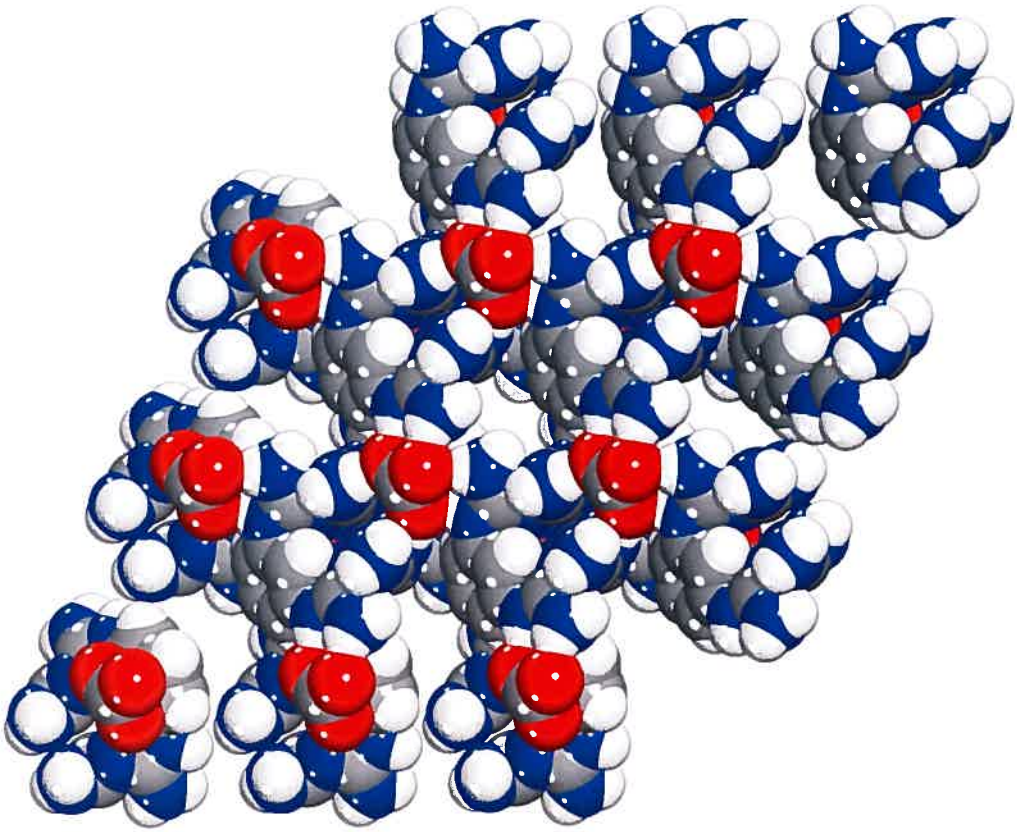

Figure A2-10. View along the *c* axis of the structure of crystals of 1,3-phenylenebis(biguanidinium) carbonate (**29** • H_2CO_3) grown from dioxane/water, showing a 3 × 3 × 1 array of unit cells with atoms represented by spheres of van der Waals radii. Hydrogen atoms appear in white, carbon in gray, nitrogen in blue, and oxygen in red. Guest molecules of water and dioxane are omitted for clarity.

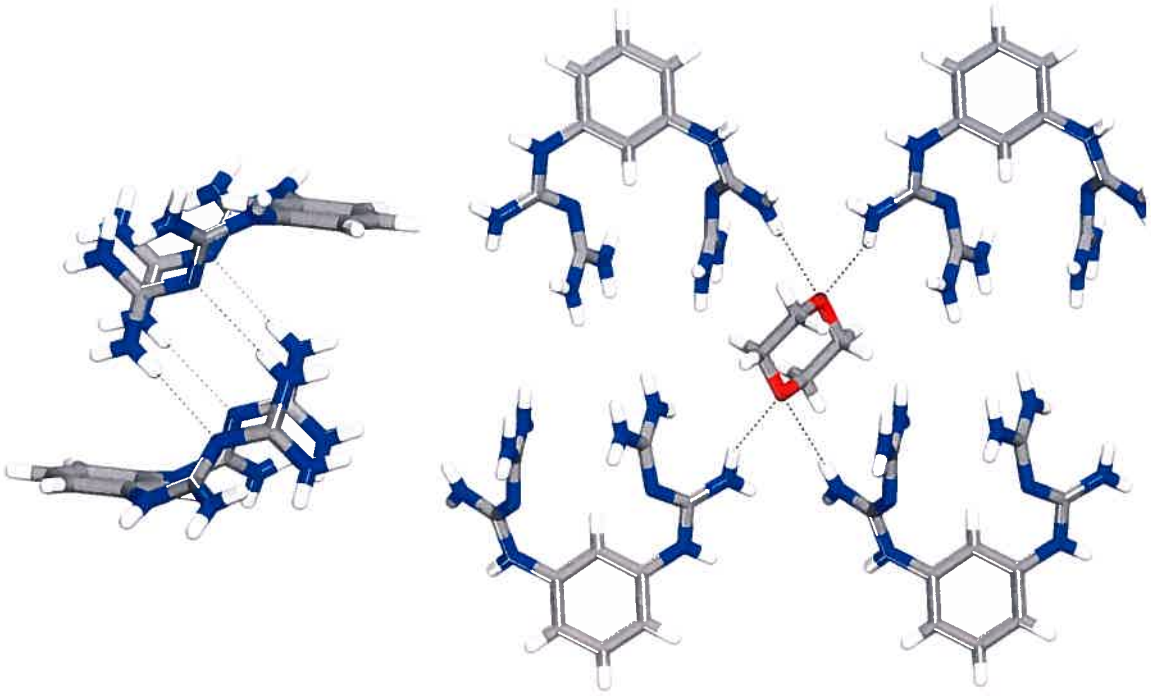

Figure A2-11. Detailed views showing interactions in the structure of crystals of 1,3-phenylenebis(biguanidinium) carbonate (**29** • H_2CO_3) grown from dioxane/water. **a**) View showing the hydrogen-bonded pairing of bis(biguanidinium) dications. **b**) View showing how included molecules of dioxane accept four hydrogen bonds from $-NH_2$ groups in four different bis(biguanidinium) dications. In both views, hydrogen bonds are represented by broken lines, and the counterions and included molecules of water are omitted for clarity. Hydrogen atoms appear in white, carbon in gray, nitrogen in blue, and oxygen in red.

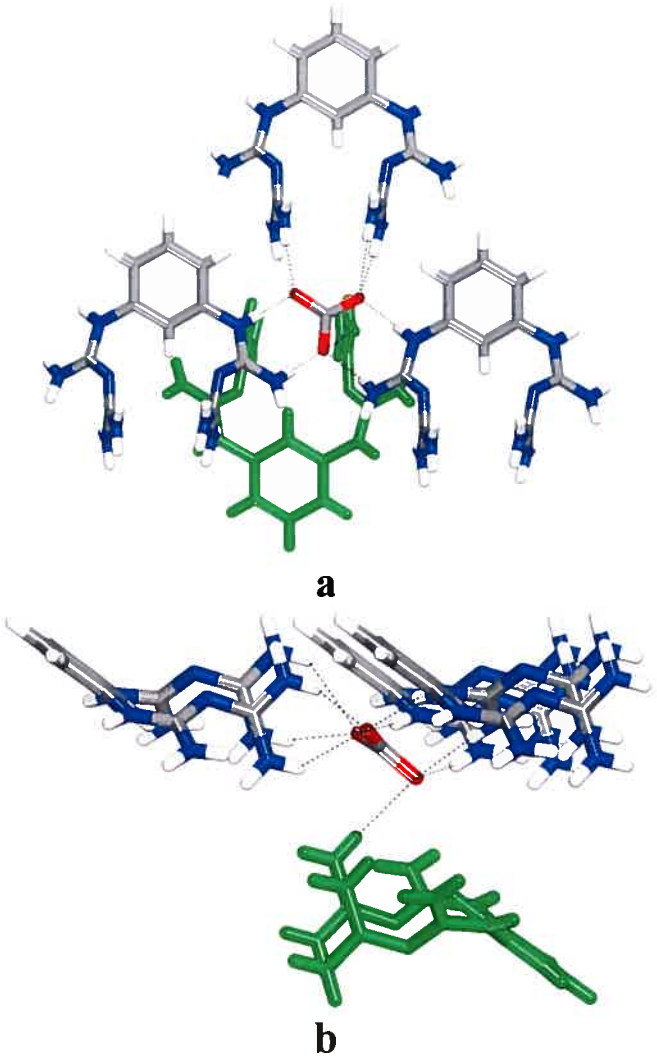

Figure A2-12. Detailed views showing hydrogen bonds involving carbonate ions in the structure of crystals of 1,3-phenylenebis(biguanidinium) carbonate (**29** • H_2CO_3) grown from dioxane/water. Each carbonate accepts four hydrogen bonds donated by a single bis(biguanidinium) dication, which adopts a characteristic pincer-like conformation. Each carbonate accepts four other hydrogen bonds contributed by two neighboring dications. Binding of carbonate in this way defines a hydrogen-bonded sheet. Each carbonate also accepts a hydrogen bond donated by a bis(biguanidinium) dication in an adjacent sheet (shown in green). This additional interaction is shown from the top (Figure A2-12a) and from the side (Figure A2-11b). Hydrogen bonds are represented by broken lines. Hydrogen atoms appear in white, carbon in gray, nitrogen in blue, and oxygen in red.

REFERENCES

International Tables for Crystallography (1992). Vol. C. Tables 4.2.6.8 and 6.1.1.4, Dordrecht: Kluwer Academic Publishers.

SAINT (2004) Release 7.06a; Integration Software for Single Crystal Data. Bruker AXS Inc., Madison, WI 53719-1173.

Sheldrick, G. M. (2001). **SADABS**, Bruker Area Detector Absorption Corrections. Bruker AXS Inc., Madison, WI 53719-1173.

Sheldrick, G. M. (2001). **TWINABS**, Bruker Area Detector Absorption Corrections. Bruker AXS Inc., Madison, WI 53719-1173.

Sheldrick, G. M. (1997). **SHELXS97**, Program for the Solution of Crystal Structures. Univ. of Gottingen, Germany.

Sheldrick, G. M. (1997). **SHELXL97**, Program for the Refinement of Crystal Structures. Univ. of Gottingen, Germany.

SHELXTL (1997) Release 5.10; The Complete Software Package for Single Crystal Structure Determination. Bruker AXS Inc., Madison, WI 53719-1173.

SMART (2003) Release 5.629; Bruker Molecular Analysis Research Tool. Bruker AXS Inc., Madison, WI 53719-1173.

Spek, A. L. (2004). **PLATON**, Molecular Geometry Program, 2000 version. University of Utrecht, Utrecht, Holland.

XPREP (1997) Release 5.10; X-Ray Data Preparation and Reciprocal Space Exploration Program. Bruker AXS Inc., Madison, WI 53719-1173.

Annexe 3 :

Information supplémentaire de l'article 3

Submitted to *Chem. Mater.*
Version of January 3, 2006

Supporting Information

A New Class of Selective Low-Molecular-Weight Gelators Based on Salts of Diaminotriazinecarboxylic Acids

Olivier LeBel,[†] Marie-Ève Perron,[†] Thierry Maris,[†] Sylvia F. Zalzal,[‡] Antonio Nanci,[‡] and James D. Wuest[*,†]

[†]*Département de Chimie, Université de Montréal*
Montréal, Québec H3C 3J7 Canada

[‡]*Laboratoire de Recherche sur les Tissus Calcifiés et Biomatériaux*
Faculté de Médecine Dentaire, Université de Montréal
Montréal, Québec H3C 3J7 Canada

Contents

III. Additional AFM Images of Gel Fibers of Sodium 4,6-Bis[(4-methylphenyl)amino)-1,3,5-triazine-2-carboxylate (43b) Spin-Cast on Quartz (A3-19-A3-20)

*Author to whom correspondence may be addressed:
[redacted]

Université de Montréal

CRYSTAL AND MOLECULAR STRUCTURE OF

C22 H28 N5 Na O4 S2 COMPOUND (JIW903)

Equipe WUEST

Département de chimie, Université de Montréal,

C.P. 6128, Succ. Centre-Ville, Montréal, Québec, H3C 3J7 (Canada)

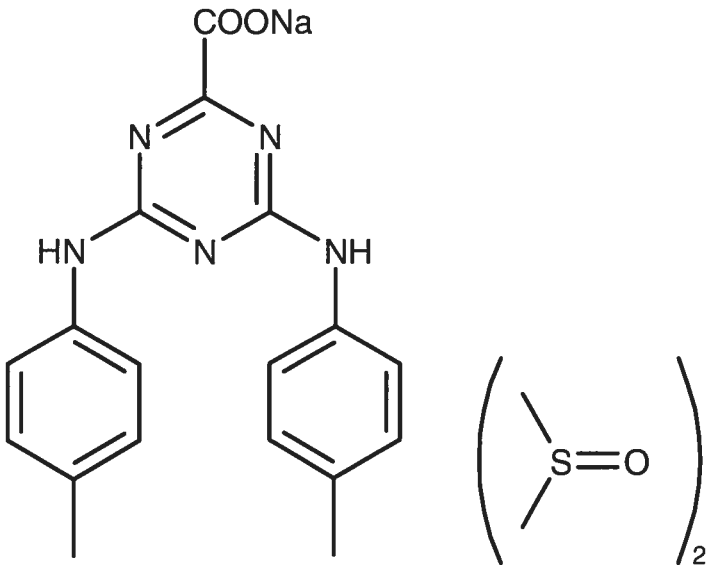

Structure solved and refined in the Laboratory of X-Ray Diffraction, Université de Montréal by Dr. Thierry Maris

Table A3-1. Crystal data and structure refinement for C22 H28 N5 Na O4 S2.

Identification code	JIW903
Empirical formula	C22 H28 N5 Na O4 S2
Formula weight	513.60
Temperature	100(2)K
Wavelength	1.54178 Å
Crystal system	Monoclinic
Space group	P21/c
Unit cell dimensions	a = 15.8524(3) Å α = 90° b = 10.4636(2) Å β = 105.0208(9)° c = 15.8729(3) Å γ = 90°
Volume	2542.93(8)Å^3
Z	4
Density (calculated)	1.342 g/cm^3
Absorption coefficient	2.384 mm^{-1}
F(000)	1080
Crystal size	0.22 x 0.07 x 0.07 mm
Theta range for data collection	2.89 to 68.05°
Index ranges	$-19 \leq h \leq 18$, $-12 \leq k \leq 11$, $-18 \leq \ell \leq 18$
Reflections collected	31713
Independent reflections	4580 [R_{int} = 0.037]
Absorption correction	Semi-empirical from equivalents
Max. and min. transmission	0.6600 and 0.5600
Refinement method	Full-matrix least-squares on F^2
Data / restraints / parameters	4580 / 0 / 314
Goodness-of-fit on F^2	1.003
Final R indices [I>2sigma(I)]	R_1 = 0.0401, wR_2 = 0.0996

R indices (all data)	R_1 = 0.0636, wR_2 = 0.1089
Extinction coefficient	0.00029(10)
Largest diff. peak and hole	0.288 and -0.378 e/Å^3

Table A3-2. Atomic coordinates (x 10^4) and equivalent isotropic displacement parameters (Å^2 x 10^3) for C22 H28 N5 Na O4 S2.

U_{eq} is defined as one third of the trace of the orthogonalized Uij tensor.

	x	y	z	U_{eq}
C(1)	5433(1)	9753(2)	2217(1)	19(1)
C(2)	4435(1)	9599(2)	2026(1)	18(1)
C(3)	3264(1)	8446(2)	2144(1)	19(1)
C(4)	3069(1)	10358(2)	1473(1)	19(1)
C(5)	2094(1)	6960(2)	2278(1)	20(1)
C(6)	1884(1)	5692(2)	2063(2)	23(1)
C(7)	1028(2)	5278(3)	1940(2)	27(1)
C(8)	368(2)	6110(3)	2009(2)	27(1)
C(9)	594(2)	7362(3)	2246(2)	28(1)
N(6)	2577(1)	11323(2)	1037(1)	22(1)
C(10)	1450(1)	7791(3)	2392(2)	25(1)
C(11)	-571(2)	5677(3)	1826(2)	36(1)
C(12)	1668(1)	11549(2)	836(1)	22(1)
C(13)	1059(2)	10720(3)	1014(2)	29(1)
C(14)	179(2)	11066(3)	800(2)	33(1)
C(15)	-112(2)	12219(3)	400(2)	28(1)
C(16)	506(2)	13023(3)	213(2)	31(1)
C(17)	1381(2)	12711(3)	428(2)	28(1)
N(5)	2973(1)	7346(2)	2400(1)	20(1)
C(18)	-1068(2)	12563(3)	165(2)	38(1)
C(20)	3484(2)	8858(3)	5562(2)	32(1)
C(21)	3427(2)	6573(3)	4748(2)	33(1)
C(30)	6043(2)	8601(3)	6299(2)	34(1)
C(31)	7219(2)	6763(3)	6333(2)	39(1)
N(1)	4150(1)	8532(2)	2314(1)	19(1)
N(2)	3946(1)	10552(2)	1600(1)	18(1)
N(3)	2700(1)	9340(2)	1732(1)	20(1)
Na(1)	5250(1)	7549(1)	3553(1)	21(1)
O(1)	5891(1)	8947(2)	2702(1)	23(1)
O(2)	5688(1)	10701(2)	1858(1)	22(1)
O(20)	4451(1)	8398(2)	4474(1)	27(1)
O(30)	6464(1)	7938(2)	4857(1)	25(1)
S(20)	3528(1)	8230(1)	4527(1)	25(1)
S(30)	6221(1)	7325(1)	5628(1)	25(1)

Table A3-3. Hydrogen coordinates (x 10^4) and isotropic displacement parameters ($Å^2$ x 10^3) for C22 H28 N5 Na O4 S2.

	x	y	z	U_{eq}
H(6)	2314	5122	2001	28
H(7)	895	4423	1809	33
H(9)	163	7930	2308	33
H(6A)	2868	11901	849	27
H(10)	1590	8630	2564	30
H(11A)	-628	4845	1563	53
H(11B)	-938	6271	1436	53
H(11C)	-743	5641	2362	53
H(13)	1235	9935	1275	35
H(14)	-224	10505	930	39
H(16)	327	13796	-65	37
H(17)	1783	13278	301	33
H(5)	3365	6815	2669	24
H(18A)	-1147	13399	-93	57
H(18B)	-1276	12559	682	57
H(18C)	-1391	11950	-244	57
H(20A)	3930	8464	6014	48
H(20B)	2922	8682	5657	48
H(20C)	3578	9765	5570	48
H(21A)	3475	6078	4254	50
H(21B)	2869	6420	4861	50
H(21C)	3883	6331	5250	50
H(30A)	6567	9099	6484	51
H(30B)	5888	8261	6800	51
H(30C)	5578	9132	5974	51
H(31A)	7449	6085	6050	58
H(31B)	7112	6449	6864	58
H(31C)	7633	7451	6463	58

Table A2-4. Anisotropic parameters ($Å^2$ x 10^3) for C22 H28 N5 Na O4 S2.

The anisotropic displacement factor exponent takes the form:

$$-2\pi^2 [h^2 a^{*2} U_{11} + ... + 2 h k a^* b^* U_{12}]$$

	U11	U22	U33	U23	U13	U12
C(1)	17(1)	22(2)	17(1)	-4(1)	4(1)	-2(1)
C(2)	20(1)	21(2)	13(1)	-3(1)	3(1)	-1(1)
C(3)	16(1)	24(2)	15(1)	-1(1)	3(1)	-1(1)
C(4)	20(1)	24(2)	14(1)	0(1)	2(1)	0(1)
C(5)	18(1)	25(2)	15(1)	3(1)	3(1)	-2(1)
C(6)	23(1)	22(2)	23(1)	3(1)	4(1)	1(1)
C(7)	29(1)	25(2)	27(1)	2(1)	5(1)	-7(1)
C(8)	21(1)	36(2)	22(1)	7(1)	1(1)	-5(1)
C(9)	20(1)	32(2)	32(1)	4(1)	8(1)	1(1)
N(6)	18(1)	21(1)	27(1)	6(1)	5(1)	2(1)
C(10)	22(1)	25(2)	28(1)	2(1)	7(1)	-2(1)
C(11)	24(1)	45(2)	36(2)	6(1)	5(1)	-11(1)
C(12)	18(1)	29(2)	18(1)	1(1)	1(1)	4(1)
C(13)	22(1)	34(2)	31(1)	9(1)	3(1)	3(1)
C(14)	21(1)	45(2)	31(1)	7(1)	5(1)	1(1)
C(15)	21(1)	40(2)	21(1)	1(1)	2(1)	8(1)
C(16)	27(1)	36(2)	28(1)	5(1)	3(1)	11(1)
C(17)	25(1)	29(2)	29(1)	8(1)	6(1)	5(1)
N(5)	15(1)	22(1)	22(1)	4(1)	3(1)	0(1)
C(18)	26(1)	55(2)	31(1)	1(1)	3(1)	9(1)
C(20)	37(2)	32(2)	29(1)	-2(1)	13(1)	2(1)
C(21)	40(2)	32(2)	34(2)	-1(1)	19(1)	-3(1)
C(30)	46(2)	35(2)	21(1)	0(1)	9(1)	-1(1)
C(31)	33(1)	46(2)	35(2)	13(1)	4(1)	4(1)
N(1)	16(1)	21(1)	18(1)	1(1)	3(1)	-2(1)
N(2)	16(1)	20(1)	18(1)	-2(1)	3(1)	0(1)
N(3)	16(1)	21(1)	21(1)	2(1)	3(1)	1(1)
Na(1)	19(1)	24(1)	18(1)	0(1)	3(1)	1(1)
O(1)	17(1)	25(1)	26(1)	4(1)	3(1)	1(1)
O(2)	17(1)	24(1)	25(1)	1(1)	5(1)	-2(1)
O(20)	29(1)	29(1)	26(1)	-1(1)	12(1)	0(1)
O(30)	28(1)	30(1)	18(1)	-1(1)	7(1)	1(1)
S(20)	27(1)	29(1)	21(1)	1(1)	8(1)	3(1)
S(30)	25(1)	26(1)	21(1)	1(1)	4(1)	0(1)

Table A3-5. Bond lengths [Å] and angles [°] for C22 H28 N5 Na O4 S2

C(1)-O(1)	1.242(3)	C(10)-C(5)-C(6)	119.5(2)
C(1)-O(2)	1.262(3)	C(10)-C(5)-N(5)	122.4(2)
C(1)-C(2)	1.541(3)	C(6)-C(5)-N(5)	118.1(2)
C(2)-N(1)	1.329(3)	C(7)-C(6)-C(5)	119.8(2)
C(2)-N(2)	1.335(3)	C(6)-C(7)-C(8)	121.5(3)
C(3)-N(3)	1.341(3)	C(9)-C(8)-C(7)	117.8(2)
C(3)-N(5)	1.341(3)	C(9)-C(8)-C(11)	120.7(2)
C(3)-N(1)	1.362(3)	C(7)-C(8)-C(11)	121.5(3)
C(4)-N(3)	1.331(3)	C(8)-C(9)-C(10)	121.6(2)
C(4)-N(6)	1.352(3)	C(4)-N(6)-C(12)	131.4(2)
C(4)-N(2)	1.367(3)	C(5)-C(10)-C(9)	119.7(2)
C(5)-C(10)	1.388(3)	C(13)-C(12)-C(17)	118.8(2)
C(5)-C(6)	1.389(3)	C(13)-C(12)-N(6)	125.0(2)
C(5)-N(5)	1.415(3)	C(17)-C(12)-N(6)	116.1(2)
C(6)-C(7)	1.388(3)	C(12)-C(13)-C(14)	119.6(2)
C(7)-C(8)	1.389(4)	C(15)-C(14)-C(13)	122.1(2)
C(8)-C(9)	1.384(4)	C(16)-C(15)-C(14)	117.3(2)
C(8)-C(11)	1.509(3)	C(16)-C(15)-C(18)	121.7(2)
C(9)-C(10)	1.390(3)	C(14)-C(15)-C(18)	121.0(2)
N(6)-C(12)	1.413(3)	C(17)-C(16)-C(15)	121.8(3)
C(12)-C(13)	1.380(3)	C(16)-C(17)-C(12)	120.4(2)
C(12)-C(17)	1.397(3)	C(3)-N(5)-C(5)	127.43(19)
C(13)-C(14)	1.395(3)	C(2)-N(1)-C(3)	114.33(19)
C(14)-C(15)	1.385(4)	C(2)-N(1)-Na(1)	112.82(13)
C(15)-C(16)	1.381(4)	C(3)-N(1)-Na(1)	127.24(15)
C(15)-C(18)	1.508(3)	C(2)-N(2)-C(4)	113.44(19)
C(16)-C(17)	1.379(3)	C(2)-N(2)-Na(1)#1	115.61(14)
C(20)-S(20)	1.787(2)	C(4)-N(2)-Na(1)#1	129.51(15)
C(21)-S(20)	1.784(3)	C(4)-N(3)-C(3)	114.73(19)
C(30)-S(30)	1.774(3)	O(20)-Na(1)-O(1)	119.92(7)
C(31)-S(30)	1.785(2)	O(20)-Na(1)-O(2)#2	94.41(6)
N(1)-Na(1)	2.4880(19)	O(1)-Na(1)-O(2)#2	131.10(6)
N(2)-Na(1)#1	2.492(2)	O(20)-Na(1)-O(30)	81.08(6)
Na(1)-O(20)	2.3433(18)	O(1)-Na(1)-O(30)	91.14(6)
Na(1)-O(1)	2.3895(18)	O(2)#2-Na(1)-O(30)	130.39(7)
Na(1)-O(2)#2	2.4243(18)	O(20)-Na(1)-N(1)	87.40(6)
Na(1)-O(30)	2.4670(17)	O(1)-Na(1)-N(1)	67.28(6)
Na(1)-N(2)#2	2.492(2)	O(2)#2-Na(1)-N(1)	82.03(6)
O(2)-Na(1)#1	2.4243(18)	O(30)-Na(1)-N(1)	146.07(7)
O(20)-S(20)	1.4962(16)	O(20)-Na(1)-N(2)#2	138.73(7)
O(30)-S(30)	1.5176(17)	O(1)-Na(1)-N(2)#2	98.91(6)
		O(2)#2-Na(1)-N(2)#2	66.32(6)
O(1)-C(1)-O(2)	127.5(2)	O(30)-Na(1)-N(2)#2	84.98(6)
O(1)-C(1)-C(2)	117.2(2)	N(1)-Na(1)-N(2)#2	122.75(7)
O(2)-C(1)-C(2)	115.32(19)	C(1)-O(1)-Na(1)	120.01(14)
N(1)-C(2)-N(2)	126.7(2)	C(1)-O(2)-Na(1)#1	120.13(14)
N(1)-C(2)-C(1)	116.37(19)	O(20)-S(20)-C(21)	105.35(11)
N(2)-C(2)-C(1)	116.9(2)	O(20)-S(20)-C(20)	106.22(11)
N(3)-C(3)-N(5)	120.52(19)	C(21)-S(20)-C(20)	98.57(13)
N(3)-C(3)-N(1)	125.0(2)	O(30)-S(30)-C(30)	106.24(11)
N(5)-C(3)-N(1)	114.5(2)	O(30)-S(30)-C(31)	105.99(11)
N(3)-C(4)-N(6)	120.9(2)	C(30)-S(30)-C(31)	97.21(13)
N(3)-C(4)-N(2)	125.8(2)	O(30)-S(30)-Na(1)	46.14(6)
N(6)-C(4)-N(2)	113.3(2)	C(30)-S(30)-Na(1)	116.41(9)

C(31)-S(30)-Na(1) 139.99(10)

Symmetry transformations: #1 -x+1,y+1/2,-z+1/2 #2 -x+1,y-1/2,-z+1/2

Table A3-6. Torsion angles [°] for C22 H28 N5 Na O4 S2.

O(1)-C(1)-C(2)-N(1)	-7.7(3)	N(3)-C(4)-N(2)-Na(1)#1	-165.62(17)
O(2)-C(1)-C(2)-N(1)	172.59(19)	N(6)-C(4)-N(2)-Na(1)#1	14.8(3)
O(1)-C(1)-C(2)-N(2)	171.6(2)	N(6)-C(4)-N(3)-C(3)	178.9(2)
O(2)-C(1)-C(2)-N(2)	-8.2(3)	N(2)-C(4)-N(3)-C(3)	-0.6(3)
C(10)-C(5)-C(6)-C(7)	1.7(3)	N(5)-C(3)-N(3)-C(4)	-176.8(2)
N(5)-C(5)-C(6)-C(7)	179.9(2)	N(1)-C(3)-N(3)-C(4)	1.1(3)
C(5)-C(6)-C(7)-C(8)	1.4(4)	C(2)-N(1)-Na(1)-O(20)	102.58(15)
C(6)-C(7)-C(8)-C(9)	-3.0(4)	C(3)-N(1)-Na(1)-O(20)	-49.20(19)
C(6)-C(7)-C(8)-C(11)	176.5(2)	C(2)-N(1)-Na(1)-O(1)	-21.49(14)
C(7)-C(8)-C(9)-C(10)	1.4(4)	C(3)-N(1)-Na(1)-O(1)	-173.3(2)
C(11)-C(8)-C(9)-C(10)	-178.0(2)	C(2)-N(1)-Na(1)-O(2)#2	-162.59(15)
N(3)-C(4)-N(6)-C(12)	6.2(4)	C(3)-N(1)-Na(1)-O(2)#2	45.63(19)
N(2)-C(4)-N(6)-C(12)	-174.2(2)	C(2)-N(1)-Na(1)-O(30)	32.8(2)
C(6)-C(5)-C(10)-C(9)	-3.2(3)	C(3)-N(1)-Na(1)-O(30)	-118.99(19)
N(5)-C(5)-C(10)-C(9)	178.7(2)	C(2)-N(1)-Na(1)-N(2)#2	-107.50(15)
C(8)-C(9)-C(10)-C(5)	1.6(4)	C(3)-N(1)-Na(1)-N(2)#2	100.72(19)
C(4)-N(6)-C(12)-C(13)	-4.7(4)	C(2)-N(1)-Na(1)-S(30)	83.92(18)
C(4)-N(6)-C(12)-C(17)	175.1(2)	C(3)-N(1)-Na(1)-S(30)	-67.9(2)
C(17)-C(12)-C(13)-C(14)	-1.2(4)	O(2)-C(1)-O(1)-Na(1)	165.62(18)
N(6)-C(12)-C(13)-C(14)	178.6(2)	C(2)-C(1)-O(1)-Na(1)	-14.1(3)
C(12)-C(13)-C(14)-C(15)	0.8(4)	O(20)-Na(1)-O(1)-C(1)	-53.72(18)
C(13)-C(14)-C(15)-C(16)	0.3(4)	O(2)#2-Na(1)-O(1)-C(1)	74.59(19)
C(13)-C(14)-C(15)-C(18)	179.2(2)	O(30)-Na(1)-O(1)-C(1)	-134.07(17)
C(14)-C(15)-C(16)-C(17)	-1.2(4)	N(1)-Na(1)-O(1)-C(1)	18.97(16)
C(18)-C(15)-C(16)-C(17)	179.9(2)	N(2)#2-Na(1)-O(1)-C(1)	140.84(17)
C(15)-C(16)-C(17)-C(12)	0.9(4)	S(30)-Na(1)-O(1)-C(1)	-129.84(16)
C(13)-C(12)-C(17)-C(16)	0.3(4)	O(1)-C(1)-O(2)-Na(1)#1	-155.17(19)
N(6)-C(12)-C(17)-C(16)	-179.4(2)	C(2)-C(1)-O(2)-Na(1)#1	24.5(2)
N(3)-C(3)-N(5)-C(5)	1.0(3)	O(1)-Na(1)-O(20)-S(20)	121.18(13)
N(1)-C(3)-N(5)-C(5)	-177.0(2)	O(2)#2-Na(1)-O(20)-S(20)	-22.44(14)
C(10)-C(5)-N(5)-C(3)	-41.8(3)	O(30)-Na(1)-O(20)-S(20)	-152.67(14)
C(6)-C(5)-N(5)-C(3)	140.1(2)	N(1)-Na(1)-O(20)-S(20)	59.36(14)
N(2)-C(2)-N(1)-C(3)	-0.2(3)	N(2)#2-Na(1)-O(20)-S(20)	-80.93(16)
C(1)-C(2)-N(1)-C(3)	178.99(18)	S(30)-Na(1)-O(20)-S(20)	-130.31(14)
N(2)-C(2)-N(1)-Na(1)	-155.77(18)	O(20)-Na(1)-O(30)-S(30)	51.37(9)
C(1)-C(2)-N(1)-Na(1)	23.4(2)	O(1)-Na(1)-O(30)-S(30)	171.49(9)
N(3)-C(3)-N(1)-C(2)	-0.7(3)	O(2)#2-Na(1)-O(30)-S(30)	-36.83(13)
N(5)-C(3)-N(1)-C(2)	177.26(19)	N(1)-Na(1)-O(30)-S(30)	122.98(12)
N(3)-C(3)-N(1)-Na(1)	150.69(17)	N(2)#2-Na(1)-O(30)-S(30)	-89.66(10)
N(5)-C(3)-N(1)-Na(1)	-31.3(3)	Na(1)-O(20)-S(20)-C(21)	61.50(16)
N(1)-C(2)-N(2)-C(4)	0.6(3)	Na(1)-O(20)-S(20)-C(20)	165.43(14)
C(1)-C(2)-N(2)-C(4)	-178.60(18)	Na(1)-O(30)-S(30)-C(30)	-111.25(11)
N(1)-C(2)-N(2)-Na(1)#1	168.19(17)	Na(1)-O(30)-S(30)-C(31)	146.07(12)
C(1)-C(2)-N(2)-Na(1)#1	-11.0(2)	O(20)-Na(1)-S(30)-O(30)	-122.09(11)
N(3)-C(4)-N(2)-C(2)	-0.1(3)	O(1)-Na(1)-S(30)-O(30)	-9.57(10)
N(6)-C(4)-N(2)-C(2)	-179.70(19)	O(2)#2-Na(1)-S(30)-O(30)	151.29(11)

N(1)-Na(1)-S(30)-O(30) -101.54(15)	O(30)-Na(1)-S(30)-C(30) 87.47(14)
N(2)#2-Na(1)-S(30)-O(30) 88.07(10)	N(1)-Na(1)-S(30)-C(30) -14.07(16)
O(20)-Na(1)-S(30)-C(30) -34.62(11)	N(2)#2-Na(1)-S(30)-C(30) 175.54(11)
O(1)-Na(1)-S(30)-C(30) 77.90(12)	O(20)-Na(1)-S(30)-C(31) -178.67(16)
O(2)#2-Na(1)-S(30)-C(30) -121.24(11)	O(1)-Na(1)-S(30)-C(31) -66.15(17)
	N(2)#2-Na(1)-S(30)-C(31) 31.49(16)

Symmetry transformations used to generate equivalent atoms:

#1 -x+1,y+1/2,-z+1/2 #2 -x+1,y-1/2,-z+1/2

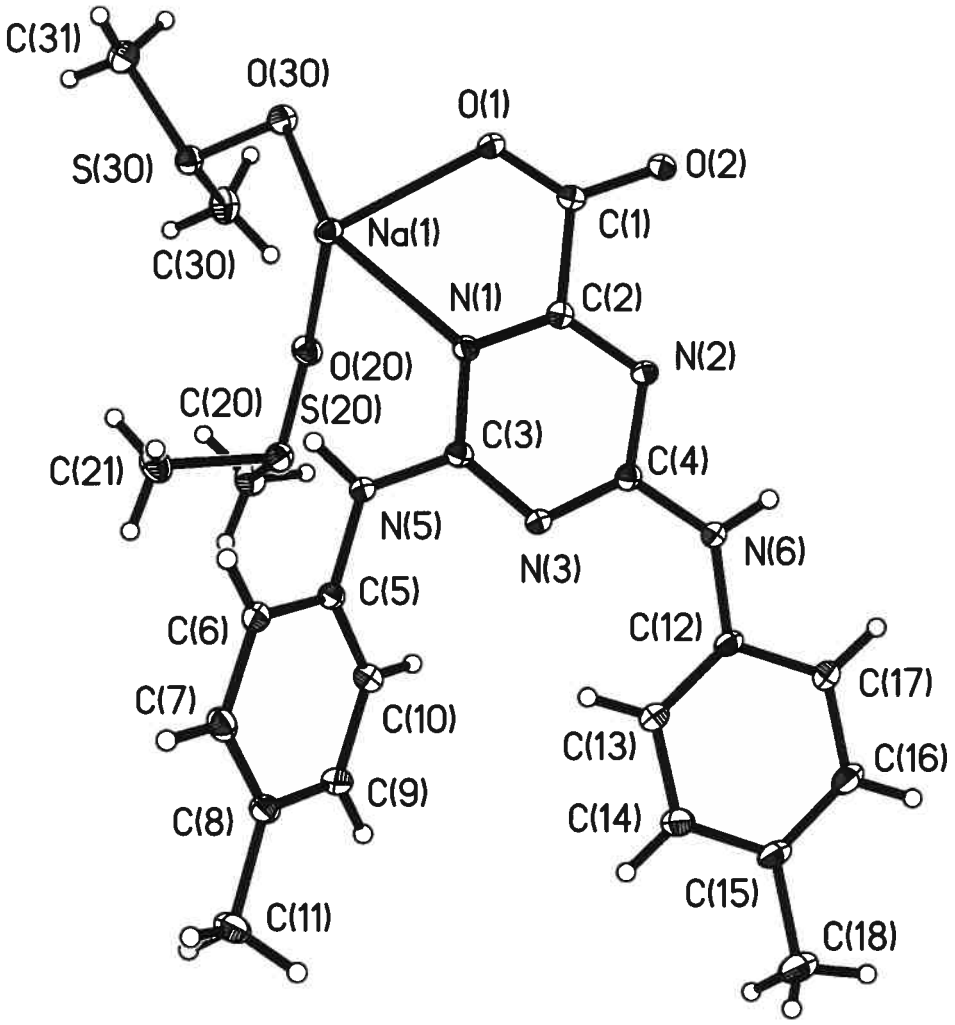

Thermal ellipsoid view of the C22 H28 N5 Na O4 S2 compound with the numbering scheme adopted. Ellipsoids are drawn at the 30% probability level. Hydrogen atoms are represented by a sphere of arbitrary size.

REFERENCES

International Tables for Crystallography (1992). Vol. C. Tables 4.2.6.8 and
6.1.1.4, Dordrecht: Kluwer Academic Publishers.

SAINT (1999) Release 6.06; Integration Software for Single Crystal Data.
Bruker AXS Inc., Madison, WI 53719-1173.

Sheldrick, G.M. (1996). SADABS, Bruker Area Detector Absorption Corrections.
Bruker AXS Inc., Madison, WI 53719-1173.

Sheldrick, G.M. (1997). SHELXS97, Program for the Solution of Crystal Structures. Univ. of Gottingen, Germany.

Sheldrick, G.M. (1997). SHELXL97, Program for the Refinement of Crystal Structures. Univ. of Gottingen, Germany.

SHELXTL (1997) Release 5.10; The Complete Software Package for Single Crystal Structure Determination. Bruker AXS Inc., Madison, WI 53719-1173.

SMART (1999) Release 5.059; Bruker Molecular Analysis Research Tool.
Bruker AXS Inc., Madison, WI 53719-1173.

Spek, A.L. (2000). PLATON, Molecular Geometry Program, 2000 version.
University of Utrecht, Utrecht, Holland.

XPREP (1997) Release 5.10; X-Ray Data Preparation and Reciprocal Space Exploration Program. Bruker AXS Inc., Madison, WI 53719-1173.

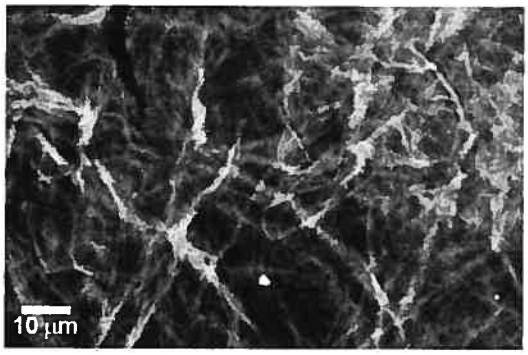

a

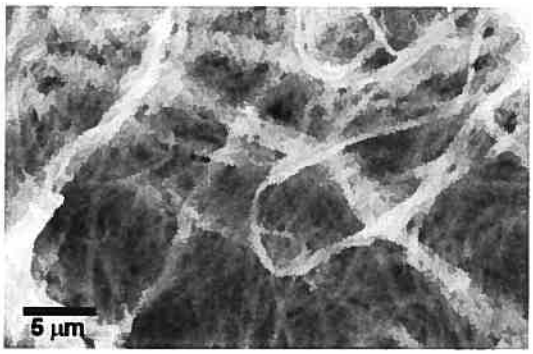

b

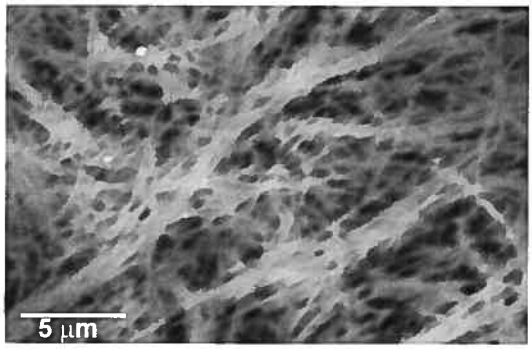

c

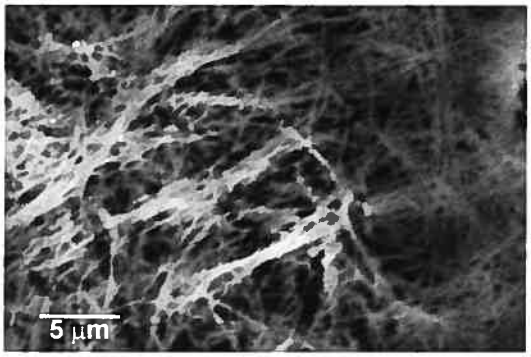

d

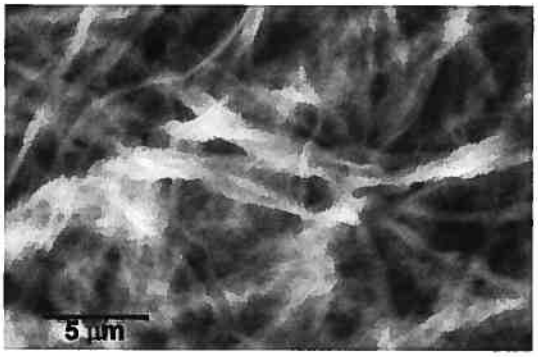

e

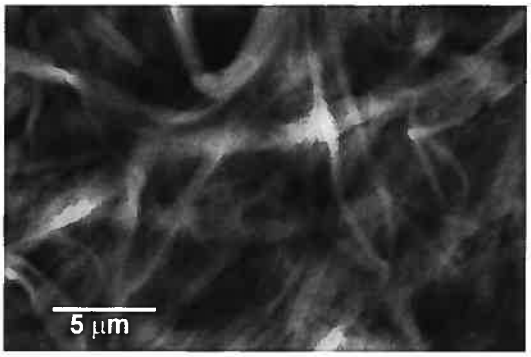

f

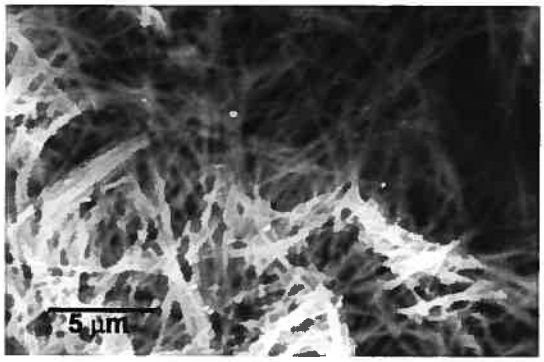

g

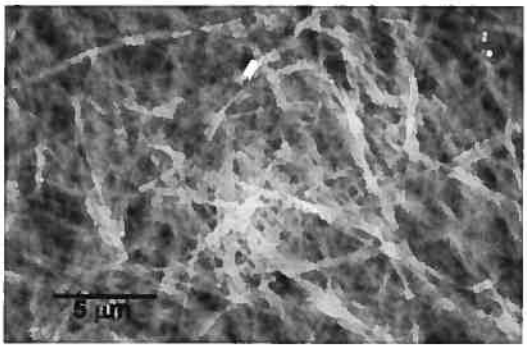

h

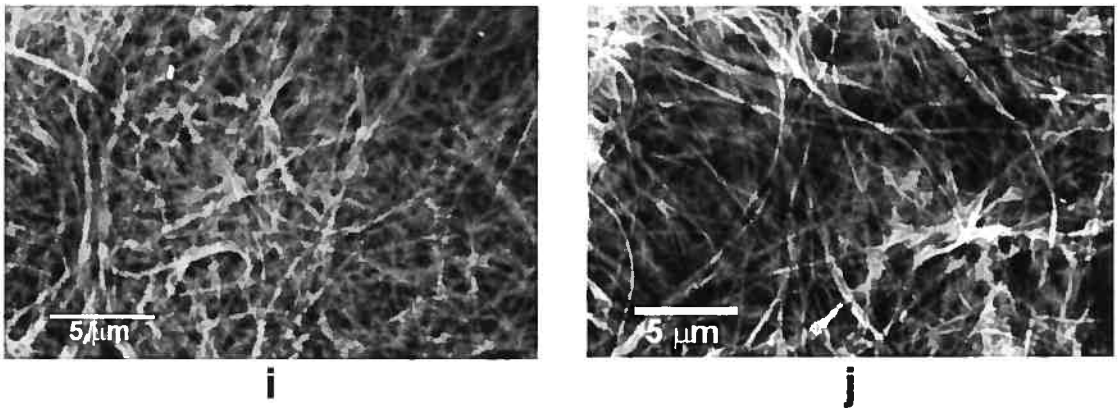

Figure A3-1. Additional variable-pressure scanning electron micrographs of the gel prepared by dissolving sodium 4,6-bis(phenylamino)-1,3,5-triazine-2-carboxylate (**43a**) in DMSO (3.0 mg/mL). Images were recorded at 27 °C and 30-50 Pa with an electron beam of 15-20 kV.

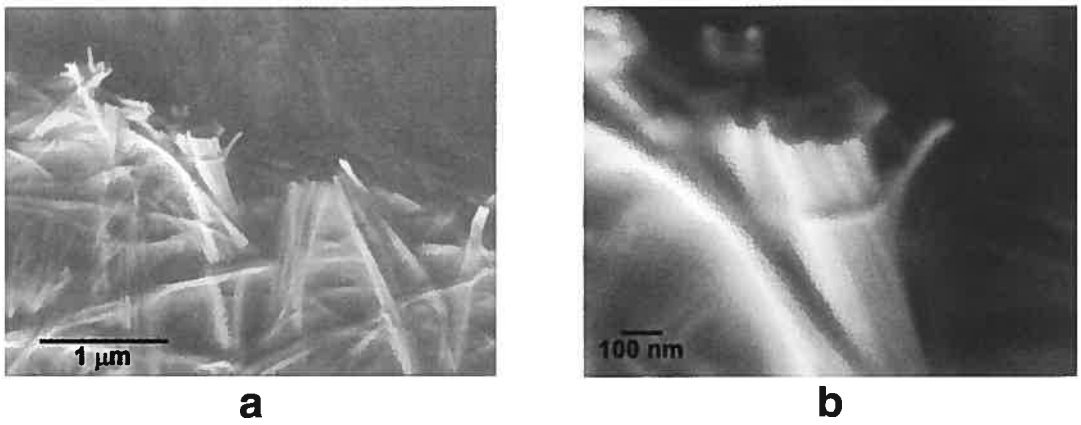

Figure A3-2. Additional field-emission scanning electron micrographs of a xerogel formed by sodium 4,6-bis(phenylamino)-1,3,5-triazine-2-carboxylate (**43a**). The gel formed by a 3.0 mg/mL solution of salt **43a** in DMSO was dried under vacuum and observed uncoated with an electron beam of 1 kV.

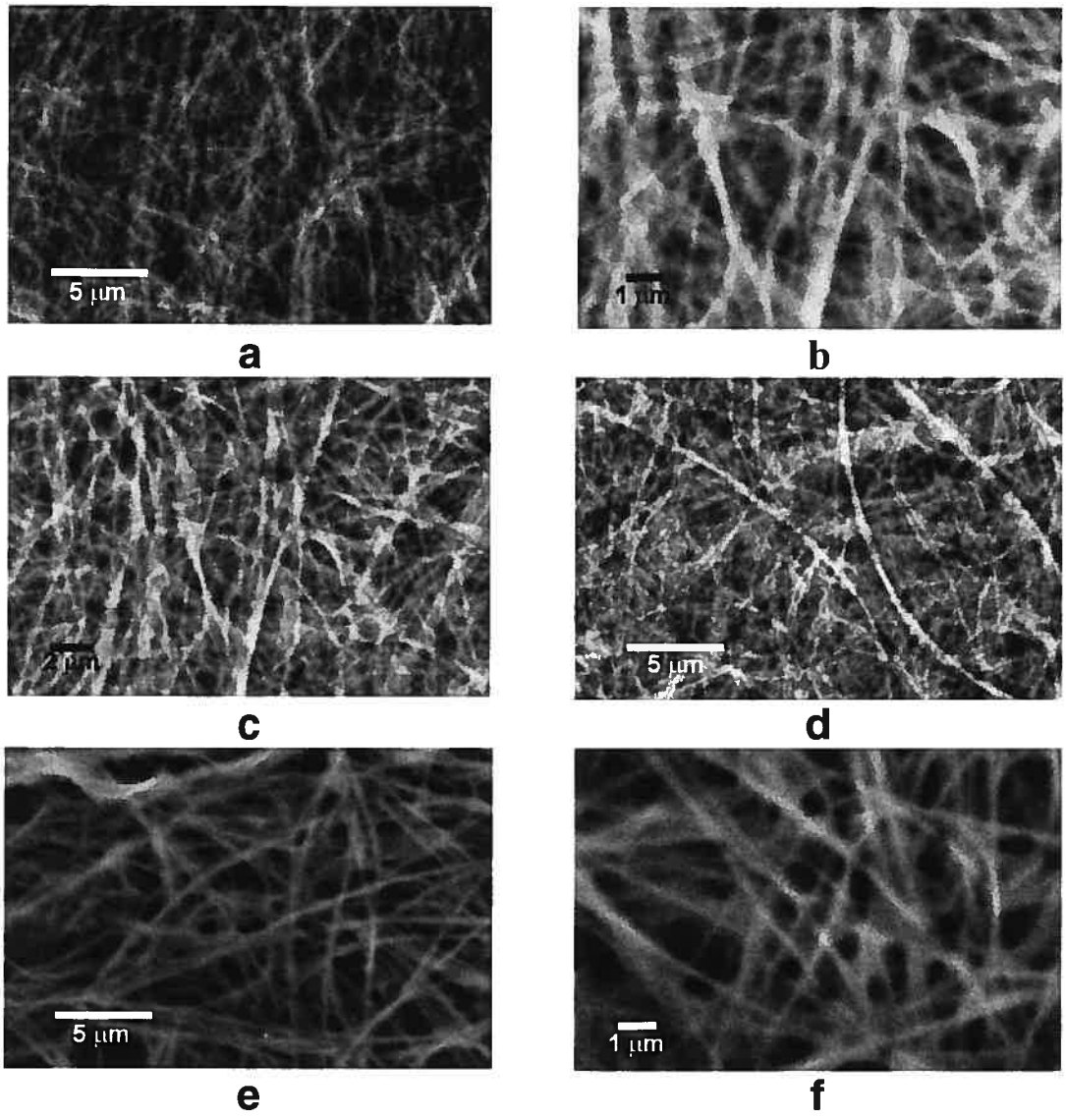

Figure A3-3. Variable-pressure scanning electron micrographs of the gel formed by dissolving sodium 4,6-bis[(4-methoxyphenyl)amino]-1,3,5-triazine-2-carboxylate (**43c**) in DMSO (3.0 mg/mL). Images were recorded at 27 °C and 30-50 Pa with an electron beam of 15-20 kV.

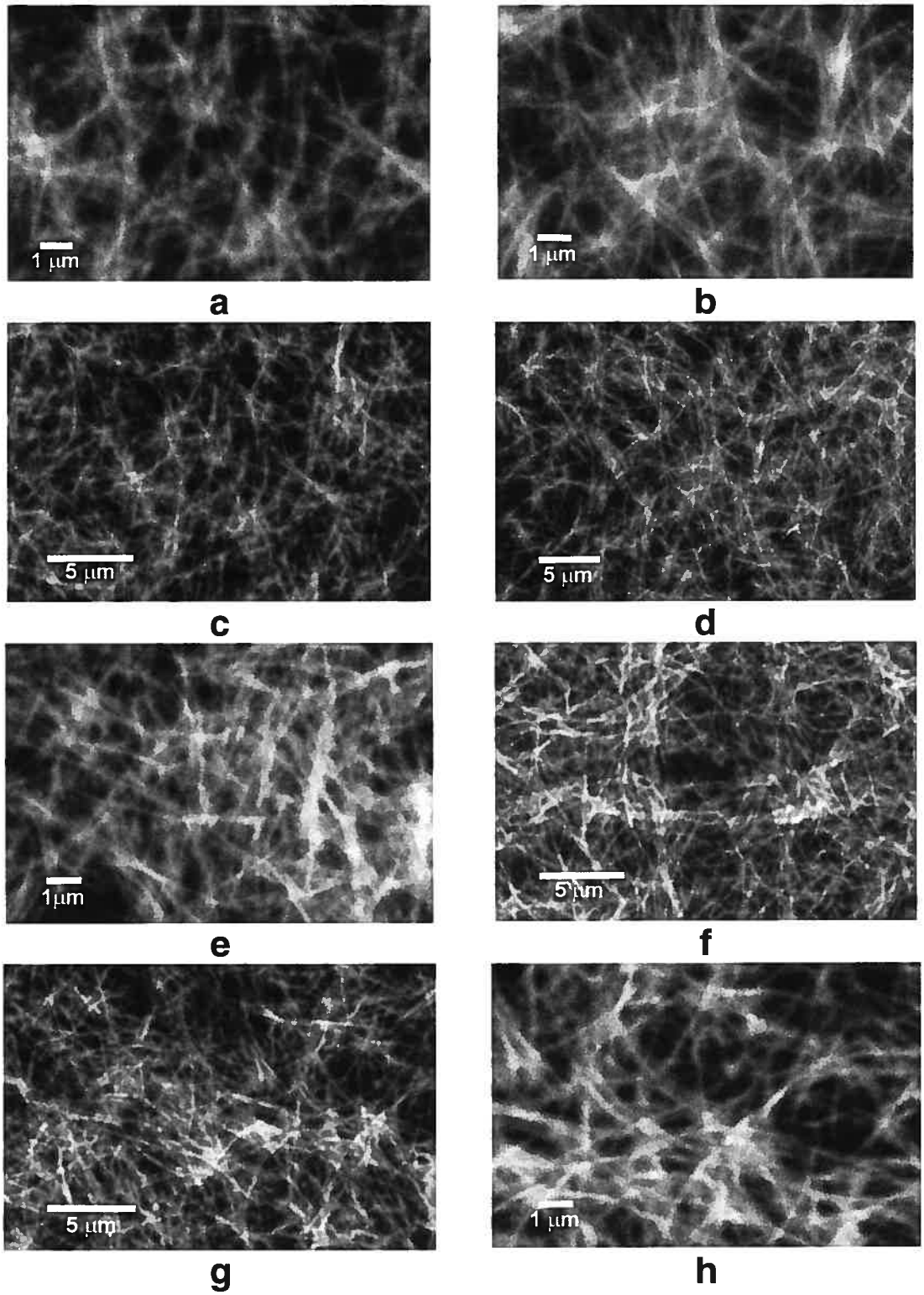
1 µm
a
1 µm
b
5 µm
c
5 µm
d
1µm
e
5 µm
f
5 µm
g
1 µm
h

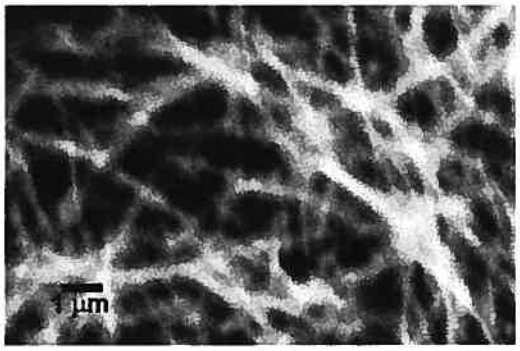

Figure A3-4. Variable-pressure scanning electron micrographs of a gel made by dissolving sodium 4,6-bis[(4-bromophenyl)amino]-1,3,5-triazine-2-carboxylate (**43e**) in DMSO (1.5 mg/mL). Images were recorded at 27 °C and 30-50 Pa with an electron beam of 15-20 kV.

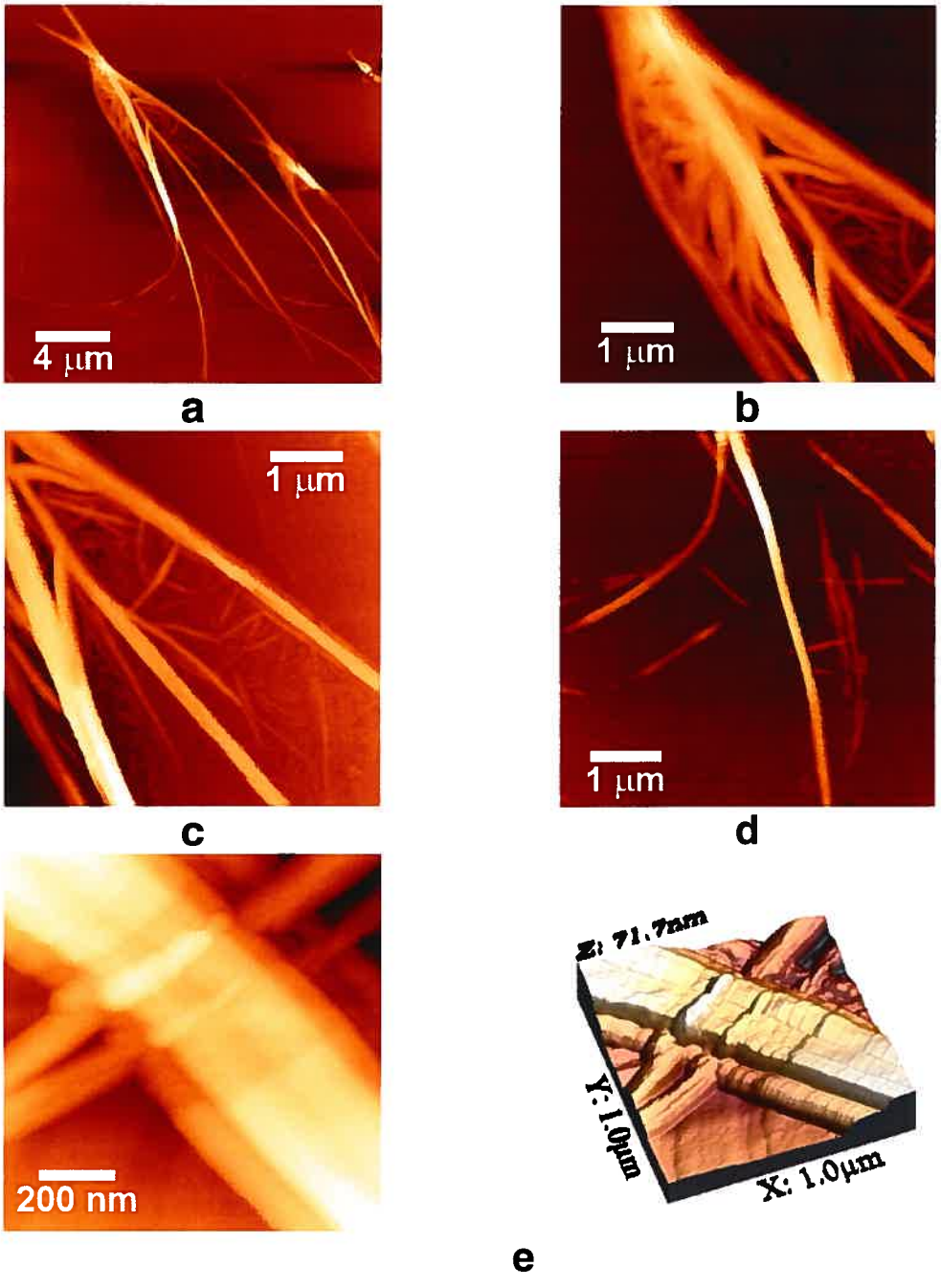
4 µm
a
1 µm
b
1 µm
c
1 µm
d
200 nm
Z: 71.7nm
Y: 1.0µm
X: 1.0µm
e

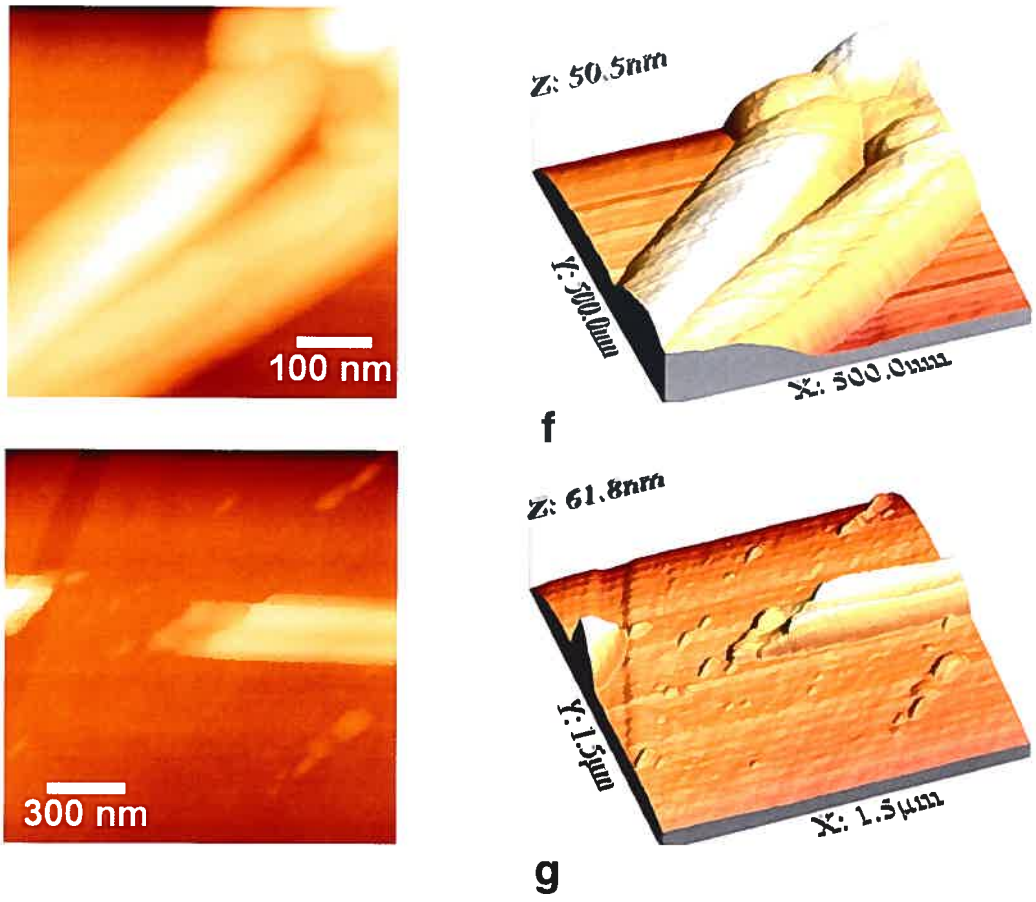

Figure A3-5. Additional tapping-mode atomic force micrographs of gel fibers spin-cast onto quartz from a 3.0 mg/mL solution of sodium 4,6-bis[(4-methylphenyl)amino)-1,3,5-triazine-2-carboxylate (**43b**) in DMSO. The images were recorded either in air or under vacuum (10^{-6} Torr). Three-dimensional perspectives are provided for some of the images.

Annexe 4 :

Information supplémentaire de l'article 4

Submitted to *J. Am. Chem. Soc.*
Version of April 27, 2005

Supporting Information

The Dark Side of Crystal Engineering: Creating Glasses from Small Symmetric Molecules that Form Multiple Hydrogen Bonds

Olivier Lebel,[†] Thierry Maris,[†] Marie-Ève Perron,[†] Eric Demers,[†] and James D. Wuest[*,†]

[†]*Département de Chimie, Université de Montréal*
Montréal, Québec H3C 3J7 Canada

Contents

*Author to whom correspondence may be addressed:
[redacted]

Experimental Section

1,5-dimexylbiguanide (**30i**),[1] Methyl 4,6-bis(dimexylamino)-1,3,5-triazine-2-carboxylate (**46k**),[2] Methyl 4,6-bis(phenylamino)-1,3,5-triazine-2-carboxylate (**46a**),[2] Methyl 4,6-bis[(4-methylphenyl)amino]-1,3,5-triazine-2-carboxylate (**46b**),[2] Methyl 4,6-bis[(3-methylphenyl)amino]-1,3,5-triazine-2-carboxylate (**46i**),[2] Methyl 4,6-bis[(2-methylphenyl)amino]-1,3,5-triazine-2-carboxylate (**46h**)[2] and 4,6-dichloro-2-methylamino-1,3,5-triazine[3] were prepared according to literature procedures.

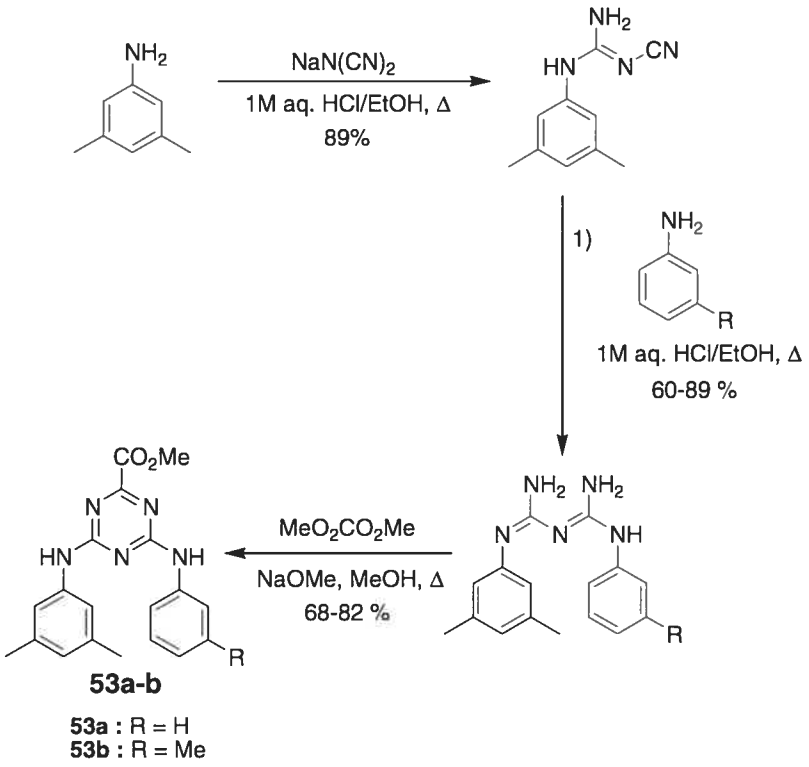

Scheme A4-1.

Methyl 4-(mexylamino)-6-phenylamino-1,3,5-triazine-2-carboxylate (53a)

3,5-dimethylaniline (6.25 mL, 6.06 g, 50.0 mmol) was added to an aqueous HCl solution (50 mL, 1M, 50 mmol) in a round-bottomed flask equipped with a magnetic stirrer. The reaction was stirred for 15 min at room temperature, then sodium dicyanamide (4.45 g, 50.0 mmol) was added and the reaction was refluxed for 2 hours. After cooling down to room temperature, AcOEt was added and the two phases were

separated. The organic phase was recovered, dried over $MgSO_4$, filtered and the solvent was evaporated. The crude product was triturated in hot hexanes to yield 8.35 g mexyldicyandiamide (44.4 mmol, 89%); mp 128 °C; IR (KBr) 3392, 3322, 3215, 3015, 2953, 2919, 2732, 2504, 2439, 2173, 1658, 1602, 1552, 1467, 1382, 1328, 1300, 1269, 1238, 1178, 1102, 1037, 891, 881, 839, 709, 682, 589, 534 cm^{-1}; ^1H NMR (400 MHz, $CDCl_3$) δ 7.92 (s, 1H), 6.88 (s, 1H), 6.87 (s, 2H), 5.91 (s, 2H), 2.29 (s, 6H); ^{13}C NMR (100 MHz, $CDCl_3$) δ 160.7, 140.0, 135.6, 129.0, 122.2, 118.4, 21.4; HRMS (ESI) calcd. for $C_{10}H_{13}N_4$ *m/e*: 189.1135, found: 189.1143; Anal. Calcd. for $C_{10}H_{13}N_4$: C, 63.81; H, 6.43; N, 29.77. Found: C, 63.75; H, 6.65; N, 29.36.

In a round-bottomed flask equipped with a magnetic stirrer was added aniline (0.243 mL, 0.248 g, 2.66 mmol) in a mixture of aqueous HCl (1M, 2.66 mL, 2.66 mmol) and EtOH (10 mL). The mixture was stirred at room temperature for 15 min., then mexyldicyandiamide (0.500 g, 2.66 mmol) was added and the reaction was refluxed overnight. The solvent was evaporated *in vacuo*, then the crude product was recrystallized from hot water and washed with dichloromethane to give 0.755 g 1-mexyl-5-phenylbiguanide hydrochloride (2.38 mmol, 89%); mp 210 °C; IR (KBr) 3428, 3308, 3178, 3120, 2994, 2945, 2912, 2605, 1635, 1615, 1602, 1582, 1523, 1494, 1447, 1377, 1300, 1249, 1178, 1088, 1036, 901, 871, 849, 759, 741, 718, 684, 627, 555, 521, 501, 473 cm^{-1}; ^1H NMR (400 MHz, DMSO-d_6) δ 9.69 (s, 1H), 9.66 (s, 1H), 7.42 (s, 2H), 7.32 (d, ^3J = 2.4 Hz, 2H), 7.31 (s, 4H), 7.10 (m, 1H), 6.88 (s, 2H), 6.75 (s, 1H), 2.20 (s, 6H); ^{13}C NMR (100 MHz, DMSO-d_6) δ 157.3, 156.6, 138.2, 138.1, 137.6, 129.0, 126.3, 124.5, 122.0, 119.9, 21.1; HRMS (ESI) calcd. for $C_{16}H_{20}N_5$ *m/e*: 282.1713, found: 282.1709; Anal. Calcd. for $C_{16}H_{20}ClN_5$: C, 60.47; H, 6.34; N, 22.04. Found: C, 60.06; H, 6.35; N, 21.97.

In a round-bottomed flask was added 1-mexyl-5-phenylbiguanide hydrochloride (0.466 g, 1.47 mmol) in MeOH (30 mL). A methanolic NaOMe solution (25%, 0.44 mL, 1.62 mmol) was added then the reaction mixture was stirred for 15 min. at room temperature. Dimethyl oxalate (0.521 g, 4.41 mmol) was added and the reaction was refluxed overnight. After the reaction mixture was brought to room temperature, H_2O and AcOEt

were added and the two phases were separated. The organic phase was recovered, dried over $MgSO_4$ and the solvent was evaporated. The crude product was then filtered on a short silica pad using 50% AcOEt/hexanes as eluent. Evaporation of the solvent thus yielded 0.421 g **53a** (1.20 mmol, 82%); T_g 51 °C; IR (KBr) 3267, 3186, 3104, 3012, 2949, 2918, 2851, 1749, 1703, 1604, 1577, 1521, 1442, 1350, 1297, 1263, 1217, 1169, 1100, 1042, 1005, 976, 911, 842, 826, 788, 754, 687, 647, 619, 541, 504 cm^{-1}; ^1H NMR (400 MHz, $CDCl_3$) δ 7.60 (d, ^3J = 7.8 Hz, 2H), 7.54 (s, 1H), 7.47 (s, 1H), 7.36 (t, ^3J = 7.9 Hz, 2H), 7.19 (s, 2H), 7.15 (t, ^3J = 7.4 Hz, 1H), 6.80 (s, 1H), 4.02 (s, 3H), 2.31 (s, 6H); ^{13}C NMR (100 MHz, $CDCl_3$) δ 164.6, 164.5, 163.5, 138.6, 137.4, 137.1, 128.9, 126.1, 124.3, 121.2, 118.6, 53.4, 21.3; HRMS (ESI) calcd. for $C_{19}H_{20}N_5O_2$ *m/e*: 350.1612, found: 350.1614; Anal. Calcd. for $C_{19}H_{19}N_5O_2$: C, 65.32; H, 5.48; N, 20.04. Found: C, 64.96; H, 5.51; N, 19.92.

Methyl 4-(mexylamino)-6-[(3-methylphenyl)amino]-1,3,5-triazine-2-carboxylate (53b)

1-mexyl-5-(3-methylphenyl)biguanide hydrochloride was prepared following a similar procedure as 1-mexyl-5-phenylbiguanide hydrochloride. Reaction of 0.569 mL 3-methylaniline (0.569 g, 5.31 mmol) with 1.00 g mexyldicyandiamide (5.31 mmol) yielded 1.06 g 1-mexyl-5-(3-methylphenyl)biguanide hydrochloride (3.20 mmol, 60%); mp 212 °C; IR (KBr) 3308, 3189, 3131, 3005, 2917, 1633, 1602, 1519, 1489, 1454, 1376, 1319, 1260, 1182, 1092, 842, 775, 719, 682, 501 cm^{-1}; ^1H NMR (400 MHz, DMSO-d_6) δ 9.67 (s, 1H), 9.65 (s, 1H), 7.38 (s, 2H), 7.34 (s, 2H), 7.20 (t, ^3J = 8.0 Hz, 1H), 7.10 (m, 2H), 6.92 (d, ^3J = 7.4 Hz, 2H), 6.89 (s, 2H), 6.75 (s, 1H), 2.25 (s, 3H), 2.20 (s, 6H); ^{13}C NMR (100 MHz, DMSO-d_6) δ 156.6, 156.3, 137.7, 137.6, 137.5, 137.4, 128.2, 125.5, 124.5, 121.9, 119.2, 118.5, 20.7, 20.6; HRMS (ESI) calcd. for $C_{17}H_{22}N_5$ *m/e*: 296.1870, found: 296.1875; Anal. Calcd. for $C_{17}H_{22}ClN_5$: C, 61.53; H, 6.68; N, 21.10. Found: C, 61.65; H, 6.94; N, 21.30.

Compound **53b** was prepared from 1-mexyl-5-(3-methylphenyl)biguanide hydrochloride using the same procedure as for **53a**. Yield : 68 %; T_g 38 °C; IR (KBr) 3266, 3181, 3104, 3013, 2950, 2918, 2851, 1749, 1702, 1583, 1525, 1489, 1428, 1345, 1300, 1256,

1220, 1164, 1104, 1044, 1000, 976, 893, 842, 827, 787, 728, 685, 648, 620, 540 cm^{-1}; ^1H NMR (400 MHz, $CDCl_3$) δ 7.62 (s, 1H), 7.57 (s, 1H), 7.52 (d, ^3J = 8.0 Hz, 1H), 7.24 (t, ^3J = 8.0 Hz, 1H), 7.17 (br s, 3H), 6.96 (d, ^3J = 8.0 Hz, 1H), 6.79 (s, 1H), 3.97 (s, 3H), 2.32 (s, 3H), 2.29 (s, 6H); ^{13}C NMR (125 MHz, $CDCl_3$, 283 K) δ 164.6, 164.5, 163.7, 163.3, 138.9, 138.6, 137.5, 137.3, 128.8, 126.2, 125.3, 121.9, 118.9, 118.7, 53.5, 21.5, 21.5; HRMS (ESI) calcd. for $C_{20}H_{22}N_5O_2$ *m/e*: 364.1768, found: 364.1779; Anal. Calcd. for $C_{20}H_{21}N_5O_2$: C, 66.10; H, 5.82; N, 19.27. Found, C, 65.86; H, 5.94; N, 19.00.

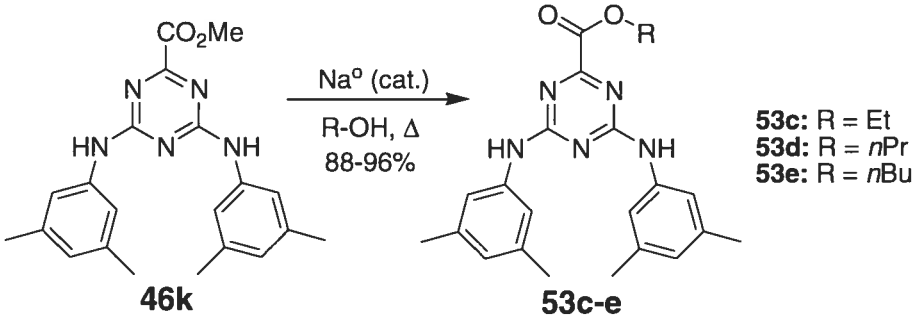

Scheme A4-2.

Ethyl 4,6-bis(mexylamino)-1,3,5-triazine-2-carboxylate (53c)

Ethanolic NaOEt was prepared by dissolving a small chunk of sodium in EtOH (30 mL) in a round-bottomed flask at room temperature. Compound **46k** (0.5 g, 1.325 mmol) was added, and the reaction was refluxed overnight. The solvent was concentrated, then H_2O and AcOEt were added. The two phases were separated, then the organic phase was recovered, dried over $MgSO_4$ and filtered. The solvent was evaporated and the remaining product was thoroughly dried on a vacuum pump for at least 2 days. The resulting glassy solid was of high enough purity to be used without further purification, yielding 0.477 g of compound **53c** (1.22 mmol, 92 %). T_g 62 °C; IR (KBr) 3271, 3186, 3102, 2977, 2917, 2857, 1746, 1613, 1586, 1524, 1432, 1368, 1336, 1301, 1260, 1213, 1162, 1104, 1053, 1021, 992, 965, 887, 865, 841, 791, 757, 684, 645, 539 cm^{-1}; ^1H NMR (400 MHz, $CDCl_3$) δ 7.47 (s, 2H), 7.14 (s, 4H), 6.79 (s, 2H), 4.49 (q, J = 7.1 Hz, 2H), 2.27 (s, 12H), 1.45 (t, J = 7.1 Hz, 3H); ^{13}C NMR (100 MHz, $CDCl_3$) δ 164.6, 163.2, 138.5, 137.3, 126.1, 119.0, 62.7, 21.2, 14.0; HRMS (ESI) calcd. for $C_{22}H_{26}N_5O_2$ *m/e*: 392.2081, found: 392.2085; Anal. Calcd. for $C_{22}H_{25}N_5O_2$: C, 67.50; H, 6.44; N, 17.89. Found, C, 67.26; H, 6.58; N, 18.12.

Compounds **53d** and **53e** were synthesized by the same procedure with the corresponding alcohols as solvents :

***n*-Propyl 4,6-bis(mexylamino)-1,3,5-triazine-2-carboxylate (53d)**

Yield : 96%; T_g 58 °C; IR (KBr) 3269, 3186, 3107, 3005, 2966, 2918, 1746, 1613, 1587, 1558, 1524, 1432, 1385, 1335, 1260, 1211, 1169, 1104, 1055, 996, 920, 886, 841, 791, 755, 684, 645, 539 cm^{-1}; ^1H NMR (400 MHz, $CDCl_3$) δ 7.47 (s, 2H), 7.14 (s, 4H), 6.78 (s, 2H), 4.36 (q, ^3J = 6.9 Hz, 2H), 2.27 (s, 12H), 1.84 (sex, ^3J = 7.2 Hz, 2H), 1.02 (br s, 3H); ^{13}C NMR (125 MHz, $CDCl_3$, 283 K) δ 164.7, 163.8, 163.5, 138.5, 137.5, 126.2, 119.3, 68.3, 21.8, 21.4, 10.2; HRMS (ESI) calcd. for $C_{23}H_{28}N_5O_2$ *m/e*: 406.2238, found: 406.2241; Anal. Calcd. for $C_{23}H_{27}N_5O_2$: C, 68.13; H, 6.71; N, 17.27. Found: C, 68.30; H, 6.91; N, 17.48.

***n*-Butyl 4,6-bis(mexylamino)-1,3,5-triazine-2-carboxylate (53e)**

Yield : 88%; T_g 54 °C; IR (KBr) 3252, 3097, 3012, 2959, 2916, 2871, 1753, 1737, 1592, 1574, 1528, 1454, 1433, 1383, 1341, 1301, 1262, 1211, 1163, 1104, 1055, 995, 969, 917, 896, 861, 839, 794, 764, 726, 676, 654, 642, 544 cm^{-1}; ^1H NMR (400 MHz, $CDCl_3$) δ 7.40 (s, 2H), 7.14 (s, 4H), 6.78 (s, 2H), 4.43 (q, ^3J = 6.8 Hz, 2H), 2.27 (s, 12H), 1.81 (quint, ^3J = 6.9 Hz, 2H), 1.47 (br s, 2H), 0.98 (t, ^3J = 7.3 Hz, 3H); ^{13}C NMR (125 MHz, $CDCl_3$, 283 K) δ 164.7, 163.7, 163.6, 138.7, 137.4, 126.3, 119.1, 66.8, 30.5, 21.5, 19.1, 13.9; HRMS (ESI) calcd. for $C_{24}H_{30}N_5O_2$ *m/e*: 420.2394, found: 420.2388; Anal. Calcd. for $C_{24}H_{29}N_5O_2$: C, 68.71; H, 6.97; N, 16.69. Found: C, 68.59; H, 7.08; N, 16.72.

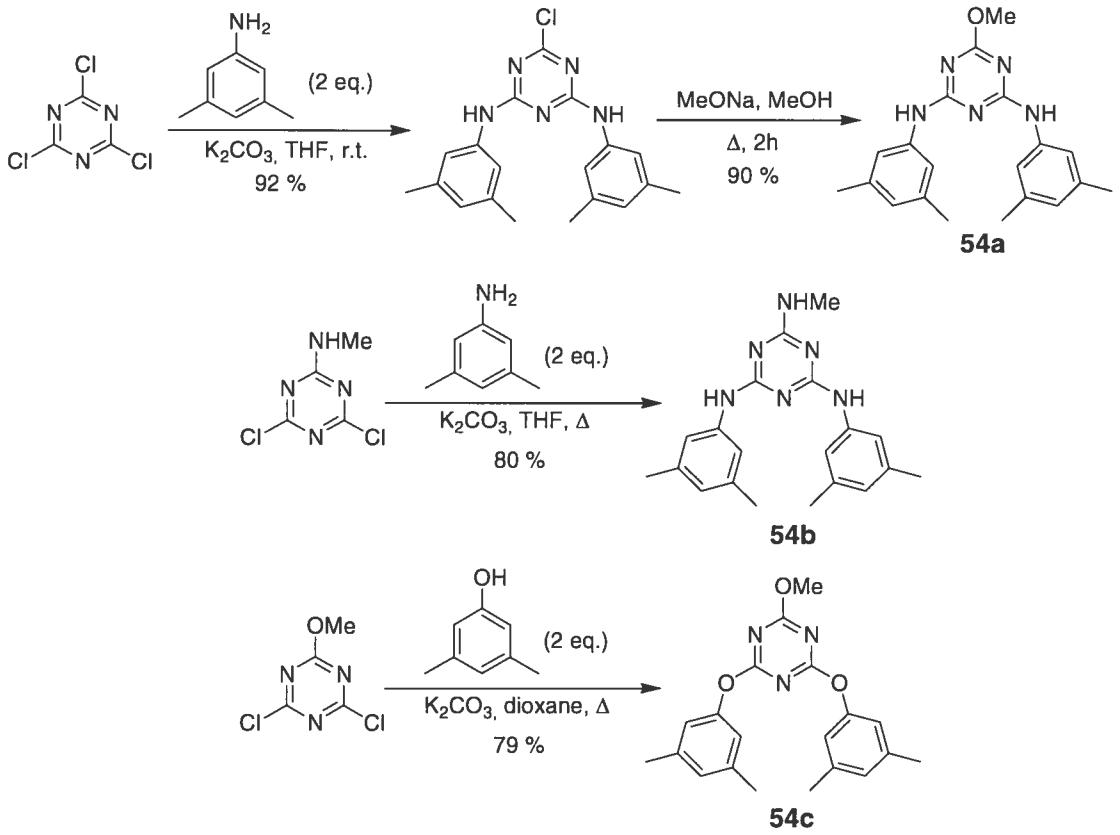

Scheme A4-3.

2-methoxy-4,6-bis(mexylamino)-1,3,5-triazine (54a)

To a solution of cyanuric chloride (5.00 g, 27.11 mmol) in acetone (100 mL) in a round-bottomed flask at 0 °C was added slowly 3,5-dimethylaniline (6.77 mL, 6.57 g, 54.23 mmol). K_2CO_3 (3.75 g, 27.11 mmol) was added, and the reaction was stirred 2 h at room temperature. H_2O was added, and the resulting precipitate was filtered off and washed thoroughly with H_2O and hexanes to yield 8.80 g 2-chloro-4,6-bis(mexylamino)-1,3,5-triazine (24.87 mmol, 92 %) which was of enough purity to be used without further purification; mp 186 °C; IR (KBr) 3259, 3185, 3139, 3096, 3015, 2955, 2916, 2853, 2474, 2343, 1710, 1622, 1604, 1592, 1577, 1525, 1441, 1386, 1305, 1275, 1248, 1230, 1167, 1047, 988, 957, 943, 885, 866, 842, 802, 755, 728, 681, 656, 641, 565, 543 cm^{-1}; ^1H NMR (400 MHz, $CDCl_3$) δ 7.63 (s, 2H), 7.12 (s, 4H), 6.79 (s, 2H), 2.27 (s, 12H); ^{13}C NMR (100 MHz, $CDCl_3$) δ 168.7 (br), 164.2, 138.6, 136.9, 126.4, 119.2, 21.3; HRMS (ESI) calcd. for $C_{19}H_{21}ClN_5$ *m/e*: 354.1480, found: 354.1487; Anal. Calcd. for $C_{19}H_{20}ClN_5$: C, 64.49; H, 5.70; N, 19.79. Found: C, 64.82; H, 5.72; N, 20.07.

A commercial solution of sodium methoxide (25 wt%, 0.300 mL, 1.1 mmol) was added in methanol (10 mL) in a round-bottomed flask. 2-chloro-4,6-bis(mexylamino)-1,3,5-triazine (0.354 g, 1.0 mmol) was added and the reaction was refluxed for 2 hours. The solvent was concentrated *in vacuo*, then H_2O and ethyl acetate were added. The two phases were separated, the organic phase was recovered, dried over $MgSO_4$, filtered and the solvent was evaporated to yield 0.316 g 5**4a** (0.90 mmol, 90 %); T_g 54 °C; IR (KBr) 3377, 3273, 3132, 3010, 2950, 2917, 2851, 1615, 1591, 1564, 1517, 1456, 1384, 1347, 1184, 1118, 1100, 1035, 993, 928, 884, 840, 811, 685, 644, 609, 539 cm^{-1}; ^1H NMR (400 MHz, C_6D_6) δ 7.00 (s, 4H), 6.82 (s, 2H), 6.58 (s, 2H), 3.71 (s, 3H), 2.13 (s, 12H); ^{13}C NMR (100 MHz, C_6D_6) δ 171.7, 166.2, 139.1, 138.1, 125.4, 119.6, 53.8, 21.5; HRMS (ESI) calcd. for $C_{20}H_{24}N_5O$ *m/e*: 350.1975, found: 350.1976; Anal. Calcd. for $C_{20}H_{23}N_5O$: C, 68.74; H, 6.63; N, 20.04. Found: C, 68.58; H, 6.75; N, 20.02.

2-methylamino-4,6-bis(mexylamino)-1,3,5-triazine (54b)

To a stirred solution of 4,6-dichloro-2-methylamino-1,3,5-triazine[3] (0.456 g, 2.55 mmol) in THF (30 mL) in a round-bottomed flask were added successively 3,5-dimethylaniline (0.637 mL, 0.618 g, 5.10 mmol) and K_2CO_3 (0.352 g, 2.55 mmol) and the reaction was refluxed overnight. After letting the reaction cool down to room temperature, AcOEt and H_2O were added, and the two phases were separated. The organic phase was then extracted with aqueous K_2CO_3 then with brine. The organic phase was then dried over $MgSO_4$ and the solvent was evaporated. The crude product was precipitated from AcOEt/hexanes to remove any unreacted 3,5-dimethylaniline, yielding 0.713 g 5**4b** (2.05 mmol, 80 %); T_g 94 °C; IR (KBr) 3401, 3274, 3148, 3013, 2945, 2916, 1587, 1555, 1515, 1426, 1355, 1318, 1180, 1092, 1034, 908, 882, 838, 808, 732, 686, 640, 538 cm^{-1}; ^1H NMR (400 MHz, $CDCl_3$) δ 7.18 (br s, 4H), 7.01 (s, 2H), 6.69 (s, 2H), 5.19 (s, 1H), 2.98 (d, ^3J = 5.0 Hz, 3H), 2.28 (s, 12H); ^{13}C NMR (100 MHz, $CDCl_3$) δ 166.5, 164.3, 164.1, 138.6, 138.2, 124.8, 124.5, 118.6, 118.1, 27.4, 21.3; HRMS (ESI) calcd. for $C_{20}H_{25}N_6$ *m/e*: 349.2135, found: 349.2137; Anal. Calcd. for $C_{20}H_{24}N_6$: C, 68.94; H, 6.94; N, 24.12. Found, C, 68.62; H, 7.25; N, 24.25.

2-methoxy-4,6-bis(mexyloxy)-1,3,5-triazine (54c)

To a solution of 4,6-dichloro-2-methoxy-1,3,5-triazine (0.500 g, 2.78 mmol) in dioxane (10 mL) were added 3,5-dimethylphenol (0.679 g, 5.56 mmol) and K_2CO_3 (0.768 g, 5.56 mmol) and the reaction was refluxed for 48 h. The solvent was concentrated, then H_2O and ethyl acetate were added. The two phases were separated, the organic phase was dried over $MgSO_4$, filtered and the solvent was evaporated. The crude product was triturated in hot hexanes to yield 0.771 g **54c** (2.19 mmol, 79 %); mp 125 °C; IR (KBr) 3017, 2955, 2919, 2863, 1620, 1598, 1567, 1503, 1470, 1452, 1431, 1360, 1285, 1199, 1153, 1114, 1091, 1036, 998, 949, 929, 901, 893, 868, 848, 813, 703, 683, 656, 634, 616, 543, 522, 508 cm^{-1}; ^1H NMR (400 MHz, C_6D_6) δ 6.73 (s, 4H), 6.58 (s, 2H), 3.55 (s, 3H), 2.00 (s, 12H); ^{13}C NMR (100 MHz, C_6D_6) δ 174.7, 174.3, 152.5, 139.2, 127.6, 119.6, 55.1, 21.1; HRMS (ESI) calcd. for $C_{20}H_{22}N_3O_3$ *m/e*: 352.1656, found: 352.1651; Anal. Calcd. for $C_{20}H_{21}N_3O_3$: C, 68.36; H, 6.02; N, 11.96. Found: C, 68.47; H, 5.83; N, 11.99.

Measurement of T_g by Modulated Differential Scanning Calorimetry (DSC). Measurements were made with a TA Instruments Q1000 calorimeter, using a 60 sec period and heating/cooling rates of 5 °C/min from 20 °C to 200 °C. Three cycles of heating and cooling were recorded.

Crystal Structure of Compound 46k. Crystals of **46k** suitable for X-ray diffractometry were obtained by slow evaporation of a saturated solution of **46k** in $CHCl_3$. Data collection was performed on a Nonius Kappa CCD diffractometer at the university of Toronto. Compound **46k** crystallizes in the monoclinic space group C2/c with cell lattice parameters a = 24.739(1) Å, b = 13.3590(6) Å, c = 19.2390(5) Å and β = 114.7900(19)°. Refinement on F^2 of 3656 observed reflections over a total of 6596 unique reflections led to residual factors R_1 = 0.0701, wR_2 = 0.1973 and Goodness of Fit of 1.035.

FTIR. KBr pellets of compound **46k** were prepared from the amorphous solid generated by heating, along with single-crystals grown from $CHCl_3$ solution. A CH_2Cl_2 solution of

46k was also prepared and the spectrum was recorded using NaCl slides. The infrared spectra were then recorded on a Perkin-Elmer Spectrum One spectrometer.

References

(1) Lebel, O.; Maris, T.; Duval, H.; Wuest, J.D. *Can. J. Chem.* **2005**, *83*, 615.

(2) Lebel, O.; Perron, M.-È.; Maris, T.; Zalzal, S.F.; Nanci, A.; Wuest, J.D. *Chem. Mater.* In press.

(3) Koopman, H.; Daams, J. *Recl. Trav. Chim. Pays-Bas Belgique* **1958**, *77*, 235.

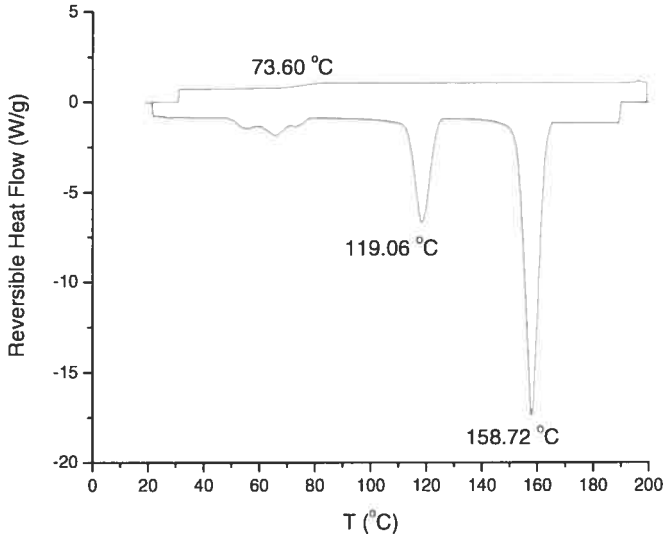

a

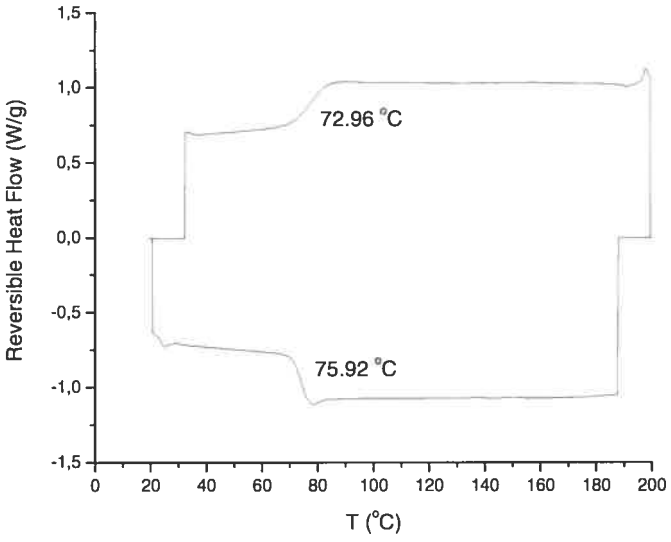

b

Figure A4-1. Representative thermograms, obtained by modulated differential scanning calorimetry (mDSC) of single crystals of compound **46k** crystallized from $CHCl_3$. a) First heating/cooling cycle. b) Second heating/cooling cycle Glass transition temperatures and melting points are indicated in each case. For the sake of simplicity, only the reversible heat flow signal is shown.

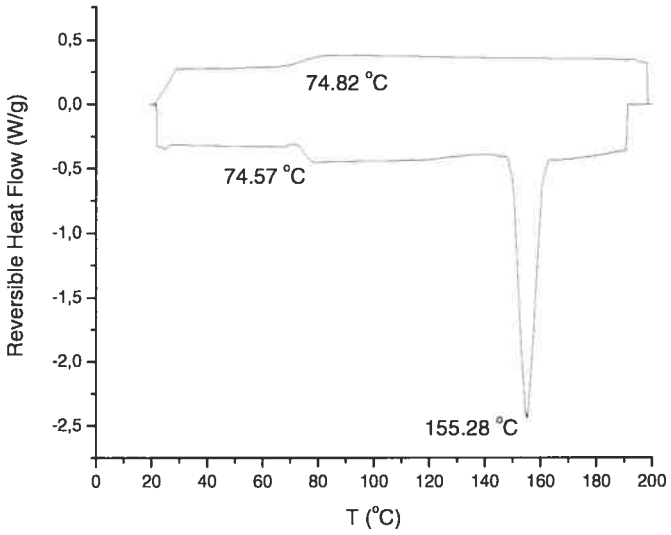

a

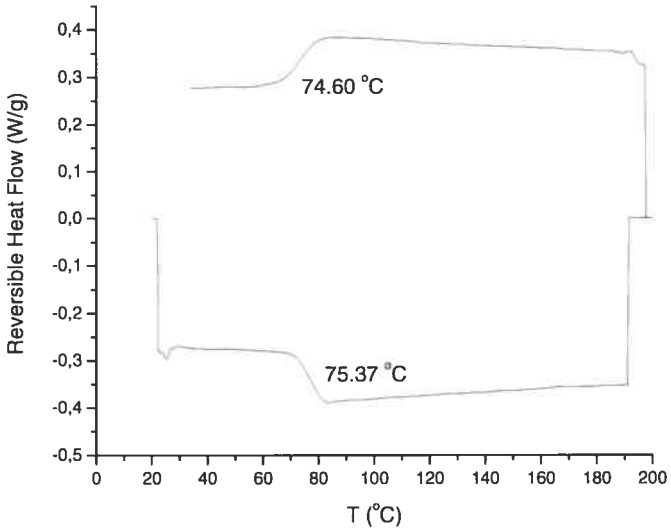

b

Figure S2. Representative thermograms, obtained by modulated differential scanning calorimetry (mDSC) of amorphous **46k**. a) First heating/cooling cycle. b) Second heating/cooling cycle Glass transition temperatures and melting points are indicated in each case. For the sake of simplicity, only the reversible heat flow signal is shown.

Université de Montréal

CRYSTAL AND MOLECULAR STRUCTURE OF

C22 H26 Cl3 N5 O3 COMPOUND (JW1027)

Equipe WUEST

Département de chimie, Université de Montréal,

C.P. 6128, Succ. Centre-Ville, Montréal, Québec, H3C 3J7 (Canada)

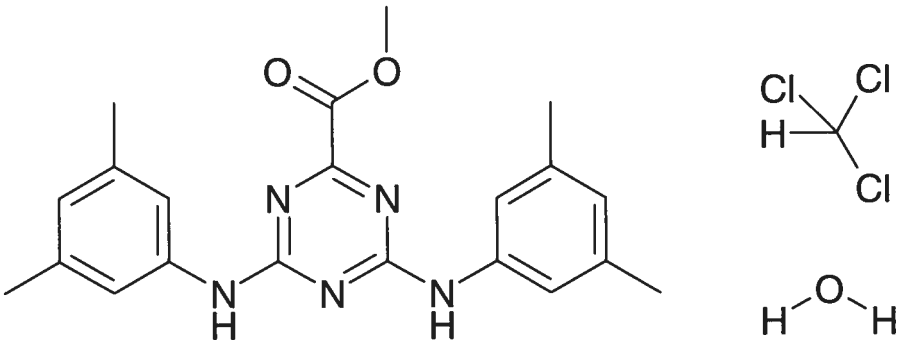

Structure solved and refined in the laboratory of X-ray diffraction Université de Montréal by Dr. Thierry Maris.

Table A4-1. Crystal data and structure refinement for C22 H26 Cl3 N5 O3.

Identification code	JW1027
Empirical formula	C22 H26 Cl3 N5 O3
Formula weight	514.83
Temperature	225(2)K
Wavelength	0.71073 Å
Crystal system	Monoclinic
Space group	C2/c
Unit cell dimensions	a = 24.739(1) Å α = 90° b = 13.3590(6) Å β = 114.7900(19)° c = 19.2390(5) Å γ = 90°
Volume	5772.4(4)Å^3
Z	8
Density (calculated)	1.185 g/cm^3
Absorption coefficient	0.346 mm^{-1}
F(000)	2144
Crystal size	0.50 x 0.40 x 0.25 mm
Theta range for data collection	2.61 to 27.55°
Index ranges	$-32 \leq h \leq 32$, $-17 \leq k \leq 17$, $-22 \leq \ell \leq 24$
Reflections collected	16419
Independent reflections	6596 [R_{int} = 0.062]
Absorption correction	Semi-empirical from equivalents
Max. and min. transmission	0.9930 and 0.7260
Refinement method	Full-matrix least-squares on F^2
Data / restraints / parameters	6596 / 0 / 295
Goodness-of-fit on F^2	1.035
Final R indices [I>2sigma(I)]	R_1 = 0.0701, wR_2 = 0.1973

R indices (all data)	R_1 = 0.1247, wR_2 = 0.2238
Extinction coefficient	0.0019(5)
Largest diff. peak and hole	0.444 and -0.454 e/Å^3

Table A4-2. Atomic coordinates (x 10^4) and equivalent isotropic displacement parameters (Å^2 x 10^3) for C22 H26 Cl3 N5 O3.

U_{eq} is defined as one third of the trace of the orthogonalized Uij tensor.

	x	y	z	U_{eq}
C(1)	3297(1)	1240(3)	2721(2)	60(1)
C(2)	3328(1)	2109(2)	1671(1)	42(1)
C(3)	3705(1)	2368(2)	1247(1)	36(1)
C(4)	4595(1)	2696(2)	1246(1)	35(1)
C(5)	3760(1)	2765(2)	151(1)	38(1)
C(6)	3712(1)	3082(2)	-1151(1)	41(1)
C(7)	4221(1)	3653(2)	-990(1)	44(1)
C(8)	4423(1)	3821(2)	-1551(2)	50(1)
C(9)	4101(2)	3416(3)	-2275(2)	64(1)
C(10)	3587(2)	2871(3)	-2451(2)	65(1)
C(11)	3400(1)	2693(2)	-1872(1)	51(1)
C(12)	4979(1)	4433(3)	-1371(2)	64(1)
C(13)	3230(2)	2436(4)	-3246(2)	106(2)
C(14)	5607(1)	3006(2)	1333(1)	36(1)
C(15)	6077(1)	3628(2)	1771(1)	40(1)
C(16)	6519(1)	3853(2)	1530(2)	45(1)
C(17)	6483(1)	3445(2)	849(2)	49(1)
C(18)	6019(1)	2819(2)	407(1)	49(1)
C(19)	5576(1)	2609(2)	654(1)	43(1)
C(20)	7024(1)	4546(3)	1997(2)	63(1)
C(21)	5994(2)	2361(3)	-318(2)	71(1)
N(1)	4287(1)	2455(2)	1666(1)	37(1)
N(2)	3406(1)	2507(2)	506(1)	42(1)
N(3)	4347(1)	2871(2)	491(1)	38(1)
N(4)	5185(1)	2766(2)	1631(1)	38(1)
N(5)	3469(1)	2905(2)	-613(1)	45(1)
O(1)	3619(1)	1530(2)	2270(1)	46(1)
O(2)	2828(1)	2406(2)	1477(1)	62(1)
C(22)	2502(2)	4466(3)	363(2)	66(1)
Cl(1)	2217(1)	5002(1)	-550(1)	98(1)
Cl(2)	2010(1)	4707(1)	786(1)	106(1)
Cl(3)	3215(1)	4925(1)	933(1)	121(1)

Table A4-3. Hydrogen coordinates (x 10^4) and isotropic displacement parameters ($Å^2$ x 10^3) for C22 H26 Cl3 N5 O3.

	x	y	z	U_{eq}
H(1A)	3246	1819	2991	89
H(1B)	3520	730	3088	89
H(1C)	2910	976	2385	89
H(7)	4428	3926	-498	53
H(9)	4239	3518	-2656	77
H(11)	3057	2305	-1975	61
H(12A)	5281	4017	-1423	96
H(12B)	5126	4683	-851	96
H(12C)	4887	4992	-1724	96
H(13A)	2838	2242	-3295	159
H(13B)	3435	1854	-3319	159
H(13C)	3191	2936	-3630	159
H(15)	6095	3897	2232	48
H(17)	6781	3597	683	59
H(19)	5254	2195	357	51
H(20A)	7315	4183	2428	95
H(20B)	6869	5102	2183	95
H(20C)	7212	4798	1679	95
H(21A)	6235	1758	-197	106
H(21B)	6147	2834	-575	106
H(21C)	5585	2194	-652	106
H(4)	5328	2650	2121	46
H(5)	3083	2884	-799	54
H(22)	2528	3733	310	79

Table A4-4. Anisotropic parameters ($Å^2$ x 10^3) for C22 H26 Cl3 N5 O3.

The anisotropic displacement factor exponent takes the form:

$$-2\pi^2 [h^2 a^{*2} U_{11} + ... + 2 h k a^* b^* U_{12}]$$

	U11	U22	U33	U23	U13	U12
C(1)	54(2)	82(2)	49(2)	1(1)	28(1)	-26(2)
C(2)	26(1)	65(2)	30(1)	-4(1)	8(1)	-11(1)
C(3)	25(1)	49(2)	32(1)	-3(1)	10(1)	-5(1)
C(4)	26(1)	44(2)	34(1)	-1(1)	12(1)	-2(1)
C(5)	25(1)	55(2)	32(1)	1(1)	10(1)	-3(1)
C(6)	32(1)	54(2)	37(1)	9(1)	16(1)	3(1)
C(7)	36(1)	54(2)	40(1)	5(1)	14(1)	0(1)
C(8)	41(2)	56(2)	56(2)	10(1)	25(1)	2(1)
C(9)	76(2)	74(2)	62(2)	0(2)	49(2)	-13(2)
C(10)	80(2)	73(2)	53(2)	-7(2)	39(2)	-17(2)
C(11)	52(2)	67(2)	39(1)	-2(1)	24(1)	-13(1)
C(12)	52(2)	66(2)	84(2)	17(2)	38(2)	-1(2)
C(13)	132(4)	150(4)	51(2)	-32(2)	54(2)	-62(3)
C(14)	25(1)	47(2)	36(1)	6(1)	12(1)	2(1)
C(15)	26(1)	51(2)	40(1)	1(1)	11(1)	1(1)
C(16)	28(1)	50(2)	56(2)	5(1)	18(1)	-1(1)
C(17)	35(1)	63(2)	56(2)	10(1)	25(1)	1(1)
C(18)	39(1)	65(2)	47(1)	2(1)	23(1)	6(1)
C(19)	29(1)	56(2)	42(1)	-3(1)	13(1)	-1(1)
C(20)	38(2)	69(2)	83(2)	-9(2)	25(2)	-17(2)
C(21)	73(2)	92(3)	63(2)	-10(2)	43(2)	6(2)
N(1)	23(1)	53(1)	34(1)	1(1)	10(1)	-3(1)
N(2)	23(1)	69(2)	32(1)	2(1)	10(1)	-4(1)
N(3)	23(1)	57(1)	31(1)	1(1)	9(1)	-2(1)
N(4)	22(1)	62(2)	29(1)	3(1)	9(1)	-2(1)
N(5)	21(1)	79(2)	32(1)	7(1)	8(1)	-4(1)
O(1)	37(1)	61(1)	43(1)	3(1)	19(1)	-9(1)
O(2)	27(1)	114(2)	45(1)	10(1)	15(1)	-2(1)
C(22)	64(2)	67(2)	60(2)	3(2)	19(2)	-4(2)
Cl(1)	119(1)	107(1)	69(1)	18(1)	40(1)	-17(1)
Cl(2)	126(1)	119(1)	94(1)	11(1)	67(1)	26(1)
Cl(3)	83(1)	91(1)	140(1)	-9(1)	-1(1)	-20(1)

Table A4-5. Bond lengths [Å] and angles [°] for C22 H26 Cl3 N5 O3

C(1)-O(1)	1.456(3)	N(4)-C(4)-N(3)	119.2(2)
C(2)-O(2)	1.200(3)	N(4)-C(4)-N(1)	116.10(19)
C(2)-O(1)	1.323(3)	N(3)-C(4)-N(1)	124.7(2)
C(2)-C(3)	1.515(3)	N(3)-C(5)-N(5)	119.7(2)
C(3)-N(2)	1.315(3)	N(3)-C(5)-N(2)	125.48(19)
C(3)-N(1)	1.329(3)	N(5)-C(5)-N(2)	114.8(2)
C(4)-N(4)	1.335(3)	C(11)-C(6)-C(7)	120.4(2)
C(4)-N(3)	1.338(3)	C(11)-C(6)-N(5)	116.3(2)
C(4)-N(1)	1.362(3)	C(7)-C(6)-N(5)	123.3(2)
C(5)-N(3)	1.327(3)	C(8)-C(7)-C(6)	120.2(2)
C(5)-N(5)	1.350(3)	C(7)-C(8)-C(9)	118.4(3)
C(5)-N(2)	1.363(3)	C(7)-C(8)-C(12)	120.1(3)
C(6)-C(11)	1.375(4)	C(9)-C(8)-C(12)	121.5(3)
C(6)-C(7)	1.390(4)	C(10)-C(9)-C(8)	122.2(3)
C(6)-N(5)	1.418(3)	C(9)-C(10)-C(11)	118.3(3)
C(7)-C(8)	1.385(4)	C(9)-C(10)-C(13)	122.2(3)
C(8)-C(9)	1.391(4)	C(11)-C(10)-C(13)	119.4(3)
C(8)-C(12)	1.510(4)	C(6)-C(11)-C(10)	120.5(3)
C(9)-C(10)	1.381(5)	C(19)-C(14)-C(15)	120.3(2)
C(10)-C(11)	1.394(4)	C(19)-C(14)-N(4)	122.3(2)
C(10)-C(13)	1.524(4)	C(15)-C(14)-N(4)	117.3(2)
C(14)-C(19)	1.382(3)	C(16)-C(15)-C(14)	120.2(2)
C(14)-C(15)	1.389(3)	C(17)-C(16)-C(15)	118.9(2)
C(14)-N(4)	1.422(3)	C(17)-C(16)-C(20)	120.8(2)
C(15)-C(16)	1.388(3)	C(15)-C(16)-C(20)	120.3(2)
C(16)-C(17)	1.387(4)	C(18)-C(17)-C(16)	121.7(2)
C(16)-C(20)	1.512(4)	C(17)-C(18)-C(19)	118.7(2)
C(17)-C(18)	1.385(4)	C(17)-C(18)-C(21)	121.1(3)
C(18)-C(19)	1.395(4)	C(19)-C(18)-C(21)	120.2(3)
C(18)-C(21)	1.501(4)	C(14)-C(19)-C(18)	120.3(2)
C(22)-Cl(1)	1.748(3)	C(3)-N(1)-C(4)	113.20(18)
C(22)-Cl(3)	1.752(3)	C(3)-N(2)-C(5)	113.02(19)
C(22)-Cl(2)	1.754(4)	C(5)-N(3)-C(4)	115.24(19)
		C(4)-N(4)-C(14)	127.43(18)
O(2)-C(2)-O(1)	125.4(2)	C(5)-N(5)-C(6)	128.5(2)
O(2)-C(2)-C(3)	123.0(2)	C(2)-O(1)-C(1)	116.1(2)
O(1)-C(2)-C(3)	111.7(2)	CL1-C(22)-CL3	111.2(2)
N(2)-C(3)-N(1)	128.3(2)	CL1-C(22)-CL2	109.0(2)
N(2)-C(3)-C(2)	114.9(2)	CL3-C(22)-CL2	111.00(19)
N(1)-C(3)-C(2)	116.67(19)		

Table A4-6. Torsion angles [°] for C22 H26 Cl3 N5 O3.

O(2)-C(2)-C(3)-N(2)	-31.0(4)	N(4)-C(14)-C(19)-C(18)	-176.1(2)
O(1)-C(2)-C(3)-N(2)	149.4(2)	C(17)-C(18)-C(19)-C(14)	-1.1(4)
O(2)-C(2)-C(3)-N(1)	147.1(3)	C(21)-C(18)-C(19)-C(14)	178.1(3)
O(1)-C(2)-C(3)-N(1)	-32.5(3)	N(2)-C(3)-N(1)-C(4)	-1.7(4)
C(11)-C(6)-C(7)-C(8)	-1.1(4)	C(2)-C(3)-N(1)-C(4)	-179.5(2)
N(5)-C(6)-C(7)-C(8)	-178.0(2)	N(4)-C(4)-N(1)-C(3)	-178.1(2)
C(6)-C(7)-C(8)-C(9)	0.8(4)	N(3)-C(4)-N(1)-C(3)	2.5(4)
C(6)-C(7)-C(8)-C(12)	-179.4(3)	N(1)-C(3)-N(2)-C(5)	0.5(4)
C(7)-C(8)-C(9)-C(10)	1.0(5)	C(2)-C(3)-N(2)-C(5)	178.3(2)
C(12)-C(8)-C(9)-C(10)	-178.8(3)	N(3)-C(5)-N(2)-C(3)	0.3(4)
C(8)-C(9)-C(10)-C(11)	-2.4(6)	N(5)-C(5)-N(2)-C(3)	179.4(2)
C(8)-C(9)-C(10)-C(13)	179.4(4)	N(5)-C(5)-N(3)-C(4)	-178.6(2)
C(7)-C(6)-C(11)-C(10)	-0.4(5)	N(2)-C(5)-N(3)-C(4)	0.4(4)
N(5)-C(6)-C(11)-C(10)	176.8(3)	N(4)-C(4)-N(3)-C(5)	178.7(2)
C(9)-C(10)-C(11)-C(6)	2.1(5)	N(1)-C(4)-N(3)-C(5)	-1.9(4)
C(13)-C(10)-C(11)-C(6)	-179.7(4)	N(3)-C(4)-N(4)-C(14)	-0.4(4)
C(19)-C(14)-C(15)-C(16)	-0.1(4)	N(1)-C(4)-N(4)-C(14)	-179.9(2)
N(4)-C(14)-C(15)-C(16)	176.9(2)	C(19)-C(14)-N(4)-C(4)	-42.9(4)
C(14)-C(15)-C(16)-C(17)	-0.1(4)	C(15)-C(14)-N(4)-C(4)	140.1(3)
C(14)-C(15)-C(16)-C(20)	178.7(3)	N(3)-C(5)-N(5)-C(6)	5.7(4)
C(15)-C(16)-C(17)-C(18)	-0.2(4)	N(2)-C(5)-N(5)-C(6)	-173.4(3)
C(20)-C(16)-C(17)-C(18)	-179.1(3)	C(11)-C(6)-N(5)-C(5)	146.7(3)
C(16)-C(17)-C(18)-C(19)	0.8(4)	C(7)-C(6)-N(5)-C(5)	-36.2(4)
C(16)-C(17)-C(18)-C(21)	-178.4(3)	O(2)-C(2)-O(1)-C(1)	0.1(4)
C(15)-C(14)-C(19)-C(18)	0.8(4)	C(3)-C(2)-O(1)-C(1)	179.7(2)

Table A4-7. Bond lengths [Å] and angles [°] related to the hydrogen bonding for C22 H26 Cl3 N5 O3.

D-H	..A	d(D-H)	d(H..A)	d(D..A)	<DHA
N(4)-H(4)	N(1)#1	0.87	2.13	3.003(3)	176.3
N(5)-H(5)	O(2)#2	0.87	2.11	2.960(3)	164.5

Symmetry transformations used to generate equivalent atoms:

#1 -x+1,y,-z+1/2 #2 -x+1/2,-y+1/2,-z

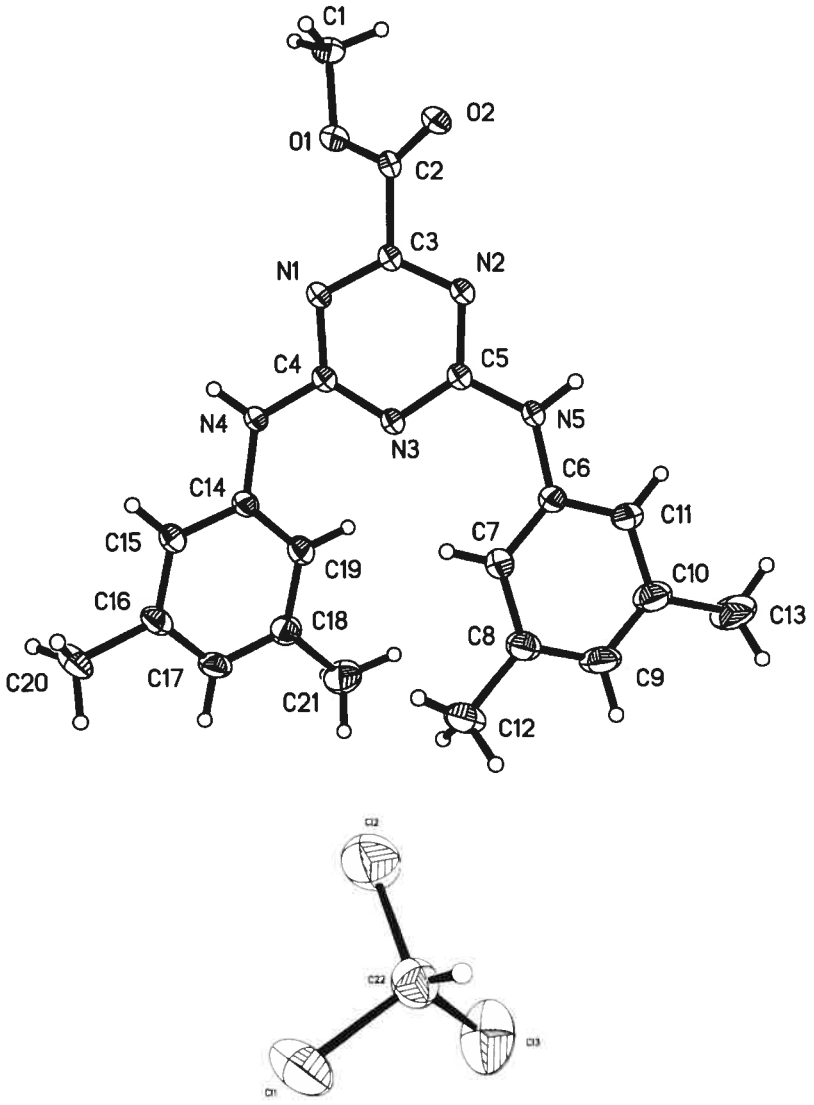

ORTEP view of the C22 H26 Cl3 N5 O3 compound with the numbering scheme adopted. Ellipsoids drawn at 30% probability level. Hydrogen atoms are represented by sphere of arbitrary size.

REFERENCES

Blessing R. H. (1995). Acta Cryst A51 33-37.

Flack, H.D. (1983). Acta Cryst. A39, 876-881.

Flack, H.D. and Schwarzenbach, D. (1988). Acta Cryst. A44, 499-506.

Nonius (1997). Kappa CCD Server software Windows 3.11 Version. Nonius BV, Delft, The Netherlands.

Otwinovski Z. & Minor W. (1997). Methods in Enzymology, Vol. 76, Macromolecular Crystallography, Part A, edited by C. W. carter Jr & R. M. Sweet, pp 307-326. New York: Academic Press.

Sheldrick, G.M. (1996). SADABS, Bruker Area Detector Absorption Corrections.
Bruker AXS Inc., Madison, WI 53719-1173.

Sheldrick, G.M. (1997). SHELXS97, Program for the Solution of Crystal Structures. Univ. of Gottingen, Germany.

Sheldrick, G.M. (1997). SHELXL97, Program for the Refinement of Crystal Structures. Univ. of Gottingen, Germany.

SHELXTL (1997) Release 5.10; The Complete Software Package for Single Crystal Structure Determination. Bruker AXS Inc., Madison, WI 53719-1173.

Spek, A.L. (2004). PLATON, Molecular Geometry Program, 2000 version. University of Utrecht, Utrecht, Holland.

XPREP (1997) Release 5.10; X-ray data Preparation and Reciprocal space Exploration Program. Bruker AXS Inc., Madison, WI 53719-11

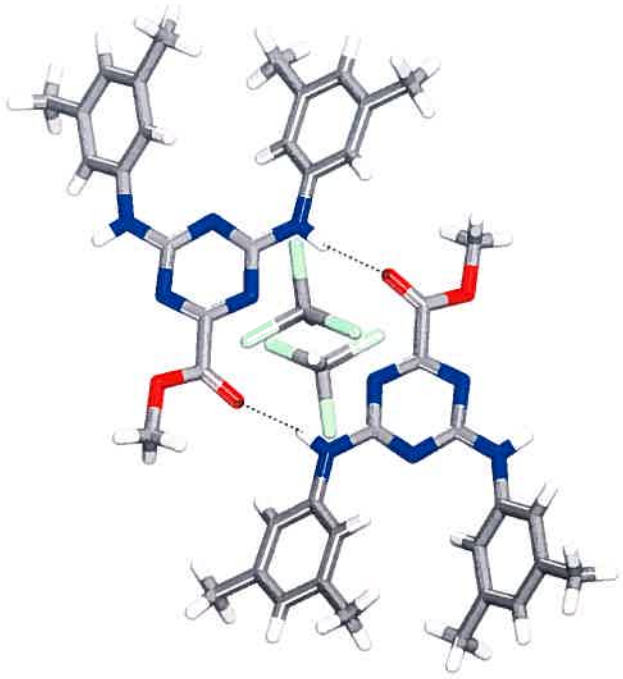

Figure A4-3. Detail of the interactions with chloroform molecules in the crystal structure of **46k**. The hydrogen atoms from two chloroform molecules point inward of a small cavity between two hydrogen-bonded molecules 46k. No notable interaction is present between **46k** molecules and chloroform molecules (the shortest N-H distance is 2.937 Å). Hydrogen bonds are represented as dotted lines. Carbon atoms are shown in gray, hydrogen atoms in white, chlorine atoms in light green, nitrogen atoms in blue and oxygen atoms in red.

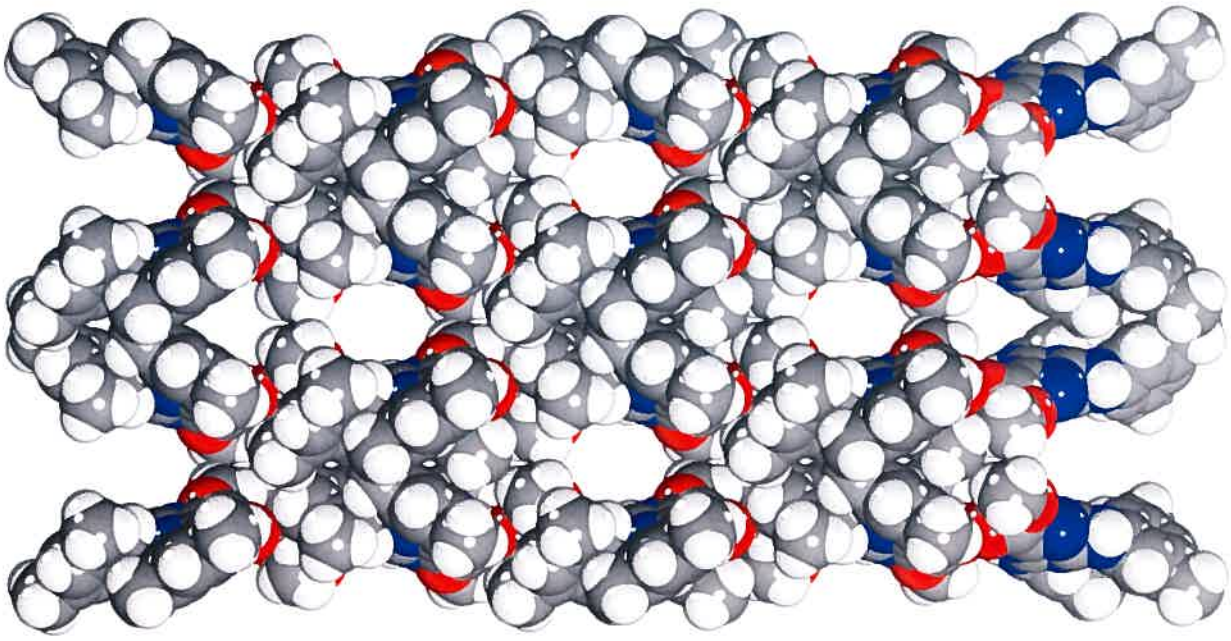

Figure A4-4. View along the *c* axis of a 2x4x1 array of unit cells in the crystal structure of **46k**. Guest molecules have been omitted for clarity, revealing the presence of small channels along the *c* axis occupied by disordered water molecules. Carbon atoms are shown in gray, hydrogen atoms in white, nitrogen atoms in blue and oxygen atoms in red.

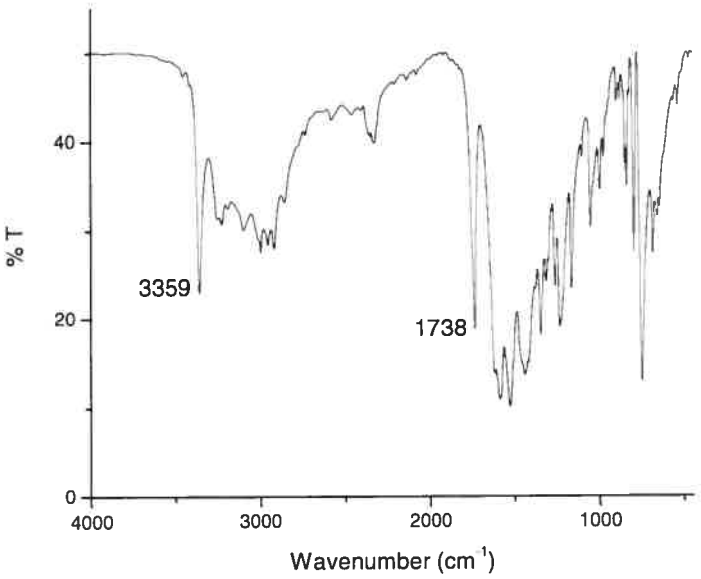
% T
40
20
0
3359
1738
4000
3000
2000
1000
Wavenumber (cm-1)

a

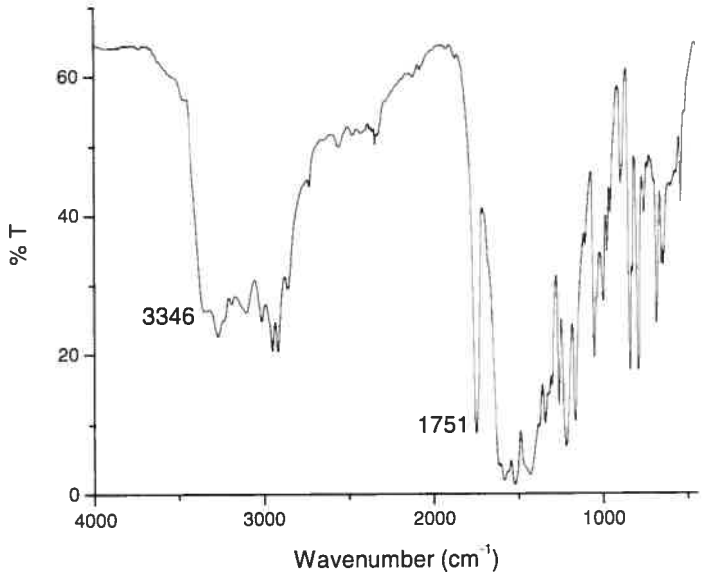
% T
60
40
20
0
3346
1751
4000
3000
2000
1000
Wavenumber (cm-1)

b

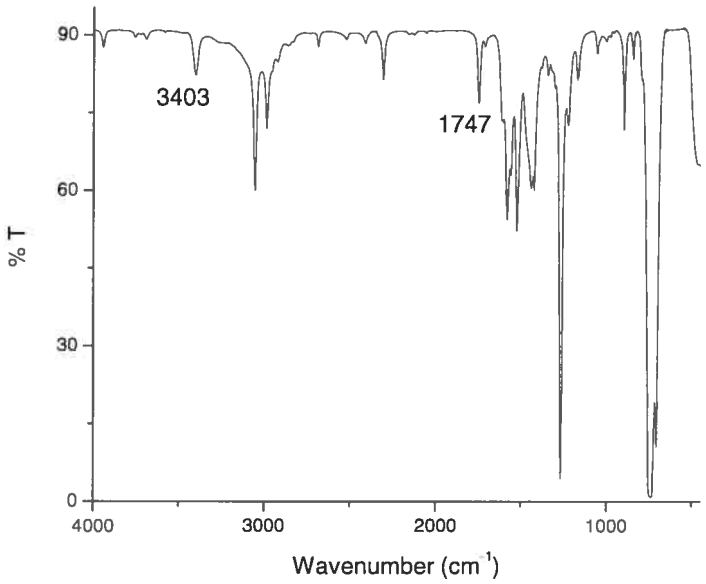

c

Figure A4-5. FTIR spectra of compound **46k** in a) single-crystalline and b) amorphous states, and c) CH_2Cl_2 solution. Wavenumbers are indicated for peaks corresponding to N-H and C=O groups.